Design, synthesis and pharmacological evaluation of nucleotidic and non-nucleotidic inhibitors and probes for the *ecto*-5′-nucleotidase (CD73)

Dissertation

zur

Erlangung des Doktorgrades (Dr. rer. nat.)

der

Mathematisch-Naturwissenschaftlichen Fakultät

der

Rheinischen Friedrich-Wilhelms-Universität Bonn

vorgelegt von

Georg Wilhelm Rolshoven

aus Köln

Bonn 2021

Die vorliegende Arbeit wurde von Mai 2017 bis November 2021 am Pharmazeutischen Institut der Rheinischen Friedrich-Wilhelms-Universität Bonn unter der Leitung von Frau Prof. Dr. Christa E. Müller angefertigt.

Table of contents

V

VII

VIII

X

XII

1   Introduction

1.1   Discovery of purinergic signaling – a historical perspective

In 1929, Drury and Szent-György investigated how the injection of heart muscle tissue extracts into the venous system might affect the heart rate of guiniea pigs. They observed changes of the heart rates depending on the injected amount, and identified the responsible compound as the nucleotide adenosine monophosphate (AMP).[1] Analytical methods were at that time limited to wet-chemical techniques and far away from instrumental devices we know nowadays, which makes their results even more remarkable. This pioneering work can be considered as starting point of research on purine-mediated signaling. The next milestone is a publication of Holton in the year 1959.[2] Herein, the authors investigated the possible role of adenosine triphosphate (ATP) in the nervous system. They reported capillary dilatatory activity for extracts of dorsal and ventral roots in which they analyzed ATP, adenosine diphosphate (ADP) and small amounts of their hydrolysis products. Due to its vasodilatatory activity, they discussed a possible role of ATP as a transmitter.[2] Geoffrey Burnstock, who died in June 2020 at the age of 92 years, is considered to be the founder of the research field "purinergic signaling" and has driven forward the research in this field to an outstanding extent in the past 60 years.[3] In the early 1960s, he and his research group postulated that nervus vagus stimulation of the guinea-pig taenia coli produced fast inhibitory junction potentials although adrenergic and cholinergic blocking agents were present. That challenged the classical view, that the autonomic control of smooth muscles is only regulated by antagonistically acting sympathetic noradrenergic and parasympathetic cholinergic nerves. They postulated that there must be a third non-adrenergic, non-cholinergic transmitter, a so called *NANC-transmitter*.[4] The next quantum leap represented the work of Geoffrey Burnstock's who published a review article entitled "purinergic nerves" in the year 1972.[5] Herein, he summed up several studies from the years before and suggested

ATP or a related purine nucleotide to be the third NANC-transmitter. Consequently, he coined the term "purinergic signaling", since the term non-adrenergic, non-cholinergic transmitter was considered to be imprecise and laborious.[5] Until that point, ATP had been well known as an intracellular energy source, but not as an extracellular messenger, and Burnstock *et al.* were repeatedly exposed to criticism for this - at that time - unconventional theory.[3] Now, after several decades of research, receptors of purines and pyrimidines have been cloned, the release and metabolic breakdown of extracellular nucleotides has been investigated, and purinergic signaling has emerged from a hypothesis to a widely accepted theory. In the following chapters, roles and functions of different members in purinergic signaling will be introduced and explained in detail.

1.2 Purinergic signaling – an introduction

1.2.1 Extracellular release and metabolic breakdown of ATP

Upon cell damage, inflammation, hypoxia, ischemia, malignancy etc., intracellular ATP is released into the extracellular compartment and is therefore considered as a "danger signal".[6–9] Independently of cell damage, ATP can also be secreted into the extracellular space by vesicular release, ABC transporters, pannexins and/or hemichannel connexins.[7, 10–12] Under physiological conditions, the extracellular ATP concentration is comparably low, namely about 10 nM, whereas the intracellular ATP concentration is between 1 and 10 mM.[7, 8] In pathophysiological conditions however, ATP accumulates in the extracellular space activating P2 receptors, which results in inflammatory and immunogenic processes.[13, 14] Metabolic degradation of ATP mediated by *ecto*-nucleotidases leads to the formation of ADP, which activates P2Y receptors (Figure 1), AMP and eventually to adenosine.[6–8, 14–16] Increased adenosine results in activation

2

of P1 receptors, which leads to the termination of inflammatory and immunogenic processes.[12, 13, 15]
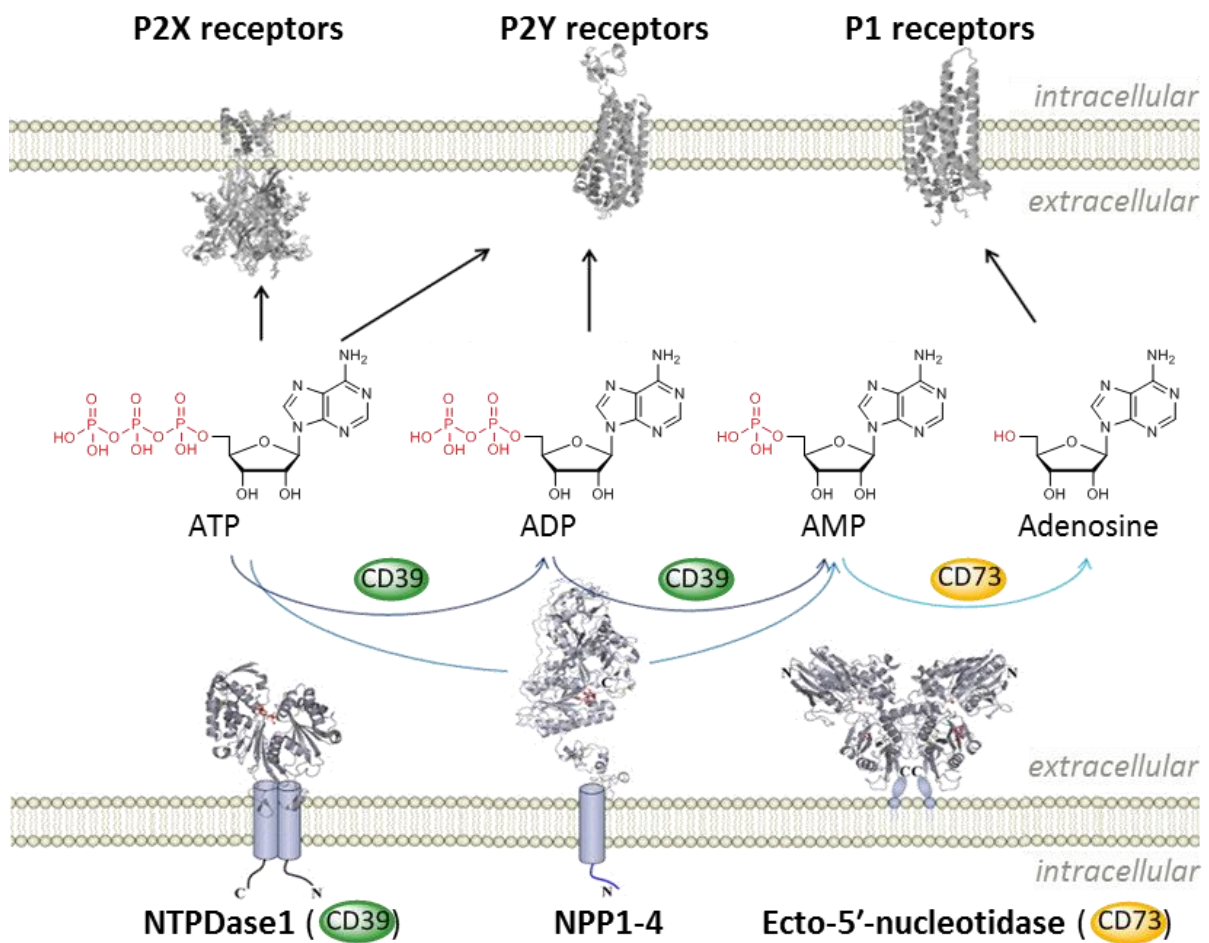
Figure 1. ATP is released and activates P2X or P2Y receptors. NTPDase1 (CD39) converts ATP to ADP, which can either activate P2Y receptors or be converted by NTPDase1 to AMP. AMP is hydrolyzed by CD73 to adenosine, which either activates P1 receptors or is taken up via nucleoside transporters into the cytosol.

1.2.2 *Ecto*-nucleotidases

Ecto-nucleotidases play the central role in the extracellular metabolism of nucleotides. After release into the extracellular space, nucleotides activate purinergic receptors and are broken down by *ecto*-nucleotidases (see Figure 1). Breakdown products of enzymatic *ecto*-nucleotidase

activity may activate other types of purinergic receptors. Purinergic receptors will be discussed in chapter 1.2.3. *Ecto*-nucleotidases consist of four major groups of enzymes: *ecto*-nucleoside triphosphate diphosphohydrolases (*e*NTPDase), *ecto*-5′-nucleotidase (*e*N, CD73), *ecto*-nucleotide pyrophosphatases/phosphodiesterases (*e*NPPs), NAD$^+$ glycohydrolase (CD38) and alkaline phosphatases (APs).[17, 18] Their main function is the hydrolysis of extracellular nucleotides and thus the control of extracellular nucleotide and adenosine levels (Figure 1).[17, 18]

1.2.2.1   *Ecto*-nucleoside triphosphate diphosphohydrolase 1 (CD39)

There are eight different members of the nucleoside triphosphate diphosphohydrolase (NTPDase) family: NTPDase 1-8. Four of them (NTPDase 1, 2, 3, 8, Figure 2) are *ecto*-nucleotidases due to their location on the cell-membrane with their catalytic site pointing towards the extracellular space. NTPDases 4-7 are located inside the cells (Figure 2).[19]
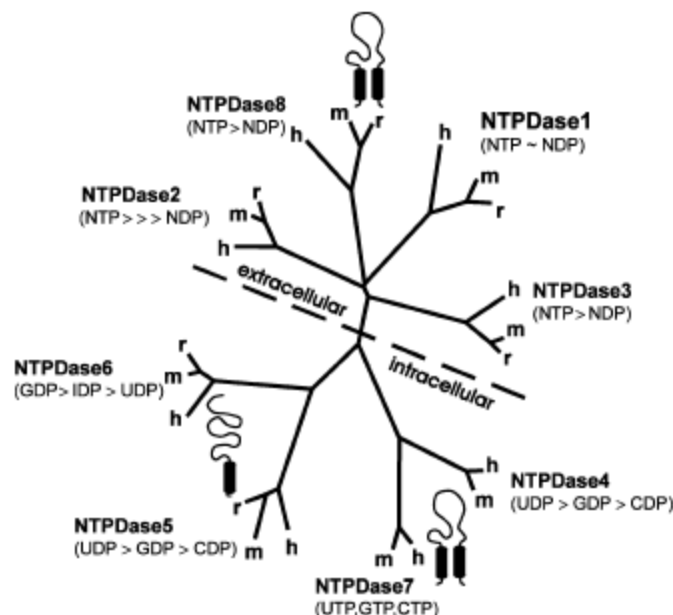
Figure 2. Phylogenetic tree of NTPDases.[19]

NTPDase1 (CD39) catalyzes the hydrolysis of ATP to AMP and thus provides the substrate for CD73. [7, 20, 15] Guidotti *et al.* were the first group that reported an apyrase activity of CD39.[20] All members of the NTPDase family possess 5 highly conserved sequence domains, which are named apyrase conserved regions (ACR).[7, 15, 19] These regions are crucial for the catabolic activity.[7, 15, 19] Like NTPDases2,-3,-4 and -7, CD39 contains two transmembrane regions,[20–22] and its catalytic activity is dependent from the presence of divalent cations in the millimolar range (Ca^{2+}, Mg^{2+}).[19, 23] Several inhibitors for CD39 have been described. There are, for example, nucleotide-derived inhibitors like N^6,N^6-diethyl-β,γ-dibromomethylene ATP (ARL67156) and 8-butylthio-AMP (8-BuS-AMP).[24, 25] Furthermore, non-nucleotide CD39 inhibitors have been reported like ticlopidine derivatives,[26] polyoxometalates,[27] and anthraquinone derivatives.[28, 29]

1.2.2.2 Further *ecto*-nucleotidases

The *e*-NPP subfamily consists of seven structurally related and cell-surface located enzymes that are capable of hydrolyzing pyrophosphate (diphosphate) and phosphodiester bonds to yield e.g. AMP.[30] In total, there are seven *ecto*-nucleotide pyrophosphatase/phosphodiesterase paralogues found to be expressed in mammals.[31] They are numbered NPP1-NPP7, whereas only NPP1-NPP3 are capable of hydrolyzing nucleotides.[32] The enzymatic activity of some members of the *e*-NPP subfamily is not limited to nucleotides.[31] *e*-NPP2 for example, besides the hydrolysis of nucleotides, is capable of hydrolyzing lysophosphatidylcholine to lysophosphatidic acid, or sphingosylphosphorylcholine to sphingosine-1-phosphate.[31] NPP6 and NPP7, are capable of hydrolyzing phospholipids only.[33, 34]

The fourth member of the *ecto*-nucleotidase family is the alkaline phosphatase (AP). The alkaline phosphatases consist of a subfamily with four members.[35] They are named by their predominant tissue distribution.[36] The tissue non-specific alkaline phosphatase (TNAP) is

highly expressed in bone, liver, kidney and in other tissues, whereas the placental AP (PLAP), gem cell AP (GCAP) and intestinal AP (IAP) are distributed in a more restricted fashion.[35] AP is the only member of the *ecto*-nucleotidase family that hydrolyzes nucleoside tri-, di-, and monophosphates, and a wide spectrum of phosphoric acid monoesters non-specifically.[9] Another member of the *ecto*-nucleotidase family is NAD+ glycohydrolase, which hydrolyses NAD leading to ADP-ribose. ADP-ribose is then hydrolysed by NPP1 leading to AMP, which is hydrolysed by CD73. This hydrolytic cascade represents an alternative pathway for the generation of extracellular adenosine.[18]

1.2.2.3 *Ecto*-5′-nucleotidase (CD73)

1.2.2.3.1 Structure and properties

Ecto-5′-nucleotidase (*e*N, EC 3.1.3.5, CD73) is a membrane-bound Zn^{2+}-binding enzyme, which mainly catalyzes the hydrolysis of extracellular AMP leading to adenosine.[17, 37–40] Human CD73 is encoded by the NT5E gene at chromosome 6q14-q21,[37] and consists of two identical monomers with a total weight of approximately 70 kDa.[37, 38, 41, 42,] Each monomer consists of a membrane-bound *C*-terminal domain, and Zn^{2+} containing *N*-terminal domain, which are attached to each other via a single α-helix comprising a hinge region.[39] The *C*-terminal domains form the dimerization interface between both monomers and are linked to the cell-membrane via a glycosylphosphatidylinositol (GPI)-anchor.[39] The GPI-anchor can be cleaved one the one hand by endogenous phospholipases, which results in a catalytically active, soluble form of CD73.[43–45] Proteolytic cleavage of the GPI-anchor, on the other hand, results either in an active or in an inactive form.[16, 43] X-ray co-crystallization studies with the non-hydrolyzable ADP analog adenosine-5′ -*O*-[(phosphonomethyl)phosphonic acid]) (AMPCP) and the hydrolysis product of AMP (adenosine), revealed that the *N*- and *C*-terminal domains

undergo a large rotation between an open and a closed conformation (see Figure 4).[39] The open state is thereby catalytically inactive, and allows the substrate to enter and leave the binding site. By domain rotation, which is mediated by a hinge region in the connecting α-helix, the Zn^{2+}-containing *N*-terminal domain rotates in the direction of the *C*-terminal domain to form the active site of the enyzme.[39] This state is the catalytically active, closed state, which prevents access of further substrates.[39, 40] Rotation back into the open state allows the hydrolyzed substrate to leave the binding site. Besides its role in purinergic signaling, CD73 is also involved in extracellular NAD^+ metabolism. CD73 dephosphorylates nicotinamide mononucleotide, which is formed from its precursor NAD^+ (Figure 3, **4**), to nicotinamide riboside for cellular uptake.[37, 46, 47]
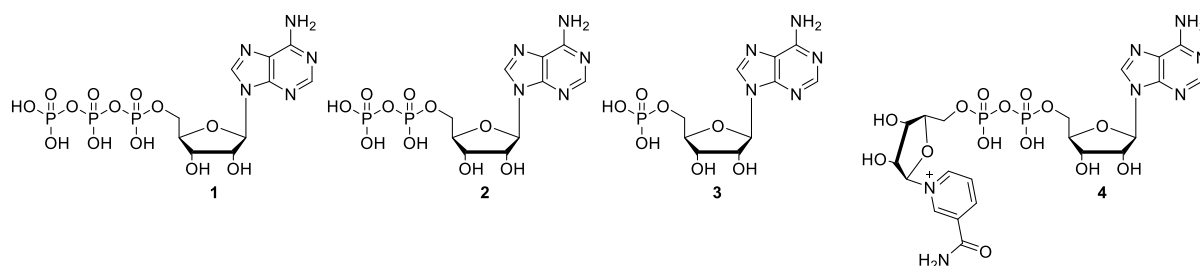
Figure 3. ATP (**1**), ADP (**2**), AMP (**3**), nicotinamide adenine dinucleotide (**4**, NAD^+).
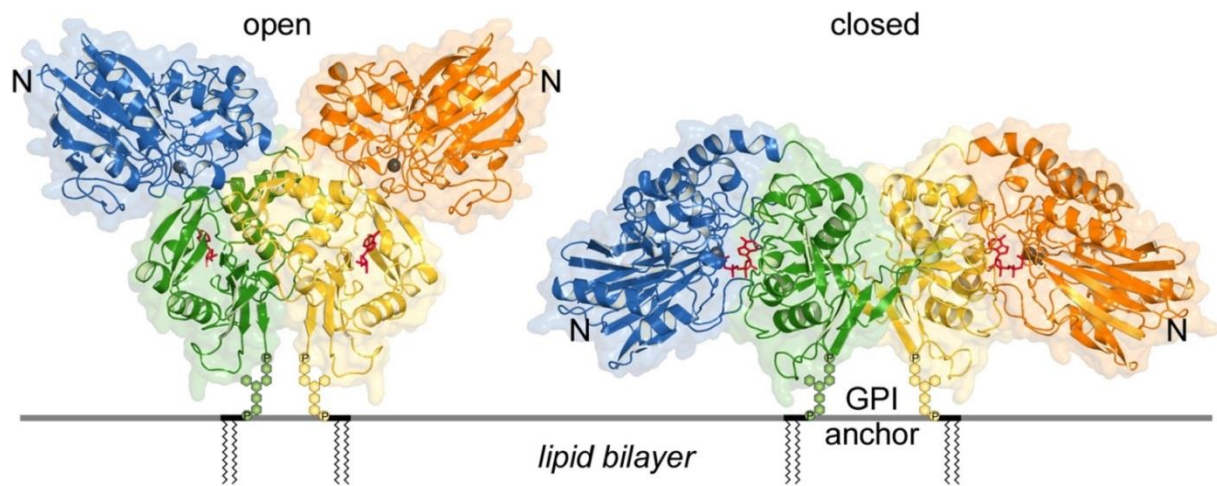
Figure 4. Crystal Structure of CD73. Depicted are the open (left) and the closed (right) conformation. The *N*-terminal domain undergoes a domain rotation of 102° to form the active site in the closed conformation.[39]

1.2.2.3.2 CD73 and its role in cancer

Adenosine, which can be generated by the enzymatic activity of CD39/CD73, plays a direct role in tumor progression. Adenosine accumulated in the extracellular space can create an immunosuppressive, pro-angiogenic, and pro-metastatic tumor microenvironment.[7, 48] Furthermore, adenosine plays a crucial role in tumor neovascularization and inhibition of tumor macrophage invasion.[48] CD73 expression levels vary in tissues, but are highly expressed in human colon, brain, kidney, heart, lung, and spleen.[16] In the immune system, CD73 is expressed on T-cells, T_{reg} cells, NK cells, macrophages, and dendritic cells, where it generates an immunosuppressive environment that fosters the progression of cancer (Figure 5). [7, 15, 16, 49–51]
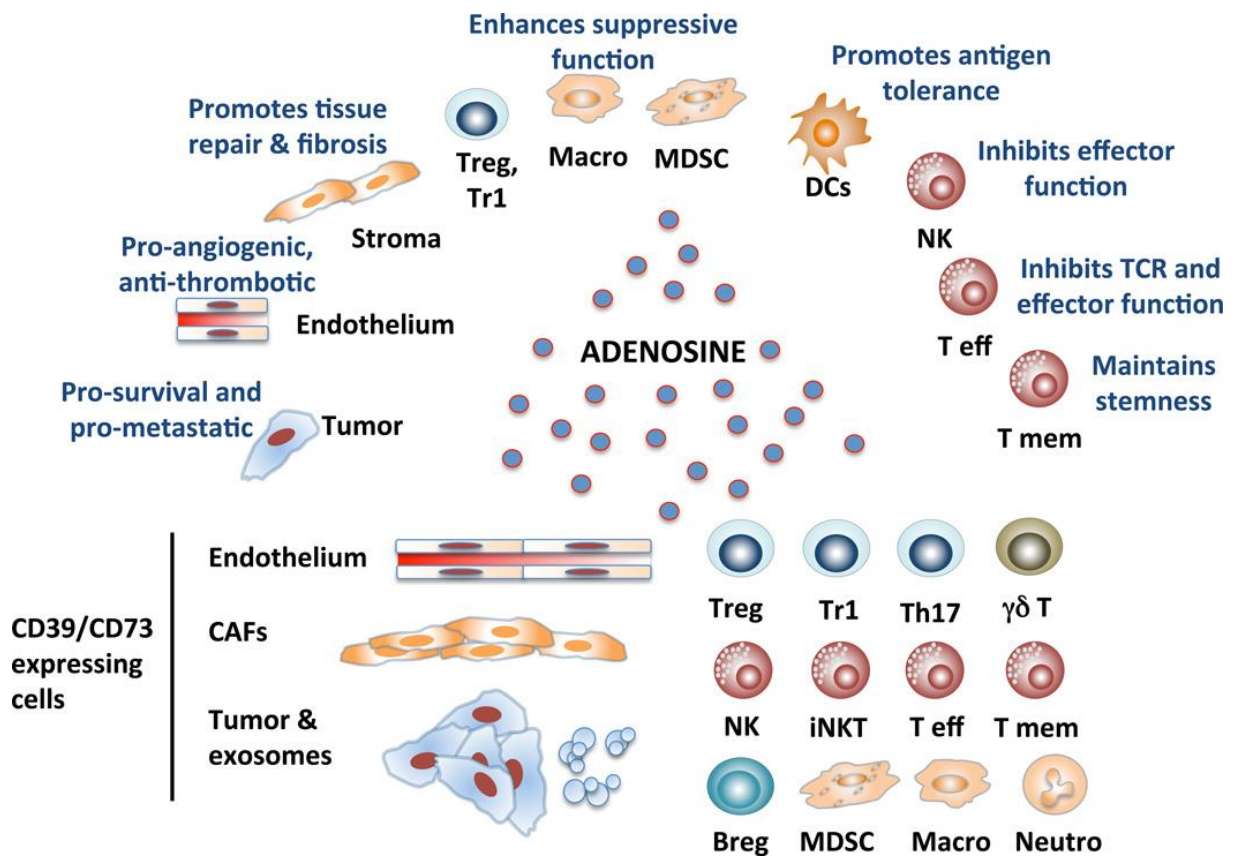
Figure 5. Adenosine and its role in tumor progression.[7]

CD73 expression is also upregulated in a variety of solid and blood cancer types as for example in colon cancer, epithelial cells of ovarian cancer, prostate cancer, thyroid, breast and, bladder cancer and in leukemia.[16, 52] Studies analyzing patients with triple-negative breast cancer cells (TNBC) showed that high CD73 expression levels were linked with poor prognosis regarding disease-free survival and overall survival.[53] The extent of immune infiltration in TNBC was found to be reduced with high CD73 expression levels, which was consistent with previous findings.[53] Application of anti-CD73 monoclonal antibodies (mAbs) significantly delayed tumor growth and metastasis in two different mouse breast cancer cell lines (4T1.2 and E0771) of immune-competent mice.[54] Importantly, it was also proven that mAb therapy against tumor-derived CD73 activates adaptive anti-tumor immunity.[54] Further methods of inhibiting the actions of CD73 were also postulated. Yegutkin *et al.*, e.g., deleted CD73 genetically. They

inoculated a CD73-lacking B16 melanoma cell line into mice and showed that tumor growth and metastasis were impaired in CD73-deficient mice. Also, pharmacological inhibition using AMPCP brought similar results as genetic deletion of CD73.[55]

1.2.2.3.3 CD73 – a new checkpoint with clinical relevance?

In the recent years, the field of cancer immunotherapy has emerged. About a decade ago, the first immune checkpoint inhibitor, the cytotoxic T-lymphocyte-associated protein 4 (CTLA4) inhibitor ipilimumab entered the market.[56] Anti-programmed cell death protein 1 (PD1) monoclonal antibodies, e.g. pembrolizumab and nivolumab, as well as the programmed cell death ligand 1 (PDL1) inhibitors atezolizumab and durvalumab followed shortly after.[57] Following the drug development of the last 10 years, Anti-PD1/PDL1 antibodies have become an inherent component anticancer therapies.[57] Apart from that, further potential checkpoint pathways have been intensively investigated. One of these additional checkpoints could be represented by CD73, generating adenosine in the tumor microenvironment.[7, 58, 59] Inhibition of tumor growth by the anti-CD73 monoclonal antibody (Mab) MEDI9447 (oleclumab) was shown in murine Balb/c (Bagg albino), syngeneic CT26 (*Colon Tumor* #26) colon carcinoma tumor models.[60] Furthermore, it was also reported that CD73 inhibition by MEDI9447 enhanced T-cell proliferation, but also timing and extent of leukocyte clustering, and levels of TH1 cytokines were increased with increasing MEDI9447 levels.[60] Studies with MEDI9447 have emerged from the preclinical phase into several clinical trials evaluating safety, pharmacokinetics and clinical efficacy.[61] It is currently being evaluated in several clinical trials phase 2 mostly in combination with immune checkpoint inhibitors, or commonly used cytostatics in the treatment of prostate cancer, pancreatic cancer.[61, 62] Besides MEDI9447, there are small-molecules being evaluated in clinical trials. The CD73 inhibitor LY3475070 from Eli Lilly and company (**6**, Figure 6) is currently being evaluated in phase 1. The goal is to see if the

inhibitor is safe and effective alone or in combination with pembrolizumab in patients with advanced cancer.[63] The nucleotide-derived small-molecule inhibitor AB680 (**5**, Figure 6) from Arcus Biosciences, Inc. is currently being tested in an open label, dose-escalation study in combination with zimberelimab (AB122), nab-paclitaxel and gemcitabine at patients with gastric cancer.[64]

AB680, **5**

hCD73 IC_{50} = 0.028 µM

6, Ex. 4, WO 2019/168744, LY3475070
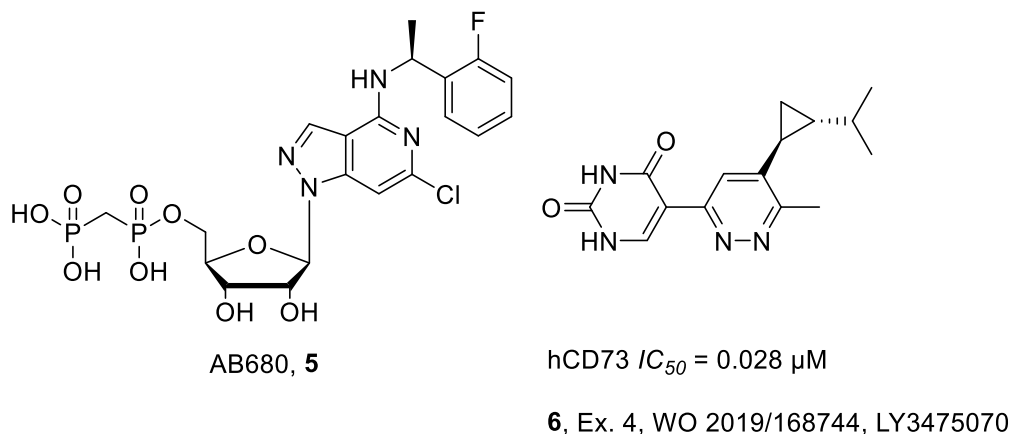
Figure 6. Small-molecule CD73 inhibitors AB680 (**5**) and LY3475070 (**6**) are currently tested in clinical trials.

1.2.2.4 Pharmacological assay systems for CD73 inhibitors

There are several assay systems that are suitable for the pharmacological evaluation of CD73 inhibitors. The following assays are most commonly used for the measurement of CD73 activity as summarized and reviewed by Jeffrey *et al.*: malachite green assay, luciferase-based luminescence assay, purine ribonucleoside phosphorylase coupled assay, radiometric assay, capillary electrophoresis (CE) assay and tandem mass spectrometry assay.[65] In the following chapter the malachite green assay and the radiometric assay will be described in more detail, since they were mainly employed in the framework of this thesis.

1.2.2.4.1 Malachite green assay

The colorimetric malachite green assay is based on the formation of inorganic phosphate (blue bubble in Figure 7, which is the reaction product of the enzymatic activity of CD73. Upon addition of malachite green and molybdate, inorganic phosphate forms under acidic conditions a complex showing an absorption maximum at a wavelength of 620 nm. Since the amount of formed inorganic phosphate correlates with the CD73 enzyme activity, the amount of the formed complex can be used to quantify the enzyme activity [66–68] Despite its lower sensitivity compared to the radiometric assay system, it is robust, easy to handle, fast, and comparably inexpensive, and therefore well-suitable for example for usage in high-throughput screenings.[69]
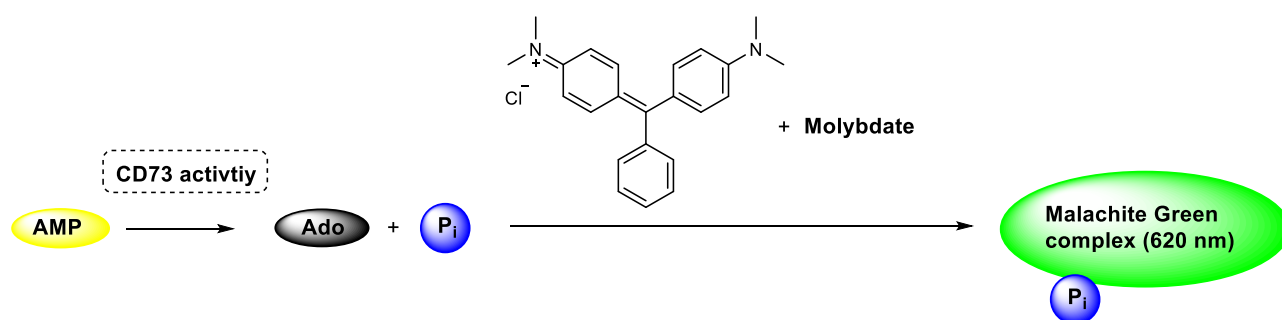
Figure 7. Principle of the malachite green assay.[66–68]

1.2.2.4.2 Radiometric assay

The radiometric assay was developed in our group by Freundlieb *et al.* and was published in 2014.[70, 71] In this assay [2,8-^{3}H]AMP is used as a substrate, which is co-incubated with CD73, and hydrolyzed to the enzymatic reaction product [2,8-^{3}H]adenosine. The second hydrolysis product, inorganic phosphate, and remaining substrate, [2,8-^{3}H]AMP, are then precipitated with lanthanum chloride. The precipitate is removed by filtration using GF/B glass fiber filters. The filtrate containing soluble [2,8-^{3}H]adenosine is collected in scintillation vials, and after addition

of scintillation cocktail, the product is quantified by scintillation counting (Figure 8). The radiometric assay shows a low limit of detection (LOD) and is thus very sensitive.[70]
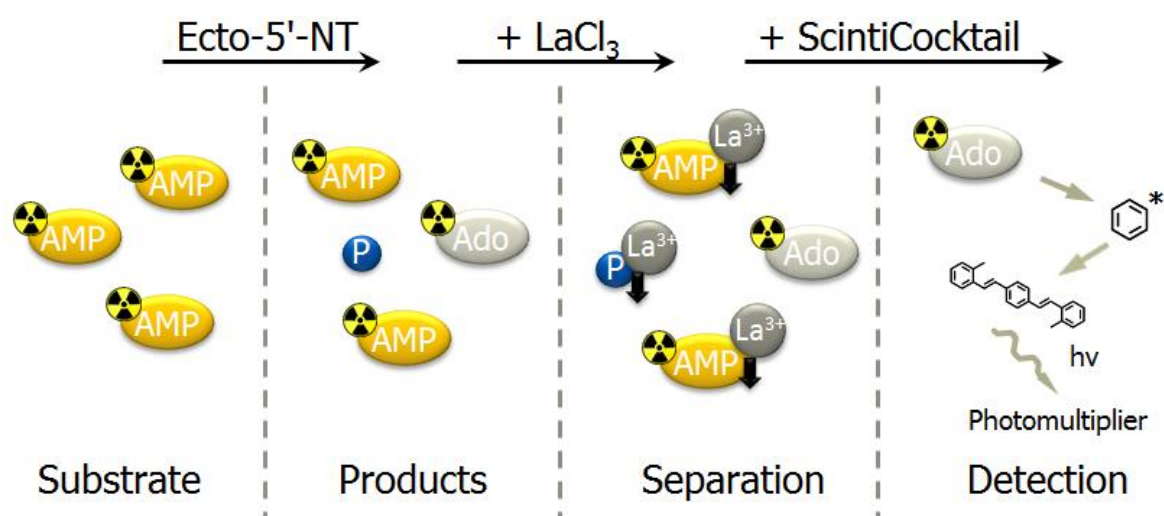
Figure 8. Principle of the radiometric assay for measuring CD73 activity.[69]

1.2.3   Purinergic receptors

Purinergic receptors are subdivided in three sub-families, P0, P1 and P2 receptors. The "youngest" member of the purinergic receptor family is the P0 receptor. P0 receptors are G protein–coupled receptors (GPCRs) that are activated by the nucleobase adenine.[72] There are furthermore the adenosine-activated P1 receptors, and P2 receptors, which are subdivided into ionotropic P2X receptors and the G protein-coupled P2Y receptors. These sub-families consist of further subtypes which will be introduced more in detail in the following chapter.[73]

1.2.3.1 P0 receptors

P0 receptors are suggested to be the latest addition to the purinergic receptor familiy.[74] This adenine-activated GPCR (AdeR), which shows high expressions levels in dorsal root ganglia, was first identified in rat by Bender *et al.* in 2002.[75] In rats, it is encoded by the mas-related gene receptor gene A1 (MrgA1).[74] Following the logic of the receptor nomenclature (ATP/ADP activate P2 receptors, adenosine activates P1 receptors), our group suggested to name this new receptor P0 (P zero) receptor.[72] Our group cloned and characterized this new adenine-activated receptor in mouse and hamster species.[74] In mice, the most-closely related receptor sequences to the rat AdeR are mMrgA10 and mMrgA9, which were previously termed mAde1R and mAde2R, respectively. Both mouse and rat receptor sequences share 76% amino acid identity.[74] The Chinese hamster adenine receptor ortholog (cAdeR) is named cMrgprA.[74.] Knospe *et al.* further characterized structure and function of the rat adenine receptor by mutagenesis studies and by a variety of binding experiments. Tissues, in which P0 receptors are relatively highly expressed, are brain cortex, hypothalamus, lung, ovaries, kidney, and small intestine.[76] To date, no human AdeR has been identified, but it is suggested that adenine plays a role as signal molecule in human pathology as well, and that G protein-coupled adenine receptors also exist in humans.[74]

1.2.3.2 P1 receptors

P1 receptors are activated by adenosine and are therefore named adenosine receptors (AR). This receptor family comprises 4 subtypes, A_1, A_{2A}, A_{2B} and A_3 ARs, and belongs to the super-family of membrane-bound GPCRs.[73, 77] A_1 and A_3 ARs are $G_{i/o}$ protein-coupled receptors, whereas A_{2A} and A_{2B} ARs belong to the G_s protein-coupled receptor family.[78] A_1 and A_3 ARs share a sequence identity of 49%, whereas A_{2A} and A_{2B} show a higher sequence identity (59%).[79] The

basal levels of stimulation by adenosine differ between the AR subtypes due to a high variability of extracellular adenosine levels between different tissues and the different sensitivities of the receptor subtypes.[77] All ARs possess various pro- and anti-tumor effects, but in general, extracellular adenosine in inflamed tissue is considered to be immunosuppressive.[80, 81] Caffeine and theophylline are prototypical non-selective antagonists of ARs,[82] but in the recent years, a variety of potent, and selective agonists and antagonists for ARs has been reported.[77, 79, 83] After approval in 2013 in Japan,[84] the FDA approved in August 2019 the A_{2A} AR antagonist istradefylline.[85] The drug with the trade name NOURIANZ® (**7**, Figure 9) is used as add-on in the treatment of Parkinson's disease with combined L-Dopa/Carbidopa for preventing "off-periods".[85] A_{2A} AR antagonists are also proposed to display neuroprotective properties.[86, 87]

7
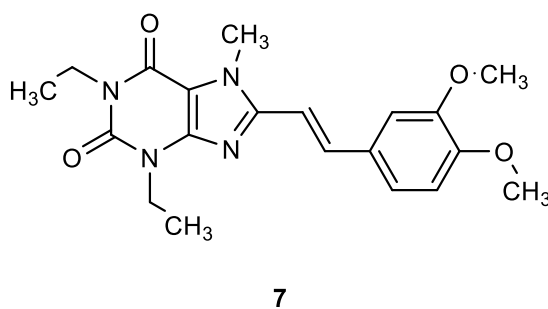
Figure 9. A_{2A} AR antagonist istradefylline (NOURIANZ®, **7**).[84, 88]

1.2.3.3   P2 receptors

P2 receptors are cell surface-located receptors activated by extracellular ATP. Depending on their structural properties they are subdivided into P2X and P2Y receptors,[73] which will be described in more detail in the following chapter.

1.2.3.3.1 P2X receptors

P2X receptors are ionotropic receptors, which consist of three subunits that form a stretched trimer or a hexamer from attached trimers.[73, 89] They are subdivided into the subtypes P2X1 – P2X7. P2X receptors are activated by ATP. By binding to the extracellular binding side, a conformational change occurs, which leads to opening of the channel that is permeable for Na^+, K^+ and Ca^{2+} ions resulting in an increase in intracellular levels of Na^+ and Ca^{2+}. The following depolarization of the cell membrane leads to an opening of voltage-gated Ca^{2+} channels provoking different cellular responses.[90, 91] P2X receptors are expressed all over the human body and are involved especially in the immune, cardiovascular and nervous system,[92] and are therefore also a target of great interest for related diseases. They are involved in a broad spectrum of physiological processes like synaptic transmission, taste, smooth muscle contraction, inflammation and nocicpetion.[7, 89, 92]

1.2.3.3.2 P2Y receptors

P2Y receptors belong to the super-family of GPCRs and are activated by various extracellular nucleotides.[93] The family of P2Y receptors comprises eight different mammalian subtypes.[94] The P2Y receptor subtypes differ in their preference towards the extracellular nucleotides, namely ADP ($P2Y_1$, $P2Y_{12}$, and $P2Y_{13}$), UTP ($P2Y_2$ and $P2Y_4$), ATP ($P2Y_2$, $P2Y_{11}$), UDP ($P2Y_6$), or UDP-glucose ($P2Y_{14}$).[72, 94, 95] The P2Y receptor family can also be clustered into two subfamilies based on sequence comparison, namely $P2Y_{1,2,4,6,11}$ ("$P2Y_1$-like") and $P2Y_{12,13,14}$ ("$P2Y_{12}$-like").[72] P2Y receptors are expressed in almost all cells in the human body, and are accordingly involved in a huge variety of physiological and pathophysiological processes.[93] As a prominent example is to mention the role of the ADP-activated $P2Y_{12}$ receptors in platelet

aggregation, which makes this receptor a drug target in the prevention and therapy of cardiovascular diseases.[96] Commercially available $P2Y_{12}$ receptor antagonists include clopidogrel (**8**), prasugrel (**9**) and ticagrelor (**10**) (Figure 10).[97, 98]

Another example of relevance for a P2Y receptor-interacting compound is diquafosol (**11**). This dinucleotide is a $P2Y_2$ receptor agonist used in the treatment of dry eye syndrome.[99] Stimulation of the G_q-coupled $P2Y_2$ receptor leads to an increase in the intracellular calcium concentration and thus to an increased mucin secretion.[100, 101]

Clopidogrel, **8**   Prasugrel, **9**   Ticagrelor, **10**
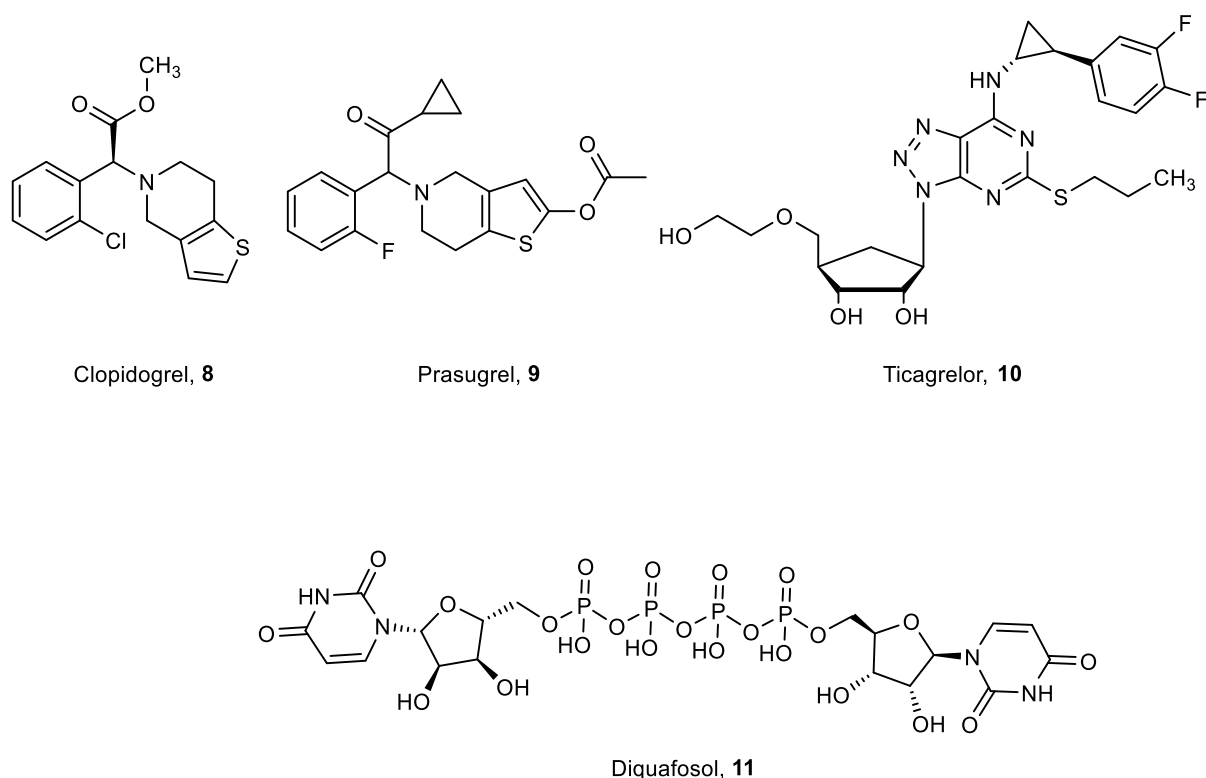
Diquafosol, **11**

Figure 10. $P2Y_{12}$ antagonists clopidogrel (**8**), prasugrel (**9**) and ticagrelor (**10**) and $P2Y_2$ agonist diquafosol (**11**).[98, 100, 101]

1.3 Recent development of small-molecule CD73 inhibitors

The following chapter will describe the development of small-molecule CD73 inhibitors, which have been developed and published in recent years. Whereas this topic was mainly addressed by academic research 10 years ago, especially the first publication of AMPCP-derived CD73

inhibitors by Bhattarai & Müller in 2015[102] sparked the interest of industrial researchers as well as by further academic research groups. Over the past years, many different compounds with various scaffolds have been published in the framework of patents and scientific publications. A selection of these will be discussed in the following chapter.

1.3.1 Binding mode of AMPCP-derived CD73 inhibitors

In 2012, Knapp *et al.* reported the first crystal structure of human CD73 in the open and closed conformation complexed with AMPCP, adenosine and two further CD73 inhibitors.[39] Co-crystallization with AMPCP revealed the binding mode of nucleotide-derived CD73 inhibitors (Figure 11). Since the majority of the CD73 inhibitors is AMPCP-derived, the binding mode will be outlined to a greater extent. The adenine base is sandwiched in the so called "adenine clamp" which consists of the aromatic rings of two phenylalanine residues forming strong hydrophobic π-π stacking. The ribose moiety forms hydrogen bonds between the side chains of two arginines (R354 and R395) and aspartic acid (D506) (Figure 11A, Figure 11B). The α-phosphonate of the diphosphonate residue interacts via hydrogen bonds with R354, R395 and N245 (asparagine) (Figure 11C).[39, 103, 104] The β-phosphonate interacts with N117, H118 and R395. It furthermore coordinates the Zn^{2+}-ions in the dimetal center and displaces a water molecule that has been observed in the E. coli 5′-nucleotidase AMPCP binding mode. The two Zn^{2+} ions are bidentally coordinated by the β-phosphonate group and are monodentally bridged by the side chain of D85 to form a distorted trigonal-bipyramidal geometry (Figure 11C). Knapp *et al.* furthermore describe a large hydrophobic cavity in proximity to the C2 atom of the adenine core.[39] This pocket is formed by the C-terminal domain and consists of the hydrophobic amino acids F421, P498, L389 and L415 and polar N390, N499 and D524 (Figure 11B). The C2-cavity was investigated in detail in subsequent publications.[103, 104] The detailed knowledge

of the binding site provided by co-crystal structures is especially for the design of new inhibitors of great value, especially for the design of new inhibitors. It facilitates the prediction of possible interactions between substituents and amino acid residues in the binding site.
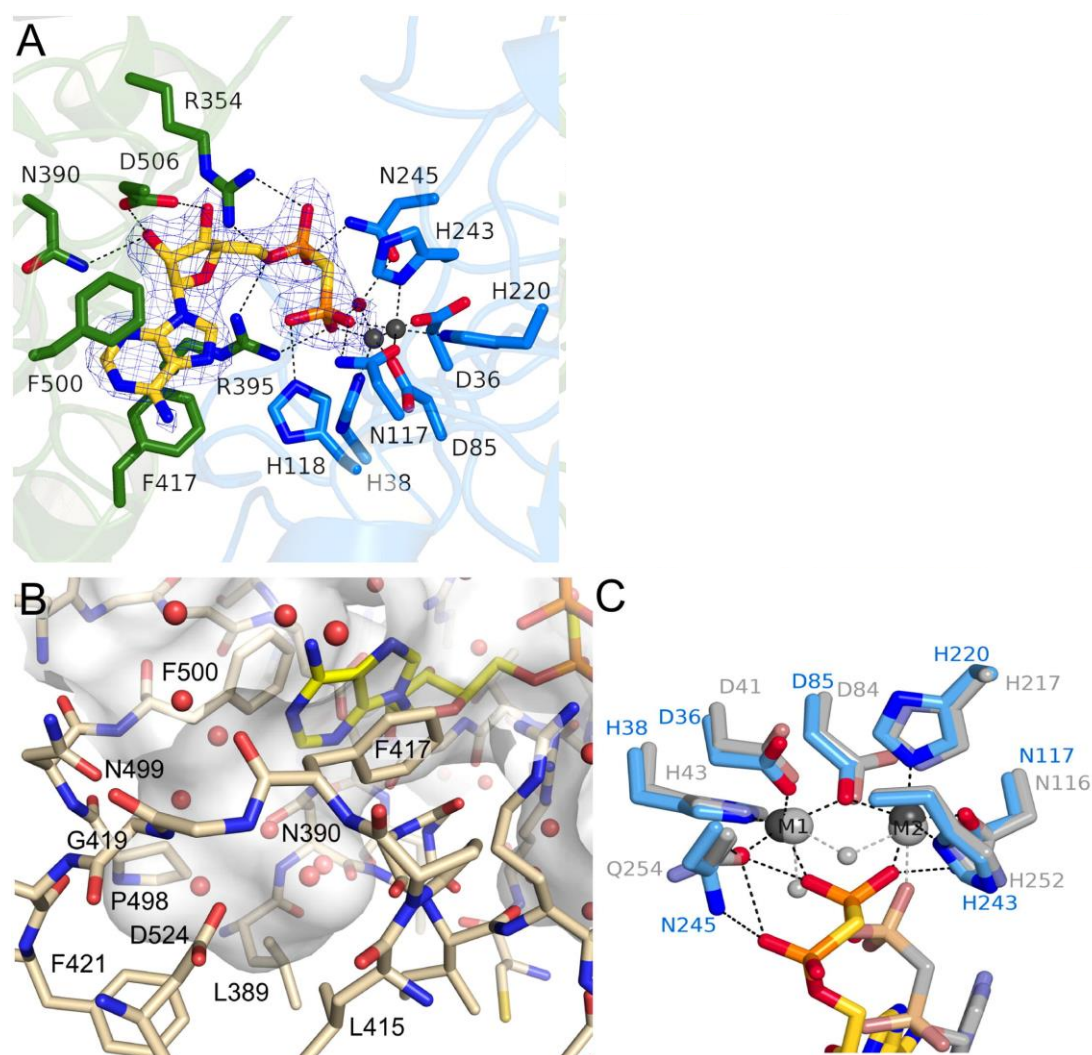
Figure 11. Co-crystal structure of AMPCP with human CD73. (A) Overview of binding: ribose interacts with R354, R395, N390 and D506. (B) "Adenine clamp" formed by F500 and F417, and C2-pocket. (C) Distorted trigonal-bipyramidal geometry between Zn^{2+} ions and β-phosphonate.[39]

1.3.2 Nucleotide-mimetics

The first described inhibitors of CD73 were the nucleotides ATP and ADP as well as the ADP analog AMPCP.[17, 105] Whereas ATP and ADP inhibited rat-derived CD73 in the low micromolar range (see Figure 12), AMPCP is a much stronger inhibitor. Its reported K_i-value of 0.85 µM was initially determined at isolated CD73 from *Torpedo marmorata*.[106] Several following publications reported further IC_{50} or K_i values for AMPCP at recombinantly generated soluble rat CD73 (sCD73), see Figure 12.[70, 107, 108]

Torpedo electric organ K_i = 48 µM[106]
K_i rat sCD73 = 8.9 µM[108]

Torpedo electric organ K_i = 48 µM[106]
IC_{50} rat sCD73 = 4.66 µM[70]
K_i rat sCD73 = 0.91[108]

K_i Torpedo electric organ = 0.85 µM[106]
K_i rat sCD73 = 0.87 µM[108]
IC_{50} rat sCD73 = 0.236 µM[70]
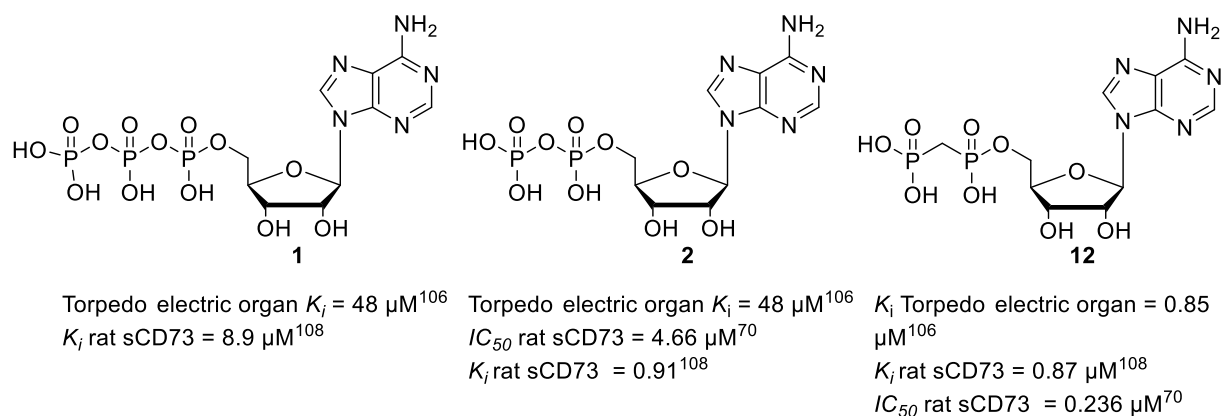
Figure 12. ATP (**1**), ADP (**2**) and AMPCP (**12**) – the first reported inhibitors of CD73.[70, 106, 108]

The pioneering work of Müller *et al.* resulted in the publication of the first potent and selective CD73 inhibitor in the low nanomolar range in 2015. [102] This coicidenced with dramatically increased interest in research on CD73 related to the field of immunotherapy in academia as well as in industry. Bhattarai *et al.* managed to strongly enhance the potency and metabolic stability of the lead structure AMPCP.[102] It is quite remarkable that only the introduction of an N^6-benzyl substituent led to such a strong enhancement in the potency. The actictiy was tested at human recombinantly generated soluble CD73 and revealed a K_i-value of 2.21 nM, see Figure **13, 13**. Metabolic studies in rat liver microsomes as well as human blood plasma indicated a high metabolic stability, which is an important factor in terms of drugability.[102] From a

structural point of view, it is also remarkable that, until now, the majority nucleotide-derived inhibitors with potencies in the low nanomolar to subnanomolar range carry a benzylamine substituent or at least a bulky, liphophilic residue in the N^6-position.[65, 103, 104, 109, 110] Further derivatization of position 2 with a chlorine atom and disubstitution of N^6 displayed the next step in the development of CD73 inhibitors. With crystal structure-aided design, compounds in the sub-nanomolar range were obtained. The most potent compound PSB-12489 (**14**) showed a potency of 0.381 nM on human soluble CD73 (Figure **13**).[103, 111] Additional substitution of the N^6-position by a small alkyl residue enhanced in some cases the potency on CD73 and – more importantly – abolishes an activation of adenosine A2 receptors by a possible adenosine conversion product.[79, 103, 112]

13, PSB-12379
K_i human sCD73: 2.21 nM
K_i rat sCD73: 9.03 nM

14, PSB-12489
K_i human sCD73: 0.381 nM
K_i rat sCD73: 0.746 nM

15, 2-I-AOPCP
K_i human sCD73: 3.59 nM
K_i rat sCD73: 3.31 nM

16, PSB-18231
K_i human sCD73: 0.010 nM
K_i rat sCD73: 0.388 nM
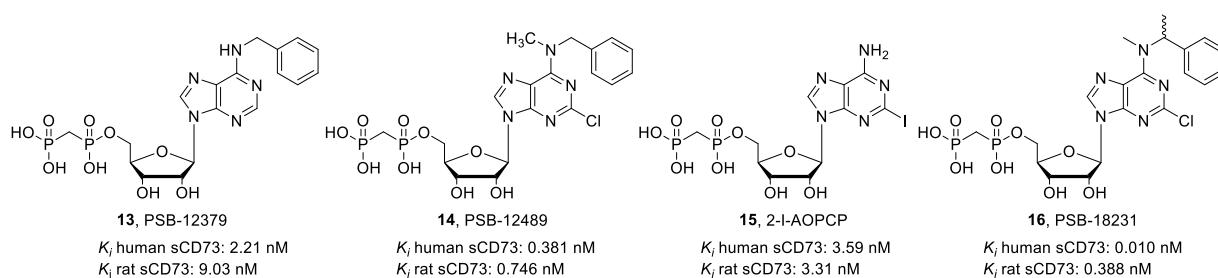
Figure 13. Development of AMPCP-derived CD73 inhibitors (**13-16**) by Müller *et al.*[102–104, 110]

Co-crystal structures with PSB-12489 (**14**) and PSB-12379 (**13**) reveal detailed interactions between the inhibitors and amino acids of the active site of the enzyme (Figure **14**). In general, the binding mode is very similar to the binding mode of AMPCP. However, there are some differences. When N^6-benzyl-substituted PSB-12489 (**14**) is bound to CD73, N186 is shifted to provide space for the aromatic benzyl residue (Figure **14**A). Co-crystallization of 2-chloro-substituted PSB-12489 (**14**) allowed detailed analysis of interactions of the chloro substituent with amino acids in the "C2-cavity". The NH group of N390 interacts with the halogen, whereas the carbonyl oxygen of N390 is too far away to form halogen bonding (Figure **14**B).[103] In 2020, Bhattarai *et al.* reported several 2-substituted AMPCP-derived CD73 inhibitors, indicating that

low nanomolar potencies can also be reached without the typical N^6-substitution pattern, if the compounds carry small polar or lipophilic substituents (I, Cl, -NH$_2$) in the 2-position (**15**, see Figure 13).[104] They reported also remarkable findings concerning the binding mode of several 2-substituted AMPCP derivatives. If the 2-position carries a bulky residue, like piperazinyl or cyclohexylethyl, the adenine base and the ribose are flipped by 180°, whereas the dipshophonate residue remains mostly in the common position (Figure 14C).[104]
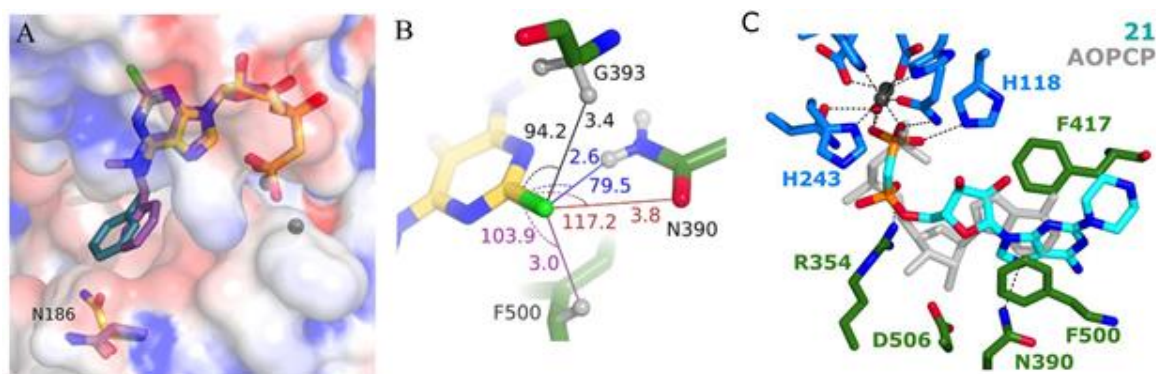
Figure 14. A) PSB-12379 (**13**) bound to CD73 shifting N186, B) Close-up of the interactions of the chloro substituent (green) in PSB12489 (A and B taken from [103]) (**14**) C) Flipped binding mode of 2-piperazinyl-substituted PSB-12604. For comparison, AMPCP depicted in gray. (taken from [104]). Distances (in A) and angles (°) are indicated.

In 2019, Arcus Biosciences presented AB680 (**5**), an AMPCP derived CD73 inhibitor with a reported potency of 5 pM.[113, 114] Essentially the same substitution pattern as described in earlier work of Müller and Bhattarai, namely N^6-benzylamine, 2-chloro and α-methyl was employed for this compound.[103, 111] The only differences are modifications of the adenine core, in which the *N1* nitrogen atom was removed and the *N7* nitrogen was shifted to position 8 (see Figure 15)[65, 78, 113, 114] In 2017, Arcus Biosciences filed a patent in which a variety of AMPCP-derived CD73 inhibitors was disclosed, also the structure of AB680, which was later on published in several publications.[115] Based on various enzyme-kinetic experiments, Bowman *et al.* characterized AB680 as "extraordinarily potent, slow-onset, reversible, competitive inhibitor

of human (h)CD73".[110] Experiments measuring the IC_{50} values of AB680 employing different hCD73 concentrations and saturating amounts of AMP indicated tight binding. Jump-dilution experiments proved the reversible inhibition mode of AB680.[110] Interestingly, the experiments showed furthermore an initial delay of time after addition of excess of substrate until enzymatic activity was recovered, indicating slow dissociation of the inhibitor.[110] Unpublished work from Müller *et al.* contains a series of compounds with potencies in the same range as AB680.[109] Besides 2-chloro substituents, also further bromo and iodo-substituents in position 2 were employed. Besides that, the *o*-position of the phenyl ring of benzyl residue was substituted with a chlorine atom leading to compounds with potencies in a range of 10 – 50 pM (**16**, **17**, Figure 15). However, the adenine core remained unchanged, what didn't impair the potency of the compounds. Tested in our system, AB680 showed a K_i value of 20 pM, which is the same range as our compounds.[109]
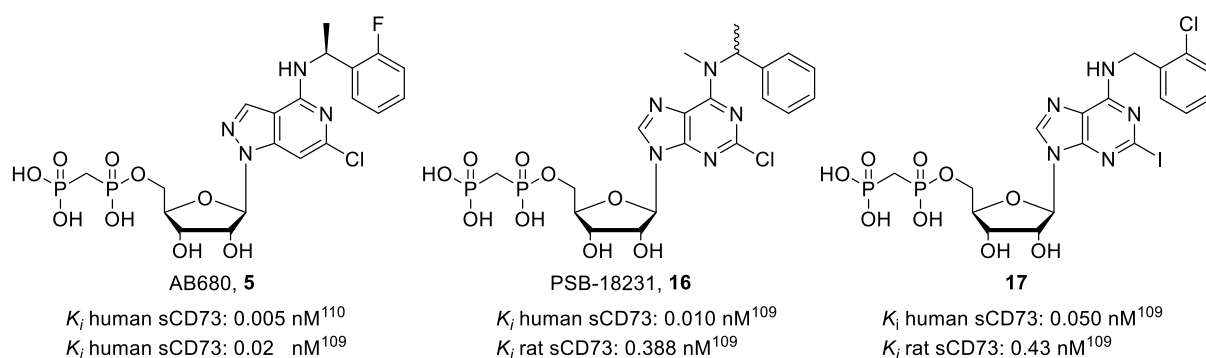
Figure 15. AB680 (**5**) and further unpublished AMPCP-derived CD73 inhibitors (**16**, **17**) with potencies in the same range.[109, 110]

In 2020, Du *et al.* from ORIC Pharmaceuticals reported the first perorally bioavailable nucleotide-derived CD73 inhibitor.[116] The monophosphonate compound **19** was developed from the diphosphonate **18** (Figure 16). With a chloro substituent in position 2 and a cyclopentyl residue at N^6, the adenine core carried a similar substitution pattern as commonly used. Also similar to AB680, the N7 was shifted to position 8, whereas the N1 was not removed. OP-5244

displays the first subnanomolar nucleotide-derived CD73 inhibitor without a diphosphonate structure. Du *et al.* removed the α-phosphonate which is esterified to the 5-OH group (**19**), and shortened the resulting alkyl chain by one methylene group leading to **20**. Shortening of the linker was crucial in terms of oral bioavailability, since the 5′-α-methylene phosphonic acid derivative (**19**) showed early signs of peroral bioavailability in rats.[117] The measured *IC50* of this compound was 29 nM. Further derivatization of the α-methylene position with a methoxymethylene or a hydroxymethylene residue provided OP-5244 (**20**), which had good oral bioavaliability and showed a 100-fold enhanced potency compared to the precursor, the methylenephosphonate **20** ($K_i = 0.25$ nM).[117] Interestingly, the group around Sharif *et al.* (Arcus Biosciences) published the identical structure of OP-5244 as a lead structure around 4 months later.[118] They reported an *IC50* of 2.5 nM, which is 10-fold more active than the reported of Du *et al.* A reason could be different incubation times of enzyme and inhibitor. Whereas Du *et al.* co-incubated only for 15 min at rt, Sharif *et al.* co-incubated for 60 min at 37 °C,[116, 118] which can have an influence on the measured *IC50*. The structurally similar AB680 showed a slow-onset inhibition, reaching a plateau of highest inhibition after around 30 minutes of co-incubation time.[110] That shows that under these conditions OP-5244 might be underrated, and would also explain why AB680 only showed an *IC50* of 0.86 nM in their assay system.[116]
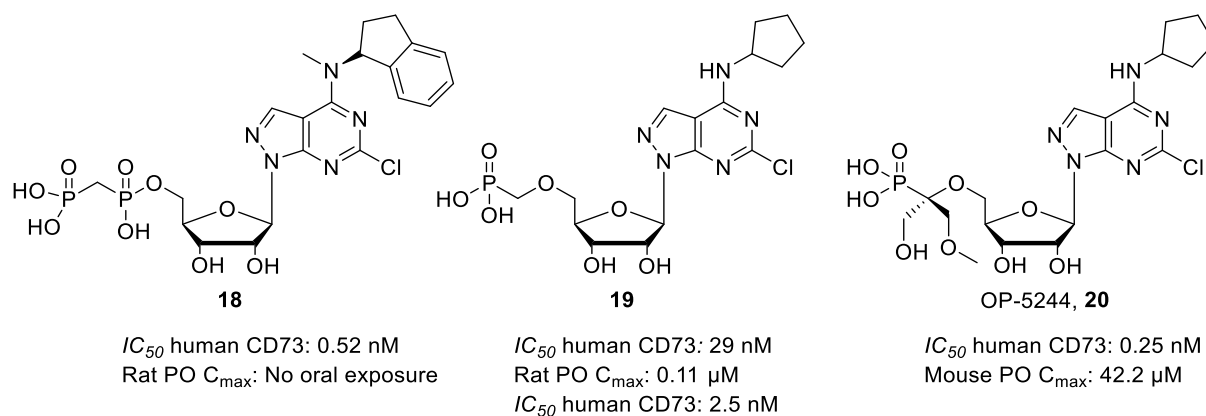
Figure 16. Development of perorally bioavailable nucleotide-derived CD73 inhibitors (**18**-**20**).[116, 117]

Dumontet *et al.* combined cytotoxic nucleosides with the diphosphonate structure in the 5′-position.[119] In contrast to the majority of the CD73 inhibitors, the 2′-OH group was substituted by a fluorine residue (Figure 17, **21**). The 2-chloro substition provided most-likely strong binding, whereas lack of an N^6-substitution might have been the reason for only moderate potency of this compound (IC_{50} = 0.18 µM). Ghoteimi *et al.* reduced the bicyclic adenine core to a monocyclic triazole ring, and **22**, which represented the most potent compound from this series (IC_{50} = 0.86 µM), carried an additional 2-naphthyl residue in position 4.[120] Compared to the AMPCP derived CD73 inhibitors, the potency of this compound (which was the best from this series) is strongly reduced. Within this publication, Ghoteimi *et al.* also reported compounds, lacking the entire ribose sugar moiety, which again led to a strong reduction in potency (4.2 µM, **23**, Figure 17). [120]
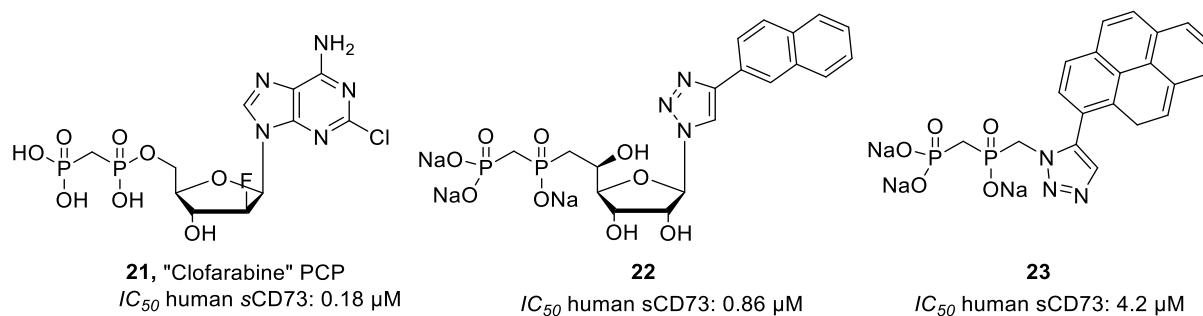
Figure 17. AMPCP-derived CD73 inhibitors with varied ribose or adenine core (**21**-**23**).[119, 120]

Substitution of the purine core by a pyrimidine core was, however, better tolerated than the previously mentioned examples. Junker *et al.* reported a series of 50 nucleotide-derived CD73 inhibitors, containing purine and mainly pyrimidine scaffolds.[121] Modifications of the sugar moiety like removal of the 2′-OH group, or (*S*)-methanocarba-based sugars were not tolerated. In case of the cytidine-derived *α,β*-methylene diphosphonates, a benzyloxy substitution at the exocyclic amino group in position 4 and a small substituent in the N3 position were tolerated best (**24**). 5-Fluorouridine was the most active compound (**25**) from those carrying a uracile base. The most potent compounds among both series were tested at different preparations of CD73 (rat-derived, soluble CD73, human-derived soluble CD73, human membrane-bound CD73). In all preparations, both compounds revealed K_i-values in the low nanomolar range (see Figure 18).[121] Furthermore, the potency of several deaza-AMPCP derivatives towards CD73 was tested. Except for 7-deaza-AMPCP (**26**) however, none of the deaza-derivatives was tolerated by CD73. Interestingly, 7-deaza AMPCP was two-fold more active than AMPCP at rat CD73 .[121]
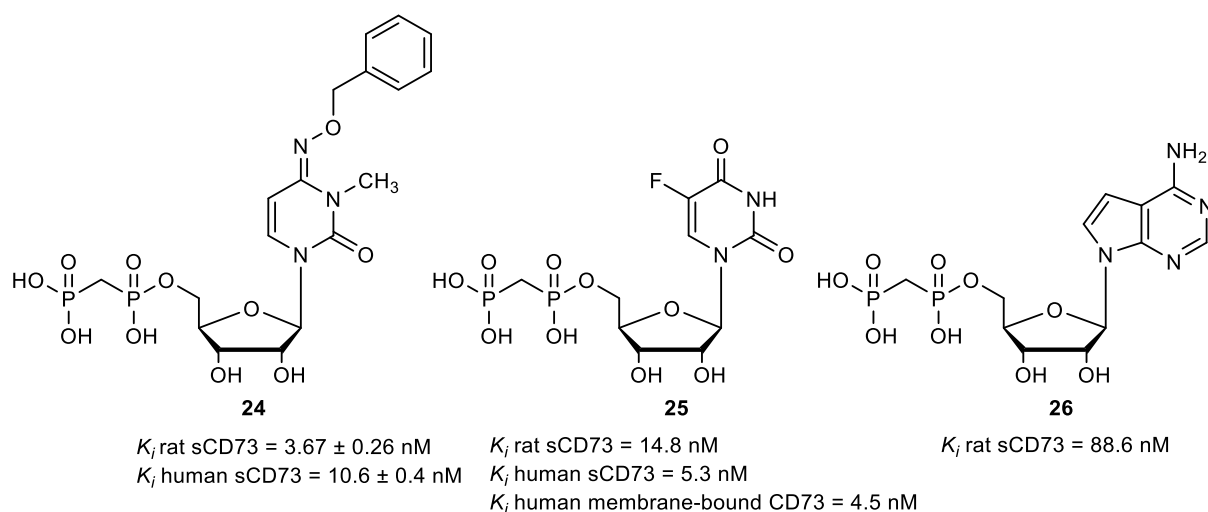
Figure 18. Pyrimidine and purine nucleotides as CD73 inhibitors (**19-21**).[121]

In a recent publication of Schäkel *et al.,* it could be shown that not only nucleoside diphosphonate, and monophosphonate compounds inhibit CD73.[25] Within the reported series of nucleoside triphosphonate derivatives (Figure 19, **27-29**), which were originally intended to be inhibitors for CD39, several compounds revealed potency at human, soluble CD73 in the sub-micromolar range.[25] However, they also reported poor metabolic stability, elaborate synthesis and thus low yields.[25] That, combined with only moderate potencies on both targets, impairs the attractiveness of the compounds.
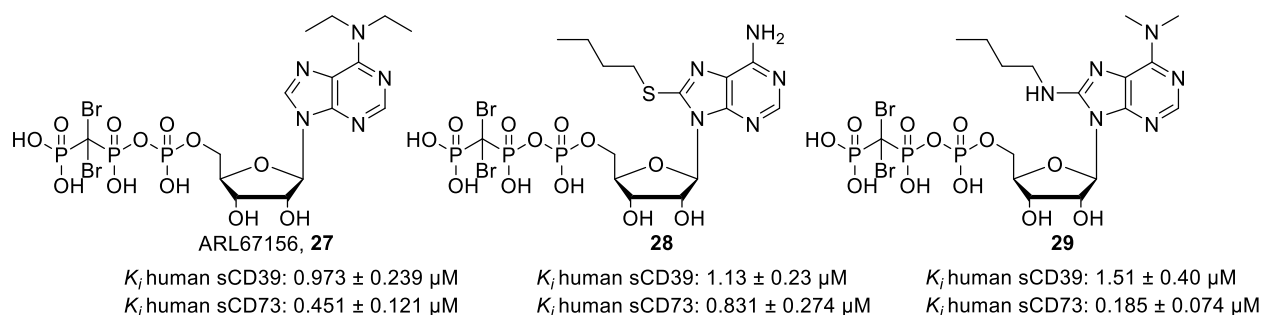
Figure 19. Dual CD39/CD73 inhibitors: triphosphonate analogs (**27-29**). [25]

In 2017, Vitae Pharmaceuticals, Washington, USA, patented a variety of CD73 inhibitors for the treatment of cancer and other CD73-mediated diseases.[122] The claimed compounds share structural elements of known AMPCP-derived CD73 inhibitors, but also vary at several positions (Figure 20). The most crucial difference is the missing diphosphonate structure. Instead, a variety of branched alkyl groups, carrying for example acetyl ester groups, phosphonic acids, malonate was introduced. Depicted are two of the most potent compounds **30** and **31**. In the patent however, no explicit K_i or IC_{50} values are mentioned. Instead, compounds with a potency below 100 nM are marked with +++, 100-1000 nM with ++ and >1000 nM with +.[122] As Dr. Christian Renn also stated in his doctoral thesis, the measured values have to be taken with a grain of salt.[69] Instead of the commonly used AMP as a substrate in the malachite green assay system, they used cytidine-5′-monophosphate (CMP), which has a higher K_m-value than AMP, which makes the assay more sensitive, because higher substrate concentrations can be used. Taking into account that the measured K_i values for AMPCP ranged between 12-25 nM (in our assay system 88 nM), we can assume that the measured K_i-values are most-likely overrated.

30, Ex. 1, Isomer 2, US 2017/0044203 A1, Inhibitory activity human sCD73: +++

31, Ex. 54a, US 2017/0044203 A1, Inhibitory activity human sCD73: +++
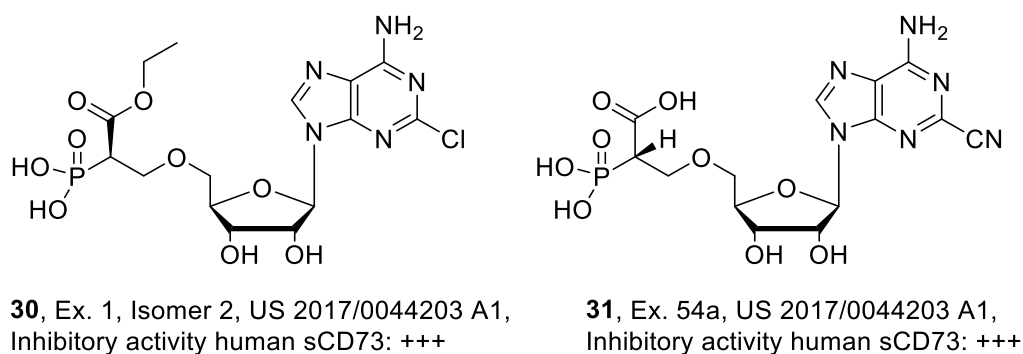
Figure 20. Nucleotide-mimetic CD73 inhibitors disclosed in the patent from Vitae Pharmaceuticals Inc. (**30, 31**).[122]

Regarding the nucleobase, the compounds patented by Calithera Biosciences Inc. are quite similar to those patented by Vitae pharmaceuticals.[123] The two most potent compounds (**32, 33**)

from the patent are depicted in Figure 21 and carry the following structural features. The stereochemistry of the 3′-position is inverted in comparison to natural nucleosides and nucleotides, and the 2′-OH group is substituted by a fluoro atom. The 5′-bound residue is again branched, but herein, similar to Du *et al.*, in the α-position. The α-position carries a malonate residue and a differently substituted, bulky, aromatic residue.[123]

Ex. 65, US2018/0186827 A1
IC$_{50}$ human membrane-bound CD73 = 0.031 µM

Ex. 58, US2018/0186827 A1
IC$_{50}$ human membrane-bound CD73 = 0.038 µM
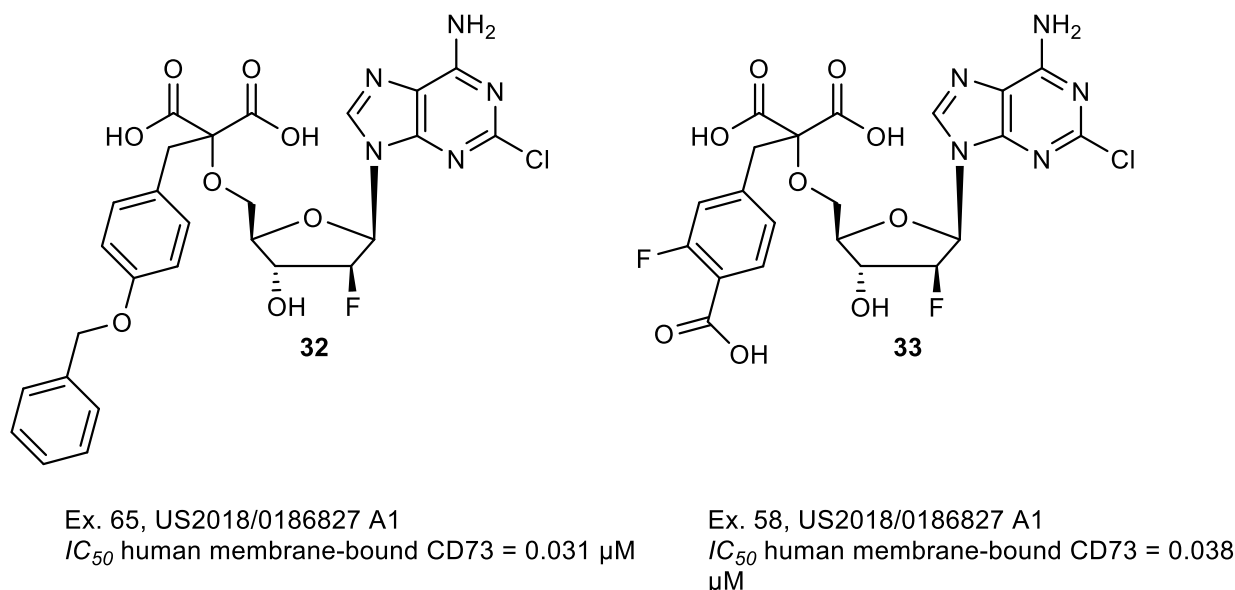
Figure 21. Selection of two of the most potent CD73 inhibitors (**32**, **33**) disclosed in the patent of Calithera Biosciences Inc.[123]

Peloton Therapeutics filed a patent for a series of nucleotides and nucleotide-mimetic derivatives in 2018.[124] Most derivatives carried either a monophosphonate residue in the 5′-position (**35**) or a sulfonylmethylphosphonate residue (**34**) as depicted in Figure 22. The substitution pattern of the adenine core was mainly the same as from previously reported AMPCP-derived CD73 inhibitors.[102–104, 116] Due to that, some compounds only vary in one substituent to already published compounds. The compounds were evaluated in an enzyme and cell-based assay and then classified into four different categories depending on their biological activity (<10 nM ++++, ≥ 10 nM < 100nM +++, ≥ 100 nM ++ <1,000 nM, ≥ 1,000 nM +).[124]
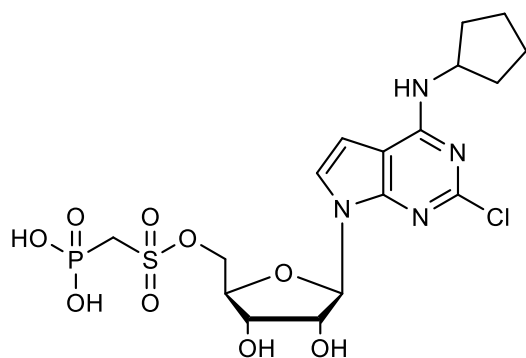
IC$_{50}$ human CD73 Cell-Based assay <10 nM
IC$_{50}$ human CD73 Enzyme assay <10 nM

34, Ex. 154, WO 2018/183635
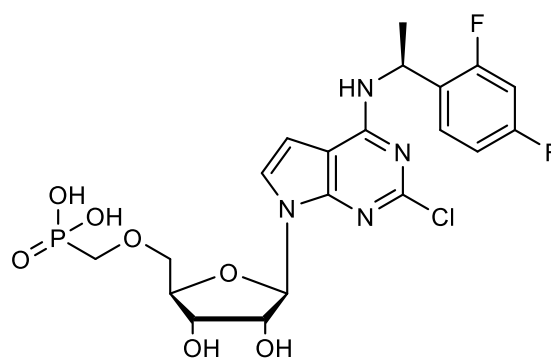
IC$_{50}$ human CD73 Cell-Based assay <10 nM
IC$_{50}$ human CD73 Enzyme assay <10 nM

35, Ex. 144, WO 2018/183635

Figure 22. Examples of disclosed compounds (**34**, **35**) by Peloton Therapeutics. [124]

1.3.3 Non-nucleotide CD73 inhibitors

Besides nucleotide-derived CD73 inhibitors, also CD73 inhibitors with different non-nucleotidic scaffolds have been targeted. These will be discussed in the following chapter. Already in 2010, Baqi & Müller *et al.* reported a series of anthraquinone-derived CD73 inhibitors.[125] Based on the anthraquinone dye *acid blue*, which was found to inhibit rat CD73 at a concentration of 15.2 µM, a series of 4-substituted anthraquinone derivatives was synthesized. Substitution of position 2 with a sulfonate moiety was essential to keep the inhibitory potency (**36**). Position 4 was derivatized with various aromatic rings, whereas 2-carboxy, 4-fluorophenyl (**37**) and 2-anthracenyl (**38**) substitution led to the most potent compounds from this series with a potency of 0.15 µM and 0.26 µM (see Figure 23), respectively, at rat sCD73.[125] Human CD73 was not tested.
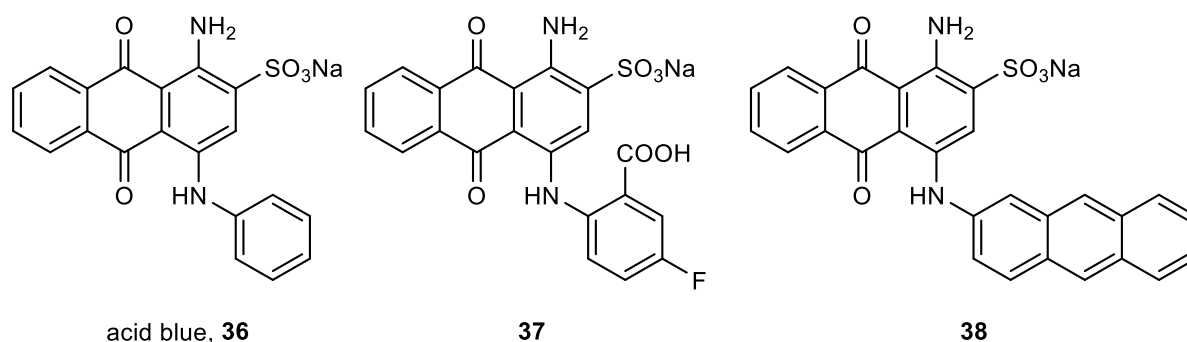
Figure 23. 4-Substituted anthraquinone-derived CD73 inhibitors (36-38).[29]

An older publication of 2007 by Braganhol *et al.* describes quercetin, a flavonoid (39) with reported multi-target bioactivtiy,[126] as inhibitor of CD73.[127] The determined IC_{50} value for inhibition of CD73, expressed in the human U138MG glioma cell line, was 45.3 µM (Figure 24). The authors also reported a reduced mRNA expression upon treatment with quercetin, which supports the hypothesis that the reduced catalytic activtiy of CD73 might be caused by down-regulation of CD73 mRNA expression and therefore a reduced protein synthesis.[127] Compared with current CD73 inhibitors nowadays, the potency is pretty low, and would probably not even be considered as hit compound in a screening campaign.
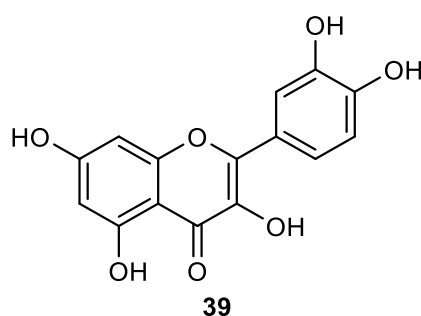
IC_{50} human CD73 = 45.3 µM

Figure 24. Quercetin (39) as inhibitor of CD73.[127]

In 2013, Iqbal *et al.* tested a series of partly commercially available and partly synthesized, mostly aromatic sulfonic acid derivatives, in order to evaluate their inhibitory potency towards

CD73.[128] The most potent compound was 6-amino-4-hydroxynaphthalene-2-sulfonic acid (**40**) also known as "Gama acid" indicating an IC_{50} value of 1.32 µM at human and 10.4 µM at rat recombinant, soluble CD73. Upon docking studies, they proposed that the sulfonic acid residue mimics the *β*-phosphonate of AMPCP binding to the Zn^{2+} ions. They also assumed that the 6-amino-group mimics the 2′- and 3′-hydroxy groups interacting with the side chain of Asp506.[128] Based on a virtual screening campaign, Ripphausen *et al.* identified out of totally 70000 candidates 51 compounds which were pharmacologically tested towards their inhibitory activity in a radiometric assay system.[129] In total, 13 of these compounds showed inhibitory activity towards CD73 with IC_{50} values between 1.90 and 74.8 µM. The most potent compound 6-chloro-2-oxo-*N*-(4-sulfamoylphenyl)-2*H*-chromene-3-carboxylic acid amide (**41**) is depicted in Figure 25, and revealed an IC_{50} value of 1.90 µM, which equals a K_i value 1.58 µM (**36**). Determination of the binding mode of this compound indicated a competitive binding mode.[129]

"Gama acid", **40**
IC_{50} human sCD73 = 1.32 µM
IC_{50} rat sCD73 = 10.4 µM

41
IC_{50} human sCD73 = 1.90 µM
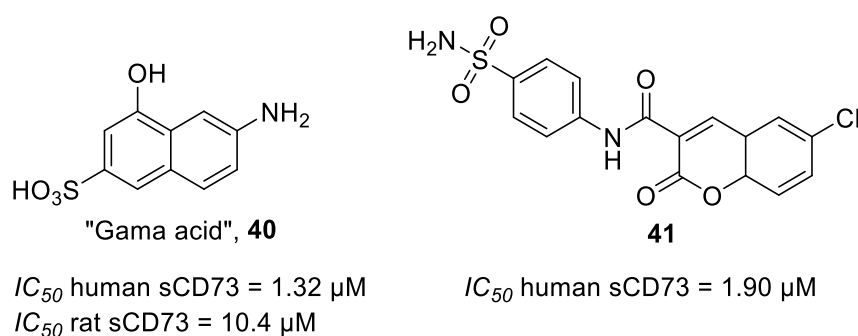
Figure 25. 6-Amino-4-hydroxynaphtalene-2-sulfonic acid (**40**) and 6-chloro-2-oxo-*N*-(4-sulfamoylphenyl)-2*H*-chromene-3-carboxylic acid amide (**41**).[128, 129]

Among the group of non-nucleotide CD73 inhibitors, the group around Lyu *et al.* published a phelligridin-based CD73 inhibitor (SMI366, **42**) with a comparably moderate inhibitory potency of 6.72 µM.[130] SMI366 did not inhibit CD39, however it would be interesting to see, how it interacts with other *ecto*-enzymes or purinergic receptors, since it carries several catechole and enone groups that are commonly known as pan-assay interference compounds

(PAINS).[131, 132] The binding mode for the phelligridin–derived SMI366 is predicted as competitive. In contrast to that, Rahimova *et al.* followed a bioinformatics approach in order to identify new *allosteric*, small-molecule CD73 inhibitors.[133] After selection of a hydrophobic cavity at the junction of the two *C*-terminal domains, they carried out a screening of 324,400 compounds consisting of five representative conformers of the cavity. The hit compounds had in common that they had branched bulky, aromatic substituents pointing in three different directions, and thus exploited the chemical space. The virtual screening hits were then validated in an assay system. The strongest inhibition was induced by RR3 (**43**) (see Figure 26). Kinetic experiments indicated a non-competitive inhibition mode for RR3 (**43**) and further compounds (not depicted), and the measured K_i-value in recombinant, human soluble CD73 expressed in insect cells was 0.53 μM, which was to our knowledge at that time the most potent, non-nucleotide CD73 inhibitor.[133]

SMI366, **42**
K_i human sCD73 = 6.72 μM

RR3, **43**
K_i human sCD73 = 0.53 μM
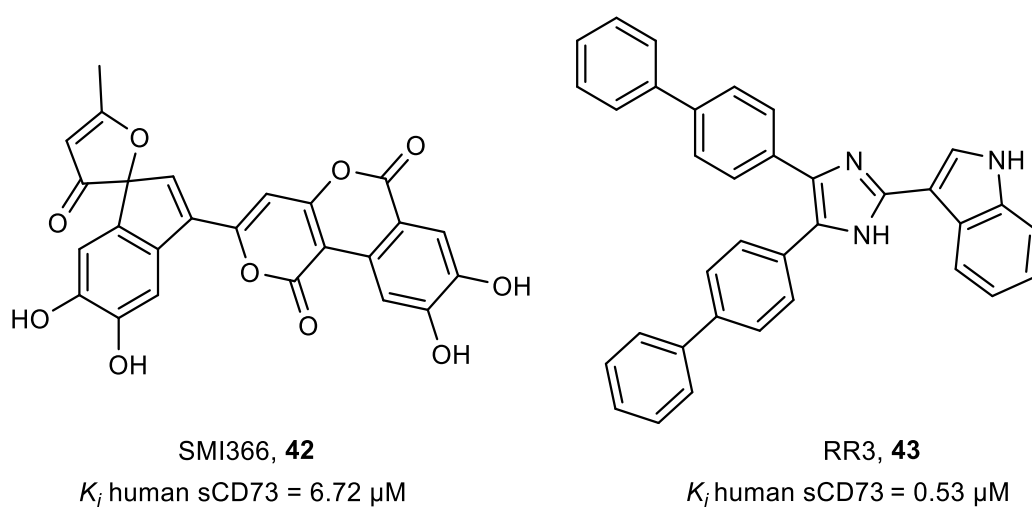
Figure 26. Non-nucleotide CD73 inhibitors **42** and **43**. [130, 133]

In 2020, Beatty *et al.* published the most potent non-nucleotide small molecule inhibitors so far.[134] A high-throughput screening campaign of a library containing more than 200000 compounds led to A00001999 (**44**) as a candidate for further optimization (see Figure 27,

hCD73 IC_{50} = 15.6 µM).[134] Besides enhancement of the potency towards CD73, enhancement of the poor metabolic stability of A00001999 was a target. Gradual optimization of the different cores of the lead structure eventually led to the most potent compounds **45** and **46** from this campaign with IC_{50} values of 12 nM and 19 nM, respectively (see Figure 27). Co-crystal structure analysis revealed binding at the active site of CD73. Incorporation of a benzimidazole moiety also substantially improved the metabolic stability.[134] These compounds are of particular interest since they do not possess a diphosphonate residue and thus no negative charge at physiological pH, which might impede membrane-permeability and bioavailability.

A00001999, **44**
IC_{50} cellular hCD73 assay = 15.6 µM

Ex 73, **45**
IC_{50} cellular hCD73 assay = 12 nM

Ex. 74, **46**
IC_{50} cellular hCD73 assay = 19 nM
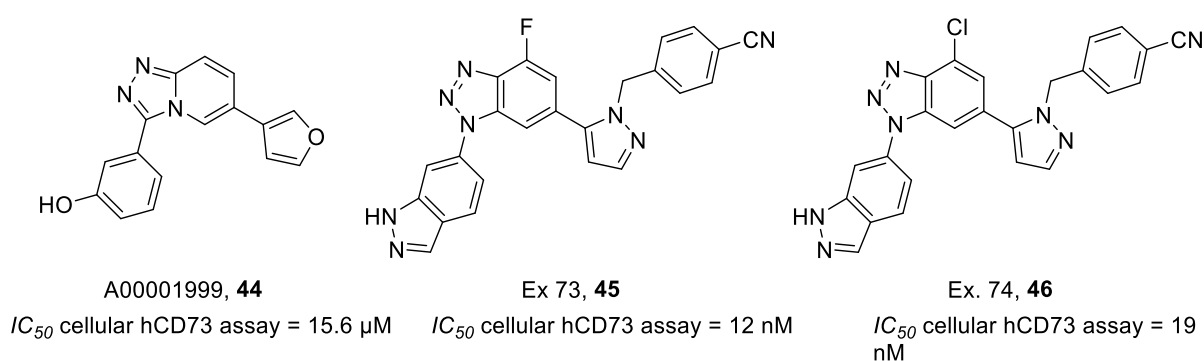
Figure 27. Non-nucleotide small molecule inhibitors (**44**-**46**) reported by Beatty *et al*.[134]

In 2017, GlaxoSmithKline (GSK) claimed a patent for in total 187 variously substituted benzothiadiazine derivatives as inhibitors of CD73.[135] The compounds were claimed for therapeutic application of various diseases like cancer, AIDS, and Parkinson's disease. The most potent compound of the claimed series is depicted in Figure 28 (**47**) and showed a quite decent potency with 16 nM.[135] In 2019, Eli Lilly and company filed a patent, in which they claimed small molecule inhibitors with potency in the low nanomolar range. The claimed compounds consist of a variously substituted pyridazinyl ring that is coupled to a pyrimidinedione ring. The compounds from this series show a comparably low molecular weight (<300 Da). The depicted compound **6** (LY3475070) is a representative compound out

of 30 examples, which all exhibit an *IC$_{50}$* value below 0.062 µM.[136] As already mentioned in chapter 1.2.2.3.3, LY3475070 (**6**) by Eli Lilly and Company is currently being evaluated in clinical trials phase 1.[63]
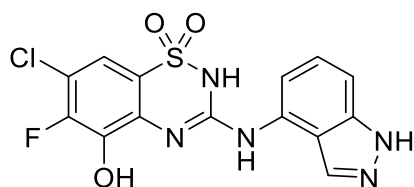
IC$_{50}$ hCD73 = 0.016 µM   *IC$_{50}$* hCD73 = 0.028 µM

47, Ex. 168, WO2017/098421   **6,** Ex. 4, WO2019/168744, LY3475070
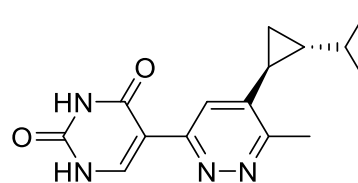
Figure 28. Patented compounds by GSK and Eli Lilly [136]

1.4   Conclusion

In the last decade, the research on CD73 inhibitors has been strongly driven forward by academia and lateron as well in industry. Numerous clincal studies that have been initiated in the recent years and that are currently ongoing, document the high relevance of the CD73-associated therapeutic approach. Especially the presence of small-molecule-derived drugs in clincial studies (besides monoclonal antibodies) indicates that the development of these compounds has gone in the right direction. For sure, the discovery of *N*-benzyl-susbtituted AMPCP derivates can be seen as a milestone in the development of CD73 inhibitors, since their discovery and advancement concerning potency, chemical stability, metabolic stability dramatacially enhanced their potential to become a future drug. Large parts of subsequent industrial and academical research is based on these findings. With regard to the fact that a modified *N*-benzyl-substituted AMPCP derivative is now being tested in clincal studies, concerns regarding drugability, and/or stability can - from today's view - be considered as

unfounded. It is exciting to see, in which direction future research on CD73 in general but especially in the discovery and development of small-molecule-derived CD73 inhibitors will go. Until now, there are only few potent, non-nucleotidic CD73 inhibitors. The same applies for allosteric CD73 inhibitors.

2 Results and discussion

2.1 AMPCP derivatives

Aim of the project

Our group initiated and has strongly driven forward the research on AMPCP-derived CD73 inhibitors.[102, 104 103, 137] With exceptionally potent inhibitors already published, it appears nearly impossible to further enhance the potency of the compounds. However, one aim was to further enhance the potency of these inhibitors e.g. by combining beneficial N^6-substituents, with optimal C2-substituents. We furthermore aimed to broaden the spectrum of substituents in the C2-position of the purine ring with further halogen substituents. By that, we wanted to explore if a substituent with a larger atomic radius might have a stronger interaction with amino acids in the C2-pocket of CD73. Another important aim was to study potential species differences (human – rat – mouse) of potent CD73 inhibitors. This information is important with regard to preclinical studies. In Figure 29, several modifications of AMPCP-derived CD73 inhibitors are depicted. Besides enhancing potency, we aimed to synthesize selective and metabolically stable compounds. We were also interested in developing a method that allows the fast re-synthesis of small amounts of the desired AMPCP derivatives. For some reaction steps, there was still

room for improvement in terms of yield, reaction time and efficiency. Therefore, we modified

different reaction parameters to optimize the reaction conditions.
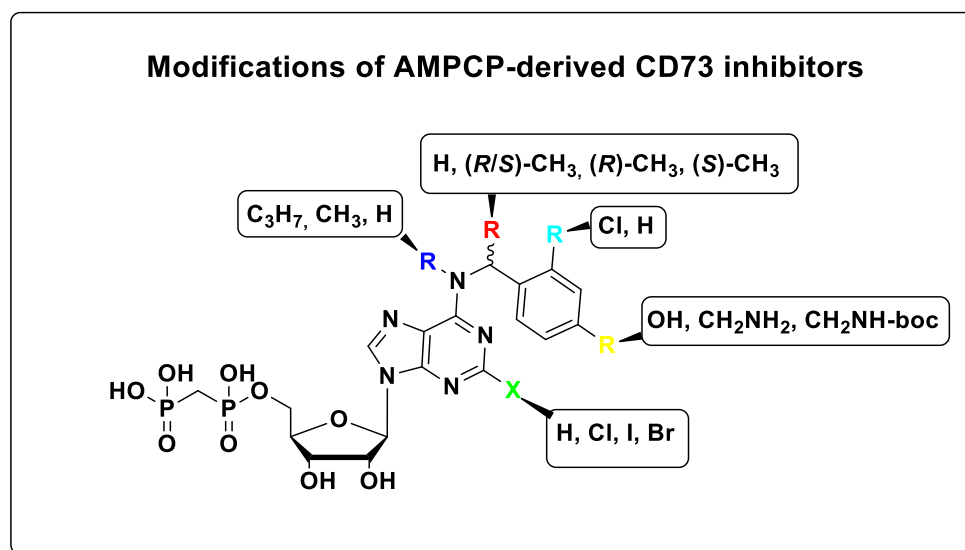
Figure 29. Planned modifications of AMPCP-derived CD73 inhibitiors

2.1.1 Chemistry

2.1.1.1 2-Chloro-AMPCP derivatives

2.1.1.1.1 Design

2-Chloro-substituted AMPCP derivatives have been evaluated in published and unpublished

work from our group, and they were found to provide the so far most potent AMPCP

derivatives, several compounds having K_i-values in the low picomolar range.[69, 102–104, 109–111, 113]

However, there was still room for further exploration of structure-activity relationship and also

for improvement of the potency.

We have observed that many of the AMPCP derivatives carry a branched methyl group in the

α-position of the N^6-benzyl substituent (see Figure 30, red substituent).[109] However, most data

are limited to the diastereomeric mixture of the R and S isomers. We therefore aimed to

37

investigate if one isomer has an advantage over the other. Initial data from Bhattarai *et al.* indicated no difference between both isomers determined at rat CD73. Unfortunately, the compounds were no longer available. We therefore resynthesized both compounds, and tested them on different species (rat and human soluble CD73, human membrane-bound). We furthermore synthesized compounds **53d** and **53e**, which carry an additional N^6-methyl group, which has the advantage that the corresponding nucleoside, which might be formed by degradation is not an AR agonist.[112] We aimed to confirm stereochemical observations obtained by compounds **53a** and **53b** which did not carry the additional methyl group (see Figure 30). Compound **53f** combines all substituents that are beneficial for the potency of AMPCP derivatives. In addition to that, we resynthesized PSB-12651 and PSB-12489 for collaboration projects and used the synthesis to optimize the reaction conditions and/or to vary the synthetic route.
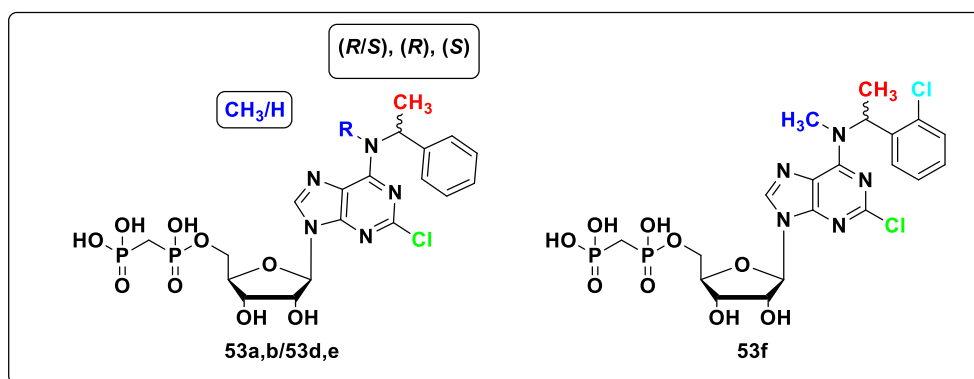
Figure 30. Investigation of stereochemical properties of *R* and *S*-configurated AMPCP derivatives.

2.1.1.1.2 Synthesis

The 2-chloro-AMPCP derivatives were synthesized according to the following synthetic route. The first step was the synthesis of 2,6-dichloro-9-(2′,3′,5′-tri-*O*-acetyl-*β*-D-ribofuranosyl)-9*H*-purine (**50**), which displays the central precursor molecule for all 2-chloro-substituted AMPCP

derivatives. For the glycosylation of 2,6-dichloropurine (**49**) with the fully acetyl-protected sugar **48**, a hybrid of the fusion method and the silyl Hilbert-Johnson reaction was employed. [138, 139] Using this method, both reagents were melted at a temperature of 108 °C, trifluoromethanesulfonic acid was added and a slight vacuum was applied. Surprisingly, liquid chromatography–mass spectrometry (LC)-MS and nuclear magnetic resonance (NMR) analysis indicated the formation of an isomeric mixture of the α- and β-conformation of the formed nucleoside. This is actually untypical and stands in contrast to the so-called Baker-1,2-trans-rule. According to Baker, the neighbouring oxygen of the 2-acyloxy group captures the carbocation which is formed after the acetyl group in C1 is cleaved (Scheme 1, step 1). By that, an acyloxonium ion is formed on the lower face of the sugar, which allows stereochemical control of the following nucleophilic substitution in the subsequent step to give the naturally occurring β-anomer (see Scheme 1, step 2).[140]

Scheme 1. Preferred formation of the *β*-nucleoside according to the 1,2-trans-Baker-rule taken and modified from [140]
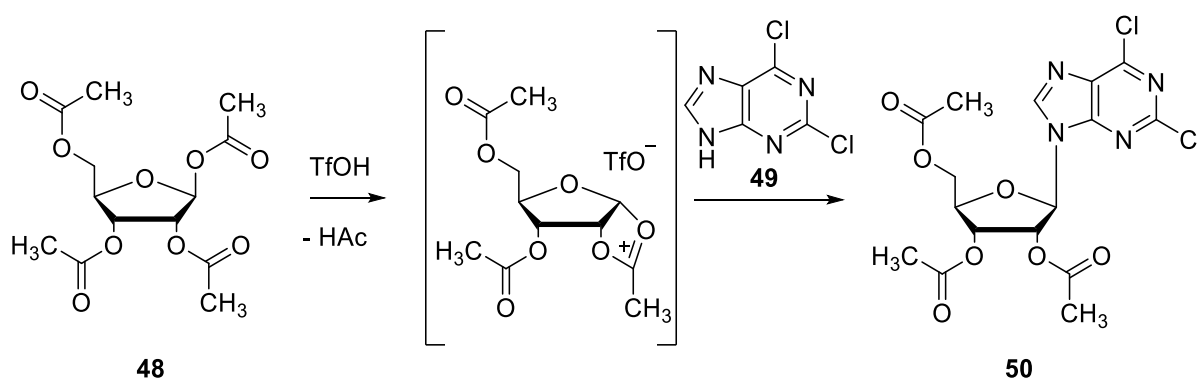
Thorough purification by normal phase column chromatography eventually led to the isolation of the desired β-anomeric nucleoside, which was confirmed by LC-MS and NMR analysis. An ^{1}H-NMR spectrum is depicted in Figure 31. However, it was not possible to me to obtain the

pure compound by recrystallization out of ethanol as Dr. Constanze Schmies had described in her PhD thesis. [141]
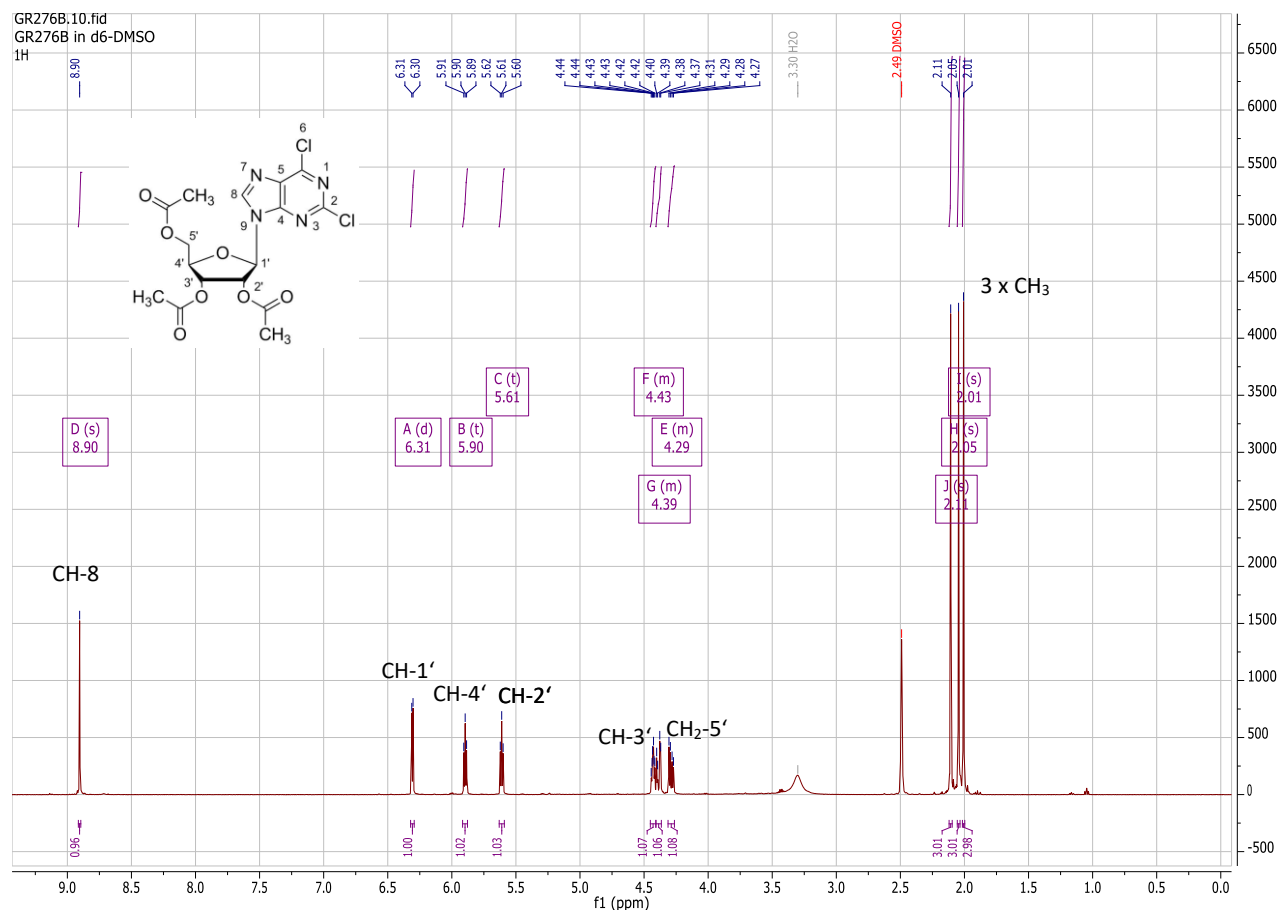
Figure 31. ^{1}H-NMR spectrum of 2,6-dichloro-9-(2′,3′,5′-tri-*O*-acetyl-*β*-D-ribo-furanosyl)-9*H*-purine **50**.

Interesting is also the comparison of the lability of the 6-chloro group with that of the 2-chloro group. Whereas the 6-chloro substituent is easy to cleave and to substitute with many different nucleophiles, the 2-chloro group is stable (see Figure 32). In all performed reactions in which the 6-chloro residue was substituted, no substitution of the 2-chloro group was observed, although various reaction conditions were employed (including temperatures around 90 °C, basic conditions, and up to 24 h reaction time).
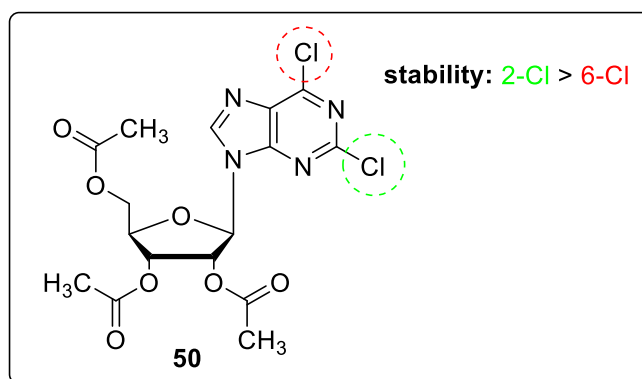
Figure 32. Stability of chloro substituents in position 2 and 6. The stable 2-chloro atom is circled in green, the 6-chloro atom is circeled in red.

In the next reaction step, the chloro substituent in position 6 was substituted with benzylamine, *N*-methylbenzylamine, or 1-methylbenzylamine, respectively. The derivatives are depicted in Table 1. Triethylamine was used as a base and ethanol as a solvent. The reaction mixture was refluxed for 3 h at 90 °C according to optimized, previously reported conditions.[102, 103] Details of the optimization procedure of this reaction are described in chapter 2.1.1.5. The progress of the reaction was monitored by frequent thin-layer chromatography (TLC) analysis. TLC-MS analysis indicated the formation of the desired products (**51a-g**), but also the already partially and fully deacetylated derivatives. Since the fully deacetylated products **52a-g** were the desired products of the next reaction step, the crude reaction mixture was evaporated. The remaining crude product was dissolved in methanol, and reacted with 7 N ammonia in methanol without prior purification. The reaction mixture was stirred overnight and subsequently purified by normal phase column chromatography dichloromethane (DCM)/methanol to give the desired deacetylated nucleoside derivatives **52a-g**. In the last step, compounds **52a-g** were then phosphonylated according to the common phosphonylation conditions.[102, 103, 141] The nucleoside was dissolved in trimethyl phosphate under cooling in an ice bath. Then, a solution of methylenbis(phosphonic dichloride) in trimethyl phosphate was slowly added to the reaction mixture which was then stirred for one hour at 0 – 4 °C. The reaction was then quenched with triethylammonium hydrogencarbonate (TEAC) buffer and extracted with 2 x 300 ml of *tert-*

butylmethyl ether (TBME). The aqueous phase was partially evaporated, frozen in liquid nitrogen and then lyophilized overnight. The resulting white solid was dissolved in water containing 0.05% trifluoroacetic acid (TFA), and purified via reversed-phase high performance liquid chromatography (RP-HPLC) (Scheme 2). The structures of the synthesized final nucleotide analogs **53a-g** were confirmed by ^{1}H, ^{13}C and ^{31}P NMR spectroscopy, additionally to liquid chromatography-electrospray ionization-mass spectrometry coupled to a UV-detector (LC/ESI-(UV)MS). UV absorption measurement confirmed a purity of higher than 95% (for examples, see Figure 33).

Scheme 2. Synthesis of **53a-g**[a]
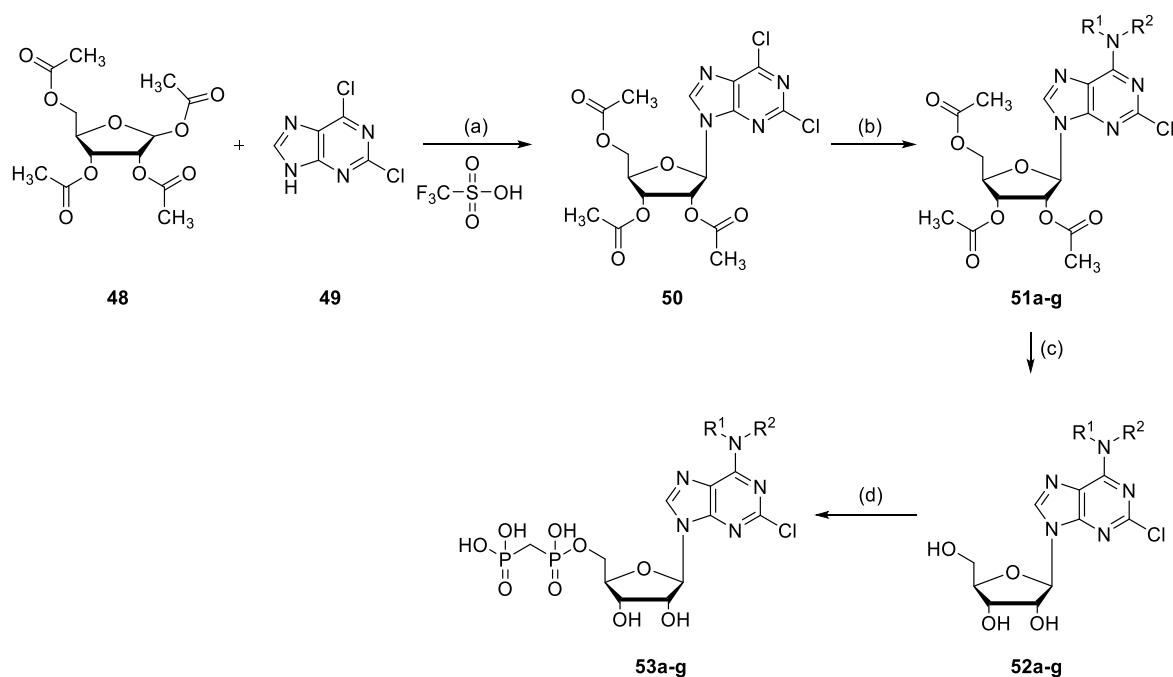
[a]Reagents and conditions: a) 90000 Pa (0.9 bar), 108 °C, 1 h; b) *N,N*-diar(alk)ylamine; or *N*-monoar(alk)ylamine, triethylamine, ethanol, 90 °C, 8 h; c) 7 N ammonia in methanol, methanol, rt, overnight d) two steps: i) methylenbis(phosphonic dichloride), trimethyl phosphate, 0-4 °C, 1 h. ii) 1 M, TEAC buffer ph 7.4-7.6, rt, 1 h.

Table 1. Substituents of 2-chloro-AMPCP derivatives (**14**, **51**-**53a-f**)

Compd.	R^1	R^2
a*	H	(*R*)-1-Methylbenzyl
b*	H	(*S*)-1-Methylbenzyl
c (PSB-12651)*	H	Benzyl
d	CH$_3$	(*R*)-1-Methylbenzyl
e	CH$_3$	(*S*)-1-Methylbenzyl
f	CH$_3$	1-(2-Chlorphenyl)ethyl
14 (PSB-12489)*	CH$_3$	Benzyl

*resynthesis
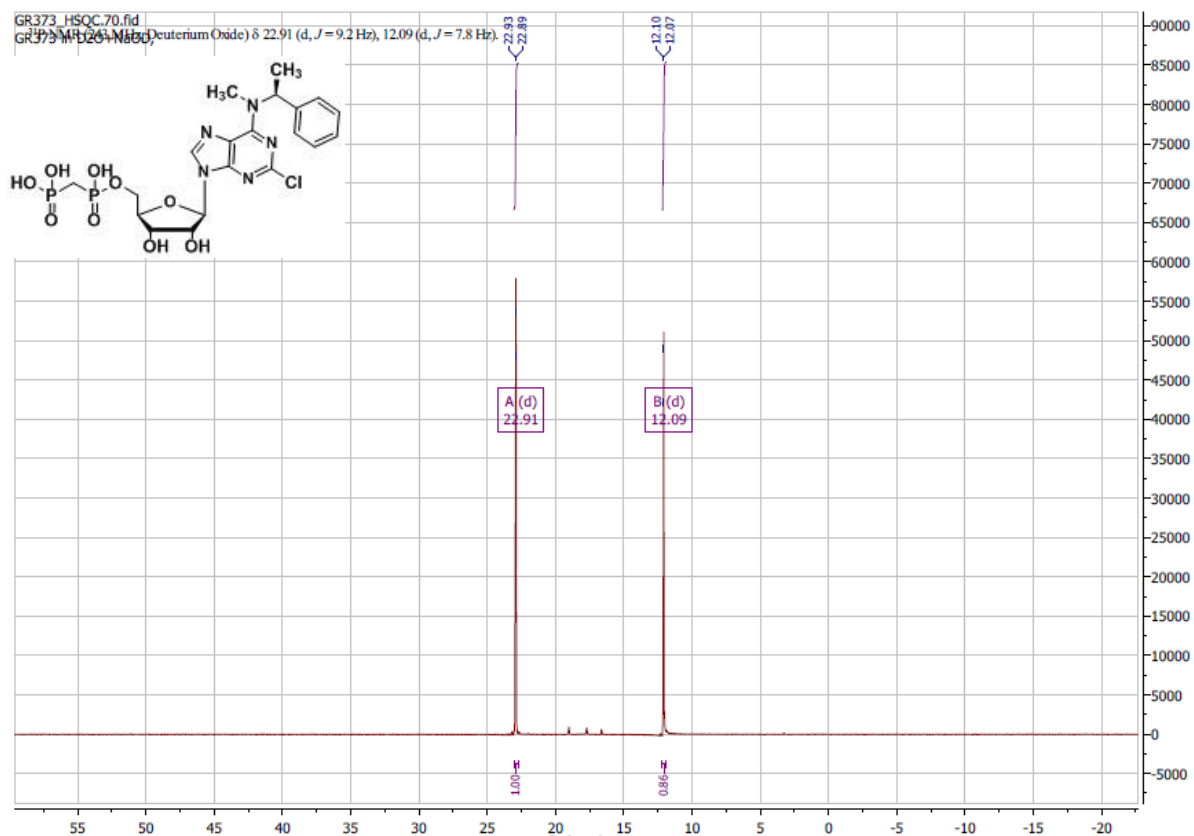
Figure 33. ^{31}P-NMR spectrum of **53e** (12.09 ppm = P$_\alpha$, 22.91 ppm = P$_\beta$).

2.1.1.2   2-Bromo-AMPCP derivatives

2.1.1.2.1   Design

As already mentioned in chapter 2.1.1.1, 2-chloro-AMPCP derivatives have been broadly pharmacologically evaluated,[102–104, 109] but 2-bromo-AMPCP derivatives have not yet been synthesized and pharmacologically evaluated to the best of my knowledge. To this end we had to establish an efficient and straightforward synthetic route. This route could later on serve for the synthesis of further compounds, e.g. combination with various substituents in the N^6-position.

2.1.1.2.2   Synthesis

The synthesis was started from commercially available 2-amino-6-chloro-9-(β-D-ribofuranosyl)-9H-purine (**54**, Scheme 3). The 2-amino group was reacted by a non-aqueous

diazotization reaction using *tert*-butyl nitrite (TBN) and trimethylsilylbromo silane (TMSBr) in analogy to Francom *et al.* [142, 143] Interestingly, the first attempt of this reaction led to a mixture of the 2-chloro- and 2-bromo substituted compounds **55** and **58** (Figure 34). This is quite surprising, since CH_2Br_2 was used as a solvent to avoid this. However, after the reaction was assumed to be completed, the extraction of the aqueous phase was carried out with DCM, and probably during this step, 2-Cl-substituted **58** was formed. By changing the extraction solvent to ethyl acetate, this issue could be fixed in the next attempt. Generally, this reaction was reported for 2′-, 3′-and 5′-protected nucleosides, but apart from the described issue, which is most-likely not related to the protection groups, it worked straightforward for the non-protected nucleoside. The desired compound **55** was obtained in 30% yield. The following reactions steps were similar to those described for the 2-chloro- and the 2-iodo-AMPCP derivatives. The 6-position was substituted by *N*-methyl-1-methylbenzylamine under reflux, in basic conditions, for 3 h.[102, 103] The desired compound **56** was purified by normal phase column chromatography. LC-MS analysis indicated also demethylation of the N^6-amino group, however only to a minor extent (6%). The following step was the phosphonylation reaction according to the the common conditions followed by hydrolsis using aqueous TEAC buffer.[102–104, 141.]Extraction with TBME, followed by RP-HPLC purification led to the desired product **57**.

Scheme 3. Synthesis of **57**[a]
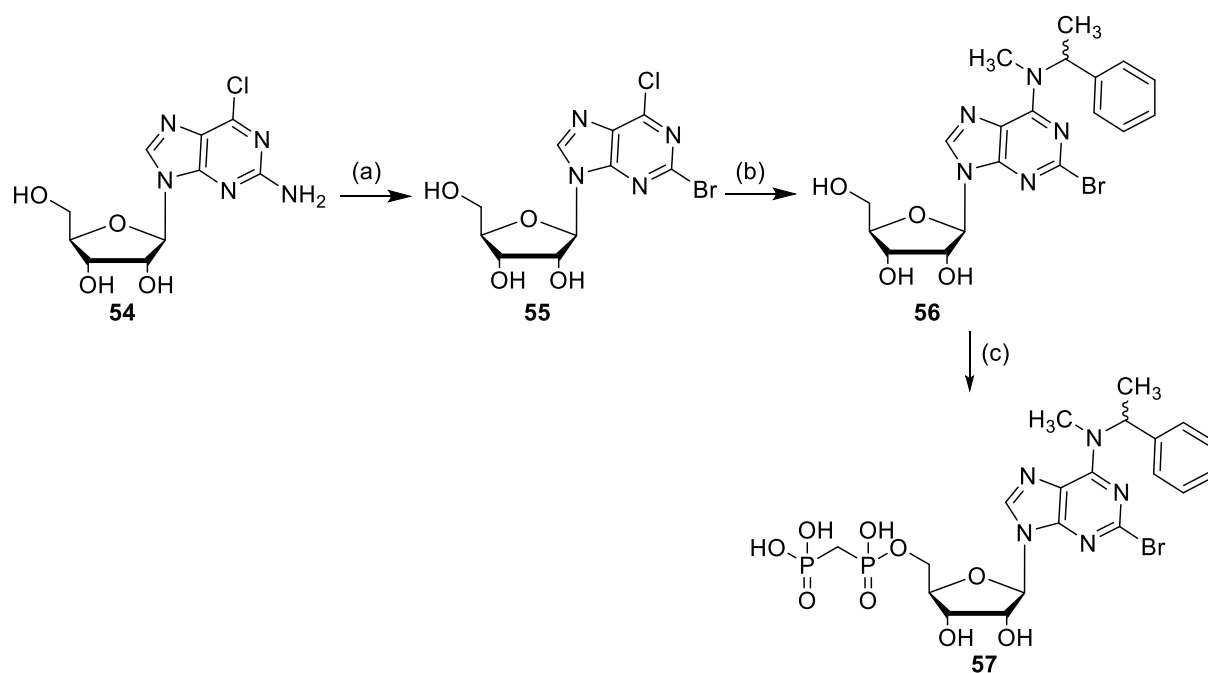
[a]Reagents and conditions: (a) TMSBr, TBN, CH$_2$Br$_2$, rt, overnight; (b) *N*-methyl-1-methylbenzylamine, triethylamine, ethanol, 90 °C, 3 h; (c) two steps: i) methylenbis(phosphonic dichloride), trimethyl phosphate, 0-4 °C, 1 h; ii) 1 M, TEAC buffer pH 7.4-7.6, rt, 1 h.
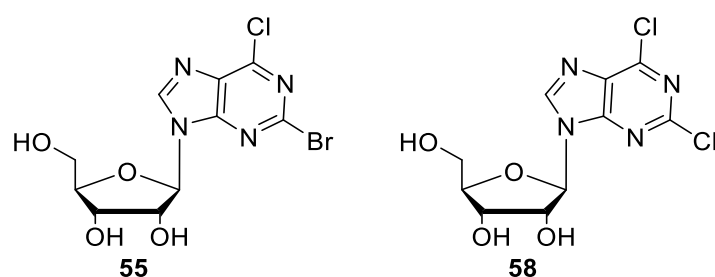
Figure 34. 2-Bromo-6-chloro-9-(β-D-ribofuranosyl)-9*H*-purine **55**, and 2,6-dichloro-9-(β-D-ribofuranosyl)-9*H*-purine **58**, which was formed as undesired side product during the synthesis of **55**.

2.1.1.3 2-Iodo-AMPCP derivatives

2.1.1.3.1 Design

Besides 2-chloro and 2-bromo-AMPCP derivatives, we also aimed to synthesize 2-iodo-AMPCP derivatives to probe the size of the respective binding pocket of CD73. First published as well as unpublished data by our group were already promising, as e.g. 2-I-AMPCP has been found to be 25-fold more potent than unsubstituted AMPCP at human CD73.[104] Therefore, we designed and synthesized a small series of AMPCP derivatives, carrying N^6-substitutents that had been shown to be most beneficial for CD73 inhibitory activity.

2.1.1.3.2 Synthesis

The synthesis of **62a-c** was started from commercially available 6-chloro-2-iodo-9-(2′,3′,5′-tri-*O*-acetyl-*β*-D-ribofuranosyl)purine (**59**), which was submitted to nucleophilic substitution with the corresponding *N,N*-diar(alk)ylamine; or *N*-monoar(alk)ylamine (the substituents are depicted in Table 2) by refluxing it in ethanol in the presence of triethylamine (Scheme 4). The reaction worked straightforward affording **60a-c**. As described in chapter 2.1.1.1.2., the nucleosides **60a-c** were partially deacetylated under the applied reaction conditions. Therefore, instead of purifying the crude reaction mixture, the solvent was evaporated, and the crude mixture was directly deprotected by stirring it with 7 N ammonia in methanol at room temperature. The deprotected nucleosides **61a-c** were then reacted with methylene(bisphosphonic dichloride) in trimethylphosphate for 1 h at 0 °C, followed by subsequent quenching with aqueous TEAC buffer and stirring for another hour at room temperature.[102] The reaction mixture was extracted with TBME and the aqueous phase was lyophilized. Purification by RP-HPLC gave the desired pure products **62a-c** (Scheme 4). The structures of the synthesized final nucleotide compounds **62a-c** were confirmed by ^{1}H, ^{13}C and ^{31}P NMR spectroscopy, additionally to LC/ESI-(UV)MS. UV absorption measurement confirmed a purity of higher than 95%.

Scheme 4. Synthesis of 2-I-AMPCP derivatives **62a-c**[a]
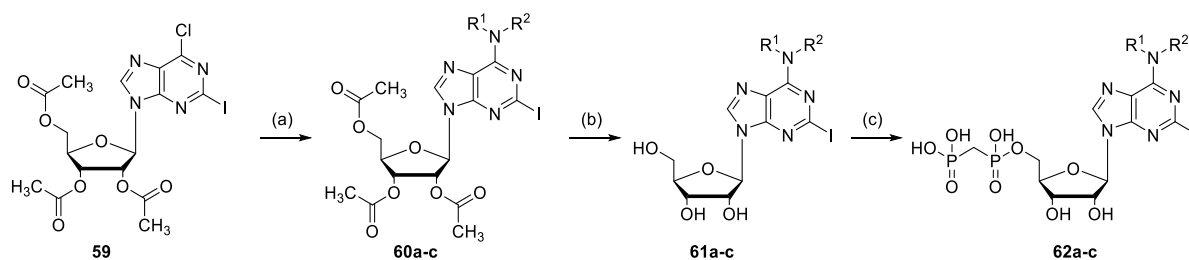
[a]Reagents and conditions: (a) *N,N*-diaralkylamine, triethylamin, ethanol, 90 °C, 3 h; (b) 7 N ammonia in methanol, methanol, rt, overnight; (c) i) methylenbis(phosphonic dichloride), trimethyl phosphate, 0-4 °C, 1h; ii) 1 M, TEAC buffer ph 7.4-7.6, rt, 1 h.

Table 2. N^6-substitution of 2-iodo-AMPCP derivatives (62a-c)

Compd.	R^1	R^2
62a	CH_3	2-Chlorobenzyl
62b	CH_3	1-Methylbenzyl
62c	CH_3	1-(2-Chlorophenyl)ethyl

2.1.1.4 Synthesis of mono-methylated benzylamine precursors

A structural motif that many of the AMPCP-derived CD73 inhibitors share is an *N*-methylated-benzylamine or methylbenzylamine residue. Since precursors are either not commercially available, or not affordable, an effective and selective synthetic route for these derivatives was developed. The first attempts for the methylation of the 2-chlorobenzylamine derivatives **63a,b** were carried out according to conditions described by Lebleu *et al.*[144] Selective monomethylation of primary amines is quite difficult, as monomethylation favors further methylation due to the increased nucleophilicity.[145] The authors Lebleu *et al.* therefore propose the very polar organic solvent 1,1,1,3,3,3-hexafluoro-2-propanole (HFIP) aiming to decrease

the nucleophilicity of the amine by its proton-donating abilities.[146] By that, formation of overalkylated side- products is to be avoided.[144] However, when methylation of **63a** using methyl triflate in HFIP was carried out, overalkylated side products **65a** and **66a** were formed besides the desired product **64a** (Scheme 5). This might be due to the fact that the reaction was carried out too long. By extraction with ethyl acetate, the quaternary ammonium derivative **66a** was removed from the reaction mixture. Since only the monomethylated derivative **64a** was able to participate in the subsequent nucleophilic substitution reaction, the obtained mixture of **64a** and **65a** was used for further synthesis. The dimethylated derivative **65a** would not react because of the lack of a hydrogen on the nitrogen atom, and could thus be eliminated from the reaction mixture in a further purification step. Compound **64b** was synthesized in a similar fashion (Scheme 5). However, the yield of the desired monomethylated product **64b** was much higher. According to LC-MS analysis, 70% of the formed product was the desired compound **64b**.

Scheme 5. Methylation of 2-chlorobenzylamine derivatives[a]
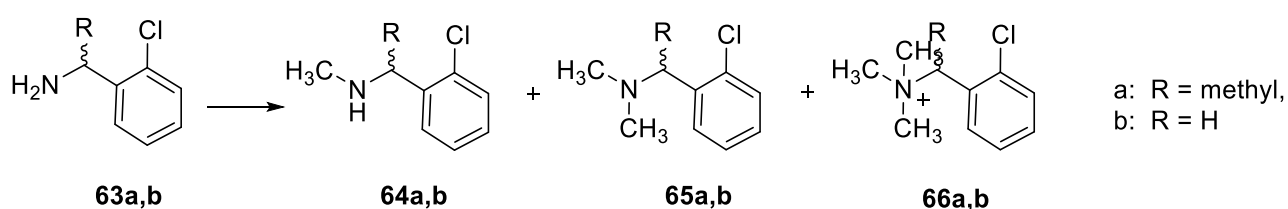
[a]Reagents and conditions: MeOTf, HFIP, rt, 1h.

However, due to the comparably high amount of side products and the high toxicity/cancerogenocity of methyl triflate,[147] an alternative synthetic route was employed. In order to circumvent the formation of side products, the benzylamine derivative was not directly methylated. The synthesis was divided into two steps. In the first step, 1-(2-chorphenyl)ethan-1-amine (**63a**) was acylated by stirring it at 80 °C in formamide for 24 h without the use of a

solvent following a modified, previously published method.[148] After 24 h, the reaction was cooled down to room temperature, and LiAlH$_4$ was carefully added to the crude reaction mixture, which was then stirred for 1 hour at room temperature. Then, the reaction temperature was raised to reflux for another hour. After completion of the reaction was indicated by TLC, the reaction was quenched by addition of water, 1 N sodium hydroxide and again water in a sequence. The crude mixture was extracted with DCM, and the organic phase was purified by normal phase column chromatography. Appropriate fractions were pooled and evaporated to give the desired product **64a** as a yellow oil (Scheme 6). Although direct methylation appears to be more straightforward, this alternative synthesis route is more effective due to almost no side product formation. With a yield of almost 70% over two reaction steps, it is well suitable for the selective monomethylation of benzylamine derivatives. Another advantage is the avoidance of the reagent methyl triflate, which is indeed a potent methylation agent, but due to that also highly cancerogenic.[144, 147] After successful establishment of this synthetic route, it was implemented in the master project of Jianyu Hou, who synthesized and purified compound **64b** under the supervision of the author.[149]

Scheme 6. Methylation by transamidation followed by reduction to yield **64a,b**[a]

63a,b   **67a,b**   **64a,b**
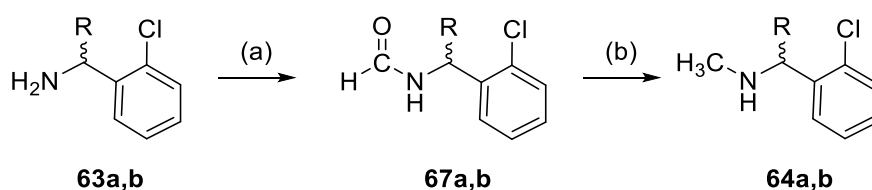
[a]Reagents and conditions: (a) Formamide, 80 °C, 24 h, (b) LiAlH$_4$, THF, rt – 1h, then 80 °C – 1 h.

2.1.1.5 Resynthesis/upscaling of 70 – optimization of nucleophilic substitution

For the preparation of a manuscript and additional pharmacological studies,[109] compound **70** needed to be resynthesized. In the framework of this study, the reaction conditions of the nucleophilic aromatic substitution were optimized (Scheme 7, step: a). Especially the reaction

time was dramatically reduced, while keeping the yield of the reaction at the same level as before. Bhattarai *et al.* stirred the reaction for 24 h at 60 °C, [102, 103] a procedure, which we intended to optimize. Since the reaction is carried out at a basic pH-value, we assumed that the nucleoside, and especially the glycosidic bond would be stable, even at higher reaction temperatures. We therefore increased the reaction temperature to 90 °C and shortened the reaction time to 3 h. After completion of the reaction, purification by normal phase column chromatography employing DCM/methanol (94:6) yielded the desired nucleoside **69**. The next reaction step was the phosphonylation of the 5′-position, which was carried out according to the commonly used reaction conditions to yield **70**. The improved reaction conditions were successfully applied to all similarly carried out reactions.

Scheme 7. Synthesis of **70**[a]
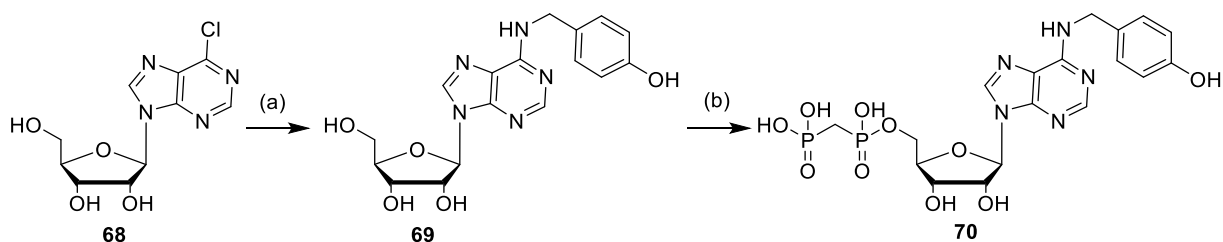
[a]Reagents and conditions: a) 4-hydroxybenzylamine, triethylamine, ethanol, 90 °C, 3 h; b) two steps: i) methylenbis(phosphonic dichloride), trimethyl phosphate, 0-4 °C, 1 h. ii) 1 M, TEAC buffer pH 7.4-7.6, rt, 1 h.

2.1.1.6 Alternative synthetic route for the preparation of PSB-12379 (13)

For a (re-)synthesis of PSB-12379 (**13**), the common synthetic route was varied. From Schmies *et al.*,[141] we know that 6-chloro-AMPCP derivatives are stable under basic conditions, even under reflux for longer reaction times. Therefore, we swapped the reaction steps. Now, the non-substituted 6-chloro-9-(β-D-ribofuranosyl)-9*H*-purine (**68**) was phosphonylated first, which led to compound **71**. After that, the 6-chloro-position of the nucleotide analog **71** was substituted with benzylamine, which afforded **13** (Scheme 8). This synthetic route is a viable alternative, if larger amounts of the precursor **71** are in stock, and only a small amount of the final product

is required. This is the case, when, for example, quick resynthesis of a compound is required and a high yield of the synthesized product is of minor interest. However, due to the polar character of the diphosphonate residue, time consuming RP-HPLC purification is required twice. It is thus advisable to synthesize larger amounts of the precursor **71**, and to derivatize it then with the corresponding primary or secondary amine.

Scheme 8. Alternative synthesic route to prepare PSB-12379 (**13**)[a]
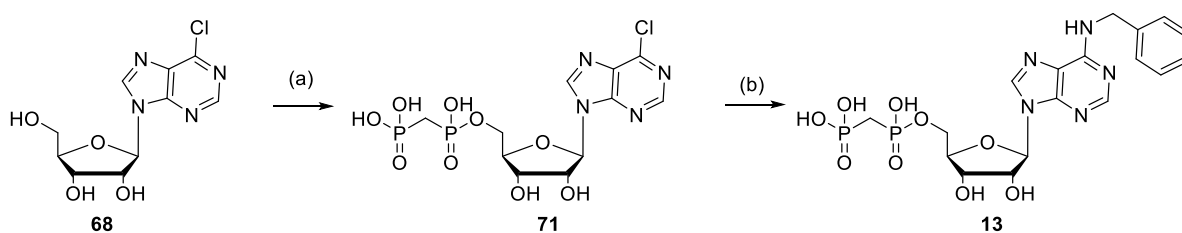
[a]Reagents and conditions: (a) two steps: i) methylenbis(phosphonic dichloride), trimethyl phosphate, 0-4 °C, 1h; ii) 1 M, TEAC buffer ph 7.4-7.6, rt, 1 h; (b) benzylamine, triethylamine, ethanol, 90 °C, 3 h.

2.1.2 Pharmacology

The pharmacological evaluation of the synthesized compounds was carried out by Riham Idris, Katharina Sylvester and Jessica Nagel. The inhibition of CD73 by the synthesized compounds was tested in a radiometric assay system using [³H]AMP as a substrate.[70] In this assay, the radioactively labeled substrate AMP and the test compound are incubated with CD73. After incubation, the remaining substrate [³H]AMP as well as the reaction product inorganic phosphate [P] are precipitated with lanthanum chloride, and then removed via filtration. The enzymatic reaction product [³H]adenosine stays in solution and is collected and transferred to scintillation vials. After addition of scintillation cocktail, the product is quantified via scintillation counting. We employed different CD73 preparations, including rat and human soluble CD73 expressed in *Spodoptera frugiperda* (*Sf9*) insect cells, as well as membrane

preparations of human triplenegative breast cancer cells (MDA-MB-231), which natively express CD73.[121] Full concentration-inhibition curves were determined and K_i values were calculated from the obtained IC_{50} values using the Cheng-Prusoff equation (Table 3).[150]

Table 3. Pharmacological evaluation of AMPCP derivatives[a]

Compd.	R^1	R^2	R^3	Human soluble CD73 $K_i \pm$ SEM (nM)	Human CD73 in MDA-MB-231 cancer cells $K_i \pm$ SEM (nM)	Rat soluble CD73 $K_i \pm$ SEM (nM)
72, AMPCP (II)[102]	H	H	H	**88.4** $\pm$ 4.0	**207** $\pm$ 6.0	**197** $\pm$ 5
14, PSB-12489[103,*]	benzyl	methyl	chloro	**0.318** $\pm$ 0.020	**1.28** $\pm$ 0.016	**0.746** $\pm$ 0.246
13, PSB-12379[102,*]	benzyl	H	H	2.21 $\pm$ 0.40	**n.d.**	9.03 $\pm$ 1.24
70*	4-hydroxybenzyl	H	H	**1.16** $\pm$ 0.095	**n.d.**	**9.06** $\pm$ 1.45
73, PSB-14650[109]	1-methylbenzyl	H	chloro	**0.0692** $\pm$ 0.0055	**0.0633** $\pm$ 0.0074	**1.20** $\pm$ 0.04

53c, PSB-12651[103],*	benzyl	H	chloro	0.134 ± 0.019	n.d.	1.23 ± 0.04
53a	(S)-1-methylbenzyl	H	chloro	0.0172 ± 0.0034	n.d.	0.525 ± 0.100
53b	(R)-1-methylbenzyl	H	chloro	0.168 ± 0.049	n.d.	0.485 ± 0.062
16, PSB-18231[141]	1-methylbenzyl	methyl	chloro	0.150 ± 0.035	0.0320 ± 0.0046	0.388 ± 0.095
53e	(S)-1-methylbenzyl	methyl	chloro	0.0522 ± 0.0126	n.d.	0.879 ± 0.095
53d	(R)-1-methylbenzyl	methyl	chloro	3.60 ± 1.32	n.d.	0.388 ± 0.016
74[109]	2-chlorobenzyl	methyl	chloro	0.0559 ± 0.0018	0.0641 ± 0.0055	2.96 ± 2.27
53f	1-(2-chlorophenyl)ethyl	methyl	chloro	0.0746 ± 0.0239	n.d.	0.815 ± 0.212
62c	1-(2-chlorophenyl)ethyl	methyl	iodo	1.77 ± 0.36	n.d.	5.35 ± 1.71
75[109]	benzyl	H	iodo	0.159 ± 0.019	0.236 ± 0.056	1.53 ± 0.24
62a	2-chlorobenzyl	methyl	iodo	0.0502 ± 0.0161	n.d.	0.432 ±0.262
62b	1-methylbenzyl	methyl	iodo	0.156 ± 0.019	n.d.	1.02 ± 0.27

76[109]	benzyl	methyl	iodo	**0.151 ±** 0.018	**0.171 ±** 0.019	**2.22 ±** 0.11
57	1-methylbenzyl	methyl	bromo	**0.0859 ±** 0.0365	**n.d.**	**0.519 ±** 0.206

[a][^{3}H]AMP (5 µM) was used a substrate; K_m value 59 µM, 17 µM and 14.8 µM respectively for purified recombinant soluble rat CD73, purified recombinant soluble human CD73, and native membrane-anchored human CD73 (in MDA-MB-231 cell membrane preparations). **n.d.** – not determined. The results at recombinat rat enzymes are also included here for comparison. *resynthesis

___

2.1.3   Structure-activity relationships

AMPCP (**72**), **73**, **16**, **75** and **76** were not synthesized, but are included in Table 3 for better comparison.[102, 103] Compound **70** has already been reported by the co-worker Dr. Sanjay Bhattarai.[109, 111] It was resynthesized, since there were only rat CD73 data available, but no data from human CD73. Similar to the publication of Bhattarai *et al.* from 2015,[102] the compound showed slight enhancement at human as compared to rat CD73 (rat: K_i = 9.06 nM and human: 1.16 nM). The inhibitory activity in both species is almost the same as for PSB12379 (**13**) indicating that a polar hydroxyl group in the para-position of the N^6-benzyl group is well tolerated by the binding pocket. Compounds **53a** and **53b** had already been reported,[109, 111] but only rat data were available and no compound was left. For that reason, the compounds were resynthesized, and the pharmacological evaluation was completely repeated (including already existing rat data). Interestingly, both compounds were generally 2-fold more active than in the experiments before on the rat enzyme. Besides that, we observed a diastereomeric selectivity between the *S* (**53a**) and the *R* (**53b**) isomer at soluble human CD73. We measured a 10-fold activity difference between the *S*-isomer and the *R*-isomer (0.0172 nM vs. 0.168 nM). With a

K_i-value of 17 pM, the compound is in the same range as the AB680 from Arcus Biosciences.[110, 113] The inhibitory activity of the isomeric mixture of both compounds was very much between both measured values (0.069 nM, **73**, PSB-14650), which is quite consistent, although the *R/S* ratio of the exact isomeric mixture is unknown. In order to further explore the diasteroselectivity of human CD73, we synthesized the N^6-methylated compounds **53e** and **53d**. Again, we observed a difference between the *S*- and the *R*-isomer, which was now almost 70-fold at human CD73 (0.052 vs. 3.6 nM). The N^6-methylated *S*-isomer **53e** was in a similar range as the non-methylated *S*-isomer **53a** with the additional advantage that its nucleoside derivative can be expected to be inactive at ARs, due to the *N*-methylation.[112] The measured K_i-value of 0.150 nM for **16** - the diastereomeric mixture of both compounds - is consistent with the the data of the pure isomers.

Compound **53f** unifies all substitutions that have been shown to be beneficial for the potency of AMPCP derivatives. With a potency of 0.0746 nM it is slightly less active at human soluble CD73 than the previously mentioned compounds, but still in the same range. This indicated that the substituents in the different positions are interdependent. Comparing 2-substituted AMPCP derivatives with unsubstituted AMPCP derivatives, we can confirm that substitution of the two position strongly enhances the potency, which is consistent with prior results. [104]

Besides 2-chloro-substituted AMPCP derivatives, also several 2-I-AMPCP derivatives were synthesized. Analyzing a 2019 published crystal structure of PSB-12489,[103] it becomes evident that the chloro-substituent is positioned for an interaction with the NH group of N390 in the binding pocket (see Figure 35).[103] However, the carbonyl group of N390 is too far away to form halogen bonding with the chloro substituent. By increasing the molecular radius of the substituent in position 2 (by introducing bromo or iodo substituents), we aimed to explore if this halogen bonding could be formed with larger halogen substituents and thus enhance the potency.
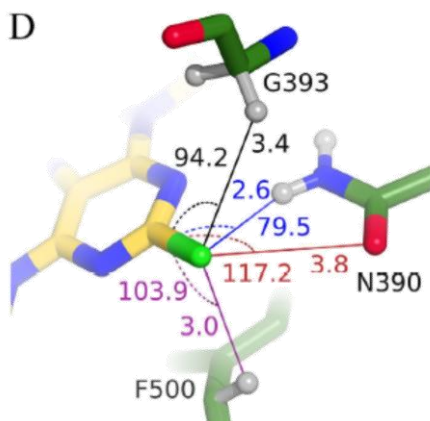
Figure 35. Close-up of the C2-binding pocket of a co-crystal of CD73 with PSB-12489. Interaction of the 2-chloro-substituent with the NH-group of N390. Depicted are also the distances between 2-chloro-substitutents and further amino acids in the binding pocket. Distances (in A) and angles (°) are indicated. Figure is taken from [103]

Besides two previously synthesized 2-I-AMPCP derivatives (**75**, **76**), three more 2-iodo-AMPCP derivatives were synthesized to further explore differences between different halogen substituents in position 2. For the N^6-substitution, we chose those substituents that had been proven to be most beneficial for potency, to especially compare 2-chloro- and 2-iodo-AMPCP derivatives with each other. Remarkable was the difference of **53f** and **62d**. Both compounds combine all substitutions in N^6 (methyl group, 2-chlorophenyl(ethyl)) which were beneficial for the potency of the 2-chloro-AMPCP derivatives. However, the 2-chloro-AMPCP derivative **53f** was 7-fold more potent in rat and a 24-fold more potent in human soluble CD73 than the 2-iodo derivative **62c**. Such a large difference in potency was, however, not representative for the whole series. The (*R*/*S*)-1-methylbenzyl-substituted derivative **62b** had a high potency of 0.156 nM and was virtually as potent its 2-chloro analog **16**. The most potent 2-iodo-AMPCP derivative at human soluble CD73 was the N^6-methyl-2-chlorobenzyl-substituted derivative **62a** (K_i = 0.0502 nM), which was as potent as its 2-chloro-analog **74** (K_i = 0.064 nM) and thus in the range of the most potent inhibitors from this series. It can be concluded, that a 2-iodo-

substitution does not enhance the potency in comparison to the 2-chloro substitution, but it also doesn't necessarily impair it. We also investigated the potency of a 2-bromo-substituted AMPCP derivative. Due to the challenging, multi-step synthesis, we decided to synthesize only one compound to get a first impression about the potency of 2-bromo-AMPCP derivatives. We synthesized N^6-methyl-N^6-1-methylbenzyl AMPCP, which showed, as all other tested 2-substituted derivatives, increased potency comparing rat (K_i = 0.519 nM) and human soluble CD73 (0.0859 nM). Compared to 2-chloro (**16**) and 2-iodo (**62b**) substituted-N^6-methyl-N^6-1-methylbenzyl AMPCP derivatives (**16**, K_i = 0.150 nM, **62b**, K_i = 0.156 nM), the 2-Br-substituted derivative **57** showed slightly increased potency at soluble human CD73 (K_i = 0.0859 nM). It could therefore be worthwile to synthesize further derivatives, in order to investigate, if this trend is also observable for other N^6-substitution patterns.

Regarding the overall results, we made another interesting observation, which had also been partly described in a previous publication.[104] Similar to 2-unsubstituted AMPCP derivatives described by Bhattarai *et al.*,[102] we observed for such compounds either no or only slight species differences between the inhibitory activity on rat and human soluble CD73. As soon as the AMPCP derivative carries a halogen substituent in position 2, large species differences between rat and human soluble CD73 emerge. Except for compound **62c**, in which the species difference between rat and human CD73 is 3-fold, all compounds have at least a species difference of 5-fold, up to 57-fold (**53a**). This phenomenon might be explained with the help of crystal structures and on a molecular biology base. With a protein sequence identity of 89%, rat and human CD73 are highly homologous.[103] There are three mutations F500Y, N499S, and L389V, of which F500 is involved in nucleobase stacking.[39, 104] N499 is involved in the formation of the so called C2-pocket, and is thus crucial for the interaction with substituents in position 2. As a consequence, 2-substituted AMPCP derivatives (Cl, I, Br) could have an increased interaction with human CD73 caused by this mutation, which could be the reason for emerging species differences. In case there is no substitution in position 2, no substituent can interact with

the mutated amino acid in this binding pocket, and thus no difference would be observed between the species.

2.1.4 Conclusion and future outlook

We synthesized a series of differently substituted AMPCP derivatives, which allowed us to further explore the structure-activity relationship of AMPCP derivatives as inhibitors of CD73. Although we could not improve the already high potency of previously synthesized compounds, we could reach the same range of potency. Moreover, we made several interesting observations: We found out that different halogen substituents do not improve, but also do not necessarily impair the potency of AMPCP, they rather lead to compounds with potencies in the same range. We furthermore found out that there is a diastereoselectivity of N^6-1-methylbenzyl-substituted AMPCP derivatives at human CD73, but not at rat CD73. This observation is new, and could be confirmed with further, slightly modified derivatives. Crystallization studies with the R and the S isomer are currently carried out by the group of Prof. Sträter (University of Leipzig). Patrick Bulambo-Riziki is currently testing selected compounds on mouse-derived breast cancer cells, which carry the same 3 mutations as the rat-derived enzyme.[151] It will thus be interesting whether the described diastereoselectivity will also be observed on mouse CD73. The experiments are currently being carried out. It may furthermore be worthwhile to synthesize more 2-bromo-substituted derivatives, since so far only a single compound with this substituent has been studied. In comparison to its 2-chloro and 2-iodo analogs, it showed slightly enhanced potency on human soluble CD73.

2.2 N^6-Propargyl-AMPCP derivatives

2.2.1 Design

In order to explore further AMPCP-derived inhibitors of CD73, we aimed to replace the commonly used N^6-benzyl/N^6-methylbenzyl-substitution[102, 103, 111] with other smaller

substituents while keeping high inhibitory potency. In addition to that, we intended to synthesize compounds that are easily functionalizable, have a feasible synthesis and show strong inhibitory potency towards CD73. For this purpose, terminal alkyne groups are of great interest, since they can easily be functionalized applying azide-alkyne Huisgen cycloaddition conditions (Scheme 9). Applying this method, a huge variety of functions could be conjugated to the highly potent ligand, as e.g. fluorescent dyes, siRNA, proteolysis targeting chmiera (PROTAC) building blocks, antibodies and nanobodies, etc.[137, 152, 153] We therefore introduced a propargyl and a butynyl residue in the N^6-position, as well as a 4-ethynylbenzylamine residue, that carries the alkynyl group in position 4. After successful completion of the synthesis, we tested the inhibitory potency towards human recombinant soluble CD73. Furthermore, the metabolic stability of one representative compound was tested.

Scheme 9. Proposed functionalizations of terminal alkyne residues
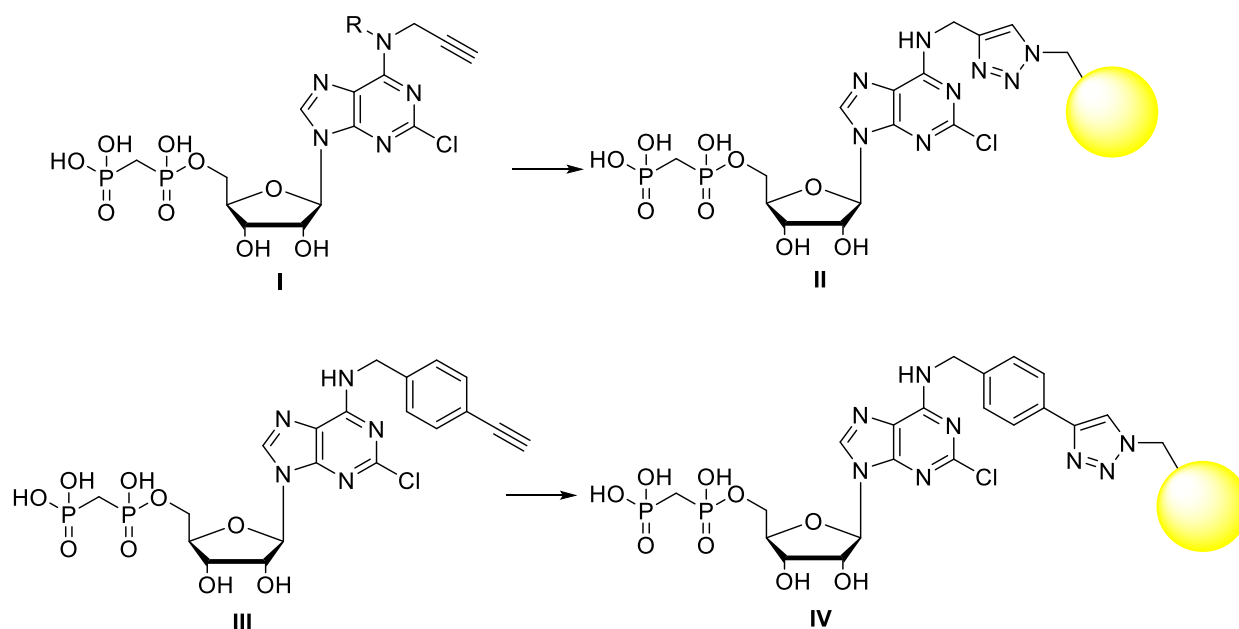
2.2.2 Chemistry

2.2.2.1 Synthesis of N^6-propargyl substituted AMPCP 78

The synthesis is depicted in Scheme **10** and was started from 6-chloro-9-(β-D-ribofuranosyl)-9*H*-purine (**68**) which was reacted with propargyl amine under basic conditions and under reflux.[102] Purification by normal phase column chromatography gave the desired product **77**. Nucleoside **77** was then phosphonylated using methylenebis(phosphonic dichloride) in trimethyl phosphate followed by hydrolyzis using aqueous TEAC buffer.[102–104] Purification by RP-HPLC gave product **78** (Scheme 10).

Scheme 10. Synthesis of N^6-propargyl substituted AMPCP **78**[a]
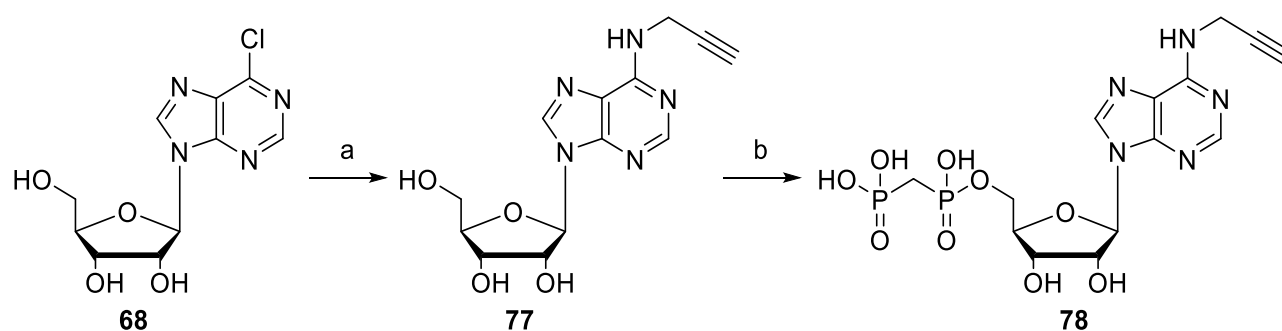
[a]Reagents and conditions: (a) propargylamine, triethylamine, ethanol, 90 °C, 8 h; c) 7N ammonia in methanol, methanol, rt, overnight, d) two steps: i) methylenbis(phosphonic dichloride), trimethyl phosphate, 0-4 °C, 1 h. ii) 1 M, TEAC buffer pH 7.4-7.6, rt, 1 h.

2.2.2.2 Synthesis of 2-Cl-N^6-alkynyle substituted AMPCP derivatives 81a-c.

The first reaction step was a glycosylation of 2,6-dichloro purine (**49**) employing the fusion method to give nucleoside **50**.[103, 138, 141] Compound **50** was then reacted with the corresponding propargylamine derivative using basic conditions under reflux at 90 °C. Compounds **79a-c** were obtained, besides partially deacetylated side-products. Since the next reaction step was a deprotection of the acetyl groups, **79a-c** were not isolated. Instead, the crude mixture containing **79a-c** was deprotected using 7N ammonia in methanol. Normal phase column chromatography yielded the nucleosides **80a-c**, which were then phosphonylated with methylenebis(phosphonic dichloride) in trimethyl phosphate and subsequently hydrolyzed with aqueous TEAC buffer according to a previously published method.[102–104] RP-HPLC purification yielded the desired products **81a-c** (see Scheme 11). A ^{31}P-NMR spectrum, which shows the signals of the diphosphonate moiety and documents the absence of further side products is depicted in Figure 36.

Scheme 11. Synthesis of 2-Cl-N^6-alkynyle substituted AMPCP derivatives **81a-c**[a]

Compd.	R^1	R^2
a	H	Propargyl
b	Methyl	Propargyl
c	H	But-3-ynyl
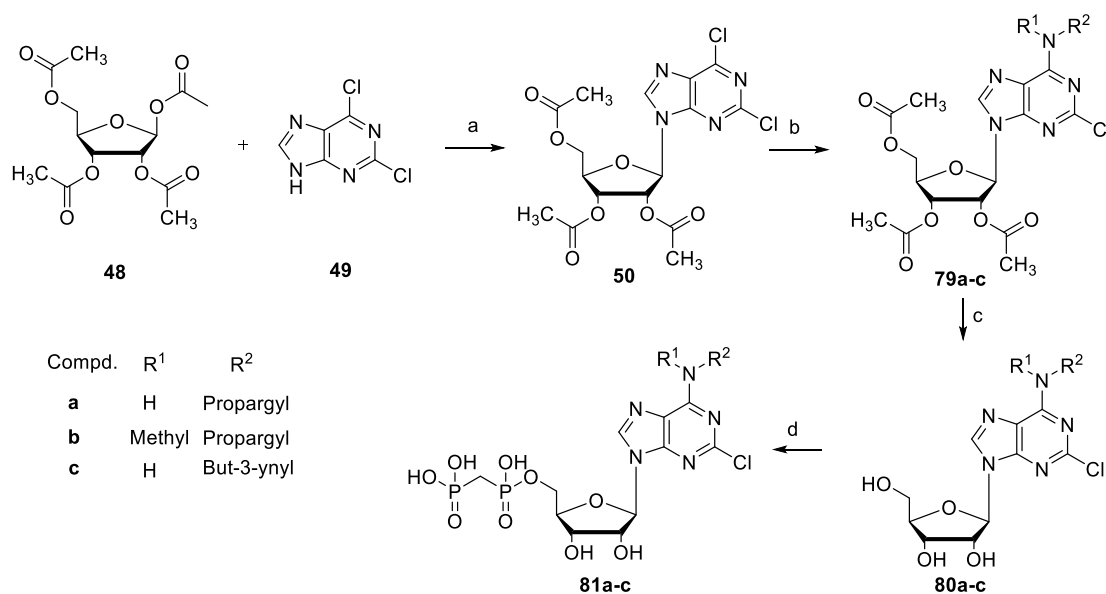
[a]Reagents and conditions: (a) 90,000 Pa (0.9 bar), 108 °C, 1 h; (b) appropriate propargylamine derivative, triethylamine, ethanol, 90 °C, 8 h; c) 7 N ammonia in methanol, methanol, rt,

overnight; d) two steps: i) methylenbis(phosphonic dichloride), trimethyl phosphate, 0-4 °C, 1 h; ii) 1 M, TEAC buffer ph 7.4-7.6, rt, 1 h.
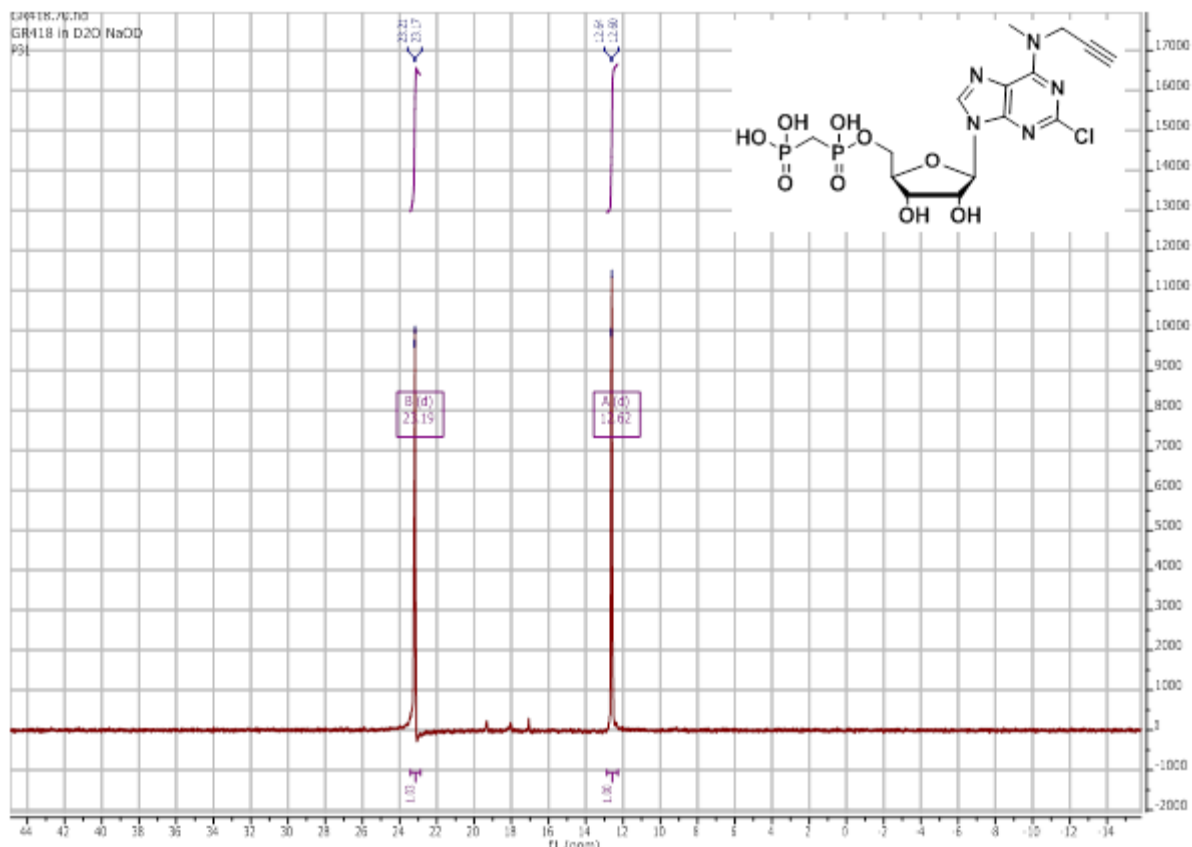
Figure 36. ^{31}P-NMR spectrum of **81b** recorded in D$_2$O and NaOD and measured at 243 MHz. (12.62 ppm = P$_\alpha$, 22.19 ppm = P$_\beta$).

2.2.2.3 Synthesis of N^6-4-ethynylbenzylamine AMPCP 83

For the synthesis of **83**, which is depicted in Scheme 12, a different synthetic approach was employed (see Scheme 12). The synthesis was started from commercially available 2,6-dichloro-9-(2′,3′,5′-tri-O-acetyl-β-D-ribofuranosyl)purine (**58**). The nucleoside was directly phosphonylated using methylenbis(phosphonic dichloride) in trimethyl phosphate, followed by subsequent hydrolysis with aqueous TEAC buffer.[102–104] Although **82** was purified by RP-

63

HPLC, it could only be obtained in a purity of 80%. However, since the next reaction step required further RP-HPLC purification, and the remaining side products would not interfere with the next reaction step, **82** was used without further purification. Next, the 6-chloro position was substituted with an excess of 4-ethynylbenzylamine according to optimized, previously reported conditions.[102, 103] Interestingly, although higher reaction temperatures (90°C) and basic conditions were applied over 3 h, no degradation of the phosphonylated product **83** was observed. Neither the glycosidic bond, nor the phosphonic ester bond showed any tendency to be cleaved. Purification by RP-HPLC gave the desired product **83**. The structure of the synthesized compounds was confirmed by ^{1}H, ^{13}C and ^{31}P NMR as well as LC/ESI-(UV)MS in positive mode confirming a purity of greater than 95% for all pharmacologically tested compounds.

Scheme 12. Synthesis of N^6-4-ethynylbenzylamine AMPCP **83**[a]
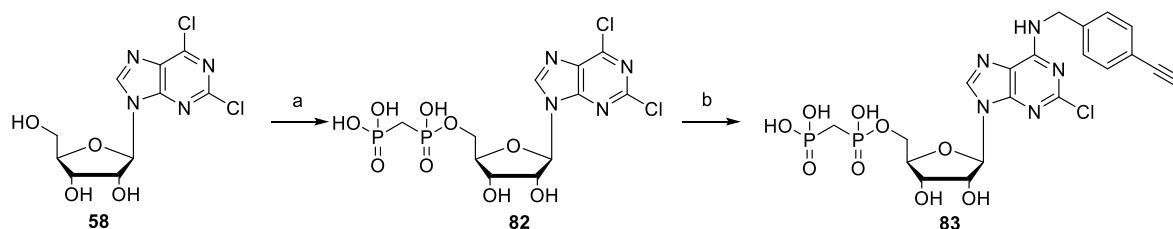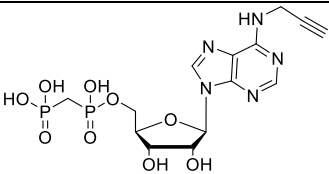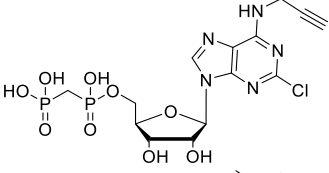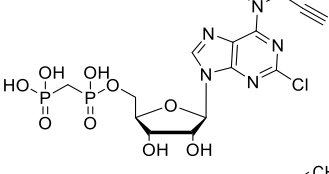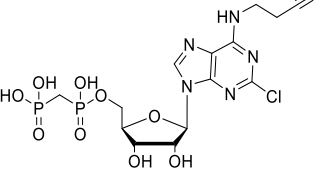
[a]Reagents and conditions: (a) two steps: i) methylenbis(phosphonic dichloride), trimethyl phosphate, 0-4 °C, 1 h. ii) 1 M, TEAC buffer ph 7.4-7.6, rt, 1 h; (b) 4-ethynylbenzylamine , triethylamin, ethanol, 90 °C, 3 h.

2.2.3 Pharmacology and structure-activity relationships

The inhibitory potency of **78**, **81a-c** and **83** was investigated on recombinant human soluble CD73 expressed in *Sf9* insect cells. Full concentration-inhibition curves were determined, and K_i values were calculated from the obtained IC_{50} values using the Cheng−Prusoff equation.[150] The inhibitory potency of **78** was already surprisingly strong (K_i = 0.894 nM, see Table 4),

although it did not carry a halogen substituent in position 2 and only a small propargyl residue in N^6. The potency was further improved by introducing a chloro-substituent in position 2 (**81a**). This is well in accordance with previously reported findings.[103] Since a second substitution at N^6 was expected to further improve the potency,[103] we also introduced an additional methyl group at N^6. However, this led to a 10-fold reduction of the potency (**81b**, see Table 4). Therefore, we omitted the disubstitution of N^6 for further compounds. Since the most potent AMPCP-derived CD73 inhibitors carry an N^6-benzylamino-substitution, [102–104, 113] we also synthesized an N^6-benzylated derivative which carries an ethynyl substitutent in position 4 of the phenyle ring. That led to a 3-fold improvement in comparison to **81a**, and thus to the most potent compound from this series **83** (Table 4). We furthermore elongated the N^6-alkynyle chain by one methylene unit (**81c**), which led to virtually the same potency as the most potent, N^6-benzylated compound **83** (**81c**, $K_i = 0.387$ nM). Compound **81c** was synthesized under my supervision by my Master student Jianyu Hou.[149]

Table 4. Inhibitory potencies of the synthesized compounds **78**, **81a-c** and **83**[a]

Compd.	Structure	Human soluble CD73 $K_i \pm \text{SEM}^a$ (nM)
78		**0.894** ± 0.175
81a		**0.573** ± 0.319
81b		**5.01** ± 1,20
81c		**0.387** ± 0.153
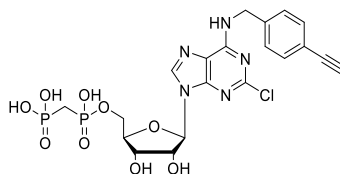
83		**0.228** ± 0.088

2.2.4 Metabolic stability

We selected propargyl derivative **81a** as representative compound for metabolic studies carried out by Pharmacelsus (Saarbrücken, Germany). The metabolic stability of compound **81a** was analyzed in human and in mouse liver microsomes. Therefore, **81a** was incubated with mouse or human liver microsomes (0.5 mg/ml, mixed gender, pooled) in a reduced nicotinamide adenine dinucleotide phosphate (NADPH) containing phosphate buffer (pH = 7.4). Degradation was determined after 0 min, 10 min, 30 min, and 60 min. Positive controls were carried out using verapamil, negative controls in an incubation medium without NADPH. Compound **81a** was found to be metabolically very stable in human liver microsomes showing a half-life of 248 min and an internal clearance of 5.6 µl/min/mg of protein Figure 37. In mouse liver microsomes a half-life of 73 min and an internal clearance of 19.0 µl/min/mg of protein was determined. Degradation that was also observed in negative controls could explain the shorter half-life in mouse liver microsomes.
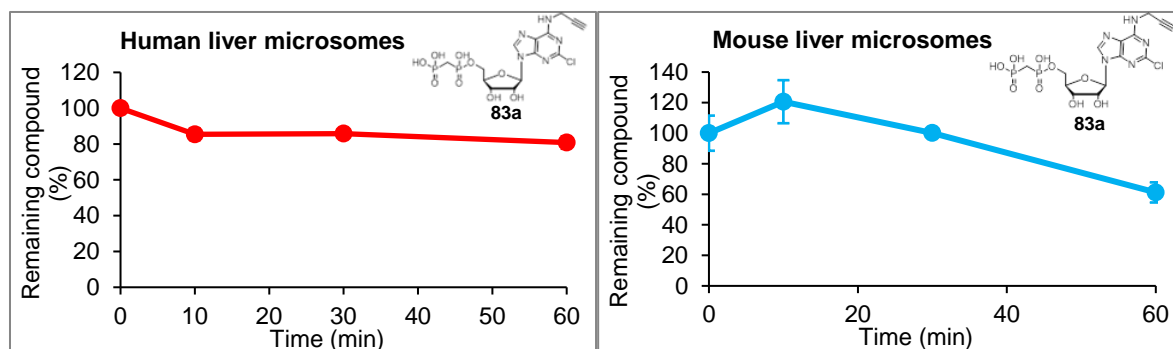
Figure 37. Metabolic stability of **81a** in human and mouse liver microsomes.

2.2.5 Conclusions and future outlook

We synthesized a small series of highly potent, metabolically stable and easily functionalizable N^6-alkynyl/N^6-alkynylbenzyle CD73 inhibitors. We could show that benzylation of the N^6-position is not necessarily required for reaching inhibitory activity in the subnanomolar range. These compounds could display promising starting points that may be employed in the synthesis of a variety of pharmacological tool compounds and probes. The next step within this project would be functionalization experiments of the triple-bond carrying AMPCP derivatives and, if the experiments are successful, first biological experiments. Further pharmacological experiments will be carried out, for determining e.g. the residence time of selected compounds.

2.3 Diagnostics and tool compounds for CD73

2.3.1 Design and synthesis of a fluorescence-labeled CD73 substrate

2.3.1.1 Design

In 2018, Lee *et al.* reported a selective and highly sensitive fluorescence assay for CD39 using fluorescein-coupled ATP as a substrate.[154] The assay showed an enhanced sensitivity compared to previous methods and was also suitable for high-throughput screening. Although already several assays for measuring the enzymatic activity of CD73 exist,[69, 70] a similar new assay could still be of interest. It is, for example, highly desirable to avoid radioactive substrates, which are expensive and accompanied with legal regulations concerning safe handling and disposal of radioactive waste. In the following chapter, the design and synthesis, as well as first biological experiments of a fluorescence-labeled CD73 substrate and its fluorescence-labeled hydrolysis product are described. With both compounds, we aimed to develop and establish a new fluorescence-based CD73 assay, which avoids the use of radioactive material and allows high sensitivity. In order to allow the best possible hydrolytic activity, we aimed to keep the

fluorescent substrate as simple and as similar as possible to AMP. The same applies for the corresponding hydrolysis product adenosine. We connected the fluorescent dye via a hexyl linker to the N^6-position of the AMP moiety, or the adenosine moiety, respectively. By that, we assumed that the bulky fluorescent dye is not directly located in the binding site, and would thus not interfere with the hydrolytic activity of the enzyme. As a fluorescent dye, we chose fluorescein, which is inexpensive and has an absorption maximum at 492 nm and an emission maximum at 517 nm.[155] A carboxylic group in position 5(6) allows easy functionalization of the fluorescent dye with e.g. a linker moiety. Figure 38 shows the targeted structure and its expected hydrolysis product by CD73 activity.
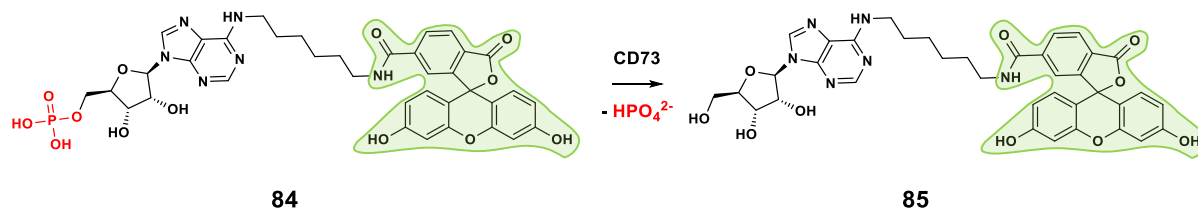
Figure 38. Enzymatic degradation of fluorescence-labeled AMP.

2.3.1.2   Chemistry

2.3.1.2.1   Synthetic route A

The originally attempted synthetic route is depicted in Scheme 14 and was started with the acetylation 2′-, 3′- and 5′- hydroxyl groups of 6-chloro-9-(β-D-ribofuranosyl)-9H-purine **68** leading to compound **86**.[156] In the next step, the protected nucleoside **86** was reacted with *N-boc*-1,6-hexanediamine under reflux and under basic conditions in ethanol (Scheme 14). Purification by normal phase column chromatography yielded the desired product **87**. Subsequently, the *boc*-protection group was cleaved using triflouoroacetic acid (TFA) in DCM and a few drops of water.[157] Again, purification employing normal phase column

chromatography yielded the desired compound **88** carrying a free primary amine. In the next step, the amino group on the hexyl linker moiety was coupled to 5(6)-carboxyfluorescein using 1-hydroxybenzotriazole (HOBt) and *N, N′*-dicyclohexylcarbodiimide (DCC).[158] We decided to use the isomeric mixture 5(6)-carboxyfluorescein for establishing the synthetic route. 5(6)-Carboxyfluorescein is more affordable than the pure isomer, and we assume that it posesses similar chemical properties. Normal phase column chromatography led to insufficient purity of (30%). However, the crude product was used for the next reaction step since we assumed that the side product wouldn't interfere with the subsequent reaction. The next reaction step was the deprotection of the sugar acetyl protection groups, carried out using 7N ammonia in methanol. After stirring overnight, the volatiles were evaporated, and the crude reaction mixture was tried to be purified by normal phase column chromatography. Repeated attempts to purify the compounds only led to a purity of 31% of **90** and a strongly reduced amount of product (Scheme 13). In order to obtain a sufficient amount of final product, we would have had to restart the synthesis from the beginning, especially since the subsequent reaction was a phosphorylation, which has usually only moderate yields.[141] Since this synthesic route became more and more elaborate, we also started an alternative synthesis pathway, which was eventually more successful and will be described in the following chapter.

Scheme 13. First synthesis pathway for compound **98**[a]
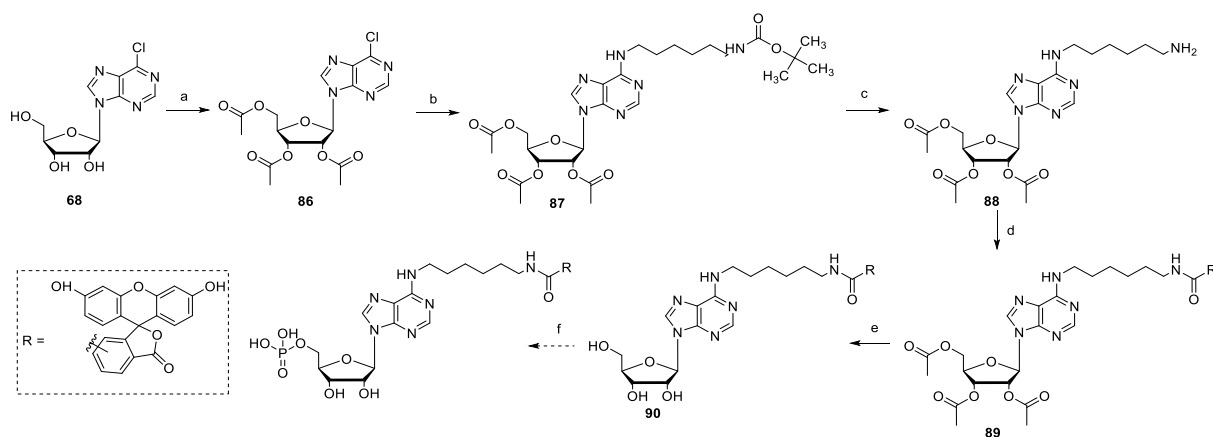
ªReagents and conditions: (a) Acetic anhydride, DMAP, triethylamine, acetonitrile, rt, 1 h; (b) *N*-Boc-1,6-hexanediamine, triethylamine, ethanol, 90 °C, 20 h; (c) TFA, DCM, water (drops), rt, 2-3 h; (d) HOBt, DCC, THF, rt, 48 h; (e) 7N NH$_3$, methanol, rt, overnight; (f) two steps: i) phosphorus oxychloride, 1,8-bis(dimethylamino)naphtalene, trimethylphosphate, 0-4° C, 4 h; ii) TEAC buffer, rt, 1 h.

2.3.1.2.2 Synthetic route B

Since the original synthetic route did not lead to the desired product, a new synthetic route was employed. Herein, the synthesis is separated into the synthesis of two building blocks, which were to be reacted with each other in the last reaction step. The two building blocks consist of the nucleotide on the one side and the linker-attached fluorescein derivative on the other side. *Note*: As for the original synthetic pathway, the synthesis was started from a commercially available isomeric mixture of 5(6)-carboxyfluorescein, which is more affordable than pure 6-carboxyfluorescein. After the synthetic route was successfully established, the synthesis was repeated starting from the pure isomer 6-carboxyfluorescein. For the sake of clarity, only the synthesis of the isomerically pure compound as well as the corresponding experimental data are reported in this chapter (Scheme 14). The synthesis was started from commercially available 6-carboxyfluorescein (**91**), which was coupled to *N-boc*-1,6-hexanediamine using standard amide coupling conditions with 1-[bis(dimethylamino)methylene]-1*H*-1,2,3-triazolo[4,5-b]pyridinium 3-oxide hexafluorophosphate (HATU) and *N,N*-diisopropylethylamine (DIPEA) in DMF.[158] The mixture was stirred under argon atmosphere for 48 h. The crude mixture was extracted with ethyl acetate and then purified by normal phase column chromatography to give the desired product (**94**). In the next step, *boc*-protected **92** was deprotected using TFA in DCM and a few drops of water.[157] Evaporation of the volatiles gave the desired product **93** without further purification. In parallel, 6-chloro-9-(*β*-D-ribofuranosyl)-9*H*-purine (**68**) was

phosphorylated using phosphorus oxychloride and 1,8-bis(dimethylamino)naphthalene (proton sponge) in trimethyl phosphate, followed by hydrolysis using aqueous TEAC buffer.[141] After extraction with TBME and purification by RP-HPLC, the desired nucleotide compound **95** was obtained. In the last step, the nucleotide compound **95** was attached to the linker-carrying fluorescent dye **93** (Scheme 14). Therefore, the compounds were reacted for 8 h under reflux in basic conditions (triethylamine) in ethanol. Frequent monitoring by normal phase TLC and subsequent analysis by TLC-coupled MS indicated that the nucleotide **95** was stable under these quite harsh reaction conditions for the entire reaction period. Neither the *N9*-bond, nor the 5′-phosphoric acid ester showed any tendency of cleavage. After TLC indicated full conversion of the starting material, the volatiles were evaporated, and the crude mixture was purified by RP-HPLC to give the desired product **96**. Furthermore, for the establishment of an assay, as a fluorescein-coupled CD73 reaction product of **96**, adenosine derivative **94** was synthesized. Except for the last reaction step, the synthesis was identical to the synthesis of the fluorescein-coupled nucleotide **96**. In the last step, the linker-attached fluorescent dye **93** is coupled to 6-chloro-9-(*β*-D-ribofuranosyl)-9*H*-purine under reflux and under basic conditions in analogy to Bhattarai *et al.*[103, 111] Normal phase colum chromatography of the crude reaction mixture yielded the desired product **94**. The structures of both fluorescent compounds **94** and **96** were confirmed by ^{1}H-, ^{13}C-,and ^{31}P NMR spectroscopy, and LC/ESI-(UV)MS analysis performed in positive mode confirming a purity of greater than 95% for both compounds.

Scheme 14. Synthesis route for compounds **94** and **96**[a]
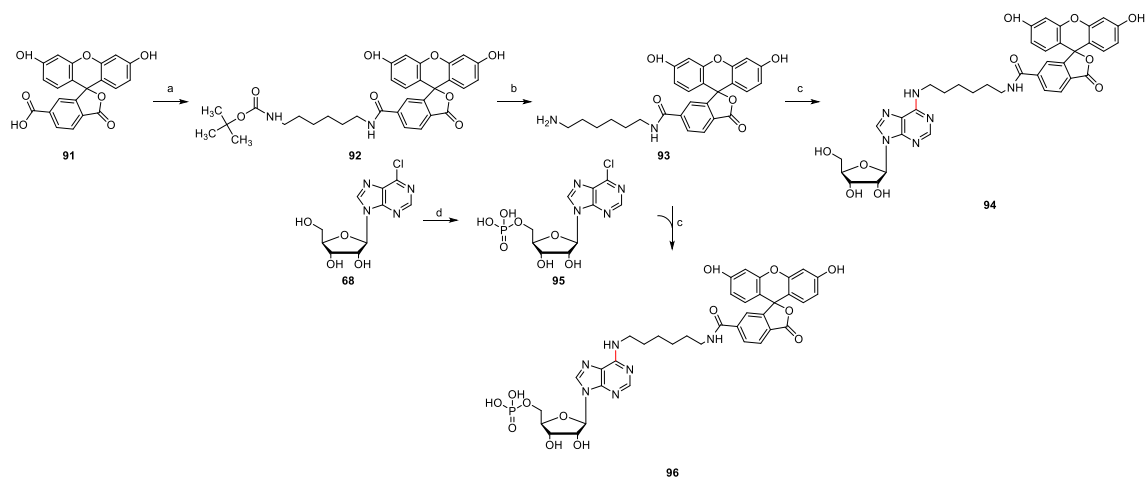
[a]Reagents and conditions: a) *N-boc*-1,6-hexanediamine, HATU, DIPEA, DMF, rt, 48 h; b) TFA, DCM, water, rt, 3 h; c) triethylamine, ethanol, 90 °C, 8 h; d) two steps i) phosphorus oxychloride, trimethyl phosphate, 0 – 4 °C, 1 h; ii) TEAC buffer, pH 7.4 – 7.6, rt, 1 h.

2.3.1.3   Biological evaluation

Initial biological studies of **94** and **96** have already been carried out by Laura Schäkel. As a first step, we aimed to evaluate, if fluorescence-labeled AMP is even hydrolyzed by CD73. In the first experiments we could see a time-dependent conversion of fluorescein-labeled AMP (**96**) leading to the enzymatic reaction product, fluorescein-labeled adenosine (**94**). Comparing a 2 minutes incubation time of **96** with CD73 with a 15 minutes incubation time, it becomes evident, that the starting material peak has become smaller and the product peak has become larger after 15 minutes (see Figure 39). Furthermore, the operation conditions for CE experiments were optimized in order to achieve the best possible seperation of fluorescence-labeled AMP **96** and adenosine **94** (see Figure 39). As can be seen, a baseline separation between starting material and product peak is achieved. However, the adenosine peak still

shows some tailing. Further experiments with the aim to optimize the operation conditions in order to resolve this issue will be carried out.
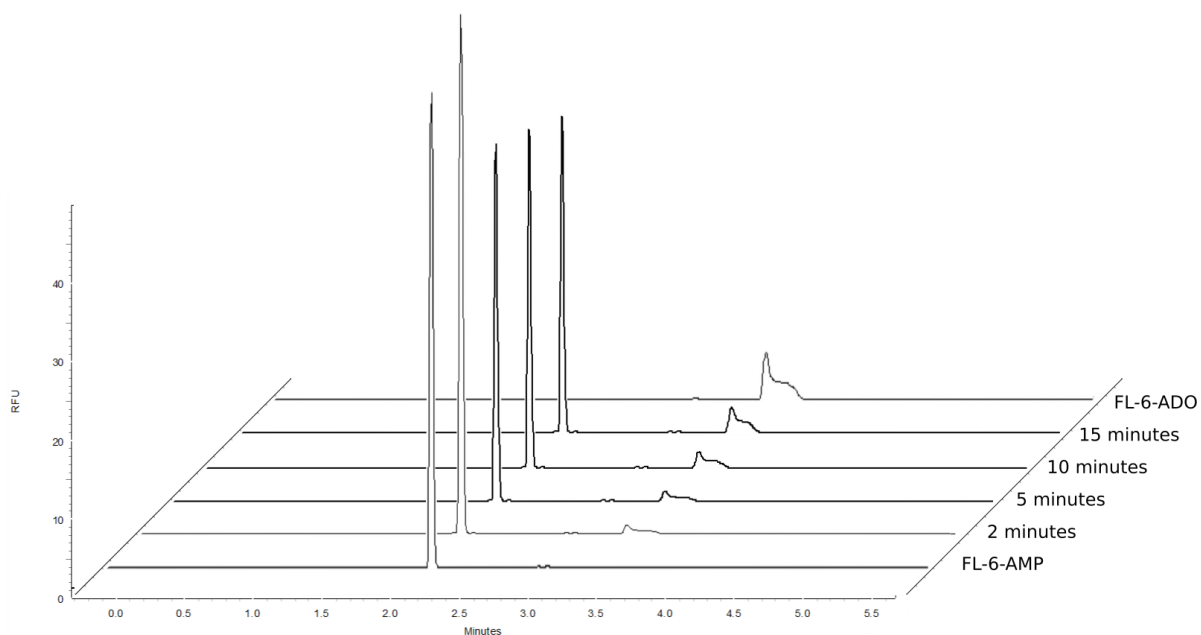
Figure 39. Electropherogram of CE with laser-induced fluorescence (LIF)-detection. The identity of the peaks is confirmed by comparison to pure samples of 6-carboxyfluorescein-coupled AMP (FL-6-AMP) (**96**) and 6-carboxyfluorescein-coupled adenosine (FL-6-ADO) (**94**) (25 nM). 500 nM of FL-6-AMP was incubated with 35.0 ng/ml of human soluble CD73 for 2, 5, 10 and 15 min at 37 °C, and the enzyme reaction was stopped by heating at 95 °C for 10 minutes (here the assay buffer was 10 mM 4-(2-hydroxyethyl)-1-piperazineethanesulfonic acid (HEPES) buffer incl. 2 mM CaCl$_2$ and 1 mM MgCl$_2$, pH 7.4). The enzyme mixtures were then diluted 1:20 with 10 mM *N*-cyclohexyl-2-aminoethanesulfonic acid (CHES) buffer (incl. 2 mM CaCl$_2$ and 1 mM MgCl$_2$, pH 9.0) before running in the CE analyses.

2.3.1.4   Conclusion and outlook

After we failed to synthesize the desired compounds following the original synthetic pathway, we managed to synthesize the desired product using an alternative synthesic route. The new

synthesic route is facile, allows fast preparation of the desired products and shows good yields. It was crucial to see that the nucleotide compound is stable under basic conditions applying high temperatures over several hours. From the chemical side, this project is completed, since both required compounds were successfully synthesized. First experiments in order to establish a new CE-fluorescence-coupled assay have been carried out. As a next step, the running conditions of the CE will be optimized, in order to achieve well shaped peaks. Later on, for example, the time-dependent formation of the fluorescent enzymatic reaction product **94** will be further evaluated. Apart from that, the K_m-value and the LOD will be investigated.

2.3.2 Design and synthesis of fluorescence-labeled 2-chloro-AMPCP derivative

A recently published study by Dr. Constanze Schmies and myself reported the first fluorescence-labeled AMPCP derivative.[137] The described synthetic route followed a similar concept as the one described in chapter 2.3.1.2.2. The fluorescent building block and the nucleotide were synthesized separately and were then coupled in the last reaction step. It was furthermore reported that the *p*-position of the N^6-benzyl moiety represents a suitable position for further derivatization. The introduction of a bulky fluorescein residue attached via a linker moiety was well tolerated leading to potent, selective, metabolically stable fluorescein-labeled CD73 inhibitors.[137] However, the synthesis of a 2-chloro substituted fluorescent AMPCP derivative had been not successful, which was why the plan to synthesize such a compound was further pursued. We also chose fluorescein as a dye for fluorescence-labeling since it represents a good starting point for initial labeling studies.

2.3.2.1 Chemistry

6-Carboxyfluorescein (**91**) was attached to commercially available *N-boc*-1,6-hexanediamine via amide coupling using HATU as a coupling reagent, and DIPEA as a base in DMF to give

92.[158] Subsequent *boc*-deprotection using TFA in DCM yielded **93**.[157] Next, 4-(*boc*-aminobenzyl)benzoic acid was coupled to the primary amino group of **93** again employing HATU and DIPEA to give **97**, followed by *boc*-deprotection with TFA in DCM yielding **98**.[157, 158] In a parallel reaction, commercially availabe 2,6-dichloro-9-(*β*-D-ribofuranosyl)purine (**50**) was phosphonylated using methylenbis(phosphonic dichloride) in trimethyl phosphate, followed by quenching with aqueous TEAC buffer according to a previously published, optimized method.[102–104, 137] RP-HPLC purification afforded the pure product **82**. In the final reaction step, nucleophilic substitution of **82** by the primary amine **98** in absolute ethanol in the presence of triethylamine under reflux conditions, followed by RP-HPLC purification, yielded the desired final product **99** (Scheme 15, yield 23%).[137] The structure of **99** was confirmed by ^{1}H, ^{13}C and ^{31}P-NMR spectroscopy and LC/ESI-(UV)MS analysis (positive and negative mode) indicating a purity of >95%.

Scheme 15. Synthetic procedure to obtain compound **99**[a]
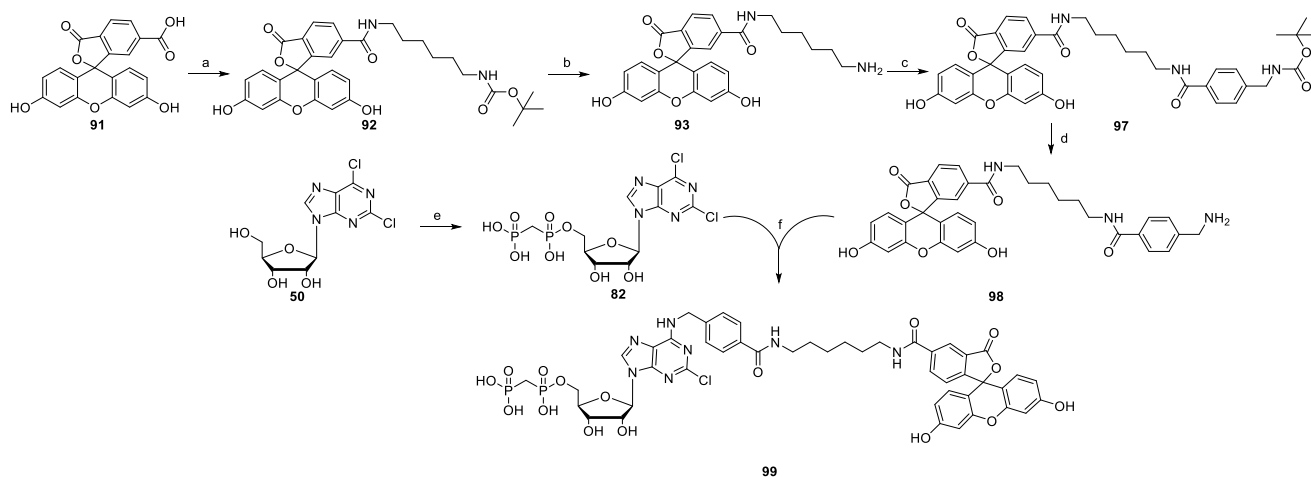
[a]Reagents and conditions: (a) *N-boc*-1,6-hexanediamine, HATU, DIPEA, rt, overnight; (b) 6-8% TFA, DCM, rt, 5 h; (c) 4-(*boc*-aminobenzyl)benzoic acid, HATU, DIPEA, rt, overnight; (d) 6-8% TFA, DCM, rt, 5 h; (e) two steps: (i) methylenebis(phosphonic dichloride), trimethyl phosphate, Ar, 0 °C, 1 h; (ii) TEAC buffer pH 7.4-7.6, rt, 1 h; (f) triethylamine, ethanol, reflux, overnight.

2.3.2.2 Pharmacology

The potency of **99** was determined by measurements of full concentration-inhibition curves. K_i values were calculated from the obtained IC_{50} values employing the Cheng-Prusoff equation.[150] For a better comparison, the K_i values of the corresponding 2-non-substituted derivative **102** (see Figure 40, taken from [137]) are depicted in Table 5.
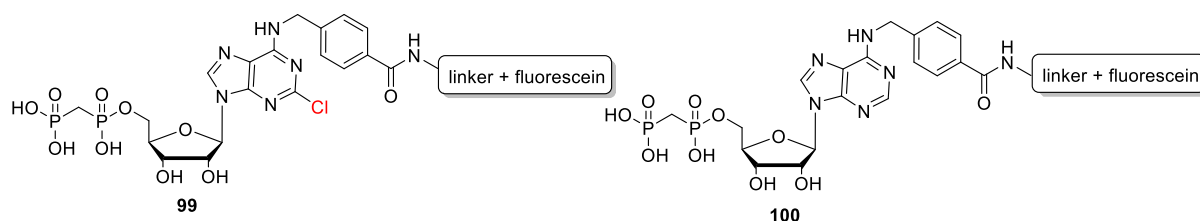
Figure 40. Comparison 2-chloro-substituted **99** and 2-unsubstituted **100**.

The pharmacological evaluation was carried out by Dr. Christian Renn and Riham Idris. As expected, compound **99** showed high potency in the low nanomolar range at human soluble CD73 (5.96 nM vs 2.98 nM) and membrane-bound CD73 (6.76 nM vs 4.59 nM) for **99** and **100**, which had virtually the same potency. The potency at rat CD73 was 3-fold lower, which met our expectations at the rat enzyme, but the newly synthesized 2-chloro derivative **99** was more potent than **100** (18.0 nM vs. 26.0 nM). This is well in accordance with results from other AMPCP derivatives (see chapter 2.1.2). However, the additional 2-chloro substitution did not lead to the expected improvement in inhibitory potency.

Table 5. Potencies of compounds **99** and **100**, and at different CD73 preparations[a]

Compd.	Human soluble CD73 $K_i \pm SEM^a$ (nM)	Human CD73 MDA-MB-231 $K_i \pm SEM^a$ (nM)	Rat soluble CD73 $K_i \pm SEM^{a,b}$ (nM)
99	5.96 ± 0.850	6.76 ± 1.25	18.0 ± 1.43
100	2.98 ± 0.77 [b]	4.59 ± 1.18[b]	26.0 ± 1.9[b]

[a][2,8-^{3}H]AMP (5 µM) was used as substrate; K_m value 59 µM, 17 µM and 14.8 µM respectively for purified recombinant soluble human CD73, native membrane-anchored human CD73 (in MDA-MB-231 cell membrane preparations), and purified recombinant soluble rat CD73; [b] data taken from [137, 141]

For a better comparison, pK_i values of **99** and **100** at different CD73 preparations are depicted in Figure 41. The pK_i value is the negative decimal logarithm of the K_i value and allows a more intuitive view, since the height of the bar correlates with the potency of the evaluated compounds. As can be seen in Table 5, the measured K_i values of the 2-chloro substituted compound **99** was in all different CD73 preparations in the same range as the non-substituted derivatives. A reason might be the large fluorescent substituent, which could hamper the compound from reaching the C2 binding pocket, which would otherwise lead to additional interaction between the inhibitor and amino acids in the binding pocket. A reason could be a different binding mode due to the large substituent. Co-crystallization studies with CD73 and both inhibitors could show similarities and differences in the binding mode and thus help to explain the findings.
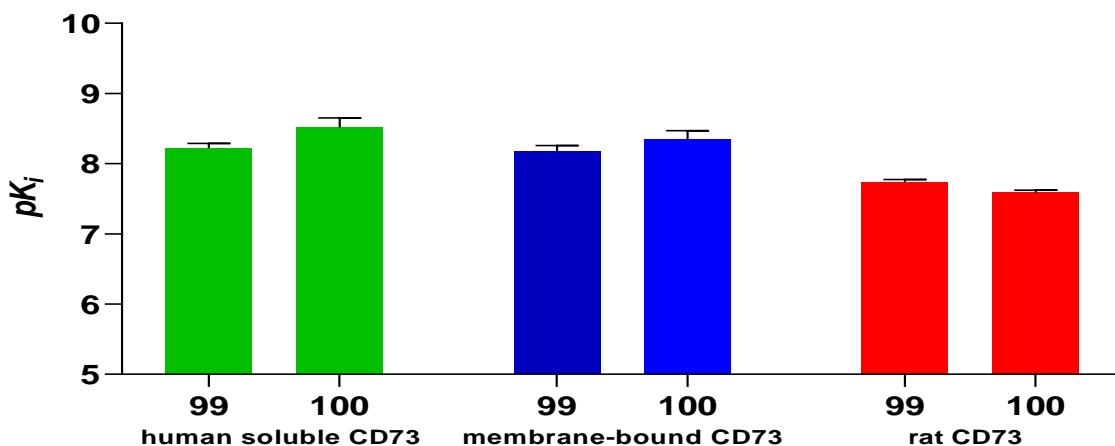
Figure 41. Comparison of potencies of compounds **99** and **100** at CD73 of different species.

2.3.2.3 Selectivity studies

We tested the selectivity of **99** for CD73. Therefore, we investigated its inhibition of human NTPDases 1, 2, 3, and 8 and furthermore antagonism as well as agonism at the ADP-activated P2Y$_{12}$ receptor.[25] The experiments were carried out by Laura Schäkel and Haneen Al-Hroub. In general, the results were well in accordance with those for previously reported AMPCP derivatives, which always showed high selectivity for CD73.[102–104, 109, 137]

2.3.2.3.1 Inhibition of human NTPDases

The inhibitory activity of the CD73 inhibitor **99** at human NTPDases 1, 2, 3, and 8 was investigated using ATP (100 µM) as a substrate according to previously published procedures.[25] ATP and **101** were co-incubated with recombinantly expressed human NTPDases at 37 °C for 30 min, and the enzymatic reaction was terminated by heating at 90 °C for 10 min. The amount of enzyme preparation was adjusted to ensure 10–20% of substrate conversion. The formed products were separated by CE and individually quantitated by a UV-detector at a wavelength

of 260 nm. For inhibition analysis, at least three independent experiments were performed, each in triplicate. The inhibition of the enzymatic activity was calculated in relation to the positive control without inhibitor and plotted by GraphPad Prism 8 software (GraphPad software, San Diego, CA, USA) (for results, see Table 6). NTPDase 2 and 8 were not inhibited at high concentrations of 50 µM of **99** while at NTPDase 1 and 3 **99** displayed an IC_{50} values of 27,6 µM and 27,7 µM which is over 4600-fold of the K_i value at human CD73.

Table 6. Interaction of compound **99** with the human NTPDases 1,3,4 and 8

Target	IC_{50} (nM) ± SEM at the indicated concentration[a] (Inhibition (%) at 50 µM ± SEM)
NTPDase1	IC_{50} = 27,600 ± 5300
NTPDase2	IC_{50} > 50,000, (10 ± 3)
NTPDase3	IC_{50} = 27,700 ± 2700
NTPDase8	IC_{50} > 50,000, (0 ± 2)

[a] Membrane-bound recombinant human NTPDase1 (CD39) enzyme with 50 µM ATP substrate (K_m value 17 µM)
[b] Membrane-bound recombinant human NTPDase2 enzyme with 100 µM ATP substrate (K_m value 70 µM)
[c] Membrane-bound recombinant human NTPDase3 enzyme with 100 µM ATP substrate (K_m value 75 µM)
[d] Membrane-bound recombinant human NTPDase8 enzyme with 100 µM ATP substrate (K_m value 46 µM)

2.3.2.3.2 Activity at the human P2Y$_{12}$ receptor

Interaction of **99** with the human P2Y$_{12}$ receptor was investigated in a β-arrestin recruitment assay using the galactosidase complementation technology as previously described.[159–161] The human P2Y$_{12}$ receptor was expressed in CHO-PK1 cells (Eurofins DiscoverX, Fremont, CA, USA). No agonism or antagonism at human P2Y$_{12}$ was observed at a concentration of 10 µM (see Table 7). Due to interference of the fluorescent compound **99** with the fluorescent dye used in a calcium mobilization assay, the activity of **99** could not be determined at P2Y$_1$ receptors.

Table 7. Interaction of compound **99** with the human ADP-activated GPCR P2Y$_{12}$ [a]

Target	IC_{50} (nM) or EC_{50} (nM)
Inhibition P2Y$_{12}$ receptor	$IC_{50} > 10,000$
Activation P2Y$_{12}$ receptor	$EC_{50} > 10,000$

[a]For antagonist testing, 2-methylthio-ADP was employed as agonist at its EC$_{80}$ concentration (3 µM).

2.3.3   Synthesis of further fluorescence-labeled CD73 inhibitors

Fluorescein that has absorption and emission maxima at relatively short wavelengths (λ_{abs}~ 500 nm, λ_{em} ~520 nm) has several limitations.[155] Due to reduced photo-toxicity, dyes that absorb and emit at longer wavelengths a more desirable.[162] Furthermore, the fluorescence quantum yield of fluorescein is strongly pH-value dependent. [163] With a pK_a value of 6.4 in water, fluorescein stays at a large proportion in the protonated, nonfluorescent form at physiological pH-values. It furthermore tends to exhibit quenching when being conjugated to proteins (relativ to the free fluorophor). This could be a problem, when high amounts of fluorescence-labeled CD73 inhibitor are binding to the target protein CD73.[164] Apart from that, fluorescein is sensitive towards photobleaching,[165] which limits is utility in biological experiments.

We therefore selected a 4,4-difluoro-4-bora-3a,4a-diaza-*s*-indacene (BODIPY) and a cyanine derivative for coupling to AMPCP derivatives. Their properties will be explained more detailed in the respective chapter. We aimed to synthesize these derivatives in a similar fashion to the already synthesized compound **99**. Therefore, we synthesized the nucleotide precursors in parallel to the fluorescent dye in order to couple both building blocks in the last reaction step.

2.3.3.1 BODIPY-coupled CD73 inhibitors

Fluorescent BODIPY dyes are widely used for protein and DNA labeling, and have become our dye of interest due to their excellent spectroscopical properties.[166, 167] They strongly absorb UV light and emit sharp fluorescence peaks possessing high fluorescent quantum yields.[162, 168] Another advantage is their insensitivity towards the polarity of the solvents as well as the pH-value.[162] The core of BODIPY derivatives, which can be substituted at different positions, is depicted in Figure 42. Absorption and emission maxima as well as water solubility can be influenced by various substituents of the BODIPY core.
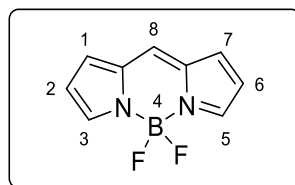
Figure 42. The BODIPY core.

The first reactions were carried out in a small scale in order to investigate if it is worthwhile to further follow the selected synthetic route. In the first step, 4-(((*tert*-butoxycarbonyl)amino)methyl)benzoic acid was reacted with BODPIY derivative **103** using HATU and DIPEA in DMF at room temperature. The reaction was followed by the deprotection of the *boc*-group, in order to obtain the free primary amino residue, which could be coupled to (((((2*R*,3*S*,4*R*,5*R*)-5-(2,6-dichloro-9*H*-purin-9-yl)-3,4-dihydroxytetrahydrofuran-2-yl)methoxy)(hydroxy)phosphoryl)methyl)phosphonic acid (**84**, Scheme 16). However, according to LC-MS analysis, the desired product could not be obtained. Only **84** could be found in the LC-MS.

Scheme 16. Synthetic route towards a BODIPY-coupled AMPCP derivative **104**[a]
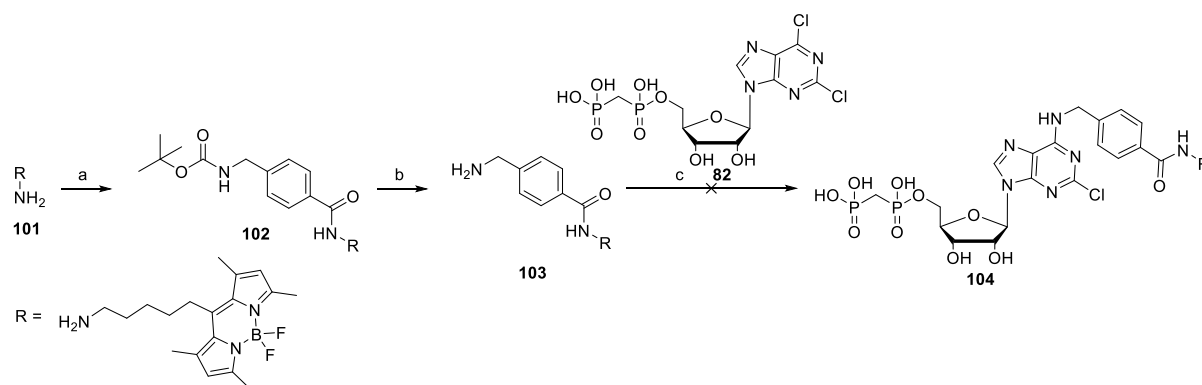
[a]Reagents and conditions: (a) 4-(((*tert*-butoxycarbonyl)amino)methyl)benzoic acid, HATU, DIPEA, rt, overnight; (b) 6-8% TFA, DCM, rt, 5 h; (c) **71**, trietylamine, ethanol, reflux, overnight.

We therefore changed the last reaction steps to an azide-alkyne cycloaddition.[169] We chose this reaction since it is, due to its character, classified as so called "click-reaction". According to Sharpless *et al.* click reactions have the following characteristics:

- High yields

- Stereoselectivity

- Wide in scope

- Easily removable solvents

- Simple isolation of the product etc[169]

These conditions seemed to be ideal for the last reaction step. The fluorescent dye was a BODIPY derivative which was synthesized by the former co-worker Dr. Tim Klapschinski. The reaction was carried out under conditions, which were previously described by Himo *et al.*[170] In order to enable the click reaction, a terminal alkyne group needed to be introduced to the nucleotide compound. The synthesis of the nucleotide precursors **81a** and **83** is described in detail in chapter 2.2.2. As a terminal group we chose a propargyl residue, since the formed

triazole ring would mimic a benzyl residue (Figure 43), which we found to be important for obtaining very potent AMPCP derived CD73 inhibitors.[102–104, 109]
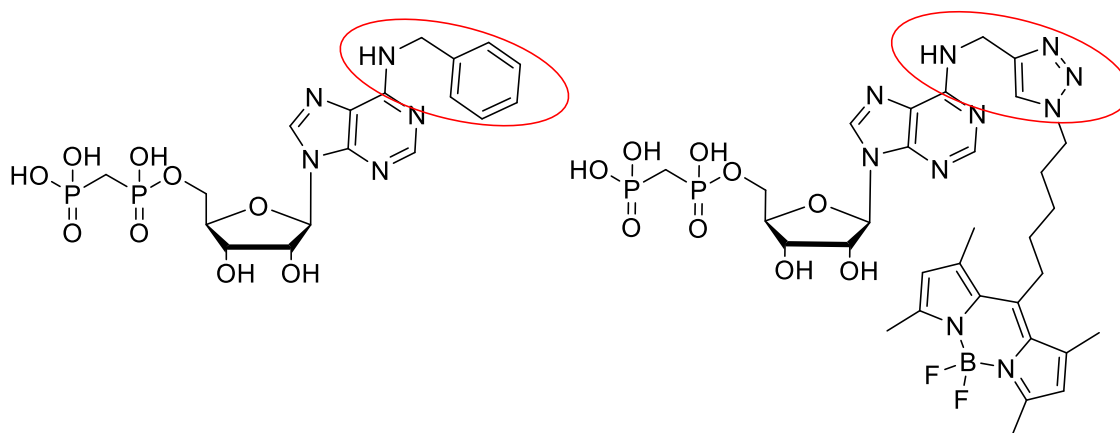
Figure 43. Bioisosteric replacement of the benzylamine residue.

Unfortunately, the synthesis of compound **108** failed. We assumed that the propargyl group might be too close to the purine ring and could thus be sterically hindered for the formation of the triazole. Therefore, we synthesized the N^6-(4-ethynylphenyl)methanamine derivative, in order to enlarge the distance between the terminal alkyne and the purine ring. However, this did not lead to the desired product **109** either (see **Scheme 17**).

Scheme 17. Click reaction between nucleotide building block **81a/83** and fluorescent building block **105**[a]
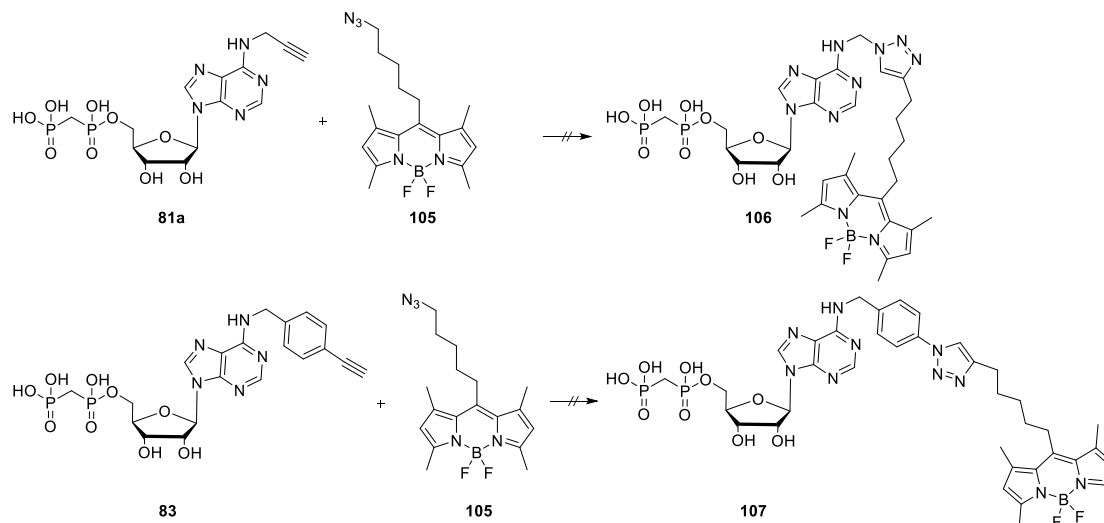
[a]Reagents and conditions: CuSO4, sodium ascorbate, H2O/*t*BuOH (1/1).

We assumed that the diphosphonate structure might interfere with the copper ions and could thus hamper the reaction. As a consequence, we changed the order of the reaction steps by coupling the nucleoside to the fluorescent dye first, and phosphonylate it then in the next step (see Scheme 18). The N^6-propargyl-substituted AMPCP derivative **81a** was coupled using copper sulfate, sodium ascorbate, and Tris((1-benzyl-4-triazolyl)methyl)amine (TBTA) at room temperature in a mixture of H2O and *tert*-butanol. In contrast to the attempts with the nucleotide derivatives, the click-reaction between the nucleoside **77** and the BODIPY derivative **105** worked straight forward in the same reaction conditions which had been used for the coupling of the nucleotide **81a** with the BODIPY derivative **105** (yield 41%).[170] The next step would be a phosphonylation of the 5′-position. Since the reaction step before was only small-scale test reaction, not enough starting material for the phosphonylation was available. Since phosphonylation reactions are usually associated with low yields,[111] the BODIPY derivative

needs to be resynthesized to a larger scale, in order to obtain at least 50 mg of the nucleoside precursor **108**.

Scheme 18. Alternative synthetic route for **107**[a]
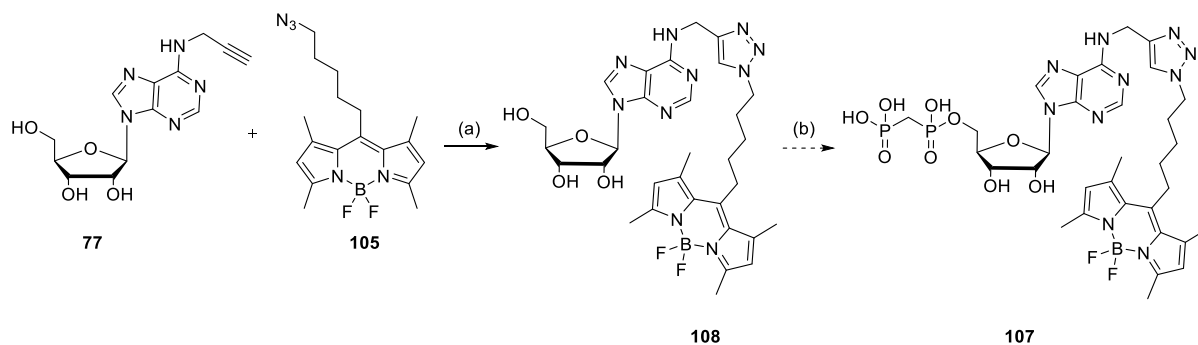
[a]Reagents and conditions: (a) CuSO₄, sodium ascorbate, tris-[(1-benzyl-1*H*-1,2,3-triazol-4-yl)-methyl]-amin (TBTA), H₂O/*t*BuOH (1/1), (b) two steps: (i) methylenebis(phosphonic dichloride), trimethyl phosphate, Ar, 0 °C, 1 h; (ii) TEAC buffer pH 7.4-7.6, rt, 1 h.

2.3.3.2 Cyanine-coupled AMPCP derivatives

To broaden the range of CD73 tool compounds, we decided to synthesize an AMPCP derivative coupled with near-infrared absorbing dye. Near infrared fluorescent dyes possess several advantages over dyes that emit at a shorter wavelength. With emission of wavelengths between 650 nm and 900 nm, interference by substances with autofluorescence is reduced. Thus, they have a high detection selectivity and sensitivity, and due to their low toxicity profile are highly biocompatible.[171,172] This excellent profile makes them ideal labels for proteins and nucleic acids in the framework of biochemical and biological experiments.[173] The general structure of cyanine dyes is depicted in Figure 44. Cyanines are named according to the number of carbon atoms between the heterocyclic moieties (Cy3, Cy5 etc.).[174]
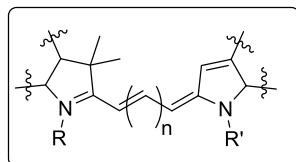
Figure 44. General structure of a fluorescent cyanine dye

For the synthesis of cyanine-labeled AMPCP derivatives a similar synthetic approach as for the fluorescein-labeled AMPCP derivatives was pursued. The alkyne moiety containing AMPCP precursor was synthesized as one building block, and the azide containing cyanine dye was synthesized as the other building block. The cyanine building block was synthesized by Tim Harms.[175] The synthesis of the AMPCP building blocks is described in chapter 2.2.2. Both building blocks were then reacted with each other via a Huisgen azide alkyne cycloaddition (Scheme 19). [169, 170] We chose this reaction for the same motifs that are described in chapter 2.3.3.1. These conditions seemed to be ideal for the last reaction step. However, although various reaction conditions were tried, it was not possible to synthesize and isolate the desired product. The carried out reaction conditions are depicted in Table 8. From attempt to attempt, one parameter was varied (solvent, temperature, reaction time, ratio and amount of catalyst), but none led to the desired product. We assumed several reasons for the failure of the reactions. One was insufficient solubility **109** in the used solvent (entry 1 and 2), which could be solved by the usage of a mixture of DMF and 1 M HEPES buffer. Furthermore, we assumed that a significant amount of copper could be bidentaley complexed by the diphosphonate moiety. Therefore, it would not be available for being reduced by sodium ascorbate and could thus not participate in the catalytic reaction. We drastically increased the amount of copper sulfate and sodium ascorbate as also described by our cooperation partners Dobelmann *et al.* (A. Juncker Group, University of Münster) in the framework of radiosynthesis.[176] That, indeed, led to the formation of desired product which could be found to some extent in an LC-MS of the crude

reaction mixture. The high amount of sodium ascorbate and copper sulfate, however, impeded the following workup. It was not possible to extract the side products with water, since the product is water-soluble as well. The starting material **109** was also only soluble in DMF which strongly limited the choice of solvents. Removal of DMF also posed problems, especially due to the high water-solubility of the product. We tried to remove as much DMF as possible by evaporation using a high vacuum pump, and removed the aqueous phase by lyophilization. The remaining solid was then dissolved in as little DMF as possible, and submitted to RP-HPLC. Unfortunately, the desired product could not be isolated by RP-HPLC due to inconsistent and unpredictable elution behavior of the compound. Also reducing the catalyst, or catalyst and reducing agent, did not lead to the desired compound. Since we also assumed that the access to the triple-bond could be hampered by its local proximity to the purine ring, we switched the precursor from an N^6-propargyl-substituted AMPCP derivative (**81**) a to a N^6-4-ethynylbenzyl residue (**83**), which provides more space between the purine ring and the triple bond due to the phenyl ring. However, different trials did not lead to the desired product. Comparing the carried out click-reaction with the carried out click reaction in chapter 2.7.2., which worked straight-forward in the very first attempt, it becomes evident that the only difference is the diphosphonate structure. It could therefore be worthwhile, similar to the synthesis of the BODIPY derivative, to couple the cyanine first to the nucleoside, and phosphonylate it then in the next step. However, phosphonylation could pose a problem due to the relatively acidic conditions that occur because of the formation of HCl during the reaction. Test reactions under acidic conditions led to degradation of the fluorescent dye. It could help to keep the reaction time as short as possible and the temperature as low as possible. Further attempts that are leading in this direction were carried out in collaboration with the Master student Jianyu Hou and are described in detail in his Master thesis.[149]

Scheme 19. Click reaction between triple-bond containing **81a**, **83** and azide-containing **109**. For reagents and conditions, see **Table 8**.

81a, 83   109   110

Table 8. Different reaction conditions for fluorescence-labeling

R	Catalyst	Reducing agent	Solvent	Temp.	Time	Obervations
Propargyl	CuSO$_4$.5H$_2$O (0.3 eq.)	Sodium ascorbate (2.5 eq)	THF/H$_2$O/tBuOH	Rt	12	No desired product, complex mixture of pro ducts
Propargyl	CuSO$_4$.5H$_2$O (1.2 eq.)	Sodium ascorbate (2.5 eq)	H$_2$O/methanol	Rt	20	No desired product, complex mixture of pro ducts
Propargyl	CuSO$_4$.5H$_2$O (20 eq.)	Sodium ascorbate (40 eq.)	H$_2$O/DMF	Rt	24	No desired product, complex mixture of pro ducts
Propargyl	CuSO$_4$.5H$_2$O (20 eq.)	Sodium ascorbate (40 eq)	HEPES/DMF	60 °C	24h	No desired product, complex mixture of pro ducts
Propargyl	CuSO$_4$.5H$_2$O (0.3 eq.)	Sodium ascorbate (40 eq)	HEPES/DMF	60 °C	24h	Product could be found in LCMS
Propargyl	CuSO$_4$.5H$_2$O (0.3 eq.)	Sodium ascorbate (40 eq)	HEPES/DMF	60 °C	24h	No desired product, complex mixture of pro ducts
Propargyl	CuSO$_4$.5H$_2$O (1.2 eq.)	Sodium ascorbate (2.5 eq)	HEPES/DMF	60 °C	24h	No desired product, complex mixture of pro ducts
4-ethynylbenzylamine	CuSO$_4$.5H$_2$O (1.2 eq.) + TBTA	Sodium ascorbate (2.5 eq.)	H$_2$O/ methanol	Rt.	24h	No desired product, complex mixture of pro ducts

4-ethynylbenzylamine	CuSO$_4$.5H$_2$O (20 eq.)	Sodium ascorbate (40 eq.)	HEPES/DMF	Rt	24h	No desired product, complex mixture of pro ducts
4-ethynylbenzylamine	CuSO$_4$.5H$_2$O (20 eq.)	Sodium ascorbate (40 eq.)	HEPES/DMF	60 °C	24h	No desired product, complex mixture of pro ducts

2.3.4 Conclusions and outlook

We could successfully synthesize a 2-chloro-substituted fluorescein-coupled AMPCP derivative, which showed strong potency and high selectivity for CD73. It remains unclear, why additional substitution in position 2 by a chlorine atom did not enhance the potency on CD73 as it is usually observed. Co-crystallization studies could help to answer this question. Pharmacological evaluation confirmed that even a large substituent like fluorescein is tolerated by CD73, which is in line with recently published results.[137]

The synthesis of a cyanine-bound AMPCP derivative has not been successful until now. Employing copper-free click reactions might help to obtain the desired product.[177–179] In the context of the Master project of Jianyu Hou, further experiments for the coupling of the cyanine dye have been carried out and the project will be further followed as a subsequent PhD project.[149]

The synthesis of a BODIPY labelled AMPCP derivative could also not be successfully completed until now. The click reaction between nucleoside and BODIPY worked straightforward, and now, larger amounts of the BODIPY and the nucleoside precursor have to be synthesized. The synthesis of the BODIPY derivative is quite laborious, especially if larger amounts are required. Therefore, it should be considered, if there are better alternatives for this fluorescent dye. It furthermore has to be awaited, if the phosphonylation would work with the BODIPY-labelled nucleoside. It is questionable if the BODIPY derivative will be stable under the phosphonylation reaction conditions.

With regards to the employed click reactions, it has to be emphasized that they worked in our experience straightforward when a *nucleoside* was used. For nucleotides, however, this cannot

be concluded at all. Yet, Dr. Constanze Schmies and Dr. Anna Junker have reported that the click reaction with nucleotide analogs can work (see also chapter 2.7.2., Scheme 35).[141, 176] These findings can only partly be transferred to the cyanine and BODIPY click reactions, since the moiety to be clicked was much smaller (2-fluoroethyl azide). This could have a decisive effect on the successful outcome of the reactions.

2.4 AMPCP-derived inhibitors for attachment to a nanogel

The following chapter deals with a cooperation project with Dr. Lutz Nuhn from the Max-Planck-Institute, Mainz. The idea was to attach a CD73 inhibitor (besides A_{2A} and A_{2B} inhibitors) to pH-dependent degradable nanogels. The drug of interest is covalently bound to a nanogel, which is, due to its physicochemical properties, formed in micelles. Upon acidic pH-values in the tumor microenvironment,[14, 180] the micelles disassemble to soluble chains, which allows the drug to access the target of interest.[181]

2.4.1 Drug-loaded nanogels

In 2016, Nuhn *et al.* demonstrated that toll-like receptor (TLR) agonists conjugated to pH-degradable, self-assembling nanogels could induce spatially limited immune activation via local toll-like receptor activation and thus reduce systemic adverse effects like inflammatory toxicity.[182] The nanogels are crosslinked via pH-degradable chains. It could also be shown that nanogel-mediated delivery of imidazoquinoline (IMDQ) led to a stronger induction of T-cell and antibody responses against admixed antigens in comparison to soluble IMDQ, which led to a reduced tumor growth in in vivo mouse models. The spatially limited effect was later on confirmed by in-vivo fluorescence-imaging studies, which showed that nanogel-conjugated and fluorescence-labeled IMDQ remained localizied at the tumor site upon peritumoral injection. Furthermore, bioluminiscence experiments confirmed a locally limited induction of interferon

(IFN) type 1, upon peritumoral injection of nanogel-bound TLR-agonists, whereas injection of soluble TLR-agonists resulted in systemic IFN type I induction.[183]

There are numerous methods for the preparation of core-crosslinked polymeric micelles.[184] The following chapter will only focus on the method, which was employed for our experiments (see Figure 45). Degradable polymer nanogels consist of an amphiphilic block copolymer consisting of a hydrophilic, PEG-like polymer and a hydrophobic component.[184] In our case, the hydrophilic component is based on tri(ethylene glycol)-methyl ether methacrylate (mTEGMA) and the hydrophobic component is based on pentafluorophenyl methacrylate (PFPMA). The precursor polymer blocks are converted into precursor micelles via reversible addition-fragmentation chain transfer (RAFT)-block copolymerization using 4-cyano-4-(phenylcarbonothioylthio)pentanoic acid as chain transfer agent and self-assemble subsequently in a polar aprotic solvent (eg. DMSO). The active pentafluorophenyl (PFP) esters of the precursor micelles are then amidated with the compound of interest (in our case a CD73 inhibitor). After loading with the drug of interest, the active PFP esters can be functionalized with non-degradable, ether-based diamine crosslinker or degradable ketal-based-diamine crosslinkers. Remaining active PFP esters are then converted into hydrophilic nanogels by coupling to ethanolamine. [182, 183, 185]
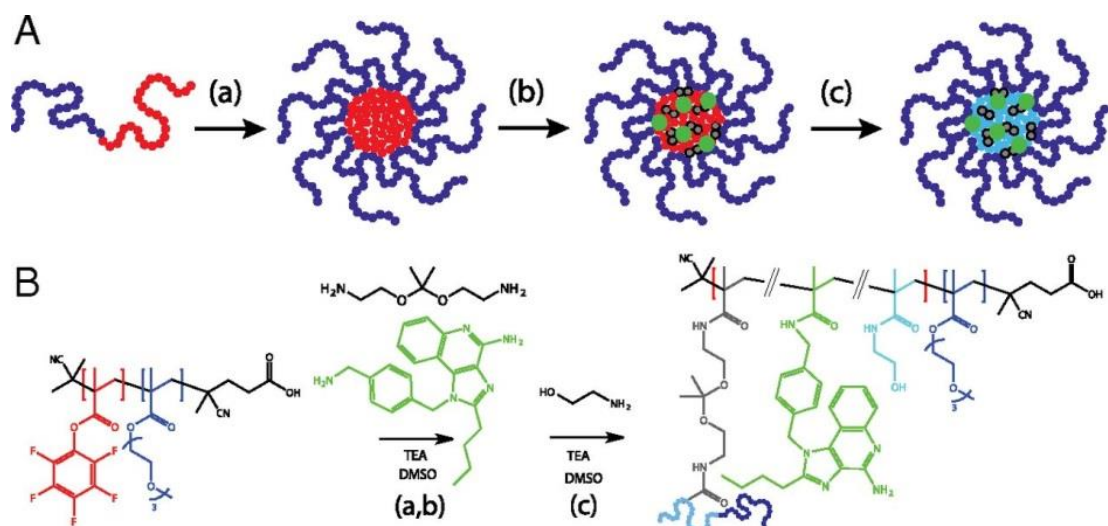
Figure 45. RAFT polymerization: Formation of degradable nanogels. (A) Schematic overview and (B) Detailed overview with correspoding chemical structures. (a) Self-assembly of block copolymers in aprotic solvent (e.g. DMSO). (b) Covalent attachment of to be attached compound (TLR7/8 agonist, green) to reactive PFP esters and cross linking. (c) Derivatization of unreacted reactive pentafluorophenyl esters with 2-ethanolamine affording fully hydrated nanogels. Taken from [182].

2.4.2 Design

To this end, we designed a CD73 inhibitor that possesses a primary amino group and allows coupling to the reactive PFP ester species while keeping its strong inhibitory potency. We chose AMPCP derivatives as compound class, since they combine strong potency with high selectivity and water solubility and possess a variety of positions for further derivatization. In previous publications of our group we could show that halogenation of the 2-position of the adenine core is a structural feature that strongly enhances the potency of AMPCP derivatives in comparison to non 2-substituted derivatives.[102–104] We therefore implemented a 2-chloro residue in our target structure. Since we could recently show that the *p*-position of the *N⁶*-benzyl ring even tolerates bulky residues, we selected this position for further derivatization.[137] We

assumed that an additional methylene group between the aromatic ring and the amine would lead to increased nucleophilicty and thus a better reactivity of the amine compared to an aniline.[186] Furthermore, we added an additional propyl substitution at the N^6-position. This is of high relevance, since a possible hydrolysis product of an AMPCP derivative – an adenosine derivative carrying a free NH group attached to C6 - might activate ARs.[112] This would counteract the intended effect of inhibiting CD73. In addition to that, N^6-disubstituted AMPCP derivatives seemed to have an even stronger potency towards CD73 than mono-substituted derivatives.[103] The compound is depicted in Figure 46.
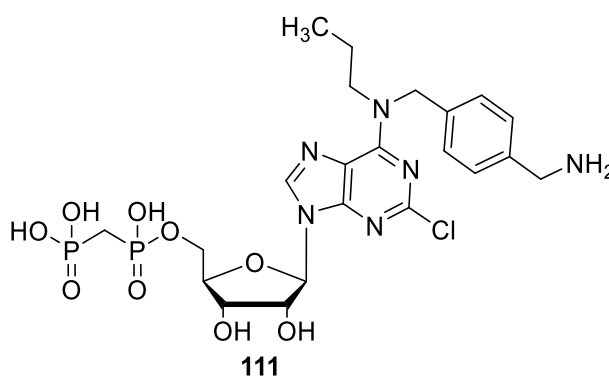
Figure 46. AMPCP derived CD73 inhibitor with free primary amino group **111**.

2.4.3   Chemistry

The synthetic approach started with glycosylation of 2,6-dichloropurine **49** using 1,2,3,5-tetra-*O*-acetyl-*β*-D-ribofuranose **48** under acidic conditions to afford compound **50**.[140] In parallel to that, 4-(*boc*-amino)benzylamine (**112**), was alkylated with 1-brompropane in DMF to give **113**.[187] Interestingly, **113** showed only a minor tendency for further alkylation. A reason might be steric hindrance that seemed to predominate the tendency of multiple nitrogen alkylation caused by increased nucleophilicity by more alkyl substituents. The benzylamine derivative **113** was then reacted with the nucleoside **50** with triethylamine in ethanol under reflux. Subsequent acetyl deprotection of **115** with 7N ammonia in methanol and purification by normal phase column chromatography gave the desired product **116**. The nucleoside **116** was

then phosphonylated using methylenbis(phosphonic dichloride) in trimethyl phosphate, followed by hydrolysis using aqueous TEAC buffer.[102–104, 109] Purification employing RP-HPLC gave the desired product **117**. The *boc*-protecting group of **117** was then cleaved using TFA in DCM mixed with a few drops of water.[157] In order to circumvent cleavage of the *N7*-bond, induced by the strong acidic conditions, the reaction time was kept as short as possible. RP-HPLC provided the desired product **111** (Scheme 20, ca. 10 mg in the first attempt). After successful completion of the synthetic route, the desired compounds were pharmacologically tested. Since further experiments were planned, the synthesis was upscaled in order to obtain about 70 mg of the final compound **111**.

Scheme 20. Synthesis of AMPCP derived CD73 inhibitor with free primary amino group **111** as precursor for ruther attachment to nanogels[a]
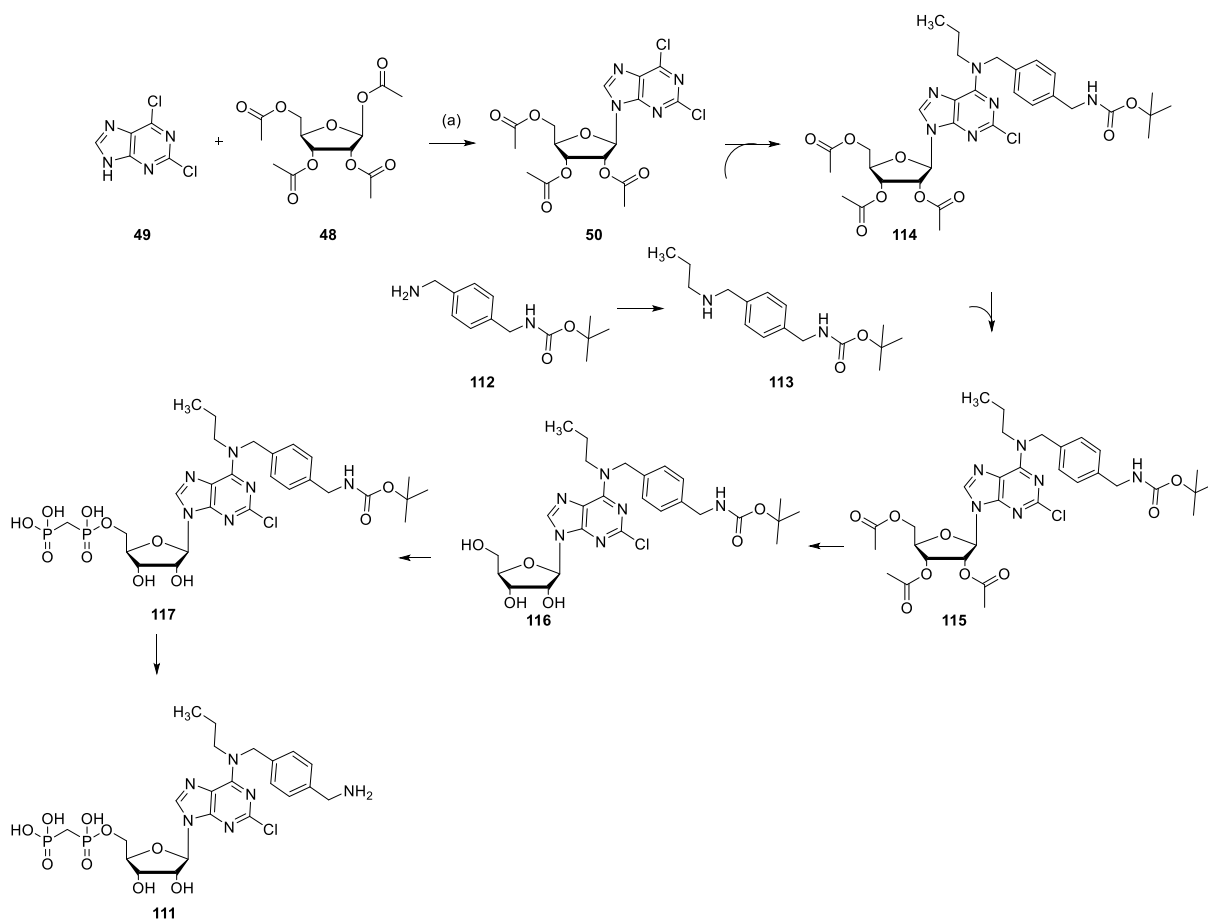
2.4.4   Synthesis of different nanogel types

Compound **111** was then sent to the group of Dr. Lutz Nuhn (Max Planck Institute for Polymer

Research, Mainz) where the drug-loaded nanogels were synthesized by Judith Stickdorn, a PhD

student from the group of Dr. Lutz Nuhn. Three different types of nanogels were loaded with

the CD73 inhibitor. The nanogels differed in their bisamine crosslinkers, which has a strong

effect on their ability to degrade under acidic pH. In the first fraction, after drug loading, the

remaining reactive PFP esters were only coupled to ethanolamine, which led to readily soluble

chains, since no cross-linking was carried out (a). The second fraction was (after drug-loading)

crosslinked with ketal-bisamines, which degrade upon acidic pH (b). The third fraction was

prepared with non-degradable ether chains (c) (see Figure 47). The different fractions a-c were

obtained with a loading volume of 18.4-21.2% (see Table 9).
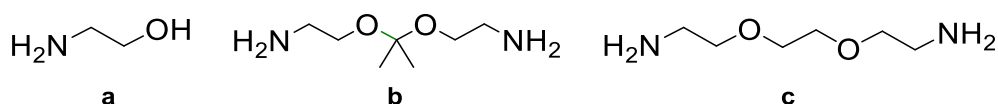
Figure 47. Soluble chain, degradable Ketal-chain (kNP), and non-degradable ether chain (eNP).

Table 9. Different fractions of CD73 inhibitor loaded nanogels

Sample	Description	Loading (wt %)	Equivalent CD73 inhibitor (CD73i) molecular weight*	Amount (mg)
a	sol. chains +CD73i	18.4	3375 g/mol	13.45
b	ketal-NP +CD73i	17.9	3469 g/mol	15.07
c	ether-NP +CD73i	21.2	2929 g/mol	10.87

* The equivalent molecular weight of polymer-bound CD73 inhibitor was calculated from the drug load (wt%). Drug loading experiments were carried out by Judith Stickdorn, Max-Planck Institute, Mainz.

2.4.5 Pharmacology

Interaction of the pure **111** as well as **111** coupled to the different nanogel fractions (**118a-c**) and of uncoupled nanogel fractions with CD73 was determined in radiometric enzyme assays using [³H]AMP as a substrate.[70, 137] Full concentration-inhibition curves were determined, and from the obtained IC_{50} values K_i values were calculated using the Cheng−Prusoff equation.[150] The activity of the samples was determined at two different pH-values (pH = 7.4 and 5.0). The acidic pH-value is supposed to display the acidic conditions in the tumor microenvironment. Since at least degradable, ketal-crosslinked nanogel-bound **J** is supposed to be degraded, we would expect improved activity upon acidic pH-value. Compound **111** showed a high potency with a K_i of 0.284 nM indicating that the free primary amino group is well accepted by the binding site of CD73. At pH 5, where the terminal primary amine is most-likely protonated, the K_i-value was virtually the same, which means that also a positively charged amine is tolerated. In addition to that, the different unloaded nanogel fractions (**118a-c**) were tested in order to exclude a possible inhibition caused by the nanogel itself. As expected, none of the non-loaded

nanogels showed any activity at a concentration of 10 µM. (see Table 10). Compound **111** coupled to three different nanogel fractions (soluble chain = **119a**, ketal-NP = **119b**, and ether NP = **119c**) was tested pH 7.4 and pH 5.0. At pH 7.4 all probes showed similar potency ranging from 0.904 nM to 1.86 nM. The strong potency is quite surprising, because except for the soluble chain probe, the nanogels Ketal-NP **119b** and Ether-NP **119c** should be assembled in micelles, which would hinder the inhibitor to reach the active site of CD73. We would therefore not expect the probes to be that potent. At the lower pH-value, in contrast, we would expect an enhanced potency for the ketal-NP bound probe **119b**, since the ketal crosslinkers are supposed to degrade and thus to disassemble into soluble chains under acidic conditions. However, the ketal-NP-bound sample showed the same potency at both pH-values. That means that decreasing the pH-value had apparently no effect on the binding of the compound. For the non-degradable ether cross-linked nanogels, we would expect no or low potency at both pH-values. However, the sample showed the same potency as the degradable nanogel and the soluble chains. The results of the soluble chain-bound sample **119a** were as expected. Due to the lack of crosslinking, the sample exists already as soluble chains, and no disassembly of a micelle is required. Therefore, we expected no change in potency depending on the pH-values. Indeed, the determined potency was at both pH-values in the same range.

2.4.6 Conclusions and future outlook

The obtained results are not consistent, since basically all results, regardless of the pH-value at which the nanogel-bound CD73 inhibitor was measured, were virtually the same. For the described reasons, this is contrary to our expectations. A possibility could be that the CD73 inhibitor was actually not covalently bound to the nanogel, but trapped in the inside of the micelle and then released upon dissolution. This could explain why there is no difference between the different micelle fractions. Nevertheless, this possibility should actually be excluded by dialysis as the final step of the conjugation process. It still has to be figured out, if

the compound is indeed covalently bound to the nanogel. As a positive results, a potent, amino-funtionalized CD73 inhibitor could be developed, which allows its coupling to e.g. polymers, fluorescent dyes, antibodies etc.
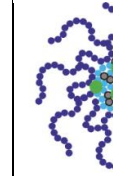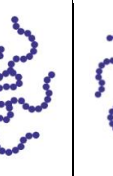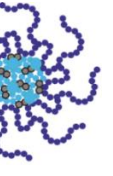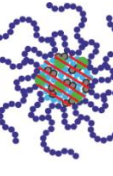
CD73							
	111	**Sol. Chain + 111 =119a**	**Sol. Chain – 111 = 118a**	**Ketal-NP + 113 = 119b**	**Ketal-NP - 113 = 118b**	**Ether-NP + 113 = 119c**	**Ether-NP - 113 = 118c**
Loading **65** (wt.%)	-	18.4	-	17.9	-	21.2	-
Eq. **65** MW (g/mol)	620.92	3375	5307	3469	5697	2929	4599
Enzyme inhibition assay — **pH = 7.4** — K_i **[nM]** (n = 1)	0.284 ± 0.100	**0.904**	> 10000* (-34 ± 6)	**1.86**	> 10000* (26 ± 10)	**0.971**	> 10000* (-23 ± 17)
pH = 5.0 — K_i **[nM]** (n = 2)	**0.375** ± 0.021	**1.70** ± 0.350	n.d.	**2.10** ± 0.357	n.d.	**1.66** ± 0.300	n.d.

Table 10. Potencies of **111** and nanogel-coupled **118** (soluble chain a, ketal-NP b, ether-NP c) at pH 5.0 and 7.4

2.5 Nucleotide mimetic compounds

2.5.1 Design of nucleotide mimetic CD73 inhibitors

Almost all recently described nucleotide-derived CD73 inhibitors carry a diphosphonate moiety, attached to the 5′-OH position.[102, 103, 110, 113] Despite high potency, this moiety is connected with several disadvantages. At physiological pH at 7.4 the diphosphonate residue is deprotonated, which, for example, hampers the ability to cross biological membranes. We synthesized a series of nucleotides and nucleotide-mimetic compounds with the aim to enhance their drugability. While keeping the adenosine moiety, the diphosphonate structure was successively replaced with monophosphonates, sulfonamides or sulfonyl groups (see Figure 48). We furthermore replaced the 5′-hydroxy group with an amino group in order to enhance the chemical stability of the compounds. First, the α-phosphonate was replaced by a carbonyl group, while keeping the β-phosphonate moiety. The carbonyl moiety could mimic the α-phosphonate group. Furthermore, in order to increase the chemical stability, the 5′-ester structure was replaced with a more stable ether, or amide bond. In the further progress, we aimed to fully replace the diphosphonate structure. Therefore, we replaced the β-phosphonate residue with a sulfonamide, since it displays the best compromise between being neutral while showing slight NH acidity. Furthermore, we replaced the β-phosphonate with a sulfonate group. We also combined the diphosphonate modifications with potency-enhancing derivatizations, e.g. benzylation of the N^6-position.

Replacement of diphosphonate structure

Substitution of N^6
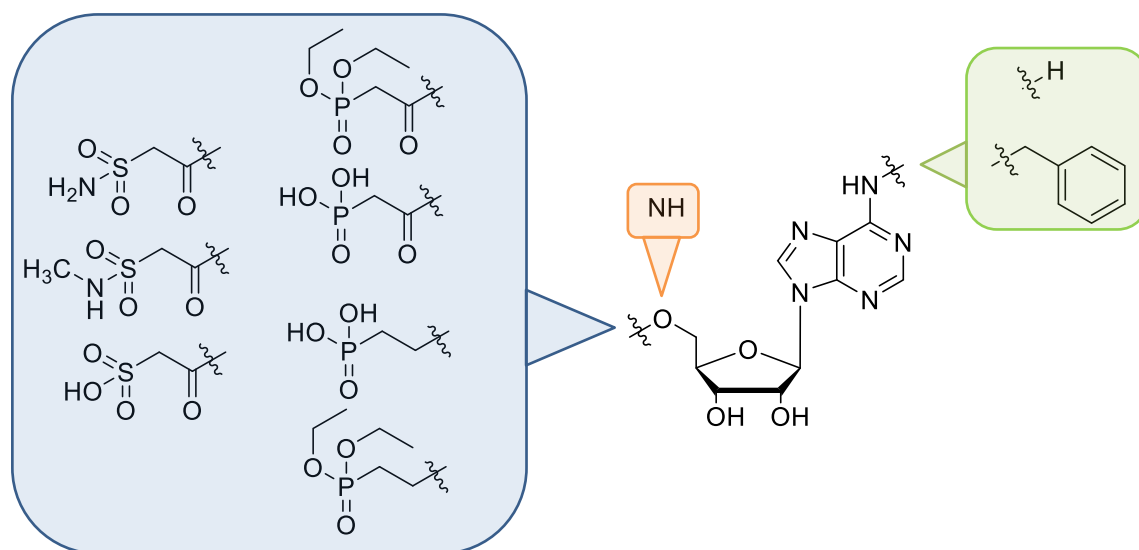
Figure 48. Design of nucleotide-mimetic CD73 inhibitor compounds.

2.5.1.1   Chemistry

2.5.1.1.1   Synthesis of N^6-benzylated, 5′-phosphonoaceticacid ester 124 -

The synthesis of **124** was started with commercially available 6-chloro-9-(β-D-ribofuranosyl)purine (**68**, Scheme 21). As a first step, 2′ and 3′-OH groups were protected with 2,2-dimethoxypropane under acidic conditions.[102] The reaction was carried out at room temperature for 30 min. In the next step, the 6-chloro group was substituted with benzylamine by refluxing at 90 °C under basic conditions for several hours. Both reactions have frequently been described and worked therefore straightforward.[102, 103] The following step was an esterification of the 5′-OH group with 2-diethylphosphonoacetic acid using N,N'-dicyclohexylcarbodiimide (DCC) as a coupling reagent and DMAP as a base applying conditions reported by Vertuani *et al.*[188] For the next step, it was planned to deprotect the 2′,3′-acetonide (the protecting group) and the diethylphosphono group in parallel as also reported by

Vertuani *et al.* [188] Several attempts following these conditions using trimethylbromosilane (TMSBr) in DCM resulted in the formation of a complex mixture of products but not the desired product **124**. This is in accordance with the PhD thesis of Dr. Andreas Brunschweiger, who also reported the formation of complex product mixtures.[189] Therefore, **122** was first deprotected using TFA in DCM at room temperature.[157] Purification by normal phase column chromatography led to the desired product **123**. This product was pharmacologically evaluated. The next reaction step was a deprotection of the phosphono group. Unfortunately, similar to the previously carried out deprotection reaction with TMSBr, the desired product could not be obtained. This might be due to the formation of hydrobromic acid during the reaction process. The strongly acidic conditions could lead to cleavage of the 5′-ester bond and also the glycosidic bond between the purine base and the sugar. We considered the ester bond in the 5′-OH position to be too instable. Therefore, we replaced the 5′-ester with an amide. In order to determine the potency of the uncharged compound **123**, it was tested in a radiometric assay.

Scheme 21. Synthesis of *N⁶*-benzylamine-5′-oxoethylphosphonic acid **124**[a]

benzylamine, triethylamine, ethanol, reflux, 90 °C, 20 h; (c) diethylphosphonoacetic acid, DCC,

DMAP, DCM, rt, 20 h; (d) TFA, DCM, H_2O, rt, 3 h (e) TMSBr, DCM, 0 °C, 1-5 h.

2.5.1.1.2 Synthesis of N^6-unsubstituted-5′-phosphonoaceticacid ester 129

The synthesis, which is depicted in Scheme 22, was started by acetonide protection of adenosine

(**125**),[102] followed by esterification using 2-diethylphosphonoacetic acid.[188] Compound **127** was

then deprotected using TFA in DCM to afford **128**. The last reaction step, similar to the

synthesis of **128**, did not lead to the desired product **129**. Compound **129** has already been

published by Vertuani *et al.*[188]

Scheme 22 Removal of P_α-atom - Synthesis of N^6-unsubstituted **129**[a]
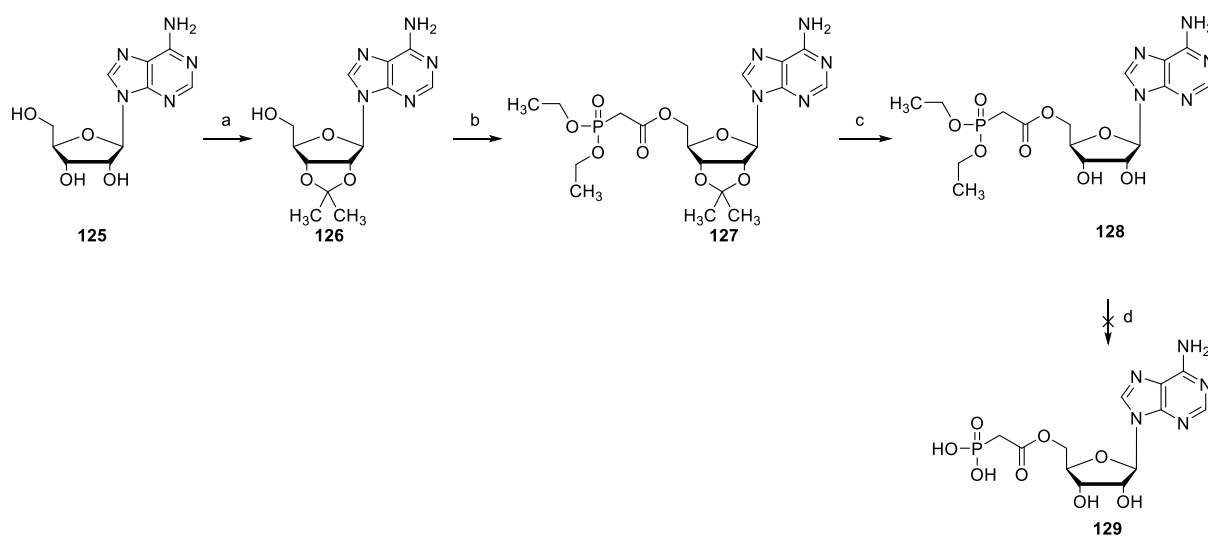
[a]Reagents and conditions: (a) 2,2-dimethoxypropane, sulfuric acid, acetone, rt, 30 min; (b)

diethylphosphonoacetic acid, DCC, DMAP, DCM, rt, 20 h; (c) TFA, DCM, H_2O, rt, 3 h; (d)

TMSBr, DCM, 0 °C, 1-5 h.

2.5.1.1.3 Replacement of 5′ester bond by an amide bond – Synthesis of 132

The synthetic pathway started from commercially available 2′, 3′-*O*-isopropylidene-5-amino-5-deoxyadenosine (**130**). Instead of protected diethylphosphonoacetic acid, unprotected phosphonoacetic acid was reacted with **131** using HATU and DIPEA as a base in DMF.[190] Surprisingly, analysis of a first test reaction indicated that the reaction worked straightforward without the use of a phosphonate-protective group. This knowledge significantly simplifies the synthesis of this target structure, since deprotection of the phosphonate residue had prevented obtaining the desired products in previous approaches (see Scheme 23). Furthermore, deprotection with TMSBr has been described as causing reduced yields.[191] As side reaction, the N^6-position was amidated besides the 5′-OH group. Due to the high polarity of both compounds, RP-HPLC was required to purify this mixture. Purification gave the desired product **131** (yield: 57%). In the next step, the isopropylidene-protected 2′-and 3′-*O* positions of **131** were deprotected using TFA in DCM. Purification by RP-HPLC gave the desired product **132**. The structure of **132** was confirmed by ^{1}H, ^{13}C and ^{31}P-NMR spectroscopy and LC/ESI-(UV)MS analysis (positive and negative mode) indicating a purity of >90%.

Scheme 23. Replacement of 5′ester bond by an amide bond to synthesize **132**[a]
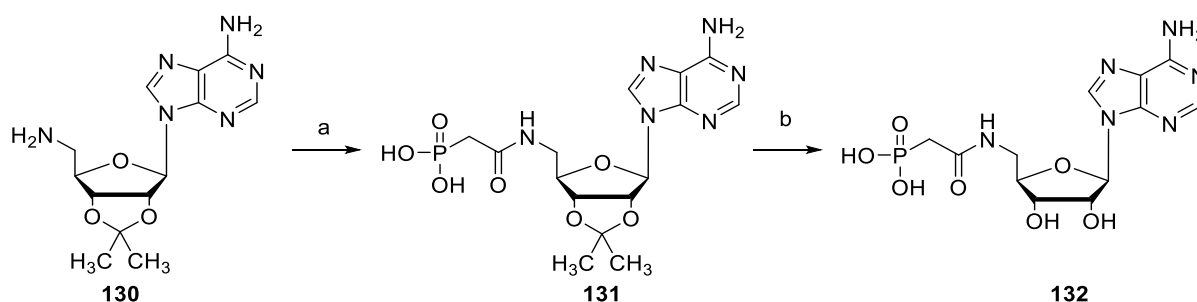
2.5.1.1.4 Substitution of P$_\alpha$ by an ether bond - Synthesis of N^6-benzylated 135

The first two reaction steps were identical to the synthesis of compound **124** (see Scheme 21). Alkylation of the 5′-OH position with diethyl (2-bromoethyl)phosphonate afforded **133** and was carried out using tetrabutylammonium hydrogen sulfate (TBAHS) in a mixture of aqueous NaOH (50%) and toluene according to Lai *et al.*[192] The next reaction step was a deprotection of the 2′-and 3′-hydroxy groups using TFA in DCM.[102, 104] Purification by normal phase column chromatography gave the desired product **134**. The last reaction step was supposed to cleave the ethoxy groups from the phosphonate, but similar to the synthesis of **124** and **129**, the deprotection did not lead to the desired product **135** (see Scheme 24).

Scheme 24. Synthesis of N^6-benzylated, 5′-etherified **135ª**
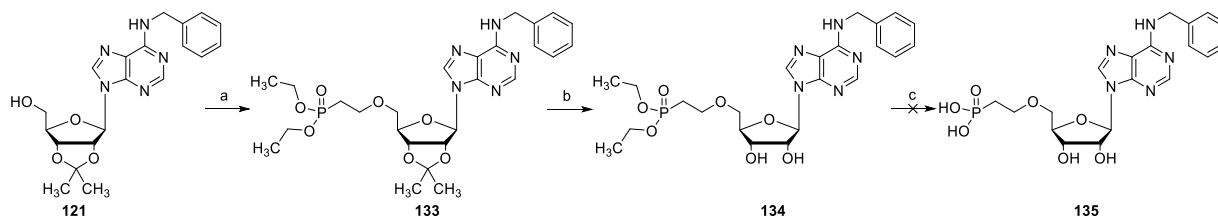
ªReagents and conditions: (a) TBAHS, aqueous NaOH solution (50%), toluene, rt, 48 h (b) TFA, DCM, water, rt, 3 h c) TMSBr, DCM, 0 °C, 1-5 h.

2.5.1.1.5 Substitution of diphosphonate structure by sulfonamide residue (137a,b)

The synthesis attempt was started from compound **121**. The first step was an esterification of the 5′-OH group with 2-sulfamoylacetic acid (a) or 2-(methylsulfamoyl) acetic acid (b), respectively, in analogy to Steglich-esterification conditions.[193] The reaction was carried out using DCC as a coupling reagent and DMAP as an auxiliary base at room temperature

overnight. In both cases, the reactions worked straightforward with 40% and 61% yield, respectively. The esterification was followed by deprotection of the acetonide-protected hydroxy groups of **136a,b** using TFA in DCM.[102] Due to the lability of the 5′-ester of **137a,b** in acidic conditions, isolation of the desired product was quite laborious. The reaction time had to be kept as short as possible, yet achieving full deprotection of **136a,b**. We eventually managed to obtain both desired products **137a,b** (Scheme 25). These compounds display the first described sulfonamide bioisosters of AMPCP compounds.

Scheme 25. Synthesis of N^6-benzyl-sulfonamide-derived AOPCP isosters **137a,b**[a]

Compd.	R
a	H
b	CH$_3$
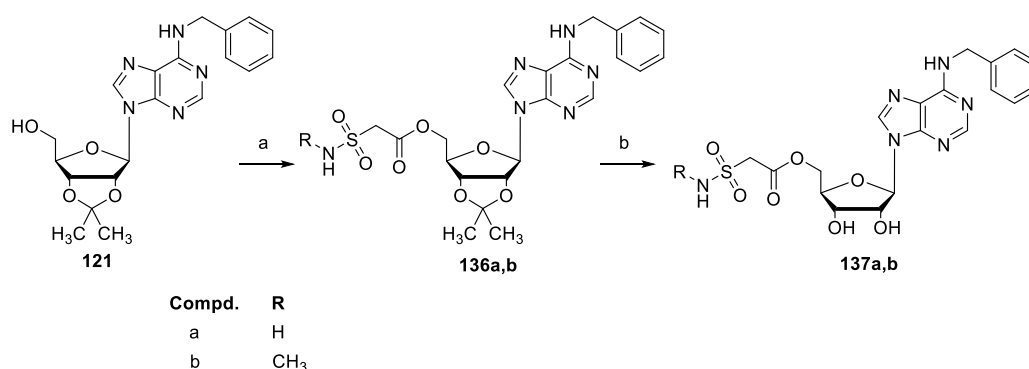
[a]Reagents and conditions: (a) DCC, DMAP, DCM, rt, 20 h (b) TFA, DCM, H$_2$O, rt, 3 h.

2.5.1.1.6 Substitution of 5-OH group by amino group – Synthesis of sulfonamide derivative 139

Similar to compound **132**, we aimed to substitute the 5′-OH group with an amino group in order to achieve higher chemical stability. The synthesis of compound **139** was started with available 2′,3′-O-isopropylidene-5′-amino-5′-deoxy adenosine (**130**). The 5′-NH group was reacted with 2-sulfamoylacetic acid using HATU as coupling reagent and triethylamine as base, achieving a moderate yield of **138** (30%).[190] Deprotection of **138** was carried out using TFA in DCM with catalytic amounts of water. Upon addition of methanol, the desired product **139** precipitated in the reaction mixture (Scheme 26).

Scheme 26. Synthesis of sulfonamide derivative **139**[a]
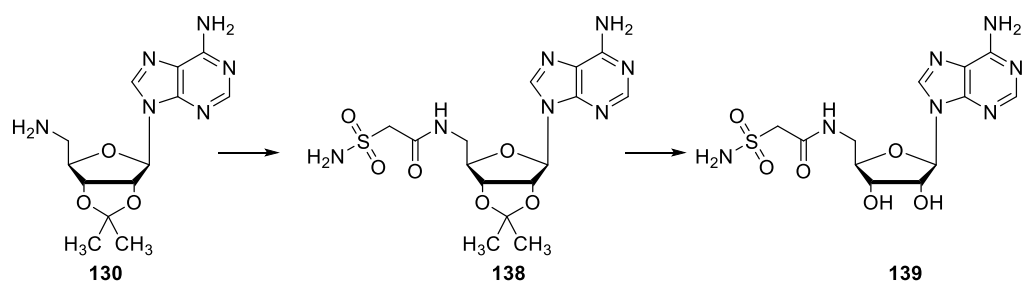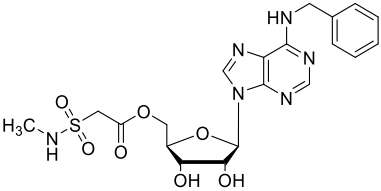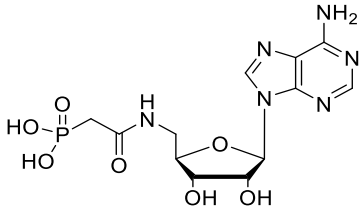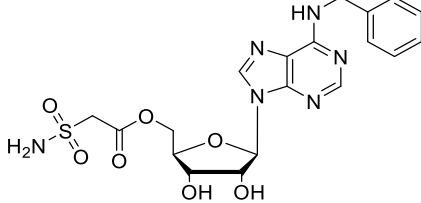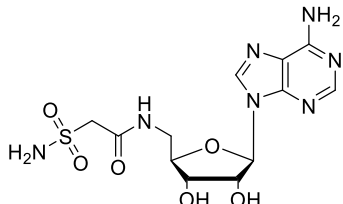
[a]Reagents and conditions: (a) HATU, Et3N, DMF, rt, overnight; (b) TFA, DCM, H2O, rt, 3 h.

2.5.2 Pharmacology

Table 11. Pharmacological evaluation of nucleotide-mimetic CD73 modulators

Compd.	Structure	Rat recombinant soluble CD73 $K_i \pm \text{SEM}^a$ (μM)	Human recombinant soluble CD73 $K_i \pm \text{SEM}^a$ (μM)
128		> 10 (5%)	n.d.
123		> 10 (5%)	n.d.
134		> 10 (11%)	n.d.

109

Compound	Structure	rat CD73	human CD73
137b		> 10 (19%)	n.d.
132		n.d.	4.22 ± 1.40
137a		n.d.	>10 (5%)
139		n.d.	> 10 (-9 ± 5) (n=2)

[a][³H]AMP (5 µM) was used a substrate; K_m value 59 µM and 17 µM for purified recombinant soluble rat CD73, purified recombinant soluble human CD73. N.d. = not determined.

The inhibitory potency of compounds **123**, **128**, **132**, **134**, **137a, 137b,** and **139** towards CD73 was determined in CD73 assays (see Table 11).[70, 71] Different preparations of CD73 were used, including rat and human recombinant soluble CD73 expressed in *Sf9* insect cells.

Compounds **123**, **128**, **134** and **137a** were screened at a concentration of 10 µM at recombinant rat CD73. In case of showing an activity of more than 50% they were supposed to be tested on human recombinant soluble CD73. With test compounds **123**, **128** and **134**, we aimed to investigate the importance of a negative charge in the *β*-phosphonate position, which is not present in the protected phosphonates **123**, **128** and **134**. Indeed, none of the compounds showed an inhibition of over 50%, which brings us to the conclusion that at least one negative charge in the *β*-position which is most likely essential for a strong interaction with the enzyme. As

described by Knapp *et al.* the *β*-phosphonate of e.g. AMPCP coordinates bidanteley with the catalytic zinc ions in the *N*-terminal domain of CD73.[39, 103] A requirement for this interaction might be the deprotonation of the terminal phosphonate, which is not possible with the two ethoxy groups present. The other reason might be the size of the two ethoxy groups which prevents access of the compounds to the limited binding space in the active site. In compound **90b** the terminal phosphonate is replaced by a smaller methylated sulfonamide residue. However, it also did not show inhibition of over 50% at 10 µM. Compounds **132**, **137a** and **139** were directly tested on recombinant human soluble CD73. Compounds **132** and **139** can directly be compared since they only differ in their residue in the *β*-position. Nucleotide analog **132** showed a K_i value of 4.22 µM and was the only compound from this series showing percentage of inhibition higher than 50% at 10 µM. Its sulfonamide analog **139** however was not active. Compound **137a** carries an additional N^6-benzyl residue, but did not inhibit CD73 at a concentration of 10 µM. However, compounds carrying a sulfonamide residue were not active, which might also be caused by the lack of a deprotonated hydroxy group coordinating the zinc ions in the binding site.

2.5.3 Conclusions and future outlook

Within this series, only **132** showed CD73 inhibition at a concentration of 10 µM. That indicates that at least one free phosphonate residue is required to have some amount of potency. In parallel to our research, the group of Peyrottes *et al.* published compound **132**,[191] which we synthesized as well and tested with a potency of 4.22 µM. The group around Du *et al.* (ORIC Pharmaceuticals) and Sharif *et al.* (Arcus Pharmaceuticals) recently published and patented variously substituted monophosphonate derivatives.[116, 118] The fact that even two pharmaceutical companies followed a very similar approach points out the competitive situation in the medicinal chemistry field of CD73. It also shows that our idea of reducing the diphosphonate moiety to a monophosphonate residue went in the right direction. Further

substitution of the N^6-position could have furthermore enhanced the potency of this compound. However, since the synthesis of these compounds appeared too elaborate considering the poor outcome, we decided to not further follow this project.

2.6 Xanthine-derived CD73 inhibitors

As already described in Chapter 2.5.1., AMPCP derivatives, despite their strong potency on CD73, possess several disadvantages, e.g. negative charges at physiological pH-values, which reduces their permeability of biomembranes.[194] Moreover, nucleotides and nucleosides display limited chemical stability under acidic conditions. Therefore, we were seeking for new scaffolds. To this end a high-throughput screening campaign was carried out, which will be described in the following chapter.

2.6.1 High throughput screening-campaign and hit-compound selection

Based on a high-throughput screening campaign (HTS-campaign), carried out by Dr. Christian Renn, several xanthine-derived hit compounds were found.[69] The campaign is reported in full detail in his PhD thesis.[69] Herein, only essential parts of the screening-campaign are described. For the high-throughput screening, an optimized malachite green phosphate assay system was employed. CD73 catalyzes the hydrolysis of AMP leading to adenosine and inorganic phosphate. In this assay, one of the enzymatic reaction products - inorganic phosphate - forms a UV-absorbing complex with ammonium heptamolybdate and malachite green.[66, 68] The UV-absorbance is caused by the formed complex and serves as a read-out for the measurement of the enzymatic activity.[66, 68] Optimization of the assay conditions provided a robust, facile, and inexpensive and thus well-suitable assay system. The assay conditions allowed an automated, robot-aided screening campaign.[69, 195] Within this screening campaign, an inhouse compound

sub-library containing over 5600 analytically and pharmacologically well characterized compounds was screened.[196] Compounds that inhibited rat soluble CD73 activity by more than 50% at a test concentration of 10 µM were declared as hits. Since this resulted in a relatively low hit-rate (0.36%), also compounds with an inhibition of more than 25% were included as hit compounds increasing the hit rate to 1.33%.[69] Hit compounds were validated by the determination of full concentration-inhibition curves in a more sensitive radiometric assay system.[70] Since most hit compounds were structurally related to the xanthine scaffold, out in-house xanthine sub-library was targeted. Compounds carrying the xanthine scaffold are well described as AR antagonists,[197–203] whereas inhibitory activity towards CD73 has to the best of our knowledge not yet been reported. These compounds caught our interest since both, inhibition of CD73 and additional antagonism of ARs, would display an intervention of two subsequent steps in purinergic signaling, and could therefore provide synergistic effects.[6, 17, 38, 59, 78, 80, 202, 204–207] The selected hit compounds consisted of a tricyclic annulated ring system, carrying methyl groups in position *N1* and *N3*. *N7* and *N9* were connected via a saturated alkyl chain to form a third ring. In position *N9*, a *para*-substituted cyclohexyl or phenyl ring was attached. The compounds were provided by Prof. Kieć-Kononowicz (Jagiellonian University, Kraków, Poland). Compounds carrying a benzyl residue in this position were found to be inactive (data not shown).[69] The potencies of the selected hits varied between 3.30 and 23.1 µM. As a lead structure for further research compounds **141** and **144** were selected. Both represent good starting points for the synthesis of a series of tricyclic xanthine-derived inhibitors for the following reasons: They carry several positions for further derivatization, they are synthetically well accessible, and with a potency of 3.30 µM for compound **144** and 23.1 µM for **141**, there is still enough room for improvement (Table 12)

Table 12. Selected hit compounds of the HTS-campaign[69]
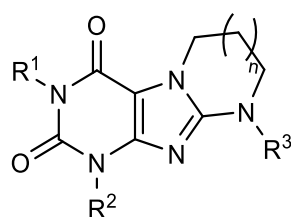
93-97

	Compound	n	R[1,2]	R[3]	Rat CD73 $IC_{50} \pm$ SEM (μM, n=3)
140	PZB01808173A	1	Methyl	3-methoxypropyl	10.0 ± 1.14
141	PZB01808014A	1	Methyl	4-hydroxyphenyl	23.1 ± 8.3
142	PZB01808055A	2	Methyl	4-hydroxycyclohexyl	13.9 ± 1.6
143	PZB01808051A	2	Methyl	4-methylphenyl	8.47 ± 1.32
144	PZB01808057A	2	Methyl	4-methoxyphenyl	3.30 ± 0.34

* or % inhibition at indicated concentration

[1]Carried out by Dr. Christian Renn

2.6.2 Design of target structures

Possible positions for modifications of the tricyclic xanthine are depicted in Figure 49. As already mentioned, we selected compounds **141** and **144** as lead structures for the synthesis of further tricyclic xanthine compounds. They differ in the ring size of ring "c". Whereas ring c of **144** is a diazepino ring, ring c of **141** is a pyrimido ring. Since almost all hit compounds as well as both lead compounds are dimethylated at *N1*- and *N9*, this derivatization pattern was kept for the first series. The alkyl chain, that connects *N7* and *N9* to form ring c, could also be further varied. For the first series, six-membered and seven-membered rings were synthesized. Furthermore, several positions of the phenyl ring, which is attached to *N9* could be investigated. The focus was set on positions 3 and 4 of the phenyl ring attached to *N9* (see Figure 49. Possible

modification of tricyclic xanthine compounds.. In these positions several substituents, like halogen atoms, trifluoromethyl, trifluoromethoxy, carboxy, sulfonamidyl etc. were to be introduced with the aim to study the SARs and to improve the potency of the lead structure.
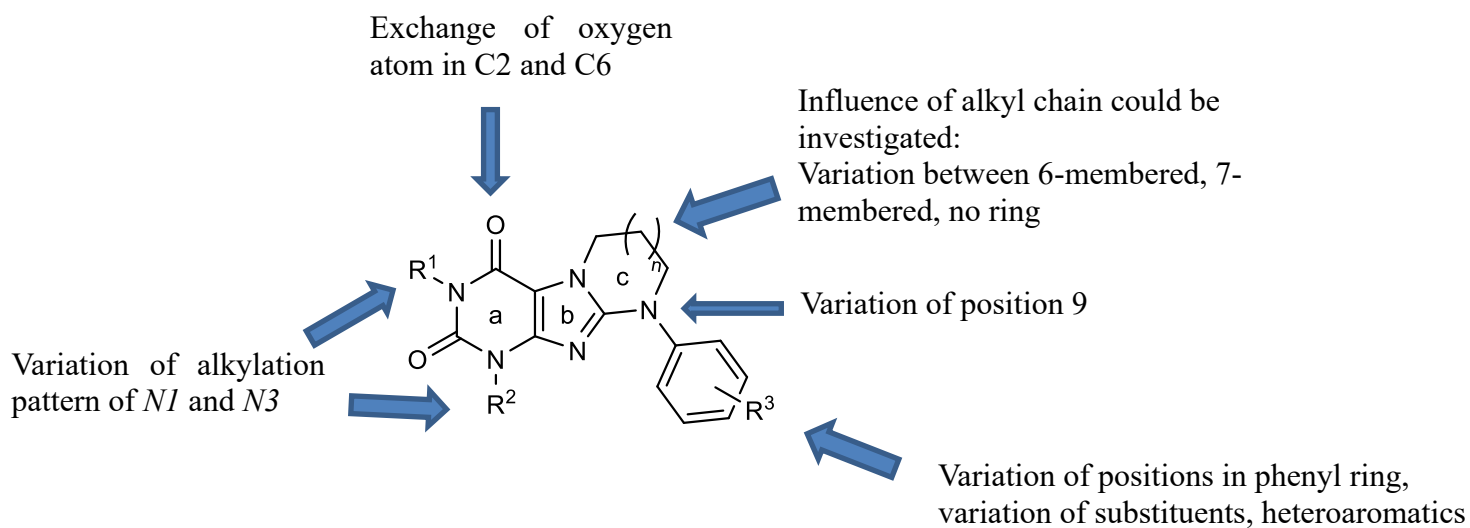
Figure 49. Possible modification of tricyclic xanthine compounds.

2.6.3   Chemistry

2.6.3.1   Synthesis of tricyclic diazepinopurinedione derivatives

Scheme 27. Synthesis of 9-phenyl-1,3-dimethyltetrahydropyrimido[2,1-*f*]purinedione derivatives[a]

Compd.	R^1	R^2
a	H	F
b	H	Cl
c	H	Br
d	H	OCF$_3$
e	CF$_3$	H
f	OCF$_3$	H
g	Cl	H
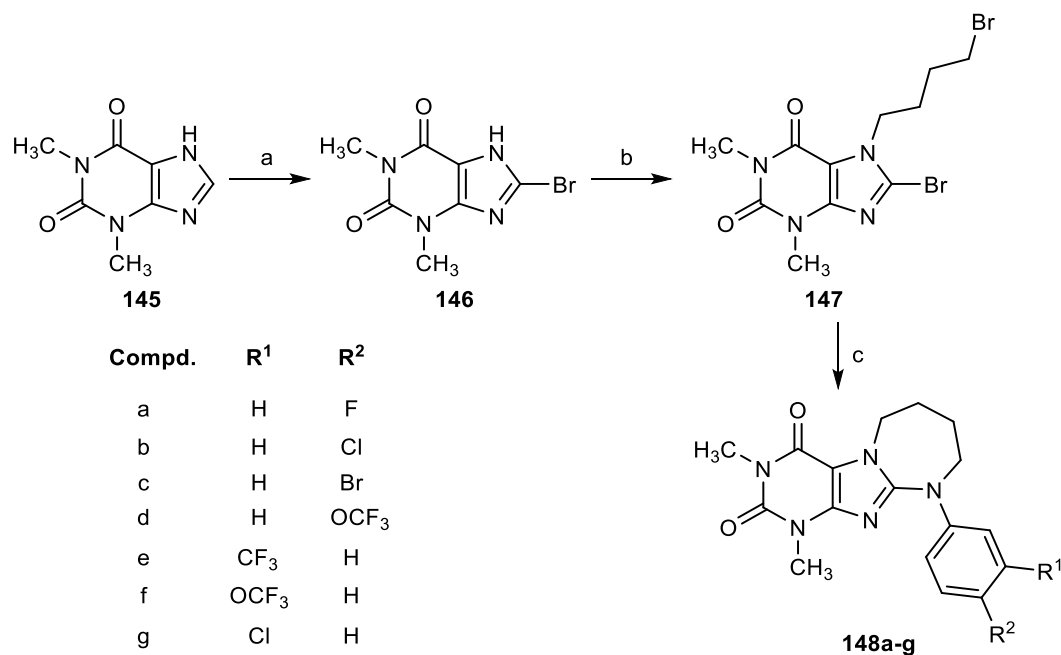
[a]Reagents and conditions: (a) bromine−H$_2$O, sodium-acetate buffer, pH 4.0, rt, overnight; (b) 1,4-dibrombutane, triethylamine, DMF, 85 °C, 2 h; (c) corresp. aniline derivative, DMF, 200 °C, 10 h.

The synthesis of the 9-phenyl-1,3-dimethyltetrahydropyrimido[2,1-*f*]purinedione derivatives was started from commercially availabe theophylline (**145**). The compound was brominated employing previously reported conditions.[102] The procedure worked straightforward for the (yield 87%) and was, due to that, upscaled to the 5 g scale. Next, 8-bromotheophylline (**146**) was alkylated at the *N7* position using 1,4-dibromobutane by stirring at 85 °C under basic conditions for 2 h affording 7-(4-bromobutyl)-8-bromo-theophylline (**147**).[197] This reaction was also up-scaled to 2 g and higher. The final reaction step was a cyclization reaction between 7-(4-bromobutyl)-8-bromo-theophylline (**148**) and the corresponding aniline derivative. The final reaction step is a cyclization reaction to form the 3-membered ring system. This reaction initially posed some problems. Various attempts using milder reaction conditions did not lead to the desired product. In the first attempts, for example, reaction conditions according to

Brunschweiger *et al.* were employed.[203] These include reacting the compounds at room temperature in DMF with DIPEA as base overnight. However, following this procedure, we could not obtain the desired product. We also tried different aniline derivatives, extended the reaction time or varied the solvents, but the desired product was not formed (see Scheme 28). Therefore, reaction conditions as described by Drabczyńska *et al.* were applied.[197] These conditions use elevated reaction temperatures without the usage of an auxiliary base. The first attempts were carried out at 170 °C for 5-10 h leading to the formation of a product mixture of mainly products **148h** and **148d** (see Scheme 29). Both products were isolated and pharmacologically evaluated. Since isolation of the respective products was rather difficult, the reaction conditions were further optimized in order to increase the yield of the desired product. Extension of the reaction time (10-12 h) and further elevation of the reaction temperature to 200 °C eventually displayed the best reaction conditions (see Scheme 27). **148c** could only be isolated in a yield of 1%, since high temperatures led to the formation of the **148i** and more side products, which complicated the isolation of the desired product. This was not observed for the 4-chloro-substituted derivative **148b**. Except for compound **148f** (yield 94%), the yields were only moderate (see Table 13). One reason for this might be high reaction temperatures that are necessary to accomplish ring closure, but also lead to side-products or degradation of the compounds. It could be discussed if the addition of an auxiliary base like DIPEA could enhance the yields.

Table 13. Yields of 9-phenyl-1,3-dimethyltetrahydropyrimido[2,1-*f*]purinedione derivatives **148a-g**

Compound	Yield
148a	24%
148b	35%
148c	1%
148d	36%
148e	35%
148f	94%
148g	43%

Scheme 28. Synthesis attempt A[a]

Compd.	R
4b	Cl
4c	Br
4d	OCF$_3$

147   **148b-d**
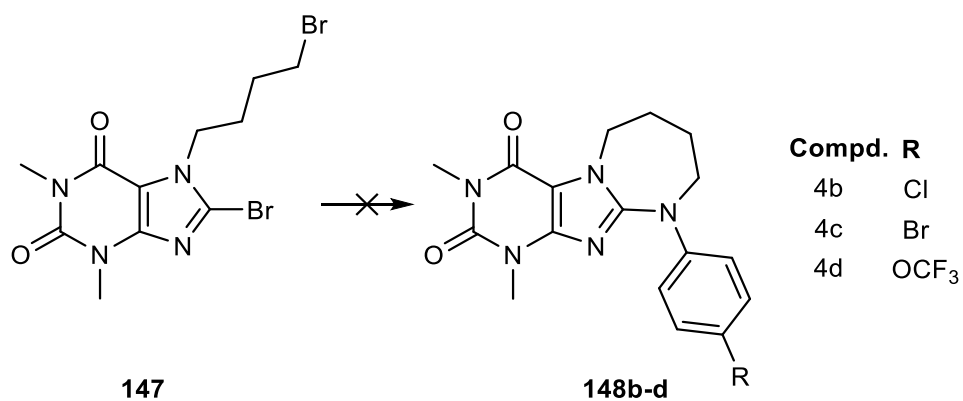
[a]Reagents and conditions: 4-trifluoromethoxyaniline/4-chloroaniline/4-bromoaniline, DIPEA, DMF, rt, overnight.

Scheme 29. Example of side-reaction[a]
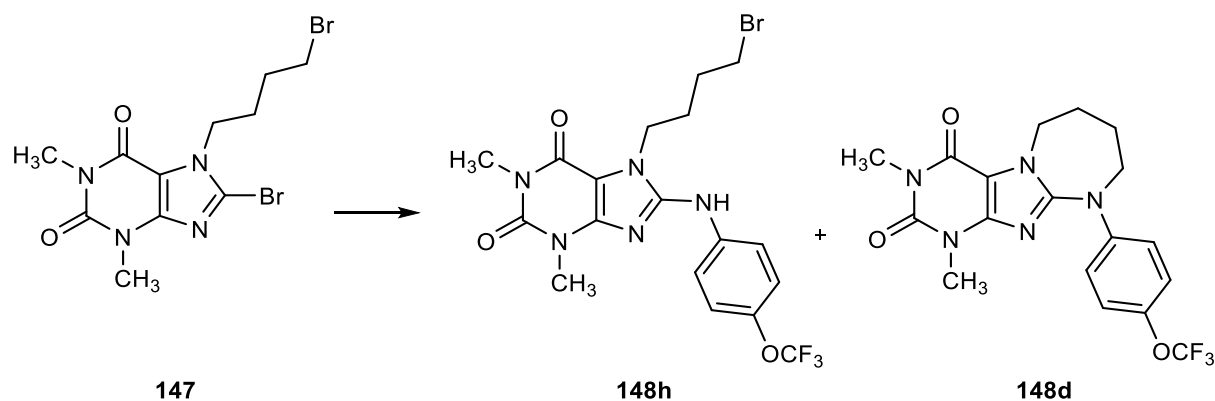
[a]Reagents and conditions: 4-trifluoromethoxyaniline, DMF, 150 °C, 10 h

Scheme 30. Formation of **148c** and side-product **148i**[a]
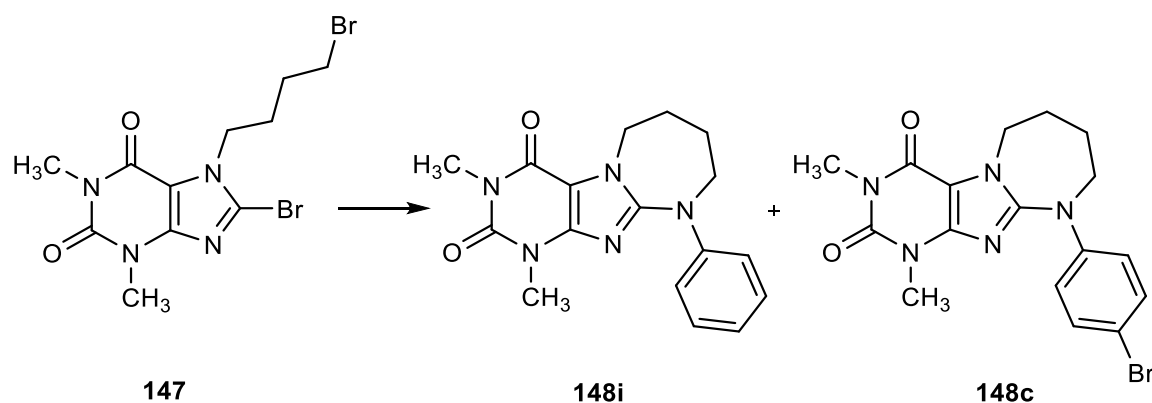
[a]Reagents and conditions: 4-bromoaniline, DMF, 200 °C, 10 h.

2.6.3.2 Synthesis of unsaturated 7-membered ring xanthines

In order to further optimize the reaction conditions (especially shortening the reaction time) another synthesis attempt was carried out. We raised the reaction temperature to 250 °C and used Dowtherm™ as solvent. This is in accordance with classical Conrad-Limpbach conditions – a synthesis for 4-hydroxyquinoline derivatives.[208] By applying this high reaction temperature, the reaction time was supposed to be shortened (3 h). However, not the desired product **148j** was formed, but product **148i**. Most likely, the high temperature has caused an oxidation of the diazepane ring leading to the 2,3-dihydro-diazepine derivative **150i** (Scheme 31). The product

119

was confirmed by ^{1}H-, and ^{13}C NMR spectroscopy, in addition to LC/ESI-(UV)MS analysis which confirmed a purity of greater than 95%.

Scheme 31. Synthesis of compound **148i** using Conrad-Limpbach reaction conditions[a]

147

148i

148g
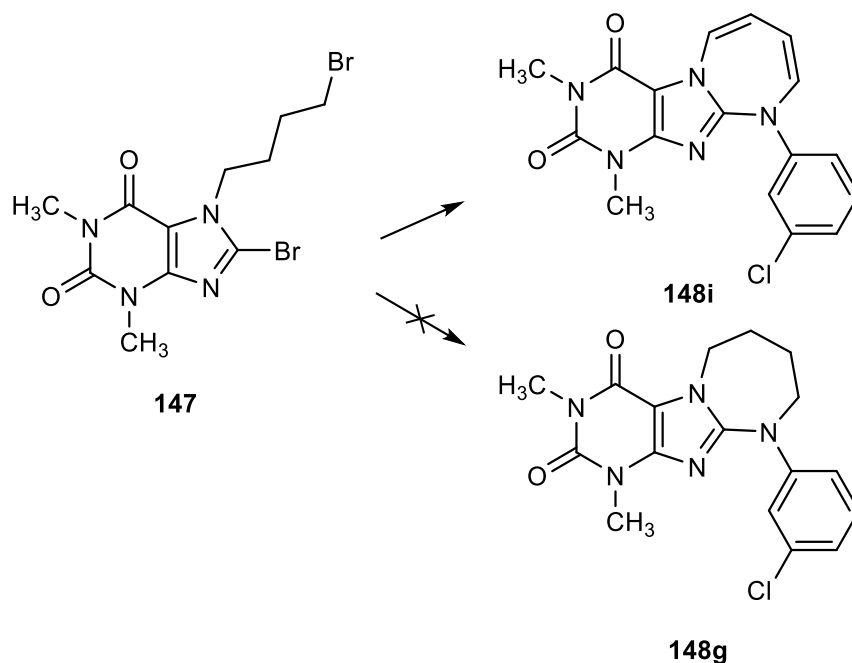
[a]Reagents and conditions: 3-Chloroaniline, Dowtherm™, 250 °C, 3 h.

2.6.3.3 Synthesis of pyrimido[2,1-*f*]purinedione derivatives

Scheme 32. Synthesis of pyrimido[2,1-*f*]purinedione derivatives **150a-i**[a]

146   **149**   **150a-i**

comp.	R$_1$	R$_2$
a	OCF$_3$	H
b	H	F
c	H	Cl
d	H	OCF$_3$
e	H	SO$_2$NH$_2$
f	H	OCHF$_2$
g	H	CF$_3$
h	Cl	F
i	H	COOH
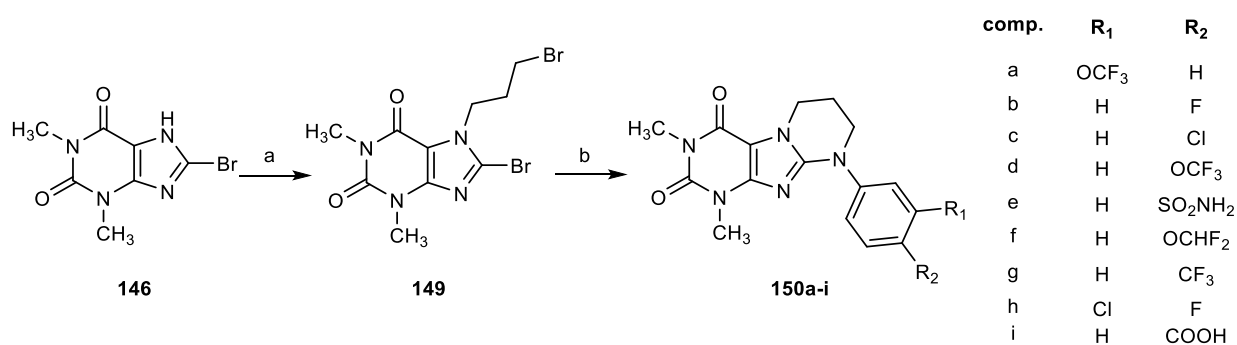
[a]Reagents and conditions: (a) 1,3-Dibromopropane, triethylamine, DMF, 85 °C, 2 h; (b) corresp. aniline-derivative, DMF, 150 °C, 10 h.

The synthetic route towards 1,3-dimethyl-9-phenyl-6,7,8,9-tetrahydropyrimido[2,1-*f*]purine-2,4(1*H*,3*H*)-dione derivatives **150a-i** is depicted in Scheme 32. The synthesis was started from 8-bromotheophylline (**146**). The bromination of theophylline has already been described in Scheme 27. The *N7*-alkylation of 8-bromotheophylline using 1,3-dibromopropane was carried out at 85 °C in triethylamine and DMF (yield: 83%). This reaction worked as straightforward as the alkylation with 1,4-dibromobutane (see Scheme 27) and was as a consequence, up-scaled. As final reaction step, 8-bromo-7-(3-bromopropyl)-1,3-dimethyl-3,7-dihydro-1*H*-purine-2,6-dione (**149**) was reacted for 10 h with the corresponding aniline derivative in DMF at 150 °C, to give the desired final products (**150a-i**). Interestingly, the cyclization reaction worked in case of the formation of 6-membered rings (**150a-i, 151a-b**) with much lower reaction temperatures than attempting the formation of 7-membered rings (**150a-i**). This is especially displayed by a lower reaction temperature. As a consequence, the formation rate of side products was reduced, which facilitated the purification process. In some cases, the desired products precipitated from the reaction mixture and only filtration and washing with different solvents was required. However, compounds with a pyridine residue required elaborate purification consisting of column chromatography, followed by RP-HPLC chromatography (Scheme 33). That led to strongly reduced yields (see Table 14). The yields of 9-phenyl-1,3-dimethyltetrahydropyrimido[2,1-*f*]purinedione derivatives (Table 13) compared with those of the 9-phenyl-1,3-dimethyltetrahydropyrimido[2,1-*f*]purinedione derivatives (Table 14) were with some exceptions in most cases lower. A reason for that might be the already mentioned milder reaction conditions, which results in lower rates of side-products and thus to facilitated purification.

Table 14. Yields of 9-phenyl-1,3-dimethyltetrahydropyrimido[2,1-*f*]purinedione derivatives

Compound	Yield
150a	72%
150b	90%
150c	53%
150d	16%
150e	42%
150f	64%
150g	32%
150h	53%
150i	9%
151a	5%
151b	7%

Scheme 33. Synthesis of pyridin-2-yl-pyrimido[2,1-*f*]purinedione derivatives (**151a,b**)[a]
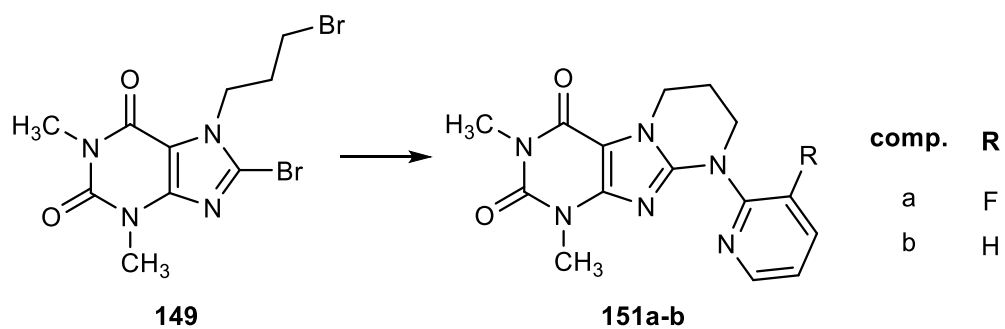
[a]Reagents and conditions: 2-aminopyridine deriv., DMF, 150 °C, 10 h.

2.6.4   Pharmacology

2.6.4.1   Hit validation as CD73 inhibitors.

After the project was in already in progress and compounds 148a-g have been synthesized, the hit compounds **140**-**144**, which had so far only been tested in a radiometric assay at recombinant soluble rat CD73 expressed in *Sf9* insect cells, and bearing a GST tag,[69] were tested at human CD73 (Dr. C. Renn).[69] Human recombinant soluble CD73 expressed in *Sf9* insect cells and membrane preparations of human triple negative breast cancer cells (MDA-MB-231), which natively (over-)express CD73, were employed.[121, 137] The results were quite surprising. Despite inhibitory potency observed at rat CD73, **140**, **142**-**144** showed no inhibition or even slight activation of soluble recombinant human CD73. Since the syntheses of compounds **148a**-**g** have already been completed at this point, they were tested on human soluble CD73 (see Table 15)**.** The results are discussed in the following chapter 2.6.4.2.

Table 15. Potencies of xanthine derivatives analyzed with different sources of CD73[69]
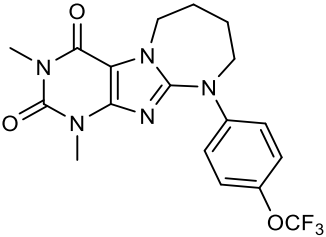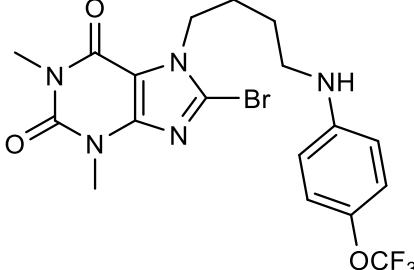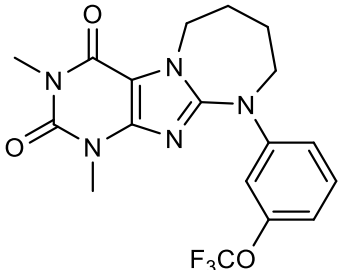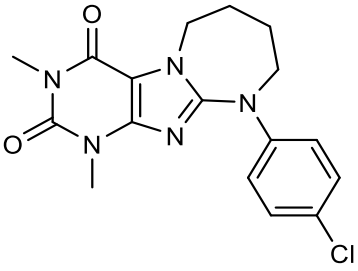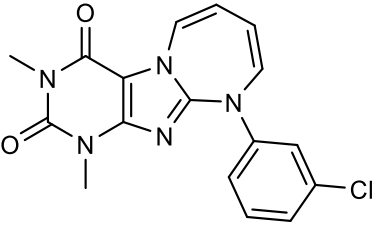
Compound	Rat CD73 $IC_{50} \pm$ SEM (μM)	Human CD73 $IC_{50} \pm$ SEM (μM)[a]	MDA-MB-231 Membrane preparation $IC_{50} \pm$ SEM (μM)
140 PZB01808173A	**10.0** $\pm$ 1.14	**> 10** (-62%)[b] **0.869** $\pm$ 0.173	**> 10** (-15%)
141 PZB01808014A	**23.1** $\pm$ 8.3	**6.57** $\pm$ 1.06	**> 10** (-8%)
142 PZB01808055A	**13.9** $\pm$ 1.6	**> 10** (-52%)*	**> 10** (-9%)
143 PZB01808051A	**8.47** $\pm$ 1.32	**> 10** (-40%)	**> 10** (-15%)
144 PZB01808057A	**3.30** $\pm$ 0.34	**> 10** (-42%)	**> 10** (-10%)
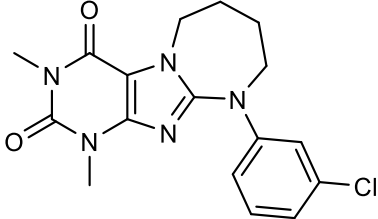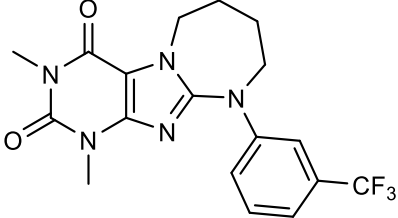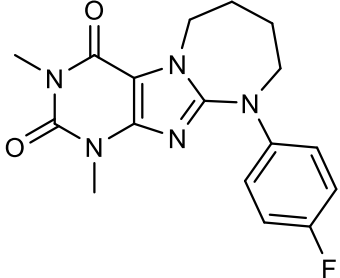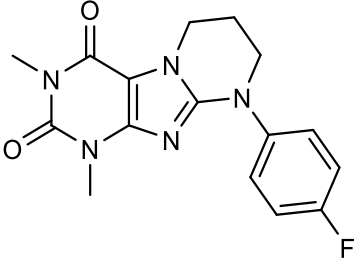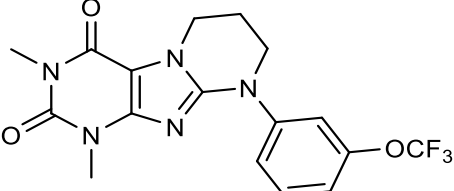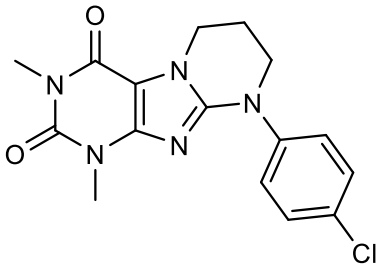
* or % inhibition at indicated concentration; [b] maximum activation
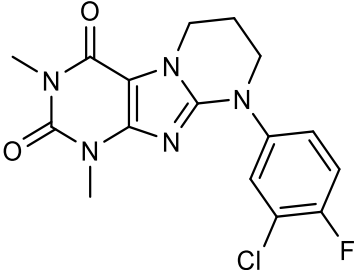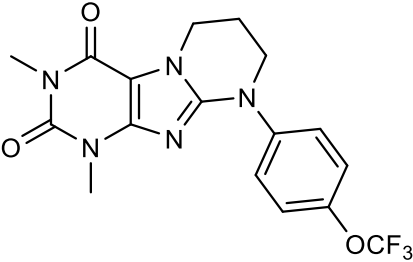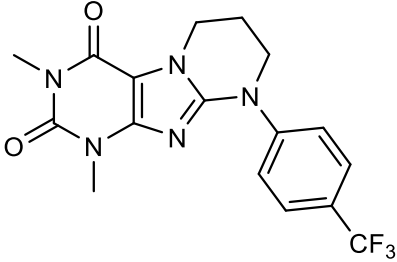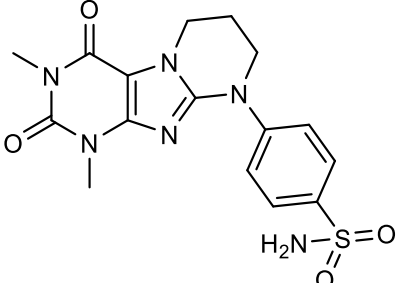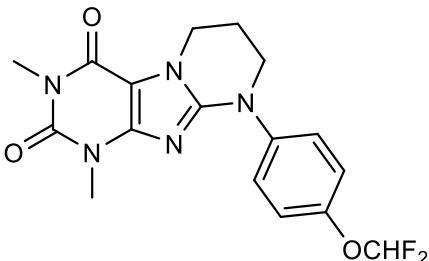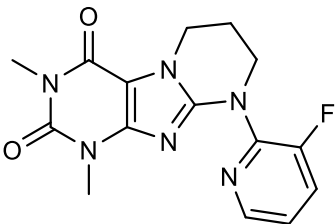
2.6.4.2 Pharmacological evaluation of synthesized xanthine derived compounds
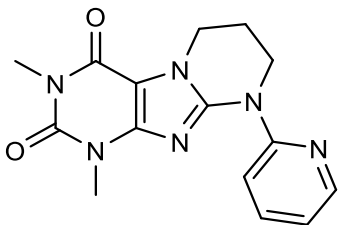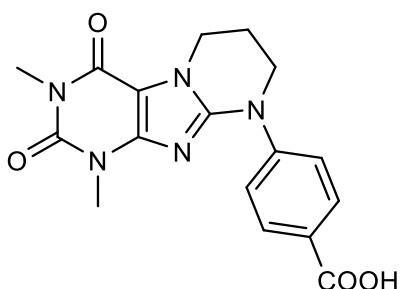
The following experiments were carried out by Dr. Christian Renn and Riham Idris. The inhibitory/activating activity of **148a-g**, **150a-i** and **151a,b** was analyzed in a radiometric enzyme assay system, which was carried out in the same fashion as already described in *Sf9* insect cells. With the exception of **148i**, test results for 9-phenyl-1,3-dimethyltetrahydropyrimido[2,1-*f*]purinedione derivatives (**148a-g**) were well in accordance with the previously described validation studies (Table 15). Except for **148i**, none of the compounds showed activity of over 50% at a concentration of 20 µM. Unfortunately, also **150a-i** and **151a-b** did not show inhibitory activity over 50% at a concentration of 20 µM. Compounds **150e** and **150f** were tested at higher concentrations (500 µM and 300µM, see

Table **16**), but did not show any activity at this high conentrations. Interestingly, **148i** was the only compound showing an activity of over 50%. However, it activated the enzymatic activity of human soluble CD73. A full concentration-response curve was determined and an *EC$_{50}$* value of 672 nM was obtained. The structurally very close compound **148g** did not show any activity. Compounds **148g** and **148i** only differ in the alkyl chain that connects *N7* and *N9*. The chain of **148i** is unsaturated, whereas the chain of **148g** is saturated. That leads to different rigidities of the alkyl chain, and **148g** is therefore a more rigid molecule. However, it is quite surprising that such small modification leads to this change in potency. Therefore, **148i** will be further investigated in different species (rat, mouse) and maybe a co-crystal structure could help to get a better understanding of the binding of these compounds. It has to be furthermore investigated, why none of the hit compounds showed activity in the MDA-MB-231 membrane preparations.

Table 16. Pharmacological evaluation of xanthine derived CD73 modulators at human soluble CD73

Compd.	Structure	Inhibition result at 20 μM (% ± SEM) (n=3)	(IC_{50} ± SEM) μM
148f		-23 ± 11%	n.d.[a]
148h		7 ± 5%	n.d.
148d		-18 ± 9%	n.d.
148b		20 ± 9%	n.d.
148i		-66 ± 3%	0.672 ± 0.327[b]

148g		9 ± 5%	n.d.
148e		-8 ± 4%	n.d.
148a		6 ± 6%	n.d.
150b		5 ± 6%	n.d.
150a		-13 ± 2%	n.d.
150c		3 ± 6%	n.d.

150h		24 ± 7%	n.d.
150d		2 ± 6%	n.d.
150g		-2 ± 8%	n.d.
150e		14 ± 3%	n.a. (no inhibition up to 500 µM)
150f		23 ± 4%	n.a. (no inhibition up to 300 µM)
151a		10 ± 6%	n.d.

| 151b | | -2 ± 3% | n.d. |

| 150i | | 8 ± 3% | n.d. |

[a][3H]AMP (5 µM) was used a substrate; K_m value 17 µM for purified recombinant soluble human CD73.[b] activation: EC_{50} ± SEM (µM), n.d. = not determined, n.a. = not active

2.6.5 Discussion and outlook

There are different reasons that could explain the large species differences between rat and human CD73. Upon binding mode experiments carried out in a malachite green assay, Dr. Christian Renn proposed a mixed inhibition mode for the xanthine compounds in his PhD thesis.[69] Only slight changes of the amino acid sequence of a less conserved allosteric binding site could lead to changes of the spatial arrangement and thus varied interactions of the binding inhibitor. Renn also proposed that the truncated *N*- and *C*-termini in combination with an additional introduction of a His-tag could led to structural modifications which again affects binding of the xanthines to an alternative binding site.[69] It was, however, not yet possible to identify an alternative binding site. Interestingly, Scaletti & Sträter *et al*., published a CD73 co-crystal structure with caffein bound to the enzyme.[209] They reported binding to the nucleoside binding site of caffein – and proposed π-stacking beween the two phenylalanine moieties Phe417 and Phe500 as single low-energy binding mode.[209] It has to be awaited, if these results can be transferred to the structurally related tricyclic xanthine derivatives. Therefore, it is

worthwile to co-crystalize the xanthine derivatives with human CD73. Selected compounds of this series will be send to Prof. Sträter, Univervisty of Leipzig, in order to further investigate the binding mode of the xanthine compounds. Compound **148i**, which activated human CD73 will also be send for co-crystallization studies, in order to investigate how the structrual variation of this compound influences the binding. In this context is to mention the 2018 reported work of Rahimova *et al.*[133] They reported non-nucleotidic compounds with mixed or allosteric binding modes, which were found in a virtual screening campaign targeting the dimer interface of human CD73. Interestingly, they observed besides moderate inhibitory potency in the low micromolar range, also activation.[133] A reason for that might be compound induced stabilizing effects of the enzymatically active conformation of CD73. On the other hand, Beatty *et al.* reported non-nucleotidic benzotriazole derivatives with strong potency ($IC_{50} = 12$ nM). X-ray co-crystallization showed binding in the active site of the enyzme, and furthermore similar binding interactions like the adenine core of AMPCP.[134] Since the newly synthesized compounds have only been tested on human soluble CD73, they will be screened on rat CD73, in order to test their activity at this species. Selected compounds could also be tested on mouse-derived CD73.

2.6.6 Conclusions

Based on a hit obtained by a screening campaign carried out at rat CD73, we synthesized a series of 19 tricyclic xanthine derivatives, which were then tested on human soluble CD73, but did not show any inhibition. Currently, confirmation experiments of the compounds depicted in Table 15 are being carried out by Patrick Bulambo-Riziki in order to verify the measured K_i value of the hit compound PZB01808014A. If the firstly reported potency could be confirmed, further compounds from the synthesized series would be tested again. Furthermore, it could be worthwhile to test representative compounds at the rat enzyme. Since the compounds are allosteric modulators, large species differences would not be surprising.

2.7 Design and synthesis of a positron emission tomography (PET) ligand

2.7.1 Background

In the framework of the design, synthesis and pharmacological evaluation of an AMPCP-derived PET-tracer, we synthesized a non-radioactive analog of the PET-Tracer (**153a**) in order to test the inhibitory potency of this compound. Furthermore, Dr. Constanze Schmies synthesized the AMPCP precursor compound (**152**),[141] which was then radioactively labeled by our cooperation partner Dr. Anna Junker (see Scheme 34) (European Institute for Molecular Imaging, University of Münster).[176] In order to carry out metabolism studies, compound **112**, which represents the unlabelled nucleoside metabolite of **155a** was synthesized.

Scheme 34. Radiosynthesis of [^{18}F]PSB-19427[a]
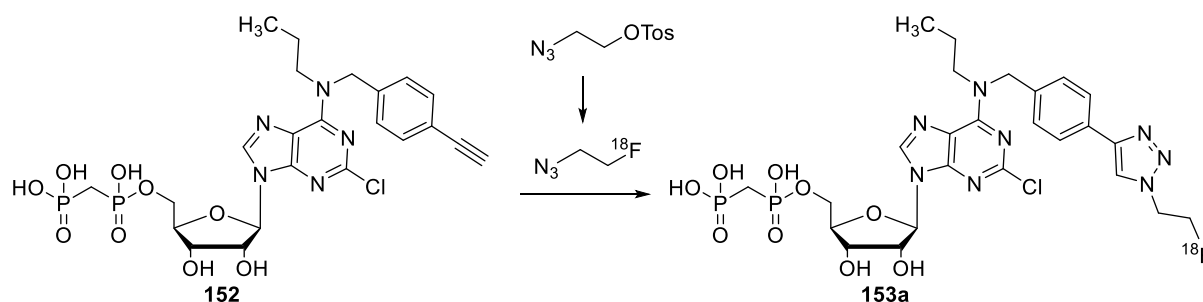
[a]Reagents and conditions: Copper sulfate, sodium ascorbate, HEPES buffer/DMF

2.7.2 Chemistry

The synthesis was started by ribosylation of 2,6-dichloropurine (**49**) with 1,2,3,5-tetraacetyl-β-D-ribofuranose (**48**) according to previously published conditions.[103] Compounds **48** and **49** were melted at 85 °C under a slight vacuum and reacted upon the addition of trifluoromethanesulfonic acid. Purification by normal phase column chromatography (DCM/methanol 98:2) led to the desired product 2,6-dichloro-9-(2′,3′,5′-tri-*O*-acetyl-*β*-D-ribofuranosyl)-9*H*-purine (**50**). In parallel, **157** (*N*-(4-ethynylbenzyl)propan-1-amine) was synthesized by alkylation of compound **156** with 1-bromopropane in methanol. By reaction of

50 with *N*-(4-ethynylbenzyl)propan-1-amine (**157**) under basic conditions in the presence of triethylamine in ethanol, the terminal alkyne group was introduced to the molecule. Basic conditions in combination with reflux led - besides the desired product - also to the partially deacetylated derivatives. Instead of purification, the crude mixture was directly employed for the next reaction step in order to obtain the fully deprotected nucleoside **158** by reacting with 1 M sodium methoxide solution in methanol.[141] The nucleoside **159** was synthesized via azide-alkyne Huisgen cycloaddition reaction.[169] 1-Azido-2-fluoroethane (**155**) was synthesized from 2-fluoroethyl-4-toluenesulfonate (**154**), which was dissolved in anhydrous DMF and sodium azide was added. The reaction was carried out for 24 h at room temperature. After TLC indicated completion of the reaction, the crude mixture was used without further purification, since isolation of 1-azido-2-fluoroethane (**155**) might lead to explosion. (2*R*,3*R*,4*S*,5*R*)-2-(2-Chloro-6-((4-ethynylbenzyl)(propyl)amino)-9*H*-purin-9-yl)-5-(hydroxymethyl)tetrahydrofuran-3,4-diol (**158**) was "clicked" to 1-azido-2-fluoroethane (**155**) using copper sulfate, sodium ascorbate and TBTA in a mixture of DMF and water (Scheme 35). After stirring overnight, the crude mixture was extracted and purified by normal phase column chromatography (yield 73%). As already described in the chapter 2.3.3.1, the click reaction worked in this case of using nucleosides as starting material straight forward, which shows, that this reaction is well-suited for the attachement of residues to nucleosides. The synthesis of **160** as well as **153b** was carried out by Dr. Constanze Schmies and is depicted in Scheme 35 for the sake of completeness.

Scheme 35. Synthesis of unlabeled analog **153b** (PSB-19427) of the selected ^{18}F-labeled PET tracer **153a** ([18F]PSB-19427) and its nucleoside metabolite **159**[176,a]
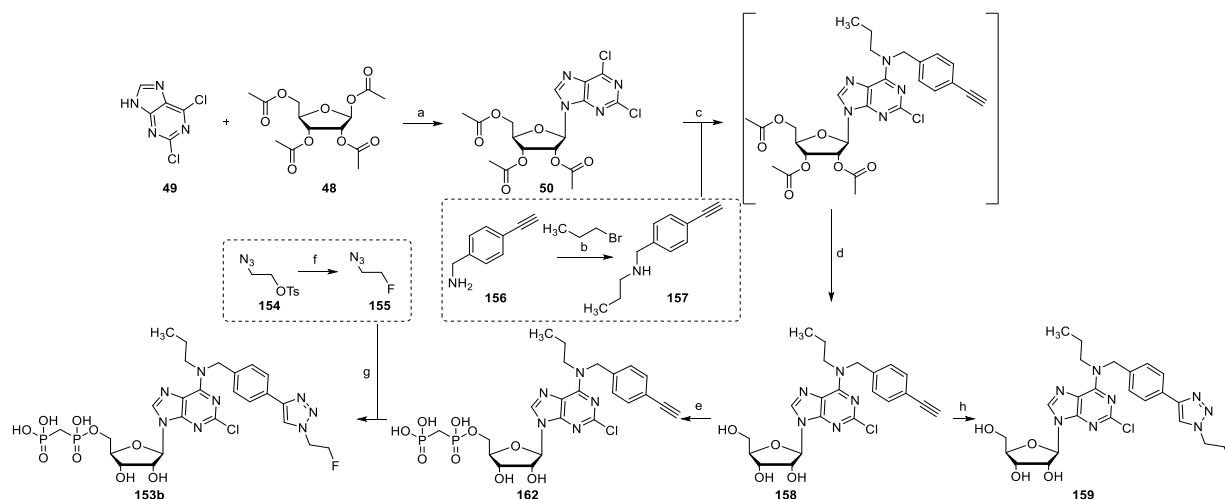
[a]Reagents and conditions: (a) Trifluoromethanesulfonic acid, 90000 Pa (0.9 bar), 85 °C –> rt, 1 h; (b) methanol, rt, 2 d; (c) triethylamine, ethanol, reflux, rt, overnight; (d) 1 M sodium methoxide, methanol, rt, overnight; (e) two steps (i) methylenebis(phosphonic dichloride), trimethyl phosphate, 0 °C, 1 h; (ii) 0.5 M TEAC buffer pH 7.4-7.6, 15 min at 0 °C, then 1 h rt; (f) sodium azide, DMF, rt, 24 h; (g) sodium ascorbate, CuSO$_4$, TBTA, THF/H$_2$O/t-BuOH, rt, overnight; (h) 2-fluoroethyl azide (**157**), sodium ascorbate, CuSO$_4$, TBTA, DMF/H$_2$O, overnight, rt.

2.7.3 Conclusions

The nucleoside was successfully synthesized and is currently being used for metabolic studies. The synthesis was straightforward. For the future it could be interesting to test the synthetic accessibility of PSB-19427 by the same sequence that was carried out for the synthesis of the nucleoside, with the addition of the phosphonylation as the final step.

3   Summary and Outlook

CD73 plays a central role in the metabolic breakdown of extracellular AMP. Overexpression of membrane-anchored CD73 in cancer and/or immune cells, which can also be released by shedding or exosomes, leads to increased extracellular adenosine levels, which activate ARs. This causes a variety of effects. In the tumor microenvironment, for example, activation of ARs leads to an immunosuppressive, proliferation-enhancing, pro-angiogenic, and pro-metastatic environment. The current situation with several clincal studies ongoing to evaluate monoclonal antibodies against CD73, in addition to the first clinical studies with small-molecule CD73 inhibitors emphasizes the clinical relevance of the target. Therefore, we drove forward the development of potent, selective and stable inhibitors as well as molecular probes. The work was divided into several sub-projects summarized in the following paragraphs.

AMPCP-derived CD73 inhibitors

-   Based on previous results, we synthesized a series of AMPCP-derived CD73 inhibitors. We selected several positions for modification of AMPCP with the aim to enhance the inhibitory potency on CD73. Our study included the investigation of further halogen atoms besides chlorine in position 2

-   the investigation of the relevance of the stereochemistry at the α-methylene position of the benzylamine residue

-   optimization of the reaction conditions (reducing formation of side-products, decreasing reaction time) to allow for an upscaling of the best inhibitors.

The compounds were tested on soluble rat and soluble human CD73. A selection of the tested compounds was furthermore tested on membrane preparations of human triple-negative breast

cancer cells (MDA-MB-231). On the basis of the results we analyzed structure-activity relationships. Halogen substitution other than chlorine were well tolerated in the 2-position (Figure 50). We furthermore found out that there is a diastereoselectivity of N^6-(1-methylbenzyl)-substituted AMPCP derivatives at human CD73, but not at rat CD73. The *S*-configurated α-methyl-substituted derivatives showed higher potencies than their *R*-configurated diastereomers. This observation is new, and could be confirmed with several derivatives. Crystallization studies with the *R*- and the *S*-isomer are currently carried out by the group of Prof. Sträter (University of Leipzig). Compounds with an *N*-methyl substitution as a second substituent on the exocyclic amino group were well accepted. The advantage of these compounds would be that their nucleoside derivative can be expected to be inactive at ARs if it were formed by metabolic reactions. Derivatization of the phenyl ring in position 2 (Cl) or 4 (OH) was well tolerated by CD73.
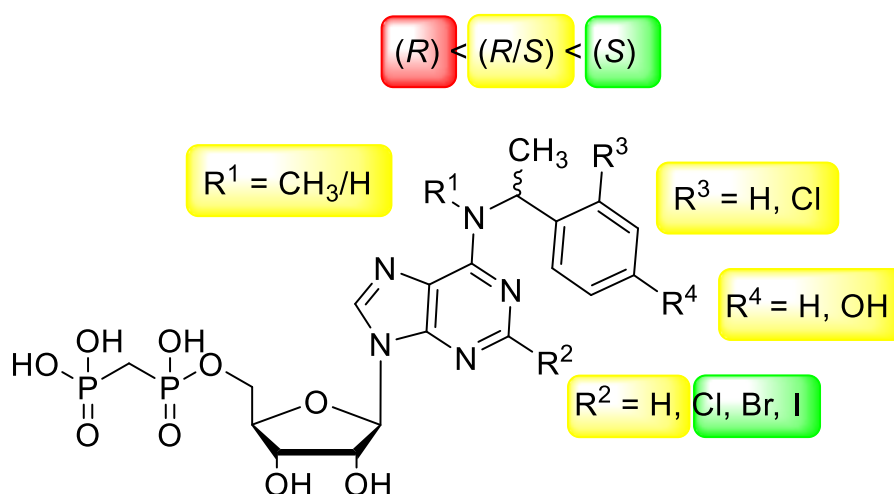
Figure 50. Structure-activity relationship of *N*-benzyl-substituted AMPCP derivatives on human CD73. Substituents that are highlighted in green are beneficial for the potency, substituents highlighted in red are not beneficial, substituents circled in yellow are accepted.

Besides the findings concerning structure-activity relationships, we improved the reaction conditions for nucleophilic substitution reactions of position 6 (see Scheme 36). We shortened

the reaction time from 24 h to 3 h. Since this reaction is frequently carried out in the synthesis of AMPCP derivatives, this improvement is quite valuable.

Scheme 36. Example for improved reaction conditions for nucleophilic substitution of position 6[a]
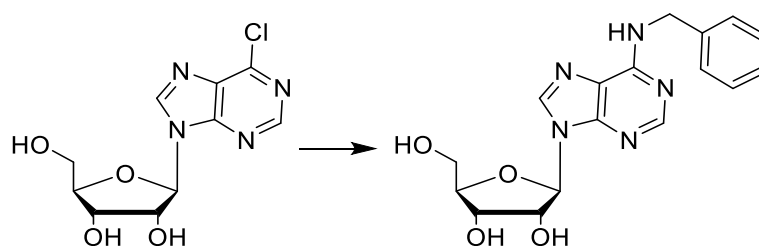
[a]Reagents and conditions: *N*-monoar(alk)ylamine or *N,N*-diar(alk)ylamine, triethylamine, ethanol, 90 °C, 3 h.

N⁶-propargyl-AMPCP derivatives

Besides the synthesis of *N*-benzyl-AMPCP derivatives, we searched for alternative residues (Figure 51). Instead of a benzylamine residue, we introduced a propargyl or butinyl residue, respectively, and evaluated their influence on CD73-inhibitory potency.
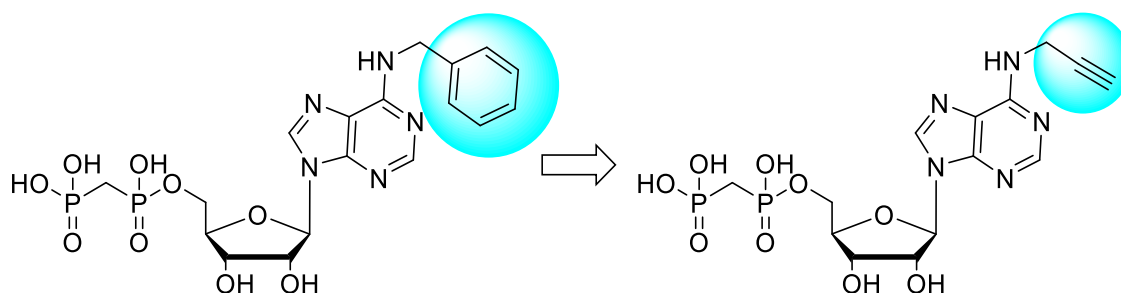
Figure 51. Reduction of the size of the *N*-benzyl residue.

From the first 5 synthesized compounds we obtained preliminary structure-activity relationships. As expected, 2-chloro-substitution enhanced the potency (see Figure 52) whereas additional methyl substitution on N^6 decreased potency significantly. The potency was improved by elongating the alkyl chain of the N^6-substituent. The resulting compound was as potent as its benzyl analog (4-ethynylbenzylamine). Besides reduction of the size, the triple-bond posseses the advantage that it can be functionalized e.g. with fluorescent dyes, nucleic acids, PROTAC moieties, antibodies or nanobodies, etc.
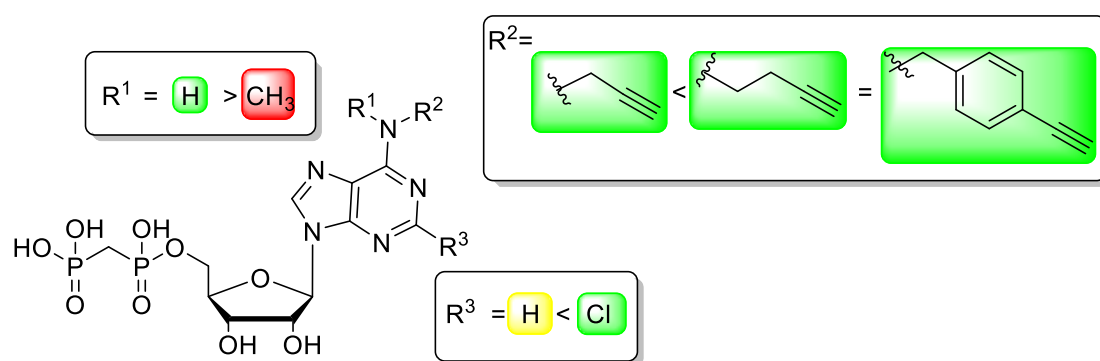
Figure 52. Structure-activity relationships of alkynyl-substituted AMPCP derivatives. Substituents that are highlighted in green are beneficial for the potency, substituents highlighted in red are not beneficial, substituents circled in yellow are accepted.

Diagnostics and tool compounds for CD73

For the development of a new fluorescence-based CD73 assay, we aimed to synthesize a fluorescein-coupled AMP derivative, which is supposed to be hydrolyzed upon incubation with CD73 (see Figure 53). After initial synthetical difficulties, we managed to establish a synthetic route that allowed us to obtain the desired product **40** as well as it nucleoside analog **41**, which is required as a reference compound being the product of the enzymatic reaction. The first

pharmacological experiments in which the substrate **40** was incubated with CD73 indicated that the fluorescent AMP derivative is indeed hydrolyzed and substrate and product could be separated by CE. Further experiments for determining for example the K_m-value and the LOD will be carried out in due course.
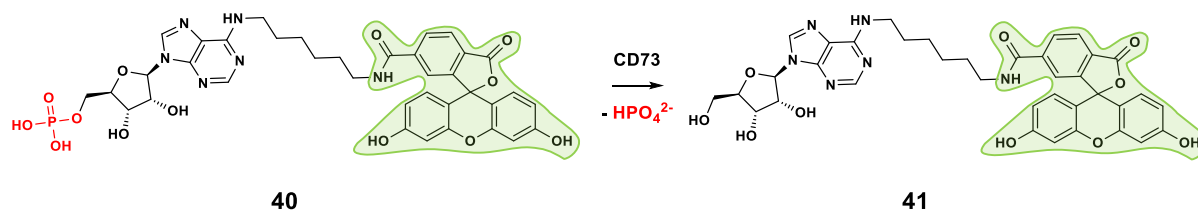
Figure 53. Hydrolysis of fluoescence-coupled AMP derivative **40** leading to fluorescence-coupled **41** via enzymatic hydrolysis by CD73

We furthermore aimed to synthesize a fluorescent ligand for CD73 in order to visualize expression levels in physiological or pathological conditions. In a recent publication by our group, we reported on a potent and selective fluorescein-labelled AMPCP-derived CD73 inhibitor. However, the originally attempted 2-chloro-substituted, fluorescein-labelled AMPCP derivative could not be synthesized during that study, and the 2-position had therefore remained unsubstituted.[137] In the present study, we successfully synthesized the desired 2-chloro-substituted compound (Figure 54), which showed high potency and selectivity for CD73. However, the additional substitution with a chlorine atom did not enhance the potency on CD73 in this case, in comparison to our previously published non-2-substituted fluorescein-labelled AMPCP derivative. Co-crystallization studies with CD73 could help to find out why the 2-chloro-substituted derivative is not as potent as would have been expected.
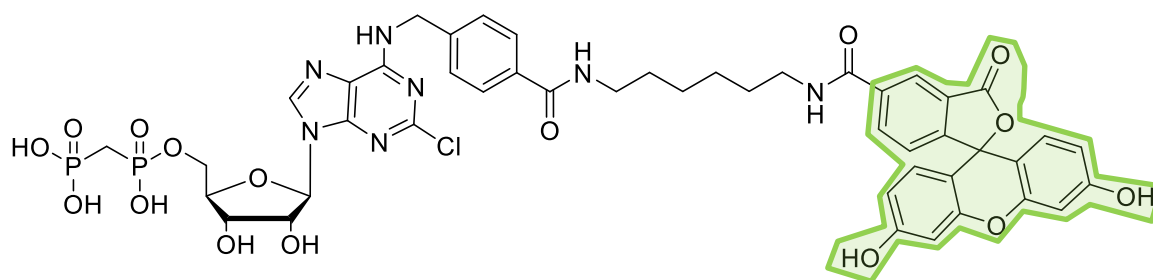
Figure 54. 2-Cl-substituted, fluorescein-labeled AMPCP **56**.

Besides fluorescein-labelled CD73 inhibitors, we selected further fluorescent dyes, e.g. BODIPY, and a near-infrared cyanine dye. The synthetic route, which we developed for the synthesis of the fluorescein-labelled CD73 inhibitors did not work for the coupling BODIPY or cyanine dyes. Despite various attempts and changes of the synthetic routes, we could not obtain the desired products. However, we succesfully synthesized a a BODIPY-labelled nucleoside derivative in low yields. For the future, this reaction could be upscaled and further attempts phosphonylating this nucleoside could be carried out. The synthesis of a cyanine-bound AMPCP derivative has not been successful until now. Since we figured that complexing of the copper ions by the diphosphonate structure might impair the click-reaction, employing a copper-free click reaction could help to obtain the desired product. Another idea could be to swap the azide and alkyne residues.

AMPCP-derived inhibitors for attachment to a nanogel

A CD73 inhibitor for covalent coupling to a nanogel was designed and synthesized. Due to its physicochemical properties, the nanogel forms micelles. Upon acidic pH-values in the tumor microenvironment, the micelles are expected to disassemble into soluble chains, which releases the drug and allows it to access the target of interest resulting in drug targeting. The obtained results were, however, not consistent. Regardless of the pH-value in which the nanogel-bound CD73 inhibitor was measured, the determined potencies were virtually the same. This means that decreasing of the pH-value had apparently no effect on the binding of the compound, which

138

is contrary to our expectations (for a detailed discussion, see chapter 2.4.6). These results suggest that the CD73 inhibitor was actually not covalently bound to the nanogel, but rather trapped in the inside of the micelle and then released upon dissolution. In the future, it has to be figured out, if the compound is indeed covalently bound to the nanogel. It should be highlighted that a potent, amino-functionalized CD73 inhibitor could be developed showing high potency (**65**, K_i = 0.284 nM, Figure 55) which allows its coupling to e.g. polymers, fluorescent dyes, antibodies etc.

65
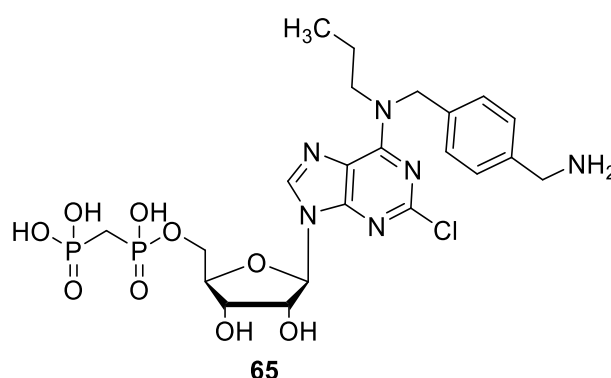
Figure 55. AMPCP-derived CD73 inhibitor containing a free primary amino group **65**

Nucleotide-mimetic compounds

Since AMPCP derived CD73 inhibitor are – despite their high potency – associated with several diasadvantages as for example high polarity, we aimed to synthesize compounds that circumvent these disadvantages by replacing the diphosphonate structure. Despite several synthetic difficulties, we could obtain seven diverse AMPCP-mimetic compounds. With the exception of compound **85** (K_i = 4.22 µM), which carried a terminal phosphonate group, none of the compounds showed activity towards CD73. These results show that at least one phosph(on)ate group has to be present for interaction with the catalytic zinc cations. Neither a diethoxy-protected phophono group was not tolerated, nor a substituted or unsubstituted sulfonamide residues (Figure 56).
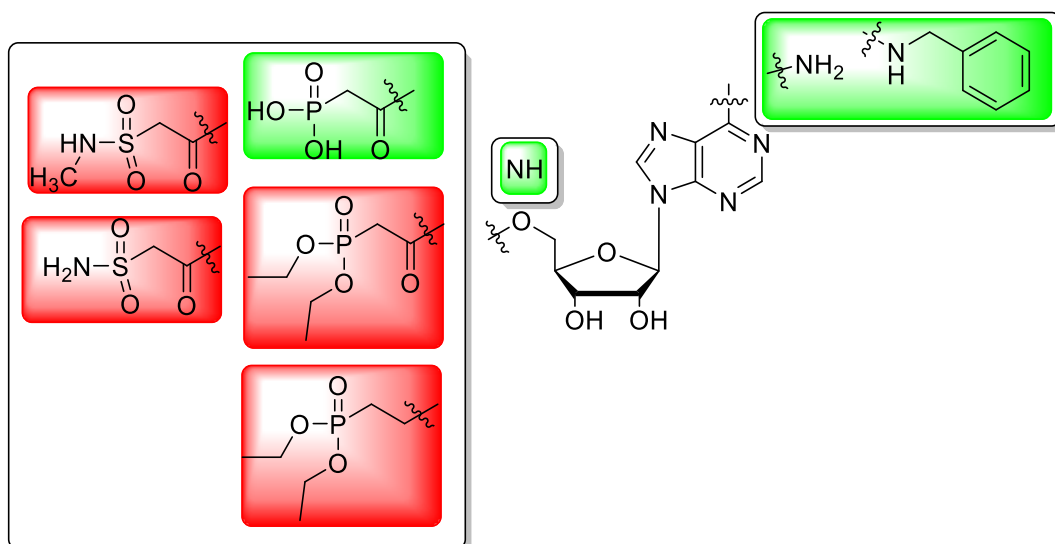
Figure 56. Structure-activity relationships of AMPCP-mimetic derivatives as inhibitors of CD73. Beneficial residues are highlighted in green, not-tolerated residues are highlighted in red.

Xanthine-derived CD73 inhibitors

In order to explore new scaffolds for inhibitors of CD73, a high-throughput screening campaign of our in-house compound library was carried out.[69] From the hit compounds, which were found to be active on rat-derived CD73, we selected a tricyclic xanthine derivatives as a lead scaffold. A series of 19 tricyclic xanthine-derived compounds was synthesized. However, none of the compounds showed inhibition of human CD73. Surprisinlgy, compound **101i** led to an activation of human soluble CD73 (EC$_{50}$ = 0.672 nM). The only structural variation compared to the other derivatives is the unsaturated diazepino ring, which gives the compound more rigidity (Figure 57, see **101g** vs. **101i**).
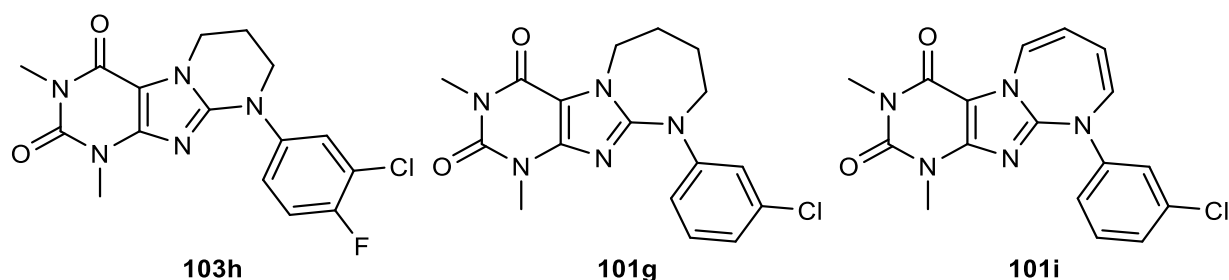
Figure 57. Examples for synthesized tricyclic xanthine derivatives.

Assuming that these compounds are allosteric modulators, large species differences would not be surprising, since an allosteric binding site might be less conserved than the substrate binding site. Crystallization studies are planned to identify the allosteric binding site.

Design and synthesis of a positron emission tomography (PET) ligand

Within a project focusing on the development of the PET-tracer **106**, we synthesized its unlabelled nucleoside derivative **112** (Figure 58) which was required for metabolic studies. From a chemical perspective, it would be interesting to see, if it is possible to phosphonylate the nucleoside **112**, since large residues in the N^6-position have often impaired the phosphonylation reactions. If the phosphonylation worked, the synthetic strategy could be changed in the future, which might provide enhanced yields of the desired nucleotide analogs.
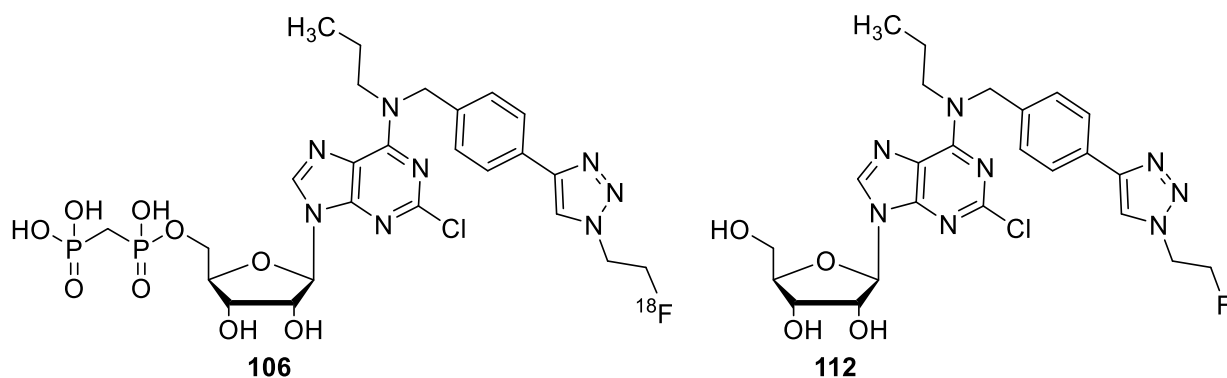
Figure 58. [^{18}F]PSB-19427 (**106**) and its unlabelled nucleoside derivative **112**.

141

The present study provides a variety of contributions to the development of CD73 modulators, that will be useful as pharmacological tools, or provide a basis for future drug development. CD73 possesses high relevance in immunity and inflammation, and is currently probed a novel drug target in cancer immunotherapy.

4   Material and Methods

4.1   Pharmacological evaluation at CD73

4.1.1   Expression of recombinant soluble CD73

Expression experiments were carried out by Dr. Christian Renn, Tobias Claff, and Riham Idris. Human soluble CD73 was expressed in *Sf9* insect cells and purified as previously described.[121] The cDNA encoding for the mature human CD73 (residues 27-549) fused to 6xHis-tag at the C-terminus (Genbank accession no. NM_002526) corresponding to the natural variant T376A (P21589/VAR_022091, UniProtKB/Swiss-Prot) was ligated into the pAcGP67B vector. For transfection, 1 µl of the recombinant vector (1000 ng/µl) blended with 2.5 µl of baculovirus genomic DNA ProEasy™ (AB vector, CA, USA) was used to transfect *Sf9* cells grown in Insect-XPRESS™ medium (#BE12-730Q, Lonza, Switzerland) supplemented with 10 mg/l gentamicin. Via ultrafiltration with Amicon® Ulta-15 filters, 10 KDa cut-off (Merck Milipore, MA, USA), the generated soluble enzyme was then concentratedand and purified by metal affinity chromatography (IMAC) over HisPur™ Ni-NTA spin columns (#88226, Thermo Fisher Scientific, MA, USA) according to the manufacturer's protocol. The purified enzyme was aliquoted and stored at -80˚C until further use. A previously published method was used to express the glutathione-S-transferase fusion protein of soluble rat CD73 in *Sf9* insect cells.[210]

4.1.2 Cell culture

The cells were cultures as previously described by Junker *et al.*[121] Natively CD73 expressing MDA-MB-231 cells were grown in Dulbecco's Modified Eagle Medium (DMEM, #: 41966, Thermo Fisher Scientific, MA, USA) supplemented with 10% fetal bovine serum (FBS, #: P30-1502, PAN Biotech, Germany) and 100 U/ml penicillin + 100 µg/ml streptomycin (#: P06-07100, PAN Biotech, Germany). The cells were incubated at 37 °C with 5% CO_2 for 72 h to reach 80 – 90% confluence. Confluent cells were washed with phosphate-buffered saline (PBS), and subsequently detached by 5-min incubation with trypsin/ethylenediaminetetraacetic acid (EDTA) (0.05%/0.6 mM, #P10-022100, PAN Biotech, Germany). Detached cells were re-suspended in culture media and split 1:20.

4.1.3 Membrane preparations

Membrane preparations were generated as described by Junker and Renn *et al.*[121] and were generated by Christian Renn.[69] Confluent cells grown in 175 cm^2 culture flasks were detached as described in chapter 4.1.2. Culture dishes (150 cm^2) were seeded with approx. 100 cells/dish and incubated at 37 ˚C, 5% CO_2 for 4 days. The growth medium was discarded, and the dishes were washed with 10 ml PBS and frozen at -20 ˚C. Frozen cells were scraped off the dishes with 1 ml of ice-cold buffer (50 mM Tris, 2 mM EDTA, pH 7.4), and were collected in a conical tube, in which they were centrifuged at 1000g at 4 ˚C for 10 min. After that, the pellets were resuspended in buffer (0.5 ml/dish; 25 mM Tris, 1 mM EDTA, 320 mM sucrose, pH 7.4, 1:1000 protease inhibitor cocktail #P8340, Sigma-Aldrich, MO, USA) and homogenized three times for 30 s each (20,500 rpm, Ultraturrax, IKA-Labortechnik, Germany). The homogenate was centrifuged for 10 min at 1000g and 4 ˚C, and the supernatant was collected and centrifuged for further 30 min at 48,000g, 4 ˚C. The obtained pellets were resuspended in washing buffer (0.5 ml/dish) and centrifuged using the same conditions. After three more times washing, the

pellets were resuspended in Tris buffer 50 mM, pH 7.4 (0.1 ml/dish), aliquoted, and stored at -80 °C until usage.

4.1.4 Enzyme inhibition assay

Inhibition of the compounds was investigated employing a previously described procedure by Junker and Renn *et al.*[69–71, 121] The experiments were carried out by Christian Renn, Riham Idris, Katharina Sylvester, Jessica Nagel and Patrick Bulambo-Riziki. Stock solutions of the corresponding compounds (10 µl) were prepared in demineralized water. Further dilutions were prepared in reaction buffer (Tris 25 mM, NaCl 140 mM, sodium dihydrogen phosphate 25 mM, pH 7.4). For screening experiments, 10 µl of the corresponding stock solution were transferred into the respective test tube supplemented with 70 µl of the reaction buffer. For generating concentration-response curves, 10 µl of different dilutions of the respective test compounds were pipetted into the test tubes. Except for the negative controls, all test tubes contained a solution or suspension of soluble or membrane-bound CD73 (10 µl, soluble rat CD73: 1.63 ng; soluble human CD73: 0.365 ng; membrane preparation of MDA-MB-231 cells expressing CD73: 7.4 ng of protein per vial). In order to start the enzymatic reaction, 10 µl (5 µM final concentration) of the radioactively-marked substrate $[2,8-^3H]AMP$ (specific activity 7.4 x 108 Bq/mmol (20 mCi/mmol)), American Radio-labeled Chemicals, MO, USA, distributed by Hartman Analytic, Germany) was added. The samples were incubated for 25 min at 37 °C in a shaking water bath, and then were cooled on ice. In order to terminate the enzymatic reaction and to enable precipitation of remaining substrate $[2,8-^3H]AMP$ and inorganic phosphate, 500 µl of precipitation buffer (lanthanum chloride, 100 mM in sodium acetate 100 mM, pH 4.0) were added. The samples were cooled over ice for at least 30 min, and subsequently filtered through GF/B glass fiber filters using a Brandel cell harvester (M-48, Brandel, MD, USA). The solution was then washed three times with 400 µl of cold (4 °C) demineralized water each and subsequently, scintillation cocktail (5ml) (ULTIMA Gold XR, PerkinElmer, MA, USA) was

added. Finally, radioactivity was measured employing a scintillation counter (Tri-Carb 2900TR, Packard/PerkinElmer). All experiments were conducted in duplicate, baseline-corrected and normalized against negative and positive controls, respectively. Data from three independent experiments were analyzed using Prism-GraphPad 8 (GraphPad Software, La Jolla, USA). With the help of the Cheng-Prusoff equation the K_i value was calculated from the obtained IC_{50} values using the following K_m values (K_m, rat CD73: 53.0 µM; K_m, human CD73: 17.0 µM; K_m, (MDA-MB-231): 14.8 µM).[150]

4.1.5 Operation conditions for CD73 CE assay with LIF detection

Analysis was carried out using P/ACE MDQ CE system (Beckman Instruments, Fullerton, CA, USA). The separation was performed in a polyacrylamide-coated capillary [30 cm (10 cm effective length) $\times$ 50 µm (id), $\times$ 360 µm (od)]. Before each run, the capillary was rinsed with the background electrolyte (50 mM phosphate buffer (pH 6.5)) for 1 min at 30 psi. Samples were electrokinetically injected by applying voltage of -6 kV for 30 s at the capillary outlet and the nucleotides were separated by voltage application of -15 kV and 0.2 psi pressure and detected with LIF-detection ($\lambda_{ex.}$ 488 nm and $\lambda_{em.}$ 510 nm).

4.1.6 Assay conditions for fluorescent CD73 assay

500 nM of FL-6-AMP was incubated with 35.0 ng/ml human CD73 for 2, 5, 10 and 15 min at 37 °C and the enzyme reaction was stopped by heating at 95 °C for 10 min (here the assay buffer was 10 mM HEPES buffer incl. 2 mM $CaCl_2$ and 1 mM $MgCl_2$, pH 7.4). The enzyme mixtures were then 1:20 diluted with 10 mM CHES buffer (incl. 2 mM $CaCl_2$ and 1 mM $MgCl_2$, pH 9.0) before running in the CE.

4.2 Pharmacological evaluation at CD39

4.2.1 Material

ATP, calcium chloride, magnesium chloride, 4-(2-hydroxyethyl)piperazine-1-ethanesulfonic acid (HEPES), ammonium heptamolybdate, Brij®L23, DMSO, malachite green and polyvinyl alcohol were obtained from Sigma (Steinheim, Germany). Disodium hydrogenphosphate and sulfuric acid were purchased from Carl Roth (Karlsruhe, Germany).

4.2.2 Malachite green assay for NTPDases-1, -2, -3 and -8

Selectivity studies at NTPDases-1, -2, -3 and -8 were conducted by Laura Schäkel. The enzyme activity assay was carried out following a modified, previously published procedure.[66] The reaction buffer contained 10 mM HEPES, 2 mM $CaCl_2$, 1 mM $MgCl_2$, pH 7.4 in a final volume of 100 µL in transparent 96-well half area plates and the compound concentration was set to 50 µM. The final concentration of DMSO was 2%. Recombinant COS-7-cell membrane preparations expressing the appropriate NTPDase isoenzyme (ca. 100 ng of protein depending on enzyme activity)[24, 211] were preincubated with or without inhibitor at 37°C and gentle shaking (Eppendorf Thermomixer comfort at 500 rpm) for 5 min. The amount of enzyme preparation was adjusted to provide 10 – 20 % substrate conversion. The reaction was started by the addition of 50 µM ATP for CD39 (K_m (CD39) = 17 µM) and 100 µM for NTPDases2, -3 and -8 (K_m (NTPDase2) = 70 µM; K_m (NTPDase3) = 75 µM; K_m (NTPDase8) = 46 µM).[212] The enzymatic reaction was stopped after 15 min by addition of the detection reagents (20 µL malachite green solution (0.6 mM) and 30 µL ammonium molybdate solution (20 mM) in sulfuric acid (1.5 M)). After 20 min, free (inorganic) phosphate was quantified at 25 °C by measuring the absorption of the malachite green-phosphomolybdate complex at a wavelength

of 600 nm. The phosphate concentration was calculated by subtracting the absorption of the negative control samples, which were incubated with denatured enzyme (90°C, 15 min), and the inhibition was calculated as follows:

$$\boldsymbol{Inhibition}\ (\%) = \frac{\boldsymbol{(B-T)}}{\boldsymbol{B}} * \boldsymbol{100}\ \%$$

where B is the average absorption of the positive control without inhibitor and T is the absorption in the presence of the test compound.

Full concentration-inhibition curves with inhibitor concentrations ranging from 0.01 to 300 μM were determined in the presence of 2% DMSO using 100 ng membrane preparations of COS-7 cells containing recombinant CD39 or NTPDase3.[24, 211] Three independent experiments were performed and the IC_{50} and values were calculated by the GraphPad Prism 8 software. K_i-values were determined with the Cheng-Prusoff equation.[150]

4.3 Chemicals

All reagents were commercially obtained from various companies (Aldrich, Enamine Building Blocks, Fluka, Merck, TCI Chemicals, abcr etc.) and were used without further purification. Commercial solvents of specific reagent grades were used, without additional purification or drying. The reactions were monitored by TLC using aluminum sheets with silica gel 60 F_{254} (Merck) and using DCM/methanol (98:2,96:4,9:1,8:2) or ethyl acetate (100%) as mobile phase. Column chromatography was carried out with silica gel 0.060-0.200 mm, pore diameter ca. 6 nm.

4.4 Instrumentation

High-resolution mass spectra were recorded on a micrOTOF-Q mass spectrometer (Bruker, Berlin, Germany) (ESI-source) coupled with a HPLC Dionex Ultimate 3000 (Thermo

Scientific, Darmstadt, Germany) using flow injection mode. Sample solution was injected to a flow of 0.3 ml/min acetonitrile containing 0.1% acetic acid or 0.1% formic acid. Positive or negative full scan MS was observed from 50 - 1000 m/z. As calibrant, sodium acetate or sodium formate was used., which can result in the formation of M+H as well as M+Na. Mass spectra were recorded on two different devices. Low-resolution mass spectra were recorded on an API2000 mass spectrometer (AB Sciex, Darmstadt, Germany) ESI-source coupled with a HPLC HP1100 (Agilent Technologies, Waldbronn, Germany) using an EC50/2 Nucleodur C18 Gravity 3 µm column (Macherey-Nagel, Düren, Germany). The column temperature was set to 25 °C. Elution was started from 90% water containing 2mM ammonium acetate following a gradient to 100% methanol containing 2mM ammonium acetate in 10 min. The column was subsequently flushed for 10 min with 100% methanol containing 2mM ammonium acetate. LCMS samples were dissolved in methanol containing 2mM ammonium acetate 1 mg/ml. A sample of 8 µl sample solution was injected into the HPLC instrument employing a flow rate of 0.3 ml/min. UV absorption was detected from 190 – 900 nm using a diode array detector (DAD). Purity was determined at 220-400 nm. Positive total ion scans were observed from 150 - 800 m/z. Low-resolution mass spectra were furthermore recorded on an Infinity Lab LC/MSD-system (Agilent Technologies, Waldbronn, Germany) (ESI-source) coupled to a HPLC 1260 Infinity II-system (Agilent Technologies, Waldbronn, Germany) using a EC50/2 Nucleodur C18 Gravity 3 µm column (Macherey-Nagel, Düren, Germany). The column temperature was 40 °C. Elution was started from 90% water containing 2mM ammonium acetate following a gradient to 100% acetonitrile. The column was subsequently flushed for 10 min with 100% acetonitrile. Samples were dissolved in water, methanol or acetonitril ~ 1 mg/ml. A sample of 2 µl sample solution was injected into the HPLC instrument employing a flow rate of 0.5 ml/min. Positive total ion scans were observed from 100 - 1000 m/z (or more if necessary). The UV absorption was detected from 190 – 600 nm using a DAD. Purity was determined at 220-600 nm. ^{1}H, ^{13}C, ^{31}P NMR spectra were recorded on Bruker Avance 500 MHz and Bruker

Avance III HD 600 MHz spectrometers. DMSO-d_6, CDCl$_3$ and D$_2$O was used as solvent. In some cases, when D$_2$O was used as solvent, 1-2 drops of NaOD were added for solubility enhancement. Shifts are given in ppm relative to the remaining protons of the deuterated solvents used as internal standard (^{1}H, ^{13}C NMR). ^{31}P-NMR was measured at room temperature with phosphoric acid (85%) as external standard and shifts are given relative to it. In spectra, recorded in D$_2$O, 3-(trimethylsilyl)propionic-2,2,3,3 acid sodium salt-d_4 was used as external standard. When DMSO-d_6 was used as a solvent, spectra were recorded at 30 °C. Shifts are provided in ppm relative to the external standard (for ^{31}P-NMR spectra) or relative to the remaining protons of the deuterated solvents used as internal standards (^{1}H, ^{13}C-NMR spectra). Coupling constants are given in Hertz (Hz). Signals in the spectra were assigned as follows: singlet (s), doublet (d), triplet (t), quartet (q), multiplet (m), broad (br). For lyophilisation, the samples were freezed in liquid nitrogen and lyophilized by a Christ Martin™ Freeze dryer alpha 1-4 LSCPLUS (Fisher scientific, Hampton, New Hampshire, USA). Melting points were determined on a Büchi B-540 melting point apparatus (Büchi Labortechnik AG, Flawil, Switzerland).

Purification of Nucleotides

Purification of nucleotides was carried out on a preparative RP-HPLC- Knauer Smartline 1800 pump (KNAUER Wissenschaftliche Geräte GmbH, Berlin, Germany), equipped with a VarioPrep HPLC column VP250/21 NUCLEODUR 100-5 C$_{18}$ ec, 250 mm x 21 mm, pore size 110 Å (Macherey-Nagel GmbH, Düren, Germany). UV absorption was detected from 200 – 400 nm using a DAD.

4.5 Experimental Procedures

4.5.1 General procedures

General procedure A. 2,6-Dichloro-9-(2′,3′,5′-tri-*O*-acetyl-β-D-ribofuranosyl)purine, 6-chloro-2-iodo-9-(2′,3′,5′-tri-*O*-acetyl-β-D-ribofuranosyl)-9*H*-purine or 6-chloro-9-(β-D-ribofuranosyl)purine (1.0 eq.) was dissolved in ethanol. Triethylamine (2.0 eq.) and the corresponding *N*-monoar(alk)ylamine or *N*,*N*-diar(alk)ylamine were added to the solution, which was then refluxed at 90 °C for 3-5 h. Progress of the reaction was monitored by silica gel TLC (DCM/methanol 9/1). After TLC indicated completion of the reaction the volatiles were evaporated. The subsequent deprotection reaction was carried out without further purification. The crude mixture was dissolved in methanol and 5 – 8 ml of 7N ammonia in methanol were added. After stirring overnight at ambient temperature, the volatiles were evaporated and the crude mixture purified by normal phase column chromatography (silca gel, DCM/methanol 96/4). Appropriate fractions were pooled and the eluents were evaporated to give the desired compound. [102, 103, 109, 111]

General procedure B. 6-Chloro-2-iodo-9-(2′,3′,5′-tri-*O*-acetyl-β-D-ribofuranosyl)-9*H*-purine (1.0 eq.) was dissolved in ethanol. Triethylamine (2.0 eq.) and the corresponding *N*-monoar(alk)ylamine or *N*,*N*-diar(alk)ylamine was added to the solution, which was then refluxed at 90 °C for 3-5 h. Progress of the reaction was monitored by silica gel TLC (DCM/methanol 9/1). After TLC indicated completion of the reaction, the volatiles were evaporated. The subsequent deprotection reaction was carried out without further purification. The crude reaction mixture was dissolved in methanol again and 5 – 8 ml of 7N ammonia in methanol were added. After stirring overnight at ambient temperature, the volatiles were evaporated and the crude mixture purified by normal phase column chromatography (silca gel,

DCM/methanol 96/4). Appropriate fractions were pooled and the eluents were evaporated to give the desired compound. [102, 103, 109, 111]

General procedure C. The nucleoside (1 eq.) was dissolved in 5 ml of trimethyl phosphate and stirred at 0 °C. Methylenbis(phosphonic dichloride) (5 eq.) was dissolved in 2 ml of trimethyl phosphate, cooled down to 0 °C and then added dropwise to the reaction mixture. The reaction was stirred at 0 °C for 1 h. After 1 h, the reaction was quenched by addition of 5 ml of 1 M TEAC buffer (pH 7.4) and stirred for 1 hour at room temperature. Next, the reaction mixture was extracted with TBME (2 x 300 ml). The obtained mixture of the desired nucleotide analog and side-products was purified by RP-HPLC using a gradient of acetonitrile/water (containing 0.05% TFA) from 20:80 to 80:20. Suitable fractions were pooled and lyophilized to obtain the desired product. [102–104, 109, 111]

General procedure D. The nucleoside monophosphate/nucleoside diphosphonate derivative (1.0 eq.) was dissolved in ethanol. Triethylamine (2.0 eq.) was added to the reaction mixture. The corresponding benzylamine derivative (2.0 eq.) was added to the reaction mixture, which was then stirred for 3-5 h at 90 °C under reflux. After completion of the reaction, the volatiles were evaporated an the crude mixture was purified by RP-HPLC using a gradient of acetonitrile/water (containing 0.05% TFA) from 20:80 to 80:20.[102, 103, 109]

General procedure E. A mixture of the respective benzylamine derivative (1 eq.) and formamide (1.3 eq.) was stirred under neat conditions at 80 °C for 24 h. The reaction mixture was then cooled to room temperature and dissolved in 10 ml of dry THF. The reaction mixture was put under Argon atmosphere and LiAlH$_4$ (3 eq.) was added portionwise. After 1 hour of stirring, the reaction mixture was heated to reflux for 1 hour. After TLC (DCM/methanol 9/1)

indicated completion of the reaction, the reaction was cooled to $0 - 4$ °C again and was carefully quenched by adding water, 1 N NaOH and water in a sequence. The mixture was extracted using DCM, and purified by normal phase column chromatography (DCM/methanol 9/1) to give the desired compound.

General Procedure F. The nucleoside (1 eq.) was dissolved in ethanol. Triethylamine (2 eq.) and the corresponding aklynylamine (2 eq.) was added to the reaction mixture, which was stirred for 3-5 h at 90 °C under reflux. After TLC indicated completion of the reaction, the volatiles were evaporated and the crude mixture was purified using normal phase column chromatography (DCM/methanol 96/4). Appropriate fractions were pooled and evaporated to give the desired product.[102, 103, 109, 111]

General procedure G. The nucleoside (1 eq.) was dissolved in 5 ml of trimethyl phosphate and stirred at 0 °C. Methylenbis(phosphonic dichloride) (5 eq.) was dissolved in 2 ml of trimethyl phosphate, cooled down to 0 °C and then added dropwise to the reaction mixture. The reaction was stirred at 0 °C for 1 h. After 1 h, the reaction was quenched by addition of 5 ml of 1 M TEAC buffer (pH 7.4) and stirred for 1 h at room temperature. Next, the reaction mixture was extracted with TBME (2 x 300 ml). The obtained mixture of the desired nucleotide analog and side-products was purified by RP-HPLC using a gradient of acetonitrile/water (containing 0.05% TFA) from 20:80 to 80:20. Suitable fractions were pooled and lyophilized to obtain the desired product. [102–104, 109]

4.5.2 (2*R*,3*R*,4*S*,5*R*)-2-(2-Bromo-6-chloro-9*H*-purin-9-yl)-5-

(hydroxymethyl)tetrahydrofuran-3,4-diol, (CAS 1359824-18-2)
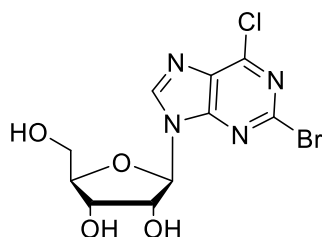
(2*R*,3*R*,4*S*,5*R*)-2-(2-Amino-6-chloro-9*H*-purin-9-yl)-5-(hydroxymethyl)tetrahydrofuran-3,4-diol (0.4 g, 1.0 g, 1.33 mmol, 1 eq.) was suspended in 20 ml of CH_2Br_2. TBN (1.57 ml, 26.5 mmol, 20 eq.) was added dropwise. TMSBr (3.94 ml, 11.9 mmol, 9 eq.) was added carefully to the reaction mixture which was then stirred overnight.[143] The reaction mixture was then transferred dropwise into a mixture of 200 ml ethyl acetate and 200 ml of sodium hydrogencarbonate. The organic phase was 2 times extracted with sodium hydrogencarbonate and subsequently washed with brine. After drying with $MgSO_4$, the mixture was filtered through a pore 4 filter and the filtrate was evaporated. The resulting residue was then purified by normal phase column chromatography (DCM/methanol 9/1). The pure fractions were pooled together and the eluents were evaporated to give the desired product (0.27 g, yield 56%). ^{1}H NMR (600 MHz, DMSO-d_6) δ 8.96 (s, 1H, C8), 5.97 (d, J = 5.0 Hz, 1H, C1′-H), 5.65 (s, 1H, OH), 5.32 (s, 1H, OH), 5.10 (s, 1H, OH), 4.52 (t, J = 5.0 Hz, 1H, C2′-H), 4.18 (t, J = 4.5 Hz, 1H, C3′-H), 3.99 (q, J = 4.0 Hz, 1H, C4′-H), 3.73 – 3.68 (m, 1H, C5′-H), 3.62 – 3.57 (m, 1H, C5′-H). ^{13}C NMR (151 MHz, DMSO-d_6) δ 153.06 (1C, C6), 151.16 (1C, C2), 149.59 (1C, C4), 141.77 (1C, C8), 131.31 (1C, C5), 88.23 (1C, C1′), 85.78 (1C, C4′), 74.07 (1C, C2′), 69.94 (1C, C3′), 60.83 (1C, C5′). LC-MS (m/z): positive mode 366.9 [M+H]$^+$. Purity determined by HPLC-UV (254 nm)-ESI-MS: 94%. HRMS (ESI): m/z [M + Na]$^+$ calcd for $C_{10}H_{10}BrClN_4O_4$ 386.9466, found: 386.9463. Mp. 176 – 178 °C.

4.5.3 (2*R*,3*R*,4*R*,5*R*)-2-(Acetoxymethyl)-5-(2,6-dichloro-9*H*-purin-9-yl)tetrahydrofuran-3,4-diyl diacetate
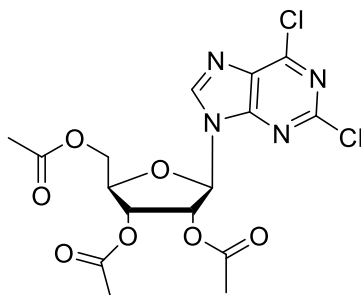
1,2,3,5-Tetra-*O*-acetyl-*β*-D-ribofuranose (5.0 g, 15.7 mmol, 1 eq.) was melted at 108 °C in a two-neck round bottomed flask. 2,6-Dichloropurine (2.97 g, 15.7 mmol, 1 eq.) was added to the reaction mixture. Trifluoromethanesulfonic acid (70 µl, 0.75 mmol, 0.05 eq.) was added to the reaction mixture and vacuum was installed at the flask. The reaction was stirred for 8 h at 108 °C.[138, 139] After TLC (DCM/methanol 9/1) indicated the end of the reaction, the volatiles were evaporated and the resulting crude mixture was purified by column chromatography (silica, DCM/methanol 9/1). Purified fractions were pooled, the solvents were evaporated and 1.88 g of a brown solid could be obtained as product (1.88, yield 27%). ^{1}H NMR (500 MHz, DMSO-*d6*) δ 8.90 (s, 1H, C8-H), 6.31 (d, *J* = 4.9 Hz, 1H, C1′-H), 5.90 (t, *J* = 5.4 Hz, 1H, C2′-H), 5.61 (t, *J* = 5.5 Hz, 1H, C3′-H), 4.45 – 4.41 (m, 1H, C4′-H), 4.41 – 4.37 (m, 1H, C5′-H), 4.31 – 4.26 (m, 1H, C5′-H), 2.11 (s, 3H, CH$_3$), 2.05 (s, 3H, CH$_3$), 2.01 (s, 3H, CH$_3$). ^{13}C NMR (126 MHz, DMSO-*d6*) δ 170.10 (1C, C=O), 169.45 (1C, C=O), 169.31 (1C, C=O), 152.91 (1C, C6), 151.45 (1C, C2), 150.40 (1C, C4), 131.37 (1C, C5), 86.37 (1C, C1′), 80.00 (1C, C4′), 72.50 (1C, C2′), 69.92 (1C, C3′), 62.75 (1C, C5′), 20.59 (1C, $\underline{C}$H$_3$), 20.47 (1C, $\underline{C}$H$_3$), 20.33 (1C, $\underline{C}$H$_3$). LC-MS (m/z): positive mode 447.1 [M+H]$^+$. Purity determined by HPLC-UV (254 nm)-ESI-MS: 93%. Mp. 159 – 161 °C

4.5.4 1-(2-Chlorophenyl)-*N*-methylethan-1-amine
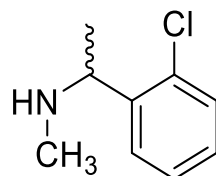
1-(2-Chlorophenyl)-*N*-methylethan-1-amine was synthesized according to general procedure E. The desired compound was obtained as yellow oil (0.21 g, yield: 64%). ^{1}H NMR (600 MHz, DMSO-*d$_6$*) δ 7.58 – 7.55 (m, 1H, aryl), 7.38 – 7.31 (m, 2H, aryl), 7.24 – 7.20 (m, 1H, aryl), 3.98 (q, *J* = 6.6 Hz, 1H, N-C<u>H</u>), 2.10 (s, 3H, N-CH$_3$), 1.19 (d, *J* = 6.6 Hz, 3H, α-CH$_3$). ^{13}C NMR (151 MHz, DMSO-*d$_6$*) δ 142.72 (1C, aryl), 132.28 (1C, aryl), 129.09 (1C, aryl), 127.88 (1C, aryl), 127.37 (1C, aryl), 127.32 (1C, aryl), 55.57 (1C, N-C<u>H</u>), 34.09 (1C, N-CH$_3$), 22.62 (1C, α-CH$_3$). LC-MS (m/z): positive mode 170.0 [M + H]$^+$. Purity determined by HPLC-UV (254 nm)-ESI-MS: 87%.

4.5.5 1-(2-Chlorophenyl)-*N*-methylmethanamine
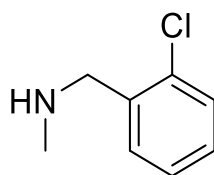
1-(2-Chlorophenyl)-*N*-methylethan-1-amine was synthesized according to general procedure E. The desired desired product was obtained as yellow oil (0.21 g, yield: 69%). ^{1}H NMR (500 MHz, DMSO-*d$_6$*) δ 7.48 (d, *J* = 7.5 Hz, 1H, aryl), 7.39 (d, *J* = 7.8 Hz, 1H, -ryl), 7.30 (m, 1H, aryl), 7.25 (m, 1H, aryl), 3.70 (s, 2H, NH-CH$_2$), 2.29 (s, 3H, CH$_3$). ^{13}C NMR (126 MHz, DMSO-*d$_6$*) δ 137.97 (1C, CH$_2$-aryl), 132.71 (1C, Cl-aryl), 129.82 (1C, aryl), 129.10 (1C, aryl), 128.31 (1C, aryl), 127.08 (1C, aryl), 52.24 (1C, CH$_2$), 35.77 (1C, CH$_3$). LC/ESI-MS (m/z):

positive mode 155.8 [M+H]$^+$ (calcd. mass for $C_8H_{11}ClN$ 156.1). Purity determined by HPLC-UV (254 nm)-ESI-MS: 95%.

4.5.6 (2R,3S,4R,5R)-2-(Hydroxymethyl)-5-(2-iodo-6-(methyl(1-phenylethyl)amino)-9H-purin-9-yl)tetrahydrofuran-3,4-diol
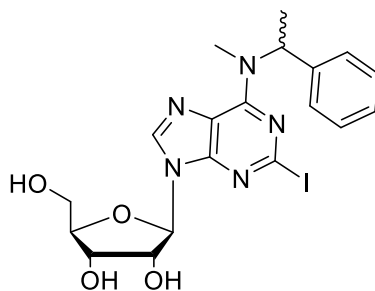
(2R,3S,4R,5R)-2-(Hydroxymethyl)-5-(2-iodo-6-(methyl(1-phenylethyl)amino)-9H-purin-9-yl)tetrahydrofuran-3,4-diol was synthesized according to general procedure B (0.14 g, overall yield: 70%). ^{1}H NMR (600 MHz, DMSO-d_6) δ 8.34 (s, 1H, C8-H), 7.37 – 7.31 (m, 4H, aryl), 7.30 – 7.26 (m, 1H, aryl), 5.85 (d, J = 5.9 Hz, 1H, C1′-H), 5.46 (d, J = 6.1 Hz, 1H, C4′-H), 5.19 (d, J = 5.0 Hz, 1H, C2′-H), 5.03 – 4.97 (m, 1H, C3′-H), 4.56 – 4.49 (m, 1H, OH), 4.12 (q, J = 4.5 Hz, 1H, OH), 3.94 (q, J = 4.5 Hz, 1H, OH), 3.67 – 3.60 (m, 1H, C5′-H), 3.57 – 3.51 (m, 1H, C5′-H), 2.82 (s br, 1H, N-C$\underline{H}_3$), 1.61 (d, J = 5.4 Hz, 3H, α-C$\underline{H}_3$). ^{13}C NMR (126 MHz, DMSO-d_6) δ 153.38 (1C, C6), 150.63 (1C, C2), 140.28 (1C, C4), 138.00 (1C, C8), 128.25 (2C, aryl), 127.03 (2C, aryl), 126.68 (2C, aryl), 119.52 (1C, C5), 87.40 (1C, C1′), 85.66 (1C, C4′), 73.63 (1C, C2′), 70.31 (1C, C3′), 61.30 (1C, C5′), 53.34 (1C, N-C$\underline{H}$), 29.84 (1C, N-CH$_3$), 15.75 (1C, α-CH$_3$). LC-MS (m/z): positive mode 512.0 [M + H]$^+$.Purity determined by HPLC-UV (254 nm)-ESI-MS: 97%. HRMS (ESI): m/z [M + Na]$^+$ calcd for $C_{19}H_{22}IN_5O_4$ 534.0609, found: 534.0620. Mp 151 - 153 °C.

N-CH peak in ^{1}H NMR not visible

4.5.7 (2*R*,3*R*,4*S*,5*R*)-2-(6-((2-Chlorobenzyl)(methyl)amino)-2-iodo-9*H*-purin-9-yl)-5-(hydroxymethyl)tetrahydrofuran-3,4-diol
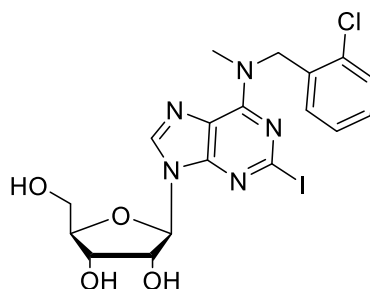
(2*R*,3*R*,4*S*,5*R*)-2-(6-((2-Chlorobenzyl)(methyl)amino)-2-iodo-9*H*-purin-9-yl)-5-(hydroxymethyl)tetrahydrofuran-3,4-diol was synthesized according to general procedure B (0.18 g, overall yield: 91%). ^{1}H NMR (500 MHz, DMSO-d_6) δ 8.23 (s, 1H, C8-H), 7.46 – 7.41 (m, 1H, aryl), 7.30 – 7.20 (m, 2H, aryl), 7.16 – 7.02 (m, 1H, aryl), 5.79 (d, J = 6.0 Hz, 1H, C1'-H), 5.59 – 5.44 (m, 1H, OH) 5.39 (d, J = 6.1 Hz, 1H, OH), 5.14 (d, J = 4.9 Hz, 1H, OH), 5.04 – 4.83 (m, 2H, CH$_2$), 4.46 (d, J = 6.1 Hz, 1H, C2'-H), 4.11 – 4.04 (m, 1H, C3'-H), 3.93 – 3.85 (m, 1H, C4'-H), 3.67 – 3.57 (m, 1H, C5'-H), 3.52 – 3.45 (m, 1H, C5'-H), 1.23 – 1.17 (m, 3H, CH$_3$). ^{13}C NMR (126 MHz, DMSO-d_6) δ 157.88 (1C, C2), 153.89 (1C, C6), 150.93 (1C, C4), 139.35 (1C, C8), 129.66 (2C, aryl), 128.96 (2C, aryl), 127.65 (2C, aryl), 119.56 (1C, C5), 87.22 (1C, C1'), 85.91 (1C, C4'), 73.72 (1C, C2'), 70.56 (1C, C3'), 61.48 (1C, C5'), 45.89 (1C, CH$_2$), 34.48 (1C, N-CH$_3$). LC-MS (m/z): positive mode 532.2 [M + H]$^+$. Purity determined by HPLC-UV (254 nm)-ESI-MS: 97%. HRMS (ESI): m/z [M + Na]$^+$ calcd. for C$_{18}$H$_{19}$ClIN$_5$O$_4$ 554.0063, found: 554.0081. Mp. 171 - 173 °C.

4.5.8 (2R,3R,4S,5R)-2-(6-((1-(2-Chlorophenyl)ethyl)(methyl)amino)-2-iodo-9H-purin-9-yl)-5-(hydroxymethyl)tetrahydrofuran-3,4-diol
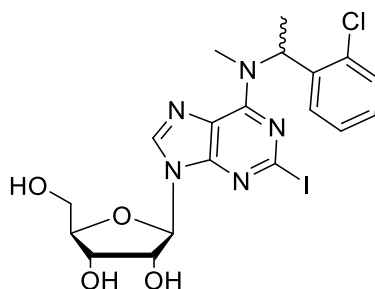
(2R,3R,4S,5R)-2-(6-((1-(2-Chlorophenyl)ethyl)(methyl)amino)-2-iodo-9H-purin-9-yl)-5-(hydroxymethyl)tetrahydrofuran-3,4-diol was synthesized according to general procedure B (0.14 g, overall yield 70%). ^{1}H NMR (600 MHz, DMSO-d_6) δ 8.38 – 8.32 (m, 1H, C8-H), 7.66 – 7.60 (m, 1H, aryl), 7.48 – 7.45 (m, 1H, aryl), 7.44 – 7.40 (m, 1H, aryl), 7.39 – 7.34 (m, 1H, aryl), 5.85 (d, J = 6.1 Hz, 1H, C1′-H), 5.48 – 5.44 (m, 1H, OH), 5.23 – 5.18 (m, 1H, OH), 5.03 – 4.98 (m, 1H, OH), 4.58 – 4.50 (m, 1H, C2′-H), 4.15 – 4.09 (m, 1H, C3′-H), 3.96 – 3.92 (m, 1H, C4′-H), 3.68 – 3.60 (m, 1H, C5′-H), 3.58 – 3.49 (m, 1H, C5′-H), 2.71 (s, 3H, N-CH$_3$), 1.67 – 1.53 (m, 3H, CH$_3$). ^{13}C NMR (151 MHz, DMSO-d_6) δ 150.71 (1C, C2), 142.56 (1C, C6), 138.40 (1C, C8), 132.29 (1C, C4), 129.70 (1C, aryl), 129.50 (1C, aryl), 129.24 (1C, aryl), 129.12 (1C, aryl), 119.59 (1C, C5), 87.01 (1C, C1′) , 85.78 (1C, C4′), 73.50 (1C, C2′), 70.45 (1C, C3′), 61.37 (1C, C5′), 55.55 (1C, N-CH), 34.04 (1C, N-CH$_3$), 22.54 (1C, α-CH$_3$). LC-MS (m/z): positive mode 546.1 [M + H]$^+$. Purity determined by HPLC-UV (254 nm)-ESI-MS: 93%. HRMS (ESI): m/z [M + H]$^+$ calcd for C$_{19}$H$_{21}$ClIN$_5$O$_4$ 546.0400, found: 546.0411. Mp. 168 – 170 °C

N-CH- peak in ^{1}H-NMR not visible

4.5.9 (2R,3R,4S,5R)-2-(2-Chloro-6-((1-(2-chlorophenyl)ethyl)(methyl)amino)-9H-purin-9-yl)-5-(hydroxymethyl)tetrahydrofuran-3,4-diol
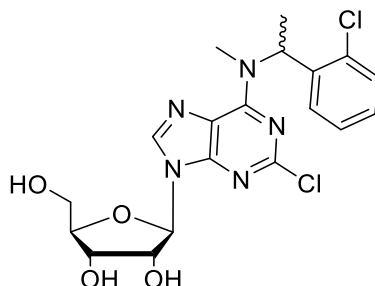
(2R,3R,4S,5R)-2-(2-Chloro-6-((1-(2-chlorophenyl)ethyl)(methyl)amino)-9H-purin-9-yl)-5-(hydroxymethyl)tetrahydrofuran-3,4-diol was synthesized according to general procedure A. (0.099 g, overall yield 46%). ^{1}H NMR (600 MHz, DMSO-d_6) δ 8.44 (s, 1H, C8-<u>H</u>), 7.65 (d, J = 7.7 Hz, 1H, aryl), 7.49 – 7.41 (m, 2H, aryl), 7.38 (t, J = 7.6 Hz, 1H, aryl), 5.86 (d, J = 5.9 Hz, 1H, C1′-<u>H</u>), 5.50 – 5.47 (m, 1H, OH), 5.22 – 5.17 (m, 1H, OH), 5.03 (q, J = 5.4 Hz, 1H, OH), 4.58 – 4.49 (m, 1H, C2′-<u>H</u>), 4.13 (q, J = 4.6 Hz, 1H, C3′-<u>H</u>), 3.94 (q, J = 3.8 Hz, 1H, C4′-H), 3.68 – 3.62 (m, 1H, C5′-H), 3.57 – 3.52 (m, 1H, C5′-H), 1.63 (s, 3H, α-CH$_3$). ^{13}C NMR (151 MHz, DMSO-d_6) δ 152.48 (1C, C2), 151.46 (1C, C6), 136.77 (1C, C4), 134.01 (1C, C8), 129.74 (1C, aryl), 129.58 (1C, aryl), 129.32 (1C, aryl), 127.33 (1C, aryl), 118.75 (1C, C5), 87.19 (1C, C1′), 85.66 (1C, C4′), 73.53 (1C, C2′), 70.28 (1C, C3′), 61.26 (1C, C5′), 55.11 (1C, N-<u>CH</u>), 30.33 (1C, N-CH$_3$), 18.52 (1C, α-CH$_3$). LC-MS (m/z): positive mode 454.2 [M + H]$^+$. Purity determined by HPLC-UV (254 nm)-ESI-MS: 96%. HRMS (ESI): m/z [M + Na] $^+$ calcd for C$_{19}$H$_{21}$O$_4$N$_5$Cl$_2$ 476.0863, found 476.0857. Mp. 193 – 195 °C.

N-CH- peak in ^{1}HNMR not visible

4.5.10 (2*R*,3*R*,4*S*,5*R*)-2-(2-Bromo-6-(methyl(1-phenylethyl)amino)-9*H*-purin-9-yl)-5-(hydroxymethyl)tetrahydrofuran-3,4-diol
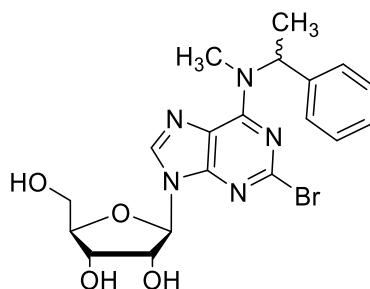
2-Bromo-, 6-chloro-9-(β-D-ribofuranosyl)purine (0.15 g, 0.41 mmol, 1 eq.) was dissolved in 10 ml of ethanol. Triethylamine (0.052 ml, 0.38 mmol, 0.92 eq.) and *N*-Methyl-1-phenylethaneamine (0.12 ml, 0.82 mmol, 2 eq.) was added to the reaction mixture, which was then stirred under reflux at 90 °C for 3 h. The progress of the reaction was monitored by TLC (DCM/methanol 9/1). After TLC indicated the end of the reaction, the volatiles were evaporated. The crude mixture was purified by normal phase column chromatography (DCM/methanol 40/1 to 9/1). The appropriate fractions were pooled together and evaporated to give the desired compound. (0.139 g, overall yield 73%). ^{1}H NMR (600 MHz, DMSO-d_6) δ 8.41 (s, 1H, C8-H), 7.38 – 7.32 (m, 4H, aryl), 7.31 – 7.27 (m, 1H, aryl), 5.86 (d, *J* = 5.8 Hz, 1H, C1′-H), 5.47 (d, *J* = 6.1 Hz, 1H, C2′-H), 5.19 (d, *J* = 5.0 Hz, 1H, C3′-H), 5.03 – 4.99 (m, 1H, C4′-H), 4.54 – 4.48 (m, 1H, OH), 4.13 (q, *J* = 4.6 Hz, 1H, OH), 3.94 (q, *J* = 3.9 Hz, 1H, OH), 3.67 – 3.62 (m, 1H, C5′-H), 3.57 – 3.52 (m, 1H, C5′-H), 2.83 (s, 3H, N-CH₃), 1.66 – 1.58 (m, 3H, α-CH₃). ^{13}C NMR (151 MHz, DMSO-d_6) δ 163.12 (1C, C2), 154.08 (1C, C6), 143.74 (1C, C4), 140.16 (1C, C8), 128.53 (2C, aryl), 127.32 (2C, aryl), 126.84 (2C, aryl), 118.75 (1C, C5), 87.25 (1C, C1′), 85.69 (1C, C4′), 73.61 (1C, C2′), 70.26 (1C, C3′), 61.26 (1C, C5′), 54.85 (1C, N-C̲H), 29.69 (1C, N-CH₃), 13.89 (1C, α-CH₃). LC-MS (m/z): positive mode 466.1 [M + H]⁺. Purity determined by HPLC-UV (254 nm)-ESI-MS: 90%. HRMS (ESI): *m/z* [M + H]⁻ calcd for C₁₉H₂₂N₅O₄Br: 486.0747; found: 486.0767. Mp. 126 - 128°C.

N-CH peak in ¹HNMR not visible

4.5.11 (2*R*,3*R*,4*S*,5*R*)-2-(2-Chloro-6-(methyl((*S*)-1-phenylethyl)amino)-9*H*-purin-9-yl)-5-(hydroxymethyl)tetrahydrofuran-3,4-diol
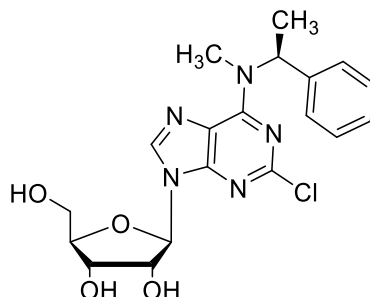
(2*R*,3*R*,4*S*,5*R*)-2-(2-Chloro-6-(methyl((*S*)-1-phenylethyl)amino)-9*H*-purin-9-yl)-5-(hydroxymethyl)tetrahydrofuran-3,4-diol was synthesized according to general procedure A (0.18 g, overall yield 96%). ¹H NMR (500 MHz, DMSO-d_6) δ 8.44 (s, 1H, C8-H), 7.39 – 7.33 (m, 4H, aryl), 7.31 – 7.27 (m, 1H, aryl), 5.88 (d, *J* = 5.7 Hz, 1H, C1′-H), 5.47 (d, *J* = 6.0 Hz, 1H, OH), 5.18 (d, *J* = 5.1 Hz, 1H, OH), 5.03 (t, *J* = 5.5 Hz, 1H, OH), 4.52 (q, *J* = 5.6 Hz, 1H, C2′-H), 4.14 (q, *J* = 4.8 Hz, 1H, C3′-H), 3.96 (q, *J* = 3.7 Hz, 1H, C4′-H), 3.70 – 3.64 (m, 1H, C5′-H), 3.59 – 3.54 (m, 1H, C5′-H), 2.97 – 2.73 (m, 3H, N-CH₃), 1.63 (d, *J* = 6.2 Hz, 3H, α-CH₃). ¹³C NMR (126 MHz, DMSO-d_6) δ 154.32 (1C, C2), 152.57 (1C, C6), 148.25 (1C, C4), 140.25 (1C, C8), 128.50 (2C, aryl), 127.29 (1C, aryl), 126.83 (2C, aryl), 118.48 (1C, C8), 87.28 (1C, C1′), 85.61 (1C, C4′), 73.70 (1C, C2′), 70.23 (1C, C3′), 61.21 (1C, C5′), 50.16 (N-CH), 30.61 (1C, N-CH₃), 16.12 (1C, α-CH₃). LC-MS (m/z): positive mode 420.2 [M + H]⁺. Purity determined by HPLC-UV (254 nm)-ESI-MS: 95%. Mp. 119 – 121 °C.

N-CH- peak in ¹HNMR not visible

4.5.12 (2*R*,3*R*,4*S*,5*R*)-2-(2-Chloro-6-(methyl((*R*)-1-phenylethyl)amino)-9*H*-purin-9-yl)-5-(hydroxymethyl)tetrahydrofuran-3,4-diol
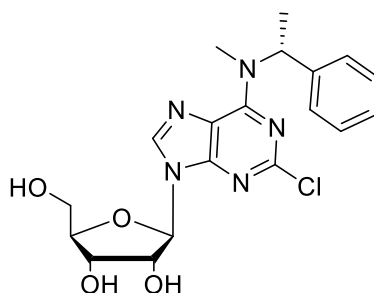
(2*R*,3*R*,4*S*,5*R*)-2-(2-Chloro-6-(methyl((*R*)-1-phenylethyl)amino)-9*H*-purin-9-yl)-5-(hydroxymethyl)tetrahydrofuran-3,4-diol was synthesized according to general procedure A (0.065 g, yield: 46%). ^{1}H NMR (600 MHz, DMSO-d_6) δ 8.44 (s, 1H, C8-H), 7.37 – 7.32 (m, 4H, aryl), 7.30 – 7.27 (m, 1H, aryl), 5.87 (d, J = 5.8 Hz, 1H, C1′-H), 5.48 (d, J = 6.0 Hz, 1H, OH), 5.19 (d, J = 5.0 Hz, 1H, OH), 5.03 (t, J = 5.6 Hz, 1H, OH), 4.52 (q, J = 5.5 Hz, 1H, C2′-H), 4.15 – 4.12 (m, 1H, C3′-H), 3.95 (q, J = 3.8 Hz, 1H, C4′-H), 3.68 – 3.63 (m, 1H, C5′-H), 3.57 – 3.53 (m, 1H, C5′-H), 3.16 (d, J = 4.3 Hz, 1H, N-CH), 2.96 – 2.76 (m, 3H, N-CH$_3$), 1.67 – 1.57 (m, 3H, α-CH$_3$). ^{13}C NMR (151 MHz, DMSO-d_6) δ 154.53 (1C, C6), 152.77 (1C, C2), 151.45 (1C, C4), 140.44 (1C, C8), 128.71 (2C, aryl), 127.49 (2C, aryl), 127.03 (2C, aryl), 118.66 (1C, C5), 87.48 (1C, C1′), 85.84 (1C, C4′), 73.83 (1C, C2′), 70.47 (1C, C3′), 61.44 (1C, C5′), 48.75 (1C, N-C̲H), 29.56 (1C, N-CH$_3$), 18.70 (1C, α-CH$_3$). LC-MS (m/z): positive mode 420.4 [M + H]$^+$. HRMS: m/z [M + H]$^+$ calcd for C$_{19}$H$_{23}$ClN$_5$O$_4$: 420.1433; found: 420.1462. Purity determined by HPLC-UV (254 nm)-ESI-MS: 97%. Mp. 120 – 122 °C.

4.5.13 (2*R*,3*R*,4*S*,5*R*)-2-(2-Chloro-6-(((*S*)-1-phenylethyl)amino)-9*H*-purin-9-yl)-5-

(hydroxymethyl)tetrahydrofuran-3,4-diol
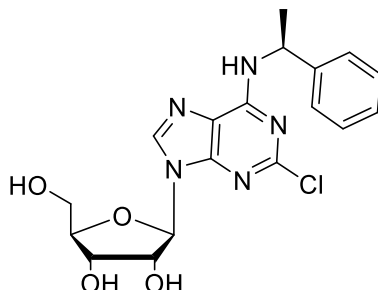
(2*R*,3*R*,4*S*,5*R*)-2-(2-Chloro-6-(((*S*)-1-phenylethyl)amino)-9*H*-purin-9-yl)-5-

(hydroxymethyl)tetrahydrofuran-3,4-diol was synthesized according to general procedure A

(0.17, yield: 37%). ^{1}H NMR (600 MHz, DMSO-d_6) δ 8.83 (d, J = 7.8 Hz, 1H, N^6-H), 8.40 (s,

1H, C8-H), 7.43 (d, J = 7.6 Hz, 2H, aryl), 7.30 (t, J = 7.6 Hz, 2H, aryl), 7.20 (t, J = 7.4 Hz, 1H,

aryl), 5.80 (d, J = 5.8 Hz, 1H, C1′-H), 5.43 (d, J = 5.9 Hz, 1H, OH), 5.16 (s br, 1H, OH), 5.02

(t, J = 5.4 Hz, 1H, OH), 4.53 – 4.45 (m, 1H, C2′-H), 4.14 – 4.08 (m, 1H, C3′-H), 3.95 – 3.89

(m, 1H, C4′-H), 3.65 – 3.61 (m, 1H, C5′-H), 3.58 – 3.51 (m, 1H, C5′-H), 1.75 (s, 1H, *N*-CH),

1.56 – 1.48 (m, 3H, CH$_3$).^{13}C NMR (151 MHz, DMSO-d_6) δ 171.58 (1C, C6) , 154.35 (1C, C2),

153.18 (1C, C4), 149.90 (1C, C1-aryl), 144.47 (1C, C8), 128.40 (2C, aryl), 126.88 (2C, aryl),

126.37 (1C, C6-aryl), 118.67 (C5, 1C), 87.63 (1C, C1′, 1C), 85.88 (1C, C4′, 1C), 73.78 (1C,

C2′, 1C), 70.53 (1C, C3′, 1C), 61.52 (1C, C5′, 1C), 49.23 (1C, NH-C, 1C), 22.11 (CH$_3$, 1C).

LC-MS (*m/z*): positive mode 405.1 [M+H]$^+$. Purity determined by HPLC-UV (254 nm)-ESI-

MS: 95%, Mp 105 °C.

4.5.14 (2*R*,3*R*,4*S*,5*R*)-2-(2-Chloro-6-(((*R*)-1-phenylethyl)amino)-9*H*-purin-9-yl)-5-(hydroxymethyl)tetrahydrofuran-3,4-diol
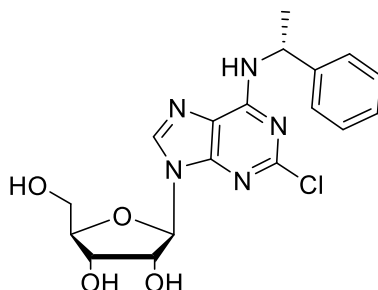
(2*R*,3*R*,4*S*,5*R*)-2-(2-chloro-6-(((*R*)-1-phenylethyl)amino)-9*H*-purin-9-yl)-5-(hydroxymethyl)tetrahydrofuran-3,4-diol was synthesized according to general procedure A (0.31 g, yield: 75%). ^{1}H NMR (600 MHz, DMSO-d_6) δ 8.83 (d, J = 8.0 Hz, 1H, NH), 8.40 (s, 1H, C8-H), 7.42 (d, J = 7.5 Hz, 2H, aryl), 7.30 (t, J = 7.5 Hz, 2H, aryl), 7.20 (t, J = 7.4 Hz, 1H, aryl), 5.80 (d, J = 5.8 Hz, 1H, C1′-H), 5.43 (d, J = 6.1 Hz, 1H, OH), 5.16 (d, J = 4.9 Hz, 1H, OH), 5.02 (t, J = 5.6 Hz, 1H, OH), 4.48 (q, J = 5.7 Hz, 1H, C2′-H), 4.13 – 4.07 (m, 1H, C3′-H), 3.96 – 3.89 (m, 1H, C4′-H), 3.68 – 3.58 (m, 1H, C5′-H), 3.58 – 3.49 (m, 1H, C5′-H), 1.57 – 1.47 (m, 3H, CH$_3$). ^{13}C NMR (151 MHz, DMSO-d_6) δ 154.34 (1C, C6), 153.18 (1C, C2), 149.90 (1C, C4), 144.51 (1C, C1-aryl), 128.39 (2C, aryl), 126.86 (2C, aryl), 126.35 (1C, C6-aryl), 118.61 (1C, C5), 87.55 (1C, C1′), 85.83 (1C, C4′), 73.91 (1C, C2′), 70.48 (1C, C3′), 61.47 (1C, C5), 49.22 (1C, NH-CH), 22.10 (1C, CH$_3$). LC-MS (*m/z*): positive mode 405.1 [M+H]$^+$. Purity determined by HPLC-UV (254 nm)-ESI-MS: 90%.

4.5.15 (2R,3R,4S,5R)-2-(6-((4-Hydroxybenzyl)amino)-9H-purin-9-yl)-5-(hydroxymethyl)tetrahydrofuran-3,4-diol

(2R,3R,4S,5R)-2-(6-((4-Hydroxybenzyl)amino)-9H-purin-9-yl)-5

(hydroxymethyl)tetrahydrofuran-3,4-diol was synthesized according to general procedure A

(0.17 g, yield: 26%). ^{1}H NMR (600 MHz, DMSO-d_6) δ 9.20 (s, 1H, NH), 8.34 (s, 1H, C2-H),

8.29 – 8.24 (m, 1H, C8-H), 8.20 (s, 1H, OH), 7.14 (d, J = 8.2 Hz, 2H, aryl), 6.68 – 6.65 (m, 2H,

aryl), 5.88 (d, J = 6.1 Hz, 1H, C1′-H), 5.41 (d, J = 6.2 Hz, 1H, OH), 5.38 – 5.35 (m, 1H, OH),

5.15 (d, J = 4.6 Hz, 1H, OH), 4.64 – 4.54 (m, 2H, N-CH$_2$), 4.16 – 4.13 (m, 1H, C2′), 4.09 –

4.05 (m, 1H, C3′), 3.97 – 3.95 (m, 1H, C4′), 3.69 – 3.64 (m, 1H, C5′-H), 3.57 – 3.52 (m, 1H,

C5′). ^{13}C NMR (151 MHz, DMSO-d_6) δ 156.29 (1C, aryl), 154.58 (1C, C6), 152.47 (1C, C2)

148.55 (1C, C4), 139.92 (1C, C8), 130.28 (1C, aryl), 128.66 (2C, aryl), 115.42 (1C, C5), 115.08

(1C, aryl), 88.11 (1C, C1′), 86.04 (1C, C4′), 73.63 (1C, C2′), 70.80 (1C, C3′), 61.81 (1C, C5′).

LC-MS (m/z): positive mode 374.2 [M + H]$^+$. Purity determined by HPLC-UV (200-600 nm)-

ESI-MS: 95%. Mp. 200 - 202 °C.

4.5.16 (2R,3R,4S,5R)-2-(6-(Benzylamino)-9H-purin-9-yl)-5-(hydroxymethyl)tetrahydrofuran-3,4-diol
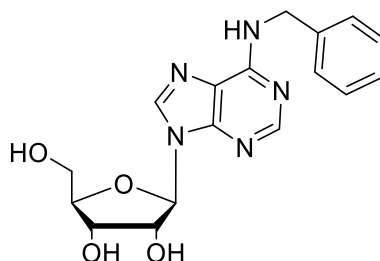
(2*R*,3*R*,4*S*,5*R*)-2-(6-(Benzylamino)-9*H*-purin-9-yl)-5-(hydroxymethyl)tetrahydrofuran-3,4-diol was synthesized according to general procedure A (0.18 g, yield: 76%). ^{1}H NMR (500 MHz, DMSO-*d₆*) δ 8.36 (s, 1H, C8-H), 8.20 (s, 1H, C2-H), 7.35 – 7.31 (m, 2H, aryl), 7.30 – 7.26 (m, 2H, aryl), 7.21 – 7.17 (m, 1H, aryl), 5.89 (d, *J* = 6.1 Hz, 1H, OH), 5.40 (d, *J* = 6.2 Hz, 1H, OH), 5.36 – 5.32 (m, 1H, C1′-H), 5.14 (d, *J* = 4.6 Hz, 1H, OH), 4.71 (s, 1H, CH₂), 4.65 – 4.58 (m, 1H, C2′-H), 4.18 – 4.13 (m, 1H, C3′-H), 3.99 – 3.95 (m, 1H, C4′-H), 3.71 – 3.64 (m, 1H, C5′-H), 3.59 – 3.52 (m, 1H, C5′-H). ^{13}C NMR (126 MHz, DMSO-*d₆*) δ 154.69 (1C, C6), 152.48 (1C, C2), 148.63 (1C, C4), 140.15 (1C, C8), 128.33 (2C, aryl), 127.25 (2C, aryl), 126.74 (2C, aryl), 119.91 (1C, C5), 88.12 (C1′, 1C), 86.05 (1C, C4′), 73.65 (1C, C2′), 70.80 (1C, C3′), 61.82 (1C, C5′), 43.09 (1C, CH₂). LC-MS (m/z): positive mode 358.2 [M + H]⁺. Purity determined by HPLC-UV (200-600 nm)-ESI-MS: 98%. Mp 147 °C.

4.5.17 (2*R*,3*R*,4*S*,5*R*)-2-(6-(Benzyl(methyl)amino)-2-chloro-9*H*-purin-9-yl)-5-(hydroxymethyl)tetrahydrofuran-3,4-diol
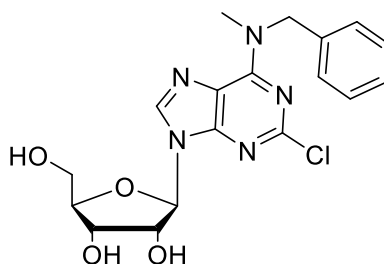
(2*R*,3*R*,4*S*,5*R*)-2-(6-(Benzyl(methyl)amino)-2-chloro-9*H*-purin-9-yl)-5-(hydroxymethyl)tetrahydrofuran-3,4-diol was synthesized according to general procedure A. (0.11 g, yield: 87%) ^{1}H NMR (600 MHz, DMSO-*d₆*) δ 8.42 (s, 1H, C8-H), 7.35 – 7.31 (m, 2H, aryl), 7.30 – 7.24 (m, 3H, aryl), 5.86 (d, *J* = 5.8 Hz, 1H, C1′-H), 5.55 (s, 1H), 5.47 (d, *J* = 6.1 Hz, 1H, OH), 5.19 (d, *J* = 5.0 Hz, 1H, OH), 5.03 (t, *J* = 5.5 Hz, 1H, OH), 4.97 – 4.79 (m, 2H,

CH₂), 4.53 – 4.49 (m, 1H, C2′-H), 4.14 – 4.11 (m, 1H, C3′-H), 3.94 (q, J = 3.8 Hz, 1H, C4′-H), 3.68 – 3.63 (m, 1H, C5′-H), 3.57 – 3.53 (m, 1H, C5′-H), 3.09 (s br, 3H, CH₃). ^{13}C NMR (151 MHz, DMSO-d_6) δ 158.39 (1C, C6), 154.66 (1C, C2), 152.81 (1C, C4), 151.44, 139.48 (1C, C8), 137.62 (1C, aryl), 128.79 (3C, aryl), 127.47 (2C, aryl), 118.62 (1C, C5), 87.47 (1C, C1′), 85.84 (1C, C4′), 73.86 (1C, C2′), 70.46 (1C, C3′), 61.44 (1C, C5′), 45.90 (1C, CH₂), 35.08 (1C, CH₃). LC-MS (m/z): positive mode 406.20 [M + H]$^+$. Purity determined by HPLC-UV (200-600 nm)-ESI-MS: 90%. Mp. 182-183 °C.

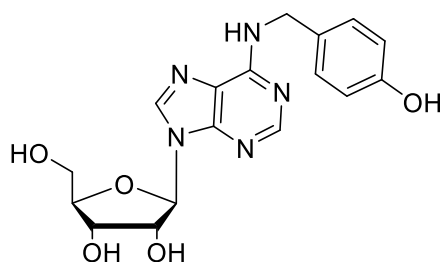### 4.5.18 (2*R*,3*R*,4*S*,5*R*)-2-(6-(Benzylamino)-2-chloro-9*H*-purin-9-yl)-5-(hydroxymethyl)tetrahydrofuran-3,4-diol
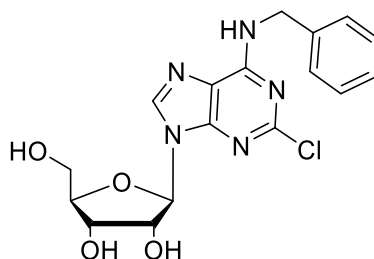
(2*R*,3*R*,4*S*,5*R*)-2-(6-(Benzylamino)-2-chloro-9*H*-purin-9-yl)-5-(hydroxymethyl)tetrahydrofuran-3,4-diol was synthesized according to general procedure A (amount: 0.21 g, yield 93%) ^{1}H NMR (600 MHz, DMSO-d_6) δ 8.92 – 8.86 (m, 1H, NH), 8.40 (s, 1H, C8-H), 7.35 – 7.28 (m, 4H, phenyl), 7.25 – 7.19 (m, 1H, phenyl), 5.82 (d, J = 5.9 Hz, 1H, C1′-H), 5.45 (d, J = 6.1 Hz, 1H, C4′-H), 5.17 (d, J = 5.0 Hz, 1H, C2′-H), 5.03 (t, J = 5.6 Hz, 1H, C3′-H), 4.66 – 4.62 (m, 1H, OH), 4.53 – 4.49 (m, 1H, OH), 4.14 – 4.10 (m, 1H, OH), 3.95 – 3.91 (m, 1H), 3.68 – 3.63 (m, 1H, C5′-H), 3.57 – 3.52 (m, 1H, C5′-H). ^{13}C NMR (151 MHz, DMSO-d_6) δ 171.58, 155.11 (1C, C6), 153.28 (1C, C2), 149.82 (1C, C4), 139.32, 128.44 (1C , 127.43, 126.99, 118.75 (1C, C5), 87.62 (1C, C1′), 85.88 (1C, C4′), 73.84 (1C, C3′), 70.52 (1C, C4′), 61.50 (1C, C5′), 43.30 (1C, N-CH₂). LC-MS (*m/z*): positive mode 392.2 [M+H]$^+$. Purity determined by HPLC-UV (254 nm)-ESI-MS: 93%.

4.5.19 (((((2*R*,3*S*,4*R*,5*R*)-5-(6-(Benzylamino)-2-chloro-9*H*-purin-9-yl)-3,4-dihydroxytetrahydrofuran-2-l)methoxy)(hydroxy)phosphoryl)methyl)phosphonic acid
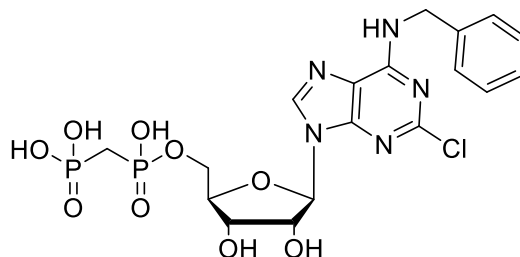
(((((2*R*,3*S*,4*R*,5*R*)-5-(6-(Benzylamino)-2-chloro-9*H*-purin-9-yl)-3,4-dihydroxytetrahydrofuran-2-yl)methoxy)(hydroxy)phosphoryl)methyl)phosphonic acid was synthesized according to general procedure B (yield: 22%, amount: 0.062 g). ^{1}H NMR (600 MHz, D$_2$O) δ 8.58 (s, 1H, C8-H), 7.38 – 7.21 (m, 5H, phenyl), 5.99 (d, J = 3.9 Hz, 1H, C1′-H), 4.72 – 4.61 (m, 3H, N-CH$_2$ + C4′-H), 4.52 – 4.47 (m, 1H, C2′-H), 4.39 – 4.33 (m, 1H, C3′-H), 4.23 – 4.13 (m, 2H, C5′-H), 3.19 (q, J = 7.3 Hz, 1H, N-C$\underline{H}_2$-CH$_3$), 2.34 (t, 2H, P-CH$_2$-P), 1.27 (t, J = 7.3 Hz, 1H, N-CH$_2$-C$\underline{H}_3$). ^{13}C NMR (151 MHz, D$_2$O) δ 157.62 (1C, C6), 157.06 (1C, C2), 151,49 (1C, C4), 140.34 (1C, C8), 131.52 (2C, phenyl), 130.35 (2C, phenyl), 130.20 (1C, phenyl), 119.12 (1C, C5), 90.48 (1C, C1′), 86.62 (1C, C2′), 77.20 (1C, C3′), 72.75 (1C, C4′), 66.43 (1C, C5′), 49.52 (1C, (1C, N-C$\underline{H}_2$-CH$_3$), 46.97 (1C, N-C$\underline{H}_2$), 29.41 (t, J = 124.5 Hz, PCP), 11.08 (1C, N-CH$_2$-C$\underline{H}_3$). ^{31}P NMR (243 MHz, D$_2$O) δ (19.03, **P$_\beta$**), (17.16, **P$_\alpha$**). LC-MS (*m/z*): negative mode 548.20 [M - H]$^{-}$, positive mode 550.30 [M + H]$^{+}$. Purity determined by HPLC-UV (254 nm)-ESI-MS: 99%, HRMS (ESI): *m/z* [M - H]$^{-}$ calcd for C$_{18}$H$_{21}$ClN$_5$O$_9$P$_2$: 548.0498; found: 548.0503. Mp. 170 – 172 °C.

4.5.20 (((((2*R*,3*S*,4*R*,5*R*)-5-(6-Chloro-9*H*-purin-9-yl)-3,4-dihydroxytetrahydrofuran-2-yl)methoxy)(hydroxy)phosphoryl)methyl)phosphonic acid
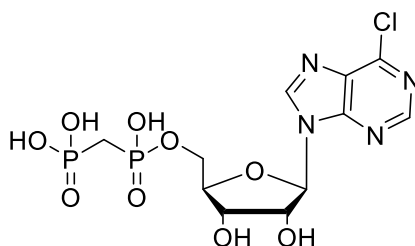
(((((2*R*,3*S*,4*R*,5*R*)-5-(6-Chloro-9*H*-purin-9-yl)-3,4-dihydroxytetrahydrofuran-2-yl)methoxy)(hydroxy)phosphoryl)methyl)phosphonic acid was synthesized according to general procedure B (yield: 27%, amount: 0.042 g). ^{1}H NMR (600 MHz, D$_2$O) δ 8.88 (s, 1H, C8-H), 8.77 (s, 1H, C2-H), 6.25 (d, *J* = 5.0 Hz, 1H, C1′-H), 4.85 (t, *J* = 5.1 Hz, 1H, C2′-H), 4.56 (t, *J* = 4.7 Hz, 1H, C3′-H), 4.43 – 4.40 (m, 1H, C4′-H), 4.28 – 4.19 (m, 2H, C5′-H), 3.19 (q, *J* = 7.3 Hz, 5H, N+-CH$_2$-C̲H$_3$), 2.42 – 2.33 (m, 2H, PCH2P), 1.27 (t, *J* = 7.3 Hz, 7H, N+-CH$_2$-C̲H$_3$). ^{13}C NMR (151 MHz, D$_2$O) δ 151.94 (1C, C8), 151.21 (1C, C6), 150.15 (1C, C4), 131.11 (1C, C2), 120.32 (1C, C5), 88.18 (1C, C1′), 83.83 (1C, C2′), 74.19 (1C, C3′), 70.04 (1C, C4′), 63.70 (1C, C5′), 46.64 (N-C̲H$_2$-CH$_3$), 27.14 – 25.29 (m, P-C̲-P), 8.19 (N-CH$_2$-C̲H$_3$). LC-MS (*m/z*): negative mode 443.10 [M - H]$^-$, positive mode 445.10 [M + H]$^+$. Purity determined by HPLC-UV DAD (200-600 nm)-ESI-MS: 97%. Mp. 156 – 158 °C.

4.5.21 (((((2*R*,3*S*,4*R*,5*R*)-5-(6-(Benzyl(methyl)amino)-2-chloro-9*H*-purin-9-yl)-3,4-dihydroxytetrahydrofuran-2-l)methoxy)(hydroxy)phosphoryl)methyl)phosphonic acid

(((((2R,3S,4R,5R)-5-(6-(Benzyl(methyl)amino)-2-chloro-9H-purin-9-yl)-3,4-dihydroxytetrahydrofuran-2-yl)methoxy)(hydroxy)phosphoryl)methyl)phosphonic acid was synthesized according to general procedure B (yield: 29%, amount: 0.041 g). ^{1}H NMR (600 MHz, D$_2$O) δ 8.36 (s, 1H, C8-H), 7.36 – 7.31 (m, 2H, aryl), 7.31 – 7.25 (m, 3H, aryl), 5.88 (d, J = 4.7 Hz, 1H, C1′-H), 5.20 (s br, 2H, N-CH$_2$), 4.63 – 4.56 (m, 1H, C2′-H), 4.31 – 4.23 (m, 2H, C3′-H + C4′-H), 4.15 – 4.04 (m, 2H, C5′-H), 3.23 (s br, 3H, N-CH$_3$), 2.01 (t, J = 19.4 Hz, 2H, P-CH$_2$-P). ^{13}C NMR (151 MHz, D$_2$O) δ 157.82 (1C, C6), 156.30 (1C, C2), 153.99 (1C, C4), 139.55 (1C, C8), 131.54 (2C, aryl), 130.34 (2C, aryl), 130.03 (2C, aryl), 120.93 (1C, C5), 90.91 (1C, C1′), 87.05 (1C, C4′), 78.47 (1C, C2′), 73.97 (1C, C3′), 66.68 (1C, C5′), 54.20 (1C, N-CH$_2$), 31.22 (dd, J = 125.6, 118.0 Hz, PCP). ^{31}P NMR (243 MHz, D$_2$O) δ 23.05 (d, J = 8.8 Hz, P$_\beta$), 12.21 (d, J = 7.4 Hz, P$_\alpha$). LC-MS (m/z): positive mode 564.2 [M - H]$^-$, negative mode 562.2 [M + H]$^+$. Purity determined by HPLC-UV (254 nm)-ESI-MS: 100%. Mp. 210 - 212 °C.

4.5.22 (((((2R,3S,4R,5R)-3,4-Dihydroxy-5-(6-((4-hydroxybenzyl)amino)-9H-purin-9-yl)tetrahydrofuran-2-yl)methoxy)(hydroxy)phosphoryl)methyl)phosphonic acid

(((((2R,3S,4R,5R)-3,4-Dihydroxy-5-(6-((4-hydroxybenzyl)amino)-9H-purin-9-yl)tetrahydrofuran-2-yl)methoxy)(hydroxy)phosphoryl)methyl)phosphonic acid was synthesized according to general procedure C (0.044 g, yield: 26%). ^{1}H NMR (600 MHz, D$_2$O) δ 8.40 (s, 1H, C8-H), 8.22 (s, 1H, C2-H), 7.15 – 7.11 (m, 2H, aryl), 6.58 – 6.54 (m, 2H, aryl), 5.90 (d, J = 5.7 Hz, 1H, C1′-H), 4.64 (t, J = 5.2 Hz, 1H, C2′-H), 4.60 (s, 2H, CH$_2$), 4.26-4.20

(m, 2H, C3′-H + C4′-H), 4.11 – 4.02 (m, 2H, C5′-H2), 1.98 (t, J = 19.5 Hz, 2H, P-CH$_2$-P). ^{13}C NMR (151 MHz, D$_2$O) δ 168.25 (1C, C6), 157.17 (1C, C2), 155.66 (1C, C4), 131.74 (2C, aryl), 126.47 (2C, aryl), 121.54 (2C, aryl), 90.80 (1C, C1′), 87.14 (1C, C4′) , 78.33 (1C, C2′), 74.10 (1C, C3′), 66.78 (1C, C5′), 39.30 (1C, N-CH$_2$), 31.19 (dd, J = 125.9, 117.9 Hz, PCP). ^{31}P NMR (243 MHz, D$_2$O) δ 23.07 (d, J = 8.6 Hz, P$_\alpha$), 12.18 (d, J = 8.2 Hz, P$_\beta$). LC-MS (m/z): positive mode 420.4 [M + H]$^+$. Purity determined by HPLC-UV (254 nm)-ESI-MS: 97%. Mp. 180 - 182 °C.

4.5.23 (((((2R,3S,4R,5R)-5-(6-(Benzylamino)-9H-purin-9-yl)-3,4-dihydroxytetrahydrofuran-2-yl)methoxy)(hydroxy)phosphoryl)methyl)phosphonic acid

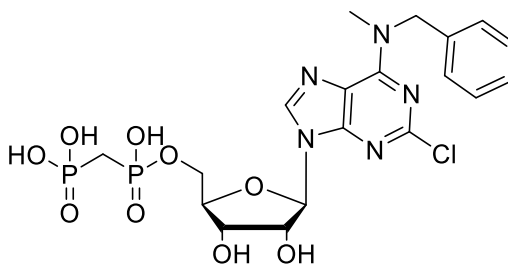(((((2R,3S,4R,5R)-5-(6-(Benzylamino)-9H-purin-9-yl)-3,4-dihydroxytetrahydrofuran-2-yl)methoxy)(hydroxy)phosphoryl)methyl)phosphonic acid was synthesized according to general procedure C (amount: 0.008 g, yield: 47%). ^{1}H NMR (600 MHz, D$_2$O) δ 8.47 (s, 1H, C2-H), 8.22 (s, 1H, C8-H), 7.43 – 7.36 (m, 4H, aryl), 7.34 – 7.29 (m, 1H, aryl), 5.97 (d, J = 5.6 Hz, 1H, C1′-H), 4.69 (t, J = 5.5 Hz, 1H, C2′-H), 4.34 – 4.31 (m, 1H, C3′-H), 4.31 – 4.28 (m, 1H, C4′-H), 4.16 – 4.08 (m, 2H, C5′-H), 2.02 (t, J = 19.5 Hz, 2H, P-CH$_2$-P). *N-CH$_2$ not visible.* ^{13}C NMR (151 MHz, D$_2$O) δ 154.61 (1C, C6), 152.88 (1C, C2), 148.51 (1C, C4), 138.47 (1C, C8), 128.74 (2C, aryl), 127.33 (2C, aryl), 126.92 (1C, aryl), 119.05 (1C, C5), 87.98 (1C, C1′), 84.33 (1C, C4′), 75.44 (1C, C2′), 71.17 (1C, C3′), 63.87 (1C, C5′), 45.32 (1C, CH$_2$), 28.57 (dd, J = 126.0, 117.9 Hz, PCP). ^{31}P NMR (243 MHz, D$_2$O) δ 23.07 (d, J = 8.8 Hz), 12.09 (d, J = 8.6

Hz). ^{31}P NMR (243 MHz, D$_2$O) δ 23.07 (d, J = 8.8 Hz, P$_\alpha$), 12.09 (d, J = 8.6 Hz, P$_\beta$). LC-MS

(m/z): positive mode 516.3 [M + H]$^+$, negative mode 514.2 [M - H]$^-$. Purity determined by

HPLC-UV (254 nm)-ESI-MS: 100%. Mp. 149 – 151 °C.

4.5.24 (((((2R,3S,4R,5R)-5-(2-Chloro-6-(((S)-1-phenylethyl)amino)-9H-purin-9-yl)-3,4-dihydroxytetrahydrofuran-2-yl)methoxy)(hydroxy)phosphoryl)methyl)phosphonic acid
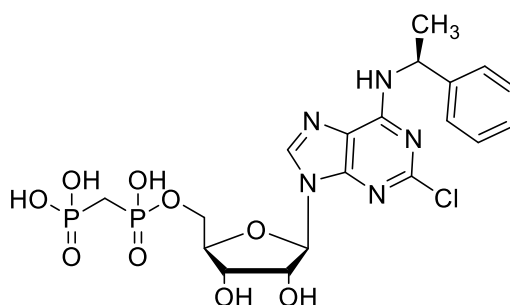
((((((2R,3S,4R,5R)-5-(2-Chloro-6-(((S)-1-phenylethyl)amino)-9H-purin-9-yl)-3,4-

dihydroxytetrahydrofuran-2-yl)methoxy)(hydroxy)phosphoryl)methyl)phosphonic acid was

synthesized according to general procedure C (0.046 g, yield: 16%). ^{1}H NMR (600 MHz, D$_2$O)

δ 8.61 (s, 1H, C8-H), 7.50 (d, J = 7.7 Hz, 2H, aryl), 7.42 (t, J = 7.3 Hz, 2H, aryl), 7.33 (t, J =

7.2 Hz, 1H, aryl), 6.05 (d, J = 5.0 Hz, 1H, C1′-H), 5.45 – 5.32 (m, 1H, N-C$\underline{H}$), 4.73 (t, J = 5.1

Hz, 1H, C2′-H), 4.52 (t, J = 4.7 Hz, 1H, C3′-H), 4.38 (s, 1H, C4′-H), 4.20 (d, J = 9.3 Hz, 2H,

C5′-$\underline{H_2}$), 2.37 – 2.27 (m, 2H, P-C$\underline{H_2}$-P), 1.64 (d, J = 6.9 Hz, 3H, α-CH$_3$). ^{13}C NMR (151 MHz,

D$_2$O) δ 152.66 (1C, C2), 146.29 (1C, C6), 145.48 (1C, C4), 140.96 (1C, C8), 131.72 (2C, aryl),

130.37 (2C, aryl), 128.83 (2C, aryl), 119.68 (1C, C5), 90.28 (1C, C1′), 86.76 (1C, C4′), 77.12

(1C, C2′), 72.84 (1C, C3′), 66.41 (1C, C5′), 48.45 (1C, N-$\underline{C}$H) 29.38 (1C, P-$\underline{C}$-P), 24.60 (1C,

α-$\underline{C}$H$_3$). ^{31}P NMR (243 MHz, D$_2$O) δ 19.00 (s, P$_\alpha$), 17.08 (s, P$_\beta$). LC-MS (m/z): negative mode

562.2 [M - H]$^-$, positive mode 564.1 [M + H]$^+$. Purity determined by HPLC-UV (254 nm)-ESI-

MS: 97%, HRMS (ESI): m/z [M - H]$^-$ calcd for C$_{19}$H$_{23}$ClN$_5$O$_9$P$_2$: 562.0654; found: 562.0677.

Mp. 174 -176 °C. $[\alpha]_D^{20}$ = - 0.046° (H$_2$O, c = 2.9 mg/ml)

4.5.25 (((((2*R*,3*S*,4*R*,5*R*)-5-(2-Chloro-6-(((*R*)-1-phenylethyl)amino)-9*H*-purin-9-yl)-3,4-

  dihydroxytetrahydrofuran-2-

  yl)methoxy)(hydroxy)phosphoryl)methyl)phosphonic acid
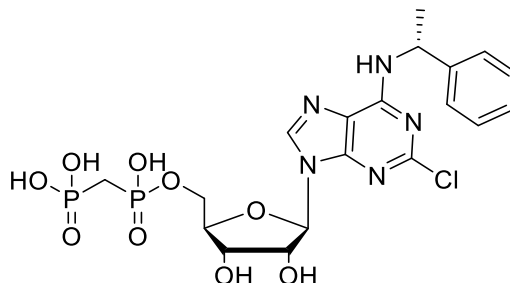
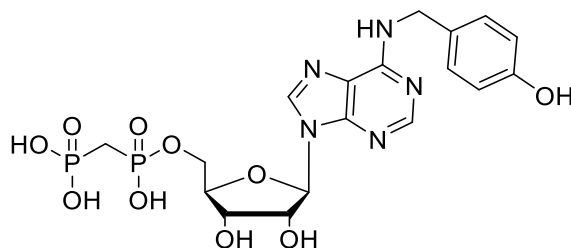(((((2*R*,3*S*,4*R*,5*R*)-5-(2-Chloro-6-(((*R*)-1-phenylethyl)amino)-9*H*-purin-9-yl)-3,4-dihydroxytetrahydrofuran-2-yl)methoxy)(hydroxy)phosphoryl)methyl)phosphonic acid was synthesized according to general procedure C. (0.042g, yield: 15%). ^{1}H NMR (600 MHz, D$_2$O) δ 8.71 (s, 1H, C8-H), 7.47 – 7.42 (m, 2H, aryl), 7.37 (t, J = 7.7 Hz, 2H, aryl), 7.29 (t, J = 7.4 Hz, 1H, aryl), 6.03 (d, J = 4.6 Hz, 1H, C1′-H), 5.37 – 5.27 (m, 1H, NC$\underline{H}$), 4.68 (t, J = 4.9 Hz, 1H, C2′-H), 4.48 (t, J = 4.8 Hz, 1H, C3′-H), 4.40 – 4.35 (m, 1H, C4′-H), 4.27 – 4.14 (m, 2H, C5′-$\underline{H}_2$), 2.36 (t, J = 20.3 Hz, 2H, P-C$\underline{H}_2$-P), 1.61 (d, J = 6.9 Hz, 3H, α-C$\underline{H}_3$). ^{13}C NMR (151 MHz, D$_2$O) δ 151.21 (1C, C2), 149.32 (1C, C6), 146.01 (1C, C4), 137.87 (1C, C8), 131.68 (2C, aryl), 130.37 (2C, aryl), 128.83 (2C, aryl), 119.51 (1C, C5), 90.86 (1C, C1′), 86.64 (1C, C4′), 77.20 (1C, C2′), 72.57 (1C, C3′), 66.35 (1C, C5′), 48.45 (1C, N-$\underline{C}$-H), 29.18 (t, J = 128.5 Hz, P-$\underline{C}$-P)., 24.52 (1C, α-$\underline{C}$H$_3$). ^{31}P NMR (243 MHz, D$_2$O) δ 19.67 (d, J = 10.8 Hz, P$_\alpha$), 16.84 (d, J = 10.8 Hz, P$_\beta$). LC-MS (*m/z*): negative mode 562.2 [M - H]$^-$, positive mode 564.2 [M + H]$^+$. Purity determined by HPLC-UV (254 nm)-ESI-MS: 98%. HRMS (ESI): *m/z* [M - H]$^-$ calcd for C$_{19}$H$_{23}$ClN$_5$O$_9$P$_2$: 562.0654; found: 566.0649. Mp. 166 - 168 °C. Specific optical rotation: $[\alpha]_D^{20}$ = - 0.03° (H$_2$O, c = 3.2 mg/ml).
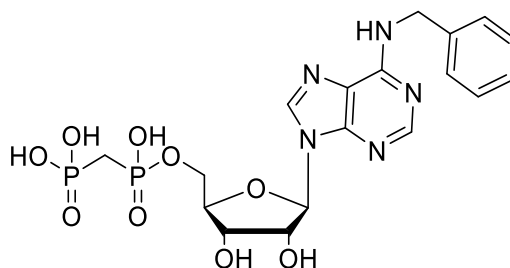
4.5.26 (((((2*R*,3*S*,4*R*,5*R*)-3,4-Dihydroxy-5-(2-iodo-6-(methyl(1-phenylethyl)amino)-9*H*-purin-9-yl)tetrahydrofuran-2-yl)methoxy)(hydroxy)phosphoryl)methyl)phosphonic acid

(((((2*R*,3*S*,4*R*,5*R*)-3,4-Dihydroxy-5-(2-iodo-6-(methyl(1-phenylethyl)amino)-9*H*-purin-9-yl)tetrahydrofuran-2-yl)methoxy)(hydroxy)phosphoryl)methyl)phosphonic acid was synthesized according to general procedure C (0.019 g, yield: 10%). ^{1}H NMR (600 MHz, D$_2$O + NaOD) δ 8.29 (s, 1H, C8-H), 7.39 – 7.33 (m, 4H, aryl), 7.32 – 7.27 (m, 1H, aryl), 5.87 (d, *J* = 5.1 Hz, 1H, C1′-H), 4.59 – 4.55 (m, 1H, C2′-H), 4.27 – 4.22 (m, 2H, C3′-H, C4′-H), 4.14 – 4.04 (m, 2H, C5′-H), 3.01 (s, 3H, N-CH$_3$), 2.00 (t, *J* = 19.4 Hz, 2H, PCH$_2$P), 1.69 – 1.58 (m, 3H, α-CH$_3$). ^{13}C NMR (151 MHz, D$_2$O) δ 156.77 (1C, C6), 153.24 (1C, C4), 142.92 (1C, C8), 131.41 (2C, aryl), 130.36 (2C, aryl), 129.94 (2C, aryl), 122.71 (1C, C2), 122.05 (1C, C5), 89.83 (1C, C1′), 86.54 (1C, C4′), 77.22 (1C, C2′), 72.96 (1C, C3′), 66.40 (1C, C5′), 57.88 (1C, N-CH), 30.34 (t, *J* = 124.5 Hz, 1C, P-C-P), 18.31 (1C, α-CH$_3$). ^{31}P NMR (243 MHz, D$_2$O + NaOD) δ 23.04 (d, *J* = 8.8 Hz, P$_\alpha$), 12.24 (d, *J* = 8.3 Hz, P$_\beta$). LC-MS (*m/z*): negative mode 668.1 [M - H]$^-$, positive mode 670.1 [M + H]$^+$. Purity determined by HPLC-UV (254 nm)-ESI-MS: 96%. HRMS (ESI): *m/z* [M - H]$^-$ calcd for C$_{20}$H$_{25}$IN$_5$O$_9$P$_2$: 668.0167; found: 668.0185. Mp. 208 – 210 °C.

N-CH not visible in ^{1}H NMR

4.5.27 (((((2*R*,3*S*,4*R*,5*R*)-5-(6-((2-Chlorobenzyl)(methyl)amino)-2-iodo-9*H*-purin-9-yl)-

3,4-dihydroxytetrahydrofuran-2-

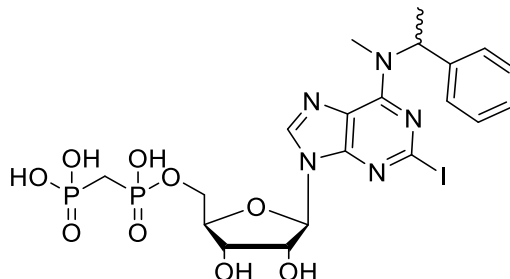**yl)methoxy)(hydroxy)phosphoryl)methyl)phosphonic acid**
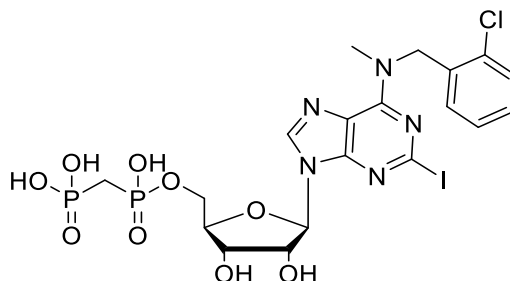
(((((2*R*,3*S*,4*R*,5*R*)-5-(6-((2-Chlorobenzyl)(methyl)amino)-2-iodo-9*H*-purin-9-yl)-3,4-dihydroxytetrahydrofuran-2-yl)methoxy)(hydroxy)phosphoryl)methyl)phosphonic acid was synthesized according to general procecure C (0.007 g, yield: 5%). ^{1}H NMR (600 MHz, D$_2$O + NaOD) δ 8.08 (s, 1H, C8′-H), 7.25 – 6.77 (m, 4H, aryl), 5.77 – 5.69 (m, 1H, C1′-H), 4.40 – 4.29 (m, 1H, C2′-H), 4.17 – 4.09 (m, 2H, C3′-H, C4′-H), 4.07 – 3.91 (m, 2H, C5′-H$_2$), 3.27 (s, 3H, N-CH$_3$), 1.92 (t, *J* = 19.2 Hz, 2H, PCH$_2$P). ^{13}C NMR (151 MHz, D$_2$O + NaOD) δ 157.14 (1C, C2), 153.61 (1C, C6), 140.55 (1C, C4) 136.98 (1C, C8), 136.11 (1C, aryl), 132.65 (1C, aryl), 131.96 (1C, aryl), 130.33 (2C, aryl), 122.82 (1C, aryl), 122.38 (1C, C5), 91.97 (1C, C1′-H), 87.13 (1C, C4′-H), 79.35 (1C, C2′-H), 74.50 (1C, C3′-H), 67.41 (1C, C5′-H), 58.73 (1C, N-CH$_2$), 31.46 (t, *J* = 121.6 Hz, P-C-P), 20.00 (1C, CH$_3$). ^{31}P NMR (243 MHz, D$_2$O + NaOD) δ 23.14 (d, *J* = 8.8 Hz, P$_\alpha$), 12.66 (d, *J* = 8.6 Hz, P$_\beta$). LC-MS (*m/z*): negative mode 689.1 [M - H]$^-$, positive mode 691.2 [M + H]$^+$. Purity determined by HPLC-UV (254 nm)-ESI-MS: 99%. HRMS (ESI): *m/z* [M - H]$^-$ calcd for C$_{19}$H$_{22}$ClIN$_5$O$_9$P$_2$: 687.9621; found: 687.9635, C$_{19}$H$_{22}$ClIN$_5$O$_9$P$_2$Na: 709.9440; found: 709.9446. Mp. 211 - 213 °C.

N-CH$_2$ not visible in ^{1}H NMR

4.5.28 (((((2*R*,3*S*,4*R*,5*R*)-5-(6-((1-(2-Chlorophenyl)ethyl)(methyl)amino)-2-iodo-9*H*-purin-9-yl)-3,4-dihydroxytetrahydrofuran-2-yl)methoxy)(hydroxy)phosphoryl)methyl)phosphonic acid
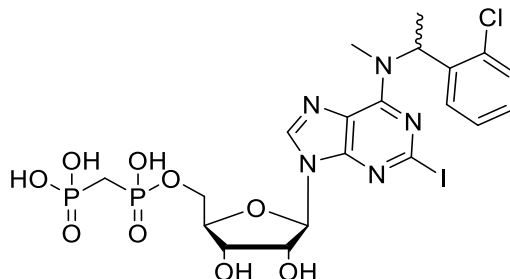
((((((2*R*,3*S*,4*R*,5*R*)-5-(6-((1-(2-Chlorophenyl)ethyl)(methyl)amino)-2-iodo-9*H*-purin-9-yl)-3,4-dihydroxytetrahydrofuran-2-yl)methoxy)(hydroxy)phosphoryl)methyl)phosphonic acid was synthesized according to general procedure C (0.028 g, yield: 18%). ^{1}H NMR (600 MHz, D$_2$O) δ 8.39 (s, 1H, C8-H), 7.67 (d, J = 7.2 Hz, 1H, aryl), 7.48 – 7.41 (m, 2H, aryl), 7.37 (t, J = 7.7 Hz, 1H, aryl), 6.07 (d, J = 5.4 Hz, 1H, C1′-H), 4.75 (d, J = 5.4 Hz, 1H, C2′-H), 4.55 – 4.52 (m, 1H, C3′-H), 4.39 – 4.36 (m, 1H, C4′-H), 4.20 – 4.14 (m, 2H, C5′-H$_2$), 2.86 (s, br, 3H, N-CH$_3$), 2.17 (t, J = 20.0 Hz, 2H, P-CH$_2$-P), 1.76 – 1.66 (m, 3H, α-CH$_3$), ^{13}C NMR (151 MHz, D$_2$O) δ 157.04 (1C, C2), 153.29 (1C, C6), 149.28 (1C, C4), 137.51 (1C, C8), 132.70 (1C, aryl), 132.36 (1C, aryl), 132.04 (1C, aryl), 129.99 (1C, aryl), 122.62 (1C, C5), 122.22 (1C, aryl), 89.66, (1C, C1′), 86.80 (1C, C4′), 77.07 (1C, C2′), 73.05 (1C, C3′), 66.38 (1C, C5′), 54.29 (1C, N-CH), 49.54 (1C, CH$_3$-C̲H$_2$)$_3$-NH$^+$-salt*) 28.41 (1C, P-C̲-P), 25.14 (1C, N-C̲H$_3$), 17.92 (1C, α-CH$_3$), 11.09 (1C, CH$_3$-C̲H$_2$)$_3$-NH$^+$-salt*) ^{31}P NMR (243 MHz, D$_2$O) δ 18.86 (s, P$_α$), 15.17 (s, P$_β$), LC-MS (m/z): negative mode 702.1 [M - H]$^-$ positive mode 704.1 [M + H]$^+$. Purity determined by HPLC-UV (254 nm)-ESI-MS: 98%. HRMS (ESI): *m/z* [M - H]$^-$ calcd for C$_{20}$H$_{24}$ClIN$_5$O$_9$P$_2$: 701.9777; found: 701.9760. Mp. 129 – 131 °C.

*compound bound to 1/3 eq. Et$_3$N

N-CH not visible in ^{1}H NMR

4.5.29 (((((2*R*,3*S*,4*R*,5*R*)-5-(2-Chloro-6-((1-(2-chlorophenyl)ethyl)(methyl)amino)-9*H*-purin-9-yl)-3,4-dihydroxytetrahydrofuran-2-yl)methoxy)(hydroxy)phosphoryl)methyl)phosphonic acid

(((((2*R*,3*S*,4*R*,5*R*)-5-(2-Chloro-6-((1-(2-chlorophenyl)ethyl)(methyl)amino)-9*H*-purin-9-yl)-3,4-dihydroxytetrahydrofuran-2-yl)methoxy)(hydroxy)phosphoryl)methyl)phosphonic acid was synthesized according to general procedure C (0.071 g, yield: 35%). ^{1}H NMR (600 MHz, D$_2$O + NaOD) δ 8.33 (s, 1H, C8-H), 7.59 – 7.54 (m, 1H, aryl), 7.38 – 7.22 (m, 3H, aryl), 5.80 (d, *J* = 5.2 Hz, 1H, C1′-H), 4.53 – 4.49 (m, 1H, C2′-H), 4.21 – 4.13 (m, 2H, C3′-H, C4′-H), 4.03 – 3.97 (m, 2H, C5′-H$_2$), 2.70 (s, br 3H, N-CH$_3$), 1.95 (t, *J* = 19.3 Hz, 2H, P-CH$_2$-P), 1.67 – 1.54 (m, 3H, α-CH$_3$). ^{13}C NMR (151 MHz, D$_2$O) δ 165.97 (1C, C2), 161.46 (1C, C6), 153.47 (1C, C4), 140.69 (1C, C8), 132.36 (1C, aryl), 132.09 (1C, aryl), 131.68 (2C, aryl), 129.80 (2C, aryl), 90.81 (1C, C1′), 86.11 (1C, C4′), 77.22 (1C, C2′), 72.41 (1C, C3′), 66.52 (1C, C5′), 54.96 (N-<u>C</u>H), 31.24 (t, *J* = 123.3, 1C, P-<u>C</u>-P), 29.00 (1C, N-CH$_3$), 17.60 (1C, α-CH$_3$). ^{31}P NMR (243 MHz, D$_2$O) δ 23.15 (d, *J* = 8.0 Hz, P$_\alpha$), 12.51 (d, *J* = 8.3 Hz, P$_\beta$). LC-MS (m/z): negative mode 610.1 [M - H]$^-$ positive mode 612.2 [M + H]$^+$. Purity determined by HPLC-UV (254 nm)-ESI-MS: 97%. HRMS (ESI): *m/z* [M - H]$^-$ calcd for C$_{20}$H$_{24}$Cl$_2$N$_5$O$_9$P$_2$: 610.0421; found: 610.0422. Mp. 159 - 161 °C.

N-CH not visible in ^{1}H NMR

4.5.30 (((((2R,3S,4R,5R)-5-(2-Bromo-6-(methyl(1-phenylethyl)amino)-9H-purin-9-yl)-3,4-dihydroxytetrahydrofuran-2-yl)methoxy)(hydroxy)phosphoryl)methyl)phosphonic acid

(((((2R,3S,4R,5R)-5-(2-Bromo-6-(methyl(1-phenylethyl)amino)-9H-purin-9-yl)-3,4-dihydroxytetrahydrofuran-2-yl)methoxy)(hydroxy)phosphoryl)methyl)phosphonic acid was synthesized according to general procedure C (0.028 g, yield: 15%). ^{1}H NMR (600 MHz, D$_2$O) δ 8.24 (s, 1H, C8-H), 7.28-7.15 (m, 5H, aryl), 5.81 – 5.72 (m, 1H, C1′-H), 4.49 – 4.42 (m, 1H, C2′-H), 4.19 – 4.10 (m, 2H, C3′-H + C4′-H), 4.06 – 3.93 (m, 2H, C5′-H$_2$), 2.91 (s, br, 3H, N-CH$_3$), 1.91 (t, J = 19.3 Hz, 2H, P-CH$_2$-P), 1.59 – 1.46 (m, 3H, α-CH$_3$). ^{13}C NMR (151 MHz, D$_2$O) δ 154.74 (1C, C2), 151.18 (1C, C6), 144.42 (1C, C4), 140.06 (1C, C8), 128.61 (2C, aryl), 127.56 (2C, aryl), 127.02 (2C, aryl), 118.62 (1C, C5), 88.49 (1C, C1′), 84.42 (1C, C4′), 76.18 (1C, C2′), 71.55 (1C, C3′), 64.15 (1C, C5′), 45.29 (1C, N-C̲H) 28.59 (t, J = 123.9 Hz, P-C-P), 20.87 (1C, N-CH$_3$), 15.34 (1C, α-CH$_3$). ^{31}P NMR (243 MHz, D$_2$O) δ 23.12 (d, J = 8.5 Hz, **P$_\alpha$**), 12.46 (d, J = 8.5 Hz, **P$_\beta$**) Purity determined by HPLC-UV (254 nm)-ESI-MS: 98%. HRMS (ESI): m/z [M + H]$^+$ calcd for C$_{20}$H$_{26}$BrN$_5$O$_9$P$_2$: 622.0462; found: 624.0445. Mp. 208 - 210 °C.

N-CH not visible in ^{1}H NMR

4.5.31 (((((2*R*,3*S*,4*R*,5*R*)-5-(2-Chloro-6-(methyl((*S*)-1-phenylethyl)amino)-9*H*-purin-9-yl)-3,4-dihydroxytetrahydrofuran-2-yl)methoxy)(hydroxy)phosphoryl)methyl)phosphonic acid

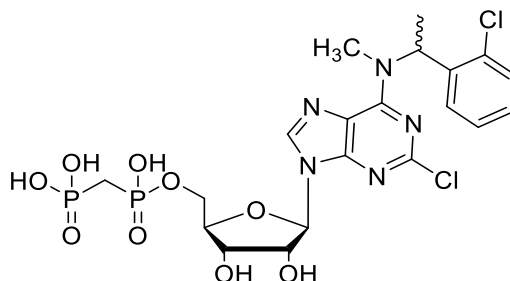(((((2*R*,3*S*,4*R*,5*R*)-5-(2-Chloro-6-(methyl((*S*)-1-phenylethyl)amino)-9*H*-purin-9-yl)-3,4-dihydroxytetrahydrofuran-2-yl)methoxy)(hydroxy)phosphoryl)methyl)phosphonic acid was synthesized according to general procedure C (0.04 g, yield: 15%). ^{1}H NMR (600 MHz, D_2O + NaOD) δ 8.27 (s, 1H, C8-H), 7.29 – 7.23 (m, 4H, aryl), 7.22 – 7.16 (m, 1H, aryl), 5.76 (d, J = 5.3 Hz, 1H, C1'-H), 4.51 – 4.46 (m, 1H, C2'-H), 4.14 – 4.12 (m, 1H, C3'-H), 4.14 – 4.12 (m, 1H, C4'-H), 4.06 – 4.00 (m, 1H, C5'-H), 3.99 – 3.93 (m, 1H, C5'-H), 2.89 (s, br, 3H, N-CH$_3$), 1.91 (t, J = 19.4 Hz, 2H, P-CH$_2$-P), 1.61 – 1.48 (m, 3H, α-CH$_3$). ^{13}C NMR (151 MHz, D_2O + NaOD) δ 157.75 (1C, C2), 156.32 (1C, C6), 154.08 (1C, C4), 142.81 (1C, C8), 131.37 (2C, aryl), 130.32 (2C, aryl), 129.79 (2C, aryl), 121.02 (1C, C5), 91.16 (1C, C1'), 87.25 (1C, C4'), 78.82 (1C, C2'), 74.32 (1C, C3'), 71.31 (1C, CH), 66.90 (1C, C5'), 56.70 (1C, α-CH), 33.43 (1C, N-CH$_3$), 31.09 (t, J = 128.8 Hz, P-C-P), 18.05 (1C, α-CH$_3$). ^{31}P NMR (243 MHz, D_2O) δ 22.91 (d, J = 9.2 Hz, **P$_α$**), 12.09 (d, J = 7.8 Hz, **P$_β$**). Purity determined by HPLC-UV (254 nm)-ESI-MS: 100% HRMS (ESI): *m/z* [M - H]$^-$ calcd for $C_{20}H_{25}ClN_5O_9P_2$: 576.081; found: 576.0831. Mp. 208 - 210 °C. Specific optical rotation: $[\alpha]_D^{20}$ = - 0.078° (H_2O, c = 5.5 mg/ml).
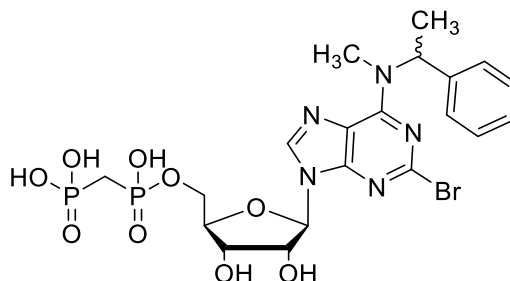
α-CH overlaping with H$_2$O peak in ^{1}H NMR

4.5.32 (((((2*R*,3*S*,4*R*,5*R*)-5-(2-Chloro-6-(methyl((*R*)-1-phenylethyl)amino)-9*H*-purin-9-yl)-3,4-dihydroxytetrahydrofuran-2-yl)methoxy)(hydroxy)phosphoryl)methyl)phosphonic acid
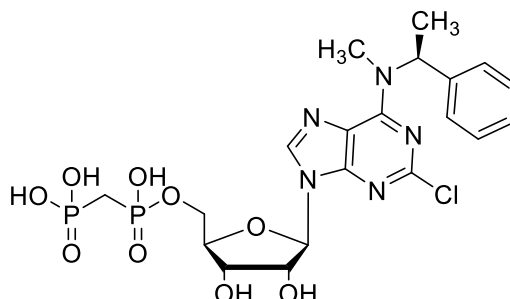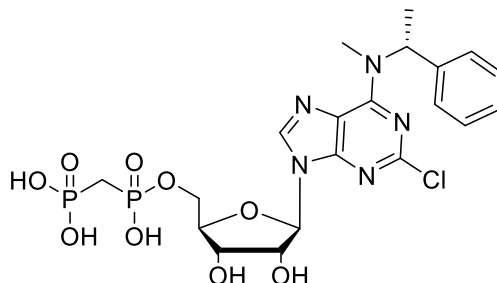

(((((2*R*,3*S*,4*R*,5*R*)-5-(2-Chloro-6-(methyl((*R*)-1-phenylethyl)amino)-9*H*-purin-9-yl)-3,4-dihydroxytetrahydrofuran-2-yl)methoxy)(hydroxy)phosphoryl)methyl)phosphonic acid was synthesized according to general procedure C (0.037 g, yield: 22%). ^{1}H NMR (600 MHz, D$_2$O) δ 8.40 (s, 1H, C8-H), 7.38 – 7.26 (m, 5H, aryl), 5.90 (d, *J* = 5.2 Hz, 1H, C1′-H), 4.63 (t, *J* = 5.2 Hz, 1H, C2′-H), 4.34 – 4.31 (m, 1H, C3′-H), 4.30 – 4.27 (m, 1H, C4′-H), 4.18 – 4.09 (m, 2H, C5′-H), 3.00 (s br, 3H, N-CH$_3$), 2.47 (q, *J* = 7.2 Hz, 1H), 2.02 (t, *J* = 19.5 Hz, 2H, P-CH$_2$-P), 1.65 (s, 3H, α-CH$_3$), 0.97 (t, *J* = 7.2 Hz, 1H). ^{13}C NMR (151 MHz, D$_2$O) δ 157.74 (1C, C6), 156.33 (1C, C2), 153.99 (1C, C4), 142.81 (1C, C8), 131.35 (1C, aryl), 130.29 (1C, aryl), 129.76 (1C, aryl), 121.00 (1C, C5), 90.78 (1C, C1′), 86.97 (1C, C4′), 78.35 (1C, C2′), 73.84 (1C, C3′), 66.59 (1C, C5′), 55.50 (1C, α-<u>C</u>H), 48.03, 31.25 (dd, *J* = 125.8, 117.9 Hz, P-<u>C</u>-P), 18.12, 12.76 (1C, α-<u>C</u>H$_3$). ^{31}P NMR (243 MHz, D$_2$O) δ 23.03 (d, *J* = 8.6 Hz, **P$_\alpha$**), 12.14 (d, *J* = 7.9 Hz, **P$_\beta$**). Purity determined by HPLC-UV (254 nm)-ESI-MS: 99% HRMS (ESI): *m/z* [M + H]$^+$ calcd for C$_{20}$H$_{27}$ClN$_5$O$_9$P$_2$: 578.0967; found: 578.0988. Mp. 157 - 159 °C.

α-CH overlapping with H$_2$O peak in ^{1}H NMR

4.5.33 (((((2*R*,3*S*,4*R*,5*R*)-5-(2,6-Dichloro-9*H*-purin-9-yl)-3,4-dihydroxytetrahydrofuran-2-yl)methoxy)(hydroxy)phosphoryl)methyl)phosphonic acid
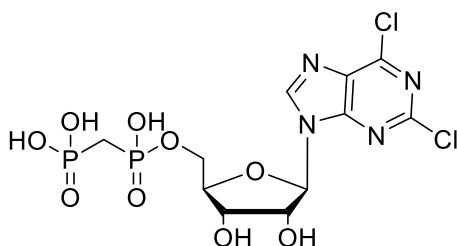
(((((2*R*,3*S*,4*R*,5*R*)-5-(2,6-Dichloro-9*H*-purin-9-yl)-3,4-dihydroxytetrahydrofuran-2-yl)methoxy)(hydroxy)phosphoryl)methyl)phosphonic acid was synthesized according to general procedure C (0.04 g , yield: 27%) ^{1}H NMR (600 MHz, D$_2$O) δ 8.24 (s, 1H, C8-H), 5.76 (d, J = 6.1 Hz, 1H, C1′-H), 4.56 (t, J = 5.8 Hz, 1H, C2′-H), 4.24 – 4.14 (m, 2H, C3′-H + C4′-H), 4.08 – 3.99 (m, 2H, C5′-H), 1.96 (t, J = 19.8 Hz, 2H, P-CH$_2$-P).^{13}C NMR (151 MHz, D$_2$O) δ 167.60 (1C, C6), 154.16 (1C, C2), 151.05 (1C, C4), 136.28 (1C, C8), 122.33 (1C, C5), 88.10 (1C, C1′), 84.42 (1C, C4′), 75.91 (1C, C2′), 71.67 (1C, C3′), 64.17 (1C, C5′), 30.15 – 26.72 (m, P-<u>C</u>-P). ^{31}P NMR (243 MHz, D$_2$O) δ 23.11 (d, J = 8.5 Hz, **P$_\alpha$**), 12.43 (d, J = 8.8 Hz, **P$_\beta$**). Purity determined by HPLC-UV (254 nm)-ESI-MS: 84%.

4.5.34 (2*R*,3*R*,4*R*,5*R*)-2-(Acetoxymethyl)-5-(6-chloro-9*H*-purin-9-yl)tetrahydrofuran-3,4-diyl diacetate
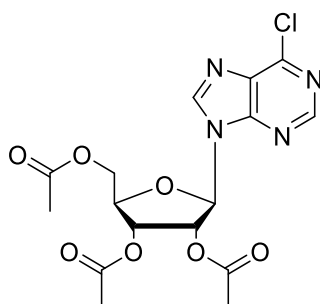
6-Chloro-9-(β-D-ribofuranosyl)purine (1 g, 3.5 mmol, 1 eq.) and 4-(dimethylamino)pyridin were suspended in a mixture of triethylamine (1.42 g, 14.0 mmol, 4 eq.), acetic anhydride (1.3 ml, 14.0 mmol, 4 eq.) and 15 ml acetonitrile. The reaction mixture was stirred for 60 minutes

at room temperature. After 60 minutes, 5 ml of methanol were added to the reaction mixture and the solvents were evaporated, which yielded a brown, viscous oil. The crude mixture was purified by normal phase column chromatography (silica gel, DCM/methanol 98/2). Appropriate fractions were pooled, the solvents were evaporated to give the desired product as colorless resin (1.25 g, yield: 87%).[156] ^{1}H NMR (500 MHz, DMSO-d_6) δ 8.89 (s, 1H, C8-H), 8.85 (s, 1H, C2-H), 6.37 (d, J = 5.1 Hz, 1H, C1'-H), 6.02 (dd, J = 5.9, 5.1 Hz, 1H, C2'-H), 5.65 (dd, J = 6.0, 5.0 Hz, 1H, C3'-H), 4.46 – 4.37 (m, 2H, C5'-H, C5''-H), 4.31 – 4.22 (m, 1H, C4'-H), 2.12 (s, 3H, CH$_3$), 2.04 (s, 3H, CH$_3$), 2.01 (s, 3H, CH$_3$). ^{13}C NMR (126 MHz, DMSO-d_6) δ 170.13 (1C, C=O), 169.51 (1C, C=O), 169.35 (1C, C=O), 152.09 (1C, C8), 151.43 (1C, C6), 149.81 (1C, C4), 146.47 (1C, C2), 131.74 (1C, C5), 86.42 (1C, C1'), 79.89 (1C, C4'), 72.26 (1C, C2'), 70.05 (1C, C3'), 62.81 (1C, C5'), 20.60 (1C, CH$_3$), 20.49 (1C, CH$_3$), 20.32 (1C, CH$_3$). LC-MS (*m/z*): positive mode 413.0 [M+H]$^+$. Purity determined by HPLC-UV (254 nm)-ESI-MS: 95%.

4.5.35 (2*R*,3*R*,4*R*,5*R*)-2-(Acetoxymethyl)-5-(6-((6-((*tert*-butoxycarbonyl)amino)hexyl)amino)-9*H*-purin-9-yl)tetrahydrofuran-3,4-diyl diacetate
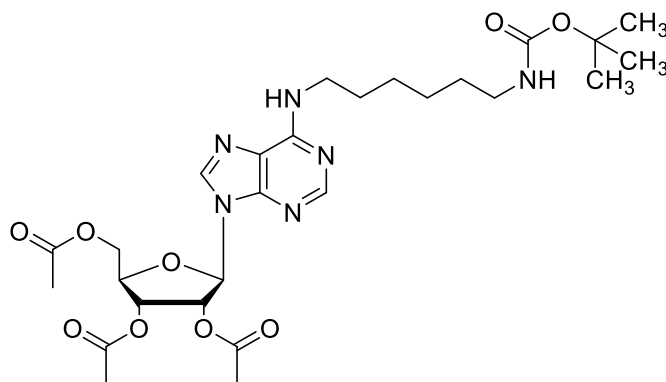
(2*R*,3*R*,4*R*,5*R*)-2-(Acetoxymethyl)-5-(6-chloro-9*H*-purin-9-yl)tetrahydrofuran-3,4-diyl diacetate (0.45 g, 1.1 mol, 1 eq.) was dissolved in 20 ml of ethanol. To the reaction mixture was

added *N-boc*-1,6-hexanediamine (0.24 g, 1.1 mmol, 1 eq.) and triethylamine (0.14 ml, 1.0 mmol, 0.9 eq.). The reaction was refluxed at 90 °C for 20 h. After TLC indicated completion of the reaction, the product was purified by normal phase column chromatography (DCM/methanol 98/2). Appropriate fractions were pooled and evaporated to give the desired product as a light brown, viscous oil (0.35 g, yield 54%).[102] ^{1}H NMR (600 MHz, DMSO-d_6) δ 8.33 (s, 1H, NH), 8.23 (s, 1H, C8-H), 7.89 (s, 1H, C2-H), 6.72 (t, J = 5.4 Hz, 1H, NH), 6.20 (d, J = 5.4 Hz, 1H, C1′-H), 6.03 (t, J = 5.7 Hz, 1H, C2′-H), 5.63 (t, J = 5.4 Hz, 1H, C3′-H), 4.41 (dd, J = 11.9, 3.8 Hz, 1H, C4′-H), 4.35 (td, J = 5.2, 3.8 Hz, 1H, C5′-H), 4.24 (dd, J = 11.9, 5.6 Hz, 1H, C5′-H), 3.45 (s, 2H, CH$_2$), 2.89 (q, J = 6.6 Hz, 2H, CH$_2$), 2.11 (s, 3H, CH$_3$), 2.04 (s, 3H, CH$_3$), 2.01 (s, 3H, CH$_3$), 1.57 (t, J = 7.2 Hz, 2H, CH$_2$), 1.38 – 1.34 (m, 11H, 3 x *boc* CH$_3$ + CH$_2$), 1.31 – 1.23 (m, 4H, 2 x CH$_2$). ^{13}C NMR (151 MHz, DMSO-d_6) δ 170.14 (1C, C=O), 169.57 (1C, C=O), 169.39 (1C, C=O), 155.69 (1C, C=O, *boc*), 154.74 (1C, C6), 152.99 (1C, C8), 151.74 (1C, C2), 148.33 (1C, C4), 145.08, 119.68 (1C, C5), 85.76 (1C, C1′), 79.53 (1C, C4′), 77.40 (1C, Cq, *boc*), 72.03 (1C, C2′), 70.22 (1C, C3′), 62.94 (1C, C5′), 29.59 (2C, 2 x CH$_2$), 29.11 (1C, CH$_2$), 28.40 (3C, CH$_3$), 26.25 (1C, CH$_2$), 26.20 (2C, 2 x CH$_2$), 20.60 (1C, CH$_3$), 20.50 (1C, CH$_3$), 20.33 (1C, CH$_3$). LC-MS (*m/z*): positive mode 593.1 [M+H]$^+$. Purity determined by HPLC-UV (254 nm)-ESI-MS: 92%.

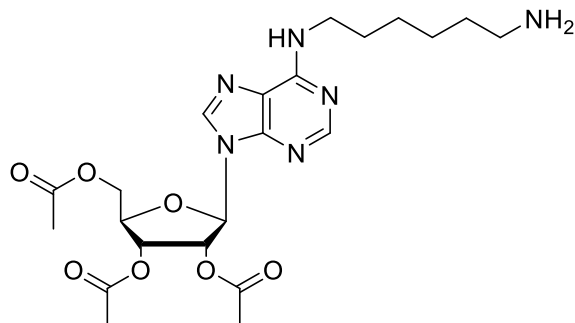### 4.5.36 (2R,3R,4R,5R)-2-(Acetoxymethyl)-5-(6-((6-aminohexyl)amino)-9H-purin-9-yl)tetrahydrofuran-3,4-diyl diacetate

(2R,3R,4R,5R)-2-(Acetoxymethyl)-5-(6-((6-((*tert*-butoxycarbonyl)amino)hexyl)amino)-9H-purin-9-yl)tetrahydrofuran-3,4-diyl diacetate (0.1 g, 0.17 mmol, 1 eq.) was dissolved in 5 ml DCM. Then, TFA (1.3 ml) and a few drops of water were added to the reaction mixture, which was then stirred for 3 h. After TLC indicated completion of the reaction, the volatiles were evaporated and the resulting crude mixture was purified by normal phase column chromatography (silica gel, DCM/methanol 9/1). Appropriate fractions were pooled and the solvents were evaporated to give the desired product as light brown, viscous oil.[156] ^{1}H NMR (500 MHz, DMSO-d_6) δ 8.33 (s, 1H, C8-H), 8.23 (s, 1H, C2-H), 7.89 (s, 1H, NH), 7.51 (s, 2H, NH$_2$), 6.20 (d, J = 5.3 Hz, 1H, C1′-H), 6.03 (t, J = 5.6 Hz, 1H, C2′-H), 5.66 – 5.61 (m, 1H, C3′-H), 4.43 – 4.39 (m, 1H, C4′-H), 4.38 – 4.33 (m, 1H, C5′-H), 4.26 – 4.21 (m, 1H, C5′-H), 3.47 (s, 2H, NH-C$\underline{H}_2$), 2.78 – 2.73 (m, 2H, NH$_2$-C$\underline{H}_2$), 2.11 (s, 3H, CH$_3$), 2.04 (s, 3H, CH$_3$), 2.00 (s, 3H, CH$_3$), 1.59 (t, J = 7.0 Hz, 2H, CH$_2$) 1.52 (t, J = 7.5 Hz, 2H, CH$_2$), 1.37 – 1.29 (m, 4H, 2 x CH$_2$). ^{13}C NMR (126 MHz, DMSO-d_6) δ 169.97 (1C, C=O), 169.40 (1C, C=O), 169.24 (1C, C=O), 85.69 (1C, C1′), 79.34 (1C, C4′), 71.88 (1C, C2′), 70.05 (1C, C3′), 62.77 (1C, C5′), 27.18 (2C, CH$_2$), 25.89 (2C, CH$_2$), 25.56 (2C, CH$_2$), 20.43 (1C, CH$_3$), 20.32 (1C, CH$_3$), 20.16 (1C, CH$_3$). LC-MS (m/z): positive mode 493.2 [M+H]+. Purity determined by HPLC-UV (254 nm)-ESI-MS: 84%.

4.5.37 (2*R*,3*R*,4*R*,5*R*)-2-(Acetoxymethyl)-5-(6-((6-(3',6'-dihydroxy-3-oxo-3*H*-spiro[isobenzofuran-1,9'-xanthene]-6-carboxamido)hexyl)amino)-9*H*-purin-9-yl)tetrahydrofuran-3,4-diyl diacetate
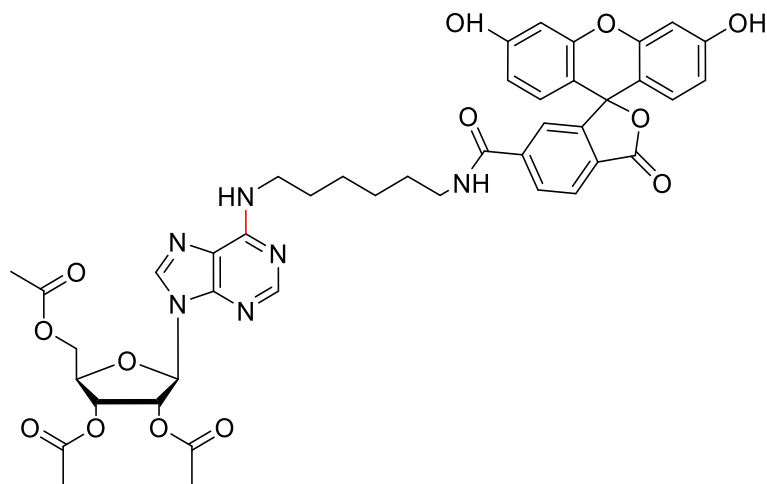
5(6)-Carboxyfluoresein (0.18 g, 1 eq., 0.47 mmol) was dissolved in 20 ml of THF. HOBt (0.072 g, 1 eq., 0.47 mmol) and DCC (0.096 g, 1 eq., 0.47 mmol) was added to the reaction mixture and was then stirred for 20 min at room temperature. After that, (2*R*,3*R*,4*R*,5*R*)-2-(acetoxymethyl)-5-(6-((6-aminohexyl)amino)-9*H*-purin-9-yl)tetrahydrofuran-3,4-diyl diacetate (0.23 g, 1 eq., 0.47 mmol) was added to the reaction mixture which was then stirred overnight at room temperature. Purification by normal phase column chromatography gave the desired product in low purity.[137] LC-MS (m/z): positive mode 851.0 [M+H]+. Purity determined by HPLC-UV (254 nm)-ESI-MS: 23%. *Due to low purity – no yield was calculated.*

4.5.38 *tert*-Butyl (6-(3',6'-dihydroxy-3-oxo-3*H*-spiro[isobenzofuran-1,9'-xanthene]-6-carboxamido)hexyl) carbamate
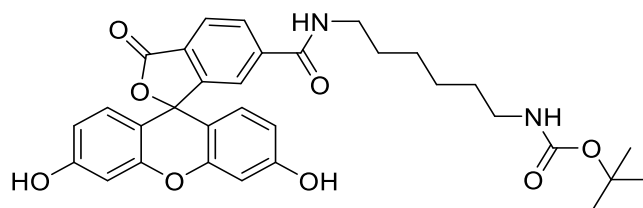
6-Carboxyfluoresein (0.33 g, 0.88 mmol, 1.0 eq.) was dissolved in 6 ml of DMF. DIPEA (0.46 ml, 2.63 mmol, 3.0 eq.) and HATU (0.37 g, 0.96 mmol, 1.1 eq.) was added to the reaction mixture which was then stirred for 20 minutes for preactivation. After that, *N-boc*-1,6-hexanediamine (0.21 ml, 0.96 mmol, 1.1 eq.) was added and the reaction was stirred overnight.[158] After TLC indicated completion of the reaction, the volatiles were evaporated and the crude mixture was diluted in ethyl acetate and extracted with water and subsequently with an aqueous solution of lithium chloride (10%). The organic phase was dried over sodium sulfate and filtrated. Solvents were evaporated and the residue was purified with normal phase column chromatography (DCM/methanol 9/1). Appropriate fractions were pooled and the solvents were evaporated to give the desired product as yellow solid. (0.49 g, yield 98%). ^{1}H NMR (500 MHz, DMSO-*d_6*) δ 8.67 (t, *J* = 5.7 Hz, 1H, NH), 8.16 (dd, *J* = 8.1, 1.4 Hz, 1H, C4-H), 8.05 (d, *J* = 8.0 Hz, 1H, C5-H), 7.66 – 7.64 (m, 1H, C7-H), 6.71 (d, *J* = 2.0 Hz, 2H, C1′-H + C8′-H), 6.57 (s br, 2H, C4′-H + C5′-H), 6.56 (d, *J* = 2.1 Hz, 2H, C2′-H + C7′-H), 3.65 – 3.56 (m, 2H, NH-C$\underline{H}_2$), 3.23 – 3.16 (m, 2H, NH-C$\underline{H}_2$), 1.60 – 1.50 (m, 8H, 4 x CH$_2$), 1.28 – 1.23 (m, 9H, 3 x CH$_3$). ^{13}C NMR (126 MHz, DMSO-*d_6*) δ 168.22 (1C, C3=O), 164.52 (1C, C=O), 159.85 (2C, C3′ + C6′), 158.56 (1C, C7a), 152.00 (2C, 4a′ + 10a′), 140.98 (1C, C6), 129.50 (1C, C4), 129.34 (2C, C1′ + C8′), 128.28 (1C, C3a), 124.98 (1C, C7), 122.35 (1C, C5), 112.94 (2C, C2′ + C7′), 109.31 (2C, 8a′ + 9a′), 102.45 (2C, C4′ + C5′), 53.61 (1C, C1), 45.74 (1C, $\underline{C}$-(CH$_3$)$_3$), 28.89 (1C, N-CH$_2$), 26.93 (2C, 2x CH$_2$), 26.13 (1C, N-CH$_2$) , 25.45 (2C, 2 x CH$_2$), 18.18 (1C, CH$_3$), 16.88 (1C, CH$_3$), 12.41 (1C, CH$_3$). LC-MS (m/z): positive mode 575.5 [M+H]$^+$. Purity determined by HPLC-UV (254 nm)-ESI-MS: 94%.

4.5.39 *N*-(6-Aminohexyl)-3′,6′-dihydroxy-3-oxo-3*H*-spiro[isobenzofuran-1,9′-xanthene]-6-carboxamide
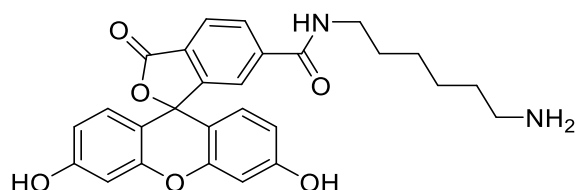
tert-Butyl (6-(3′,6′-dihydroxy-3-oxo-3*H*-spiro[isobenzofuran-1,9′-xanthene]-6-carboxamido)hexyl) carbamate (0.46 g, 8.0 mmol, 1.0 eq.) was dissolved in 10 ml of dry DCM. Upon stirring, TFA (3 ml) and a drop of water was added to the reaction mixture and the reaction was stirred for 5 h at room temperature.[137] Evaporation of the volatiles gave the desired product without further purification. ^{1}H NMR (600 MHz, DMSO-*d$_6$*) δ 8.79 (s, 1H, NH), 8.08 (d, *J* = 8.0 Hz, 1H, C4-H), 8.01 (d, *J* = 8.1 Hz, 1H, C5-H), 7.63 (s, 1H, C7-H), 6.59 (d, *J* = 8.8 Hz, 2H, C1′-H + C8′-H), 6.52 (s br, 2H, C2′-H, C7′-H), 6.40 (d, *J* = 8.9 Hz, 2H, C4′-H, C5′-H), 3.22 – 3.15 (m, 2H, NH-C$\underline{H}_2$), 2.62 – 2.57 (m, 2H, NH$_2$-C$\underline{H}_2$), 1.44 (t, *J* = 6.9 Hz, 2H, NH-CH$_2$-C$\underline{H}_2$), 1.37 (t, *J* = 7.4 Hz, 2H, NH$_2$-CH$_2$-C$\underline{H}_2$), 1.24 – 1.18 (m, 4H, 2 x CH$_2$). ^{13}C NMR (151 MHz, DMSO-*d$_6$*) δ 168.36 (1C, C3=O), 164.95 (1C, C=O), 156.34 (2C, C3′ + C6′), 153.83 (1C, C7a), 153.68 (2C, C4a′ + C10a′), 138.86 (1C, C6), 129.76 (2C, C1′ + C8′), 128.93 (1C, C3a), 126.51 (1C, C4), 122.10 (1C, C7), 121.04 (1C, C5), 117.86 (1C, C2′), 112.18 (1C, C7′), 109.95 (2C, C8a′ + 9a′), 102.56 (2C, C4′ + C5′), 84.86 (1C, C1), 48.89 (1C, NH$_2$-CH$_2$), 40.23 (1C, NH-CH$_2$, *overlapping with solvent peak*), 28.97 (1C, CH$_2$), 28.71 (1C, CH$_2$), 26.31 (1C, CH$_2$), 25.91 (1C, CH$_2$). LC-MS (m/z): positive mode 475.5 [M+H]$^+$. Purity determined by HPLC-UV (254 nm)-ESI-MS: 95%.

4.5.40 ((2R,3S,4R,5R)-5-(6-Chloro-9H-purin-9-yl)-3,4-dihydroxytetrahydrofuran-2-yl)methyl dihydrogen phosphate
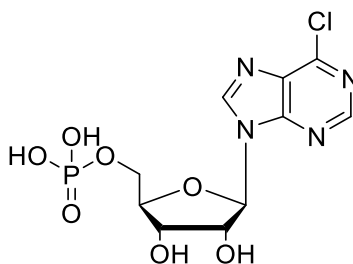
6-Chloro-9-(β-D-ribofuranosyl)purine (0.1 g, 0.35 mmol, 1 eq.) was dissolved in 5 ml of trimethyl phosphate and stirred under ice cooling. 1,8-Bis(dimethylamino)naphthalene (Proton sponge) (0.1 g, 0.52 mmol, 1.5 eq.) was added, followed by addition of phosphorus oxychloride (0.1 ml, 1.1 mmol, 3.1 eq.). The reaction mixture was stirred for 4 h under argon. After 4 h, 0.5 M TEAC buffer was (10 ml) was slowly added. The reaction mixture was stirred for another 30 minutes at 0 °C, and for 1 h at room temperature. The reaction mixture was afterwards extracted two times with TBME. The aqueous phase was lyophilized and purified by RP-HPLC.[141] ^{1}H NMR (600 MHz, D$_2$O) δ 9.00 (s, 1H, C8-H), 8.79 (s, 1H, C2-H), 6.29 (d, J = 5.5 Hz, 1H, C1′-H), 4.84 (t, J = 5.3 Hz, 1H, C2′-H), 4.55 – 4.53 (m, 1H, C3′-H), 4.42 – 4.40 (m, 1H, C4′-H), 4.11 – 4.04 (m, 2H, C5′-H). ^{13}C NMR (151 MHz, D$_2$O) δ 154.76 (1C, C2), 154.30 (1C, C4), 153.05 (1C, C6), 146.45 (1C, C8), 134.09 (1C, C5), 90.66 (1C, C1′), 87.68 (1C, C4′), 77.57 (1C, C2′), 73.43 (1C, C3′), 66.40 (1C, C5′). ^{31}P NMR (202 MHz, D$_2$O) δ 3.21. LC-MS (*m/z*): positive mode 366.9 [M+H]$^+$. Purity determined by HPLC-UV (254 nm)-ESI-MS: 100%.

4.5.41 ((2R,3S,4R,5R)-5-(6-((6-(3′,6′-Dihydroxy-3-oxo-3H-spiro[isobenzofuran-1,9′-xanthene]-6-carboxamido)hexyl)amino)-9H-purin-9-yl)-3,4-dihydroxytetrahydrofuran-2-yl)methyl dihydrogen phosphate
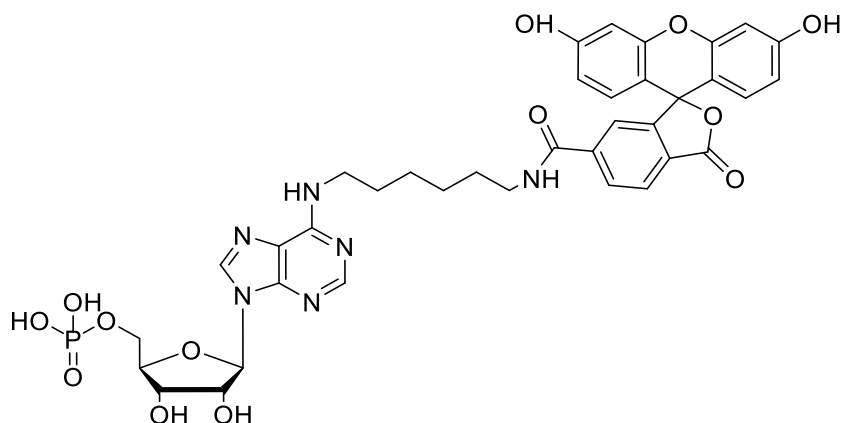
((2R,3S,4R,5R)-5-(6-Chloro-9H-purin-9-yl)-3,4-dihydroxytetrahydrofuran-2-yl)methyl dihydrogen phosphate (0.2 g, 0.55 mmol, 2.0 eq.) was dissolved in 6 ml of ethanol. Triethylamine (0.035 ml, 0.25 mmol, 0.9 eq.) was added to the reaction mixture. *N*-(6-aminohexyl)-3′6′dihydroxy-3-oxo-3H-spiro[isobenzofuran-1,9′-xanthene]-6-carboxamide (0.13 g, 0.27 mmol, 1.0 eq.) was added to the reaction mixture, which was then refluxed for 8 h at 90 °C. After completion of the reaction, the volatiles were evaporated and the crude mixture was purified by RP-HPLC. Appropriate fractions were pooled and evaporated. Remaining aqueous eluent was frozen with liquid nitrogen and lyophilized to give the desired product as fluffy, orange powder (0.052 g, yield: 23%).[102] ^{1}H NMR (600 MHz, D$_2$O) δ 8.24 (s, 1H, C8-H), 7.91 (s br, 2H, C5-H + C7-H, FL), 7.88 (s, 1H, C2-H), 7.57 (s, 1H, C4, FL), 6.96 – 6.89 (m, 2H, C1′-H + C8′-H, FL), 6.60 – 6.58 (m, 1H, C5′, FL), 6.58 – 6.53 (m, 3H, C2′-H + C4′-H + C7′-H, FL), 6.01 – 5.98 (m, 1H, C1′-H), 4.65 (s, 1H, C2′-H), 4.47 (t, J = 4.9 Hz, 1H, C3′-H), 4.36 (s, 1H, C4′-H), 4.18 – 4.10 (m, 2H, C5′-H), 3.29 (t, J = 6.4 Hz, 2H, N-CH$_2$), 3.13 (s br, 1H, N-CH$_2$), 1.49 – 1.44 (m, 2H, N-CH$_2$-C$\underline{H}_2$), 1.38 (t, *J* = 7.1 Hz, 2H, N-CH$_2$-C$\underline{H}_2$), 1.29 –

1.22 (m, 4H, -CH$_2$-CH$_2$-). ^{13}C NMR (151 MHz, D$_2$O) δ 175.55 (1C, C̲=O), 171.67 (1C, C̲=O), 159.49 (2C, C3′ + C6′, FL), 138.77 (1C, C6, FL), 133.74 (1C, C4-H, FL), 131.65 (2C, C1′-H + C8′-H, FL), 131.47 (1C, C7-H, FL), 130.28 (1C, C5-H, FL), 122.63 (1C, C2′, FL), 122.63 (1C, C7′, FL), 121.43 (1C, C8), 116.84 (2C, C8a′-H + C9a′-H, FL), 105.84 (1C, C4′-H, FL), 105.80 (1C, C5′-H, FL), 89.95 (1C, C1′), 89.71 (1C, C1, FL), 86.62 (1C, C4′), 77.39 (1C, C2′), 73.17 (1C, C3′), 67.25 (d, J = 4.3 Hz, 1C, C5′), 42.72 (2C, CH$_2$), 30.59 (2C, CH$_2$), 28.25 (1C, CH$_2$), 28.20 (1C, CH$_2$). ^{31}P NMR (243 MHz, D$_2$O) δ 0.70. LC-MS (*m/z*): positive mode 805.4 [M+H]$^+$. Purity determined by HPLC-UV (254 nm)-ESI-MS: 95%. Mp. 232-233 °C.

4.5.42 *N*-(6-((9-((2*R*,3*R*,4*S*,5*R*)-3,4-Dihydroxy-5-(hydroxymethyl)tetrahydrofuran-2-yl)-9*H*-purin-6-yl)amino)hexyl)-3',6'-dihydroxy-3-oxo-3*H*-spiro[isobenzofuran-1,9'-xanthene]-6-carboxamide
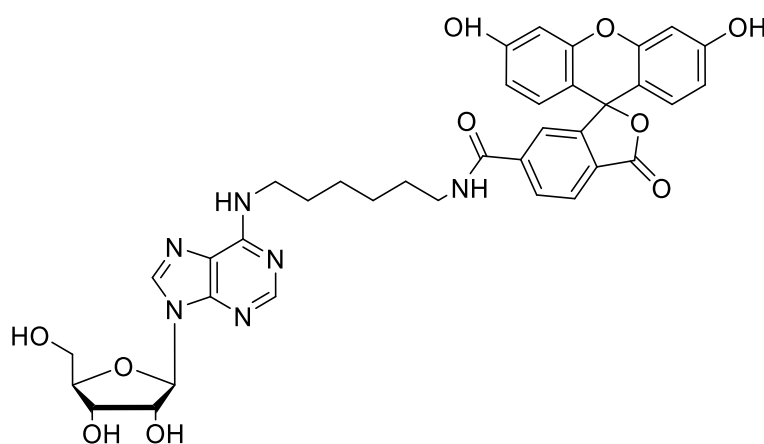
6-Chloro-9-(β-D-ribofuranosyl)purine (0.060 g, 0.21 mmol, 1 eq.) was dissolved in 8 ml of ethanol. Triethylamine (0.019 ml, 0.21 mmol, 0.92 eq.) was added to the reaction mixture. *N*-(6-Aminohexyl)-3′6′dihydroxy-3-oxo-3*H*-spiro[isobenzofuran-1,9′-xanthene]-6-carboxamide (0.10 g, 0.21 mmol, 1 eq.) was added to the reaction mixture, which was then refluxed for 8 h at 90 °C. After TLC indicated completion of the reaction, the volatiles were evaporated and the crude mixture was purified by normal phase column-chromatography. Appropriate fractions

were pooled and evaporated to give the desired compound as orange powder (0.052 g, yield: 23%).[102] ^{1}H NMR (600 MHz, DMSO-d_6) δ 10.26 – 10.09 (m, 2H, 2 x OH, FL), 8.63 (t, J = 5.6 Hz, 1H, C4-H, FL), 8.29 (s, 1H, C8-H), 8.16 – 8.11 (m, 1H, C5-H), 8.05 (d, J = 8.0 Hz, 1H, C7, FL), 7.79 (s, 1H, NH), 7.64 (s, 1H, C2-H), 6.68 (d, J = 2.3 Hz, 2H, C1′-H + C8′-H, FL), 6.59 – 6.53 (m, 3H, C2′-H + C4′-H + C7′-H, FL), 5.85 (d, J = 6.2 Hz, 1H, C1′-H), 5.45 – 5.39 (m, 2H, 2X OH), 5.17 (d, J = 4.5 Hz, 1H, OH), 4.58 (q, J = 5.6 Hz, 1H, C2′-H), 4.13 (q, J = 4.0 Hz, 1H, C3′-H), 3.95 (q, J = 3.4 Hz, 1H, C4′-H), 3.68 – 3.63 (m, 1H, C5′-H), 3.56 – 3.51 (m, 1H, C5′-H, *overlapping with solvent peak*), 3.17 (q, J = 6.7 Hz, 2H, CH$_2$), 1.54 (t, J = 7.1 Hz, 2H, CH$_2$), 1.44 (t, J = 7.1 Hz, 2H, CH$_2$), 1.32 – 1.23 (m, 4H, CH$_2$-CH$_2$). ^{13}C NMR (151 MHz, DMSO-d_6) δ 168.56 (1C, C3=O), 164.87 (1C, C=O), 160.13 (1C, C6), 155.10 (2C, C3′ + C6′, FL), 152.80 (1C, C2), 152.33 (2C, C4a′ + C10a′, FL), 148.62 (1C, C7a, FL), 141.27 (1C, C6, FL), 140.04 (1C, C8), 129.81 (1C, C4, FL), 129.70 (1C, C1′-H + C8′-H, FL), 128.66 (1C, C3a), 125.35 (1C, C7, FL), 122.69 (1C, C5, FL), 120.16 (1C, C5), 113.28, 109.69, 102.73, 88.43 (1C, C1′), 86.38 (1C, C4′), 73.93 (1C, C2′), 71.12 (1C, C3′), 62.15 (1C, C5′), 29.35 (1C, CH$_2$), 26.73 (1C, CH$_2$), 26.55 (2C, CH$_2$-CH$_2$). 2 x CH$_2$ overlapping with solvent peak., C1-FL not visibile. LC-MS (*m/z*): positive mode 725.4 [M+H]$^+$. Purity determined by HPLC-UV (254 nm)-ESI-MS: 90%.

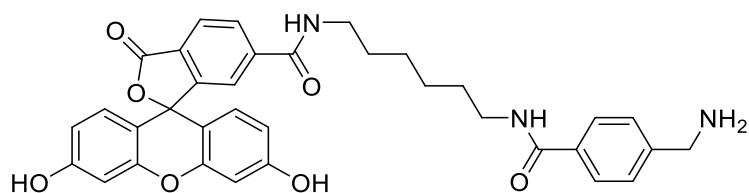### 4.5.43 *tert*-Butyl (4-((6-(3′,6′-dihydroxy-3-oxo-3*H*-spiro[isobenzofuran-1,9′-xanthene]-6-carboxamido)hexyl)carbamoyl)benzyl) carbamate
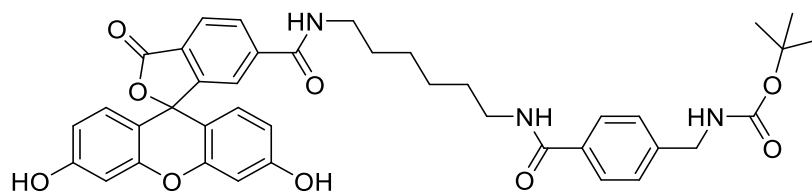
4-(*Boc*-aminobenzyl)benzoic acid (0.32 g, 1.3 mmol, 1.0 eq.) was dissolved in 5 ml of DMF. DIPEA (0.66 ml, 3.8 mmol, 3.0 eq.) and HATU (0.53 g, 1.4 mmol, 1.1 eq.) was added to the reaction mixture. The mixture was stirred for 20 min at room temperature for preactivation. Then, *N*-(6-aminohexyl)-3′,6′-dihydroxy-3-oxo-3*H*-spiro[isobenzofuran-1,9′-xanthene]-6-carboxamide (0.6 g, 1.3 mmol, 1.0 eq.) was added to the reation mixture which was stirred overnight at room temperature.[158] After the reaction was finished, the volatiles were evaporated and the crude mixture was diluted in ethyl acetate and extracted with water and subsequently with an aqueous solution of lithium chloride (10%). The organic phase was dried over sodium sulfate and filtrated. The solvent was evaporated and the residue was purified with normal phase column chromatography (DCM/methanol 8/2). Appropriate fractions were pooled and evaporated to give the desired compound (0.51 g, yield 56%). ^{1}H NMR (600 MHz, DMSO-*d6*) δ 10.15 (s, 2H, OH), 8.67 (t, *J* = 5.6 Hz, 1H, NH), 8.35 (t, *J* = 5.6 Hz, 1H, NH), 8.19 (dd, *J* = 8.0, 1.4 Hz, 1H, NH), 8.09 (d, *J* = 8.0, 0.7 Hz, 1H, C4-H), 7.78 (d, *J* = 8.0 Hz, 2H, C5-H + C7-H), 7.70 – 7.68 (m, 1H, C2-H, benzylamine), 7.43 (t, *J* = 6.2 Hz, 1H, C6-H, benzylamine), 7.30 (d, *J* = 8.0 Hz, 2H, C3-H + C5-H, benzylamine), 6.72 (d, *J* = 2.3 Hz, 2H, C1′-H + C8′-H), 6.61 (d, *J* = 8.7 Hz, 2H, C2′-H + C7′-H), 6.58 (dd, *J* = 8.7, 2.3 Hz, 2H, C4′-H + C5′-H), 4.18 (d, *J* = 6.1 Hz, 2H, CH$_2$-NH), 3.25 – 3.19 (m, 2H, 2 x CH$_2$-NH), 1.60 – 1.50 (m, 8H, 4 x CH$_2$), 1.30 – 1.22 (m, 9H, C-(CH$_3$)$_3$). ^{13}C NMR (151 MHz, DMSO-*d6*) δ 168.20 (1C, C=O), 166.03 (1C, C=O), 164.46 (1C, C=O), 159.75 (2C, C3′ + C6′, Fl), 155.95 (1C, C=O), 152.82 (1C, C7a), 151.99 (2C, C4a′ + C10a′, Fl), 143.36 (1C, C4, benzylamine), 141.00 (1C, C6, Fl), 133.32 (1C, C1, benzylamine), 129.50 (1C, C4, Fl), 129.38 (2C, C1′ + C8′, Fl), 128.26 (1C, C3a, Fl), 127.25 (C2 + C6, benzylamine), 126.73 (2C, C3 + C5, benzylamine), 124.96 (1C, C7), 122.34 (1C, C5), 112.88 (2C, C2′ + C7′, Fl), 109.34 (2C, C8a′ + C9a′, Fl), 102.40 (2C, C4′ + C5′, Fl), 83.43 (1C, C1, Fl), 78.04 (1C, C-(CH$_3$)$_3$), 56.17 (1C, NH-CH$_2$), 45.93 (1C, NH-CH$_2$), 43.29 (1C, NH-CH$_2$), 29.19 (1C, CH$_2$), 29.02 (1C, CH$_2$), 28.38 (3C, 3 x CH$_3$), 26.37 (1C, CH$_2$), 26.30 (1C,

CH$_2$). LC-MS (m/z): positive mode 708.8 [M+H]$^+$. Purity determined by HPLC-UV (254 nm)-ESI-MS: 96%.

4.5.44 *N*-(6-(4-(Aminomethyl)benzamido)hexyl)-3′,6′-dihydroxy-3-oxo-3*H*-spiro[isobenzofuran-1,9′-xanthene]-6-carboxamide

tert-Butyl (4-((6-(3′,6′-dihydroxy-3-oxo-3*H*-spiro[isobenzofuran-1,9′-xanthene]-6-carboxamido)hexyl)carbamoyl)benzyl) carbamate (0.35 g, 5.8 mmol, 1.0 eq.) was dissolved in DCM and a few drops of water were added to the reaction mixture.[137] TFA (2 ml) was added to the reaction mixture, which was then stirred for 5 hours at room temperature. After TLC indicated completion of the reaction, the volatiles were evaporated to give the desired product without further purification (0.42 g, yield: 96%). ^{1}H NMR (500 MHz, DMSO-*d$_6$*) δ 8.64 (t, *J* = 5.5 Hz, 1H, NH), 8.41 (t, *J* = 5.6 Hz, 1H, NH), 8.21 (s br, 2H, NH$_2$), 8.15 (d, *J* = 8.1 Hz, 1H, C4-H), 8.05 (d, *J* = 8.0 Hz, 1H, C5-H), 7.84 (d, *J* = 7.3 Hz, 2H, C2 + C6, benzylamine), 7.65 (s, 1H, C7-H), 7.50 (d, *J* = 7.5 Hz, 2H, C3 + C5, benzylamin, 6.69 (s, 2H, C1′-H + C8′-H), 6.59 – 6.53 (m, 4H, C2′-H, C4′-H, C5′-H, C7′-H), 4.07 (q, *J* = 5.5 Hz, 2H, NH$_2$-C<u>H$_2$</u>), 3.24 – 3.15 (m, 4H, 2x NH-C<u>H$_2$</u>), 1.52 – 1.42 (m, 4H, 2 x CH$_2$), 1.31 – 1.25 (m, 4H, 2 x CH$_2$). ^{13}C NMR (126 MHz, DMSO-*d$_6$*) δ 168.20 (1C, C=O), 165.66 (1C, C=O), 164.50 (1C, C=O), 159.82 (2C, C3′ + C6′, FL), 152.79 (1C, C7a), 152.03 (2C, C4a′ + C10a′, FL), 141.00 (1C, C6, Fl), 136.89 (1C, C4, benzylamine), 134.87 (1C, C1, benzylamine), 129.49 (1C, C4, Fl), 129.36 (2C, C1′ + C8′, Fl), 128.71 (C2 + C6, benzylamine), 128.30 (1C, C3a, Fl), 127.52 (2C, C3 + C5, benzylamin), 124.98 (1C, C7), 122.37 (1C, C5), 112.92 (2C, C2′ + C7′, FL), 109.37 (2C, C8a′ + C9a′, FL), 102.43 (2C, C4′ + C5′, FL), 53.75 (1C, <u>C</u>-(CH$_3$)$_3$), 45.93 (1C, NH-<u>C</u>H$_2$), 42.10

(NH₂-C̲H₂), 4̲1.98 (1C, NH-C̲H₂), 29.15 (1C, CH₂), 29.03 (1C, CH₂), 26.36 (1C, CH₂), 26.29 (1C, CH₂). LC-MS (m/z): positive mode 608.3 [M+H]⁺. Purity determined by HPLC-UV (254 nm)-ESI-MS: 96%.
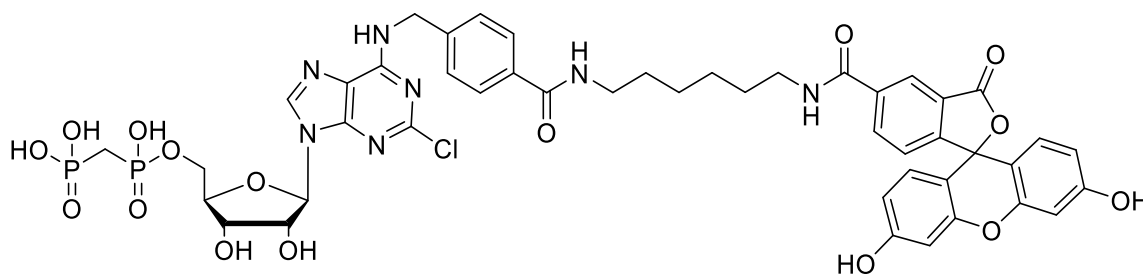
4.5.45 **(((((2*R*,3*S*,4*R*,5*R*)-5-(2-Chloro-6-((4-((6-(3′,6′-dihydroxy-3-oxo-3*H*-spiro[isobenzofuran-1,9′-xanthene]-6-carboxamido)hexyl)carbamoyl)benzyl)amino)-9*H*-purin-9-yl)-3,4-dihydroxytetrahydrofuran-2-yl)methoxy)(hydroxy)phosphoryl)methyl)phosphonic acid**

((((((2*R*,3*S*,4*R*,5*R*)-5-(2,6-Dichloro-9*H*-purin-9-yl)-3,4-dihydroxytetrahydrofuran-2-yl)methoxy)(hydroxy)phosphoryl)methyl)phosphonic acid (0.02 g, 1.0 eq., 0.042 mmol) was dissolved in absolute ethanol (5 ml). *N*-(6-(4-(Aminomethyl)benzamido)hexyl)-3′,6′-dihydroxy-3-oxo-3*H*-spiro[isobenzofuran-1,9′-xanthene]-6-carboxamide (0.051 g, 2.0 eq., 0.083 mmol) was added to the reaction mixture which stirred for 3 h under reflux at 90 °C. After 3 h, the volatiles were evaporated and the crude mixture was purified by RP-HPLC using a gradient of acetonitrile/water (containing 0.05% TFA) from 20:80 to 80:20. Appropriate fractions were pooled, evaporated and lyophilized to give the desired product as orange solid. [137] (0.01 g, yield: 23%). ¹H NMR (600 MHz, D₂O) δ 8.29 (s, 1H, C8-H), 7.80 – 7.69 (m, 2H, aryl), 7.41 – 7.27 (m, 3H, aryl), 7.14 – 7.01 (m, 2H, aryl), 6.86 – 6.75 (m, 2H, C1′-H + C8′-H, Fl), 6.44 – 6.32 (m, 4H, C2′-H, C4′-H, C5′-H, C7′-H, Fl), 5.80 – 5.71 (m, 1H, C1′-H, rib), 4.83

(d, J = 3.6 Hz, 1H, C2′-H, rib) 4.51 – 4.37 (m, 2H, C3′-H + C4′-H, rib), 4.25 – 4.17 (m, 2H, C5′-H$_2$, rib), 4.14 – 3.98 (m, 2H, NH-C$\underline{H}_2$, benzylamine), 3.10 – 2.98 (m, 4H, 2 x NH-C$\underline{H}_2$), 1.97 (t, J = 19.2 Hz, 2H, P-C$\underline{H}_2$-P), 1.29 – 1.15 (m, 4H, 2 x NH-CH$_2$-C$\underline{H}_2$), 1.09 – 0.96 (m, 4H, 2 x C$\underline{H}_2$). ^{13}C NMR (151 MHz, D$_2$O) δ 183.53 (1C, C=O), 176.57 (1C, C=O), 172.11 (1C, C3′, Fl), 171.54 (1C, C6′, Fl), 161.22 (1C, C=O), 160.04 (1C, C7′, Fl), 157.70 (1C, C6), 156.82 (1C, C4), 152.15 (1C, C2), 145.21 (1C, C3′, Fl) , 144.71 (1C, C4′, Fl), 139.70 (1C, C8), 137.31 (1C, C3a, Fl), 135.16 (1C, C1, Fl), 134.69 (1C, C4, benzyl), 133.80 (1C, CH-aryl), 131.79 (1C, CH-aryl), 131.19 (1C, CH-aryl), 130.96 (1C, CH-aryl), 130.13 (1C, CH-aryl), 129.85 (1C, CH-aryl), 125.89 (2C, C1′-H + C8′-H, Fl), 120.92 (1C, C5), 114.72 (2C, C8′a + C9′a, Fl), 106.62 (2C, C2′-H + C7′-H, Fl), 106.58 (2C, C4′-H + C5′-H, Fl), 91.47 (1C, C1′, rib), 87.18 (1C, C4′, rib), 85.89 (1C, C1, Fl), 78.86 (1C, C2′, rib), 74.24 (1C, C3′, rib), 66.95 (1C, C5′, rib), 47.21 (1C, N-C$\underline{H}_2$), 42.74 (1C, CH$_2$, linker), 42.42 (1C, CH$_2$, linker), 32.18 – 30.84 (1C, P-C$\underline{H}_2$-P), 31.10 (1C, CH$_2$, linker), 31.02 (1C, CH$_2$, linker), 28.53 (2C, 2 x CH$_2$-linker). ^{31}P NMR (243 MHz, D$_2$O) δ 23.14 (d, J = 9.1 Hz, P$_\alpha$), 12.46 (d, J = 7.6 Hz, P$_\beta$). LC-MS (*m/z*): positive mode 1050.70 [M+H]$^+$, negative mode 1048.80 [M+H]$^+$. Purity determined by HPLC-UV (254 nm)-ESI-MS: 97%. Mp. Decomp. > 290 °C.

4.5.46 (2*R*,3*R*,4*S*,5*R*)-2-(6-(((2-(5-(5,5-Difluoro-1,3,7,9-tetramethyl-5*H*-4l4,5l4-dipyrrolo[1,2-c:2',1'-f][1,3,2]diazaborinin-10-yl)pentyl)-2*H*-1,2,3-triazol-4-yl)methyl)amino)-9*H*-purin-9-yl)-5-(hydroxymethyl)tetrahydrofuran-3,4-diol
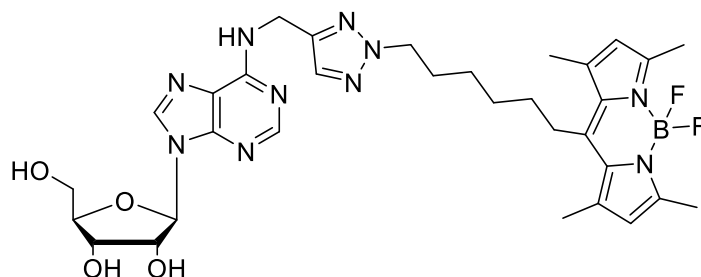
The BODIPY derivative (0.01g, 0.0028 mmol, 1eq.) was dissolved in 10 ml of a mixture of tBuOH/H_2O 1/1. CuSO$_4$ (catal. amount) and sodium ascorbate were added to the reaction mixture. N^6-Propinyl adenosine was added to the reaction mixture which was stirred overnight at room temperature. After stirring overnight, the volatiles were evaporated. It was then dissolved in a small volume of acetonitrile, filtered over a milipore filter an then purified by RP-HPLC. The pure fractions were pooled together and the eluents were lyophilized. After lyophilization overnight 9 mg of the desired product were obtained (yield 41%).[177, 179] ^{1}H NMR (600 MHz, DMSO-d_6) δ 8.38 (s, 1H, C8), 8.24 (s, 1H, C2), 7.88 (s, 1H, H-Triazole), 6.19 (s, 2H, N-CH$_2$), 5.89 (d, J = 6.1 Hz, 1H, C1'-H), 4.60 (t, J = 5.5 Hz, 1H, C2'), 4.30 (t, J = 7.0 Hz, 1H, OH), 4.18 (q, J = 7.1 Hz, 1H, OH), 4.15 – 4.13 (m, 1H, C3'-H), 3.97 – 3.94 (m, 1H, C4'-H), 3.66 (dd, J = 12.1, 3.7 Hz, 1H, C5'-H), 3.54 (dd, J = 12.0, 3.7 Hz, 1H, C5'-H), 3.43 (q, J = 7.0 Hz, 1H, OH), 2.90 – 2.85 (m, 2H, CH$_2$), 2.38 (s, 6H, 2 x CH$_3$), 2.34 (s, 6H, 2 x CH$_3$), 1.88 – 1.82 (m, 2H, CH$_2$), 1.59 – 1.53 (m, 2H, CH$_2$), 1.41 – 1.35 (m, 2H, CH$_2$), 1.23 (t, J = 7.1 Hz, 3H), 1.04 (t, J = 7.0 Hz, 2H, CH$_2$). ^{13}C NMR (151 MHz, DMSO-d_6) δ 153.19, 152.44 (1C, a), 146.69 (1C, C4), 145.52 (1C, b), 140.97 (1C, c), 130.84 (Cq, d), 129.80, 121.81 (2C, 2 x CH,

e), 88.09 (1C, C1′), 86.07 (1C; C2′), 73.67 (1C, C3′), 70.79 (1C, C4′), 61.73 (1C, C5′), 56.18, 48.97 (1C, N-$\underline{C}$H$_2$), 45.88, 30.75 (1C, CH$_2$), 29.47 (1C, CH$_2$), 27.80 (1C, CH$_2$), 26.49 (1C, CH$_2$), 18.71, 15.98 (1C, CH$_3$), 15.97 (1C, CH$_3$), 14.23 (1C, CH$_3$), 13.98 (1C, CH$_3)$. LC-MS (*m/z*): positive mode 665.5 [M+H]$^+$. Purity determined by HPLC-UV (254 nm)-ESI-MS: 95%.

4.5.47 *N*-(4-Ethynylbenzyl)propan-1-amine
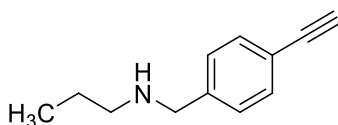
(4-Ethynylphenyl)methanamine (0.3 g, 2.29 mmol, 2 eq) was dissolved in DMF. Then, cesium carbonate (0.27 g, 1.1 mmol, 1 eq.) and 1-bromopropane (0.10 ml, 1.14 mmol, 1.0 eq) were added, and the reaction was stirred for 24 h at room temperature. After completion of the reaction, a maximum of DMF was evaporated and the reaction mixture was extracted with water and ethyl acetate. The organic phase was then washed with 10% LiCl solution and dried over sodium sulfate. The crude mixture was subsequently purified by normal phase column chromatography (DCM/methanol 98/2). Appropriate fraction were pooled and evaporated to give the desired product (0.28 g, yield: 71%). ^{1}H NMR (500 MHz, DMSO-*d$_6$*) δ 7.44 – 7.40 (m, 2H, aryl), 7.37 – 7.33 (m, 2H, aryl), 4.13 (d, J = 1.5 Hz, 1H, NH), 3.74 (s, 2H, N-CH$_2$), 2.46 (d, J = 7.3 Hz, 2H, CH$_2$), 1.48 – 1.40 (m, 2H, CH$_2$), 0.87 – 0.82 (m, 3H, CH$_3$). ^{13}C NMR (126 MHz, DMSO-*d$_6$*) δ 141.03 (1C, C1), 131.72 (2C, aryl), 128.62 (2C, aryl), 120.31 (1C, C4), 83.72 (1C, C-CH), 80.65 (1C, C-CH), 52.28 (1C, N-CH2), 50.42 (1C, aryl-N-CH$_2$), 22.23 (1C, CH$_2$), 11.89 (1C, CH$_3$). LC-MS (m/z): positive mode 174.1 [M+H]$^+$. Purity determined by HPLC-UV (254 nm)-ESI-MS: 98%.

4.5.48 (2*R*,3*R*,4*S*,5*R*)-2-(2-Chloro-6-((4-ethynylbenzyl)(propyl)amino)-9*H*-purin-9-yl)-5-(hydroxymethyl)tetrahydrofuran-3,4-diol
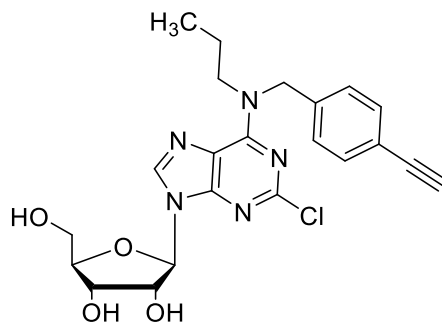
2,6-Dichloro-9-(β-D-ribofuranosyl)purine (0.077 g, 0.24 mmol, 1.0 eq) was suspended in absolute ethanol. Triethylamine (0.067 ml, 0.48 mmol, 2.0 eq) and *N*-(4-ethynylbenzyl)propan-1-amine (0.058 g, 0.48 mmol, 2.0 eq) were added to the suspension which was refluxed overnight. The progress of the reaction was monitored by TLC (DCM/methanol 9/1). After TLC indicated completion of the reaction, the solvent was evaporated. Purification by column chromatography (DCM/methanol 94/6) yielded the desired product as a white solid (0.091 g, 83%).[102] ^{1}H NMR (500 MHz, DMSO-*d₆*) δ 8.49 – 8.35 (m, 1H, C8-H), 7.42 (d, *J* = 7.7 Hz, 2H, aryl), 7.28 (m, 2H, aryl), 5.85 (d, *J* = 5.7 Hz, 1H, C1′-H), 5.62 – 5.48 (m, 1H, 1x N-CH₂), 5.45 (d, *J* = 6.0 Hz, 1H, OH), 5.16 (dd, *J* = 5.2, 1.3 Hz, 1H, OH), 5.00 (t, *J* = 5.5 Hz, 1H, OH), 4.97 – 4.86 (m, 1H, 1x N-CH₂), 4.51 (q, *J* = 5.6 Hz, 1H, C2′-H), 4.14 – 4.11 (m, 1H, C3′-H), 4.12 – 4.11 (m, 1H, C-CH), 4.09 – 3.99 (m, 1H, N-C<u>H</u>₂-CH₂), 3.94 (q, J = 3.8 Hz, 1H, C4′-H), 3.68 – 3.61 (m, 1H, C5′-H), 3.58 – 3.51 (m, 1H, C5′-H), 1.68 – 1.56 (m, 2H, C<u>H</u>₂-CH₃), 0.85 (t, *J* = 7.3 Hz, 3H, CH₃). ^{13}C NMR (126 MHz, DMSO-*d₆*) δ 154.35 (1C, C6), 152.75 (1C, C2), 151.72 (1C, C4), 138.83 (1C, C8), 135.22 (1C, C1-aryl), 132.02 (2C, aryl), 127.79 (2C, aryl), 120.67 (1C, C4-aryl), 118.39 (1C, C5), 87.46 (1C, C1′), 85.84 (1C, C4′), 83.45 (1C; <u>C</u>-CH), 80.81 (1C, C-<u>C</u>H), 73.82 (1C, C3′), 70.47 (1C, C4′), 61.43 (1C, C5′), 50.07 (1C, N-<u>C</u>H₂), 45.92 (1C, N-

$\underline{C}H_2$), 21.39 (1C, $\underline{C}H_2$-CH$_3$, 10.84 (1C, CH$_3$). LC-MS (m/z): positive mode 458.2 [M+H]$^+$.

Purity determined by HPLC-UV (254 nm)-ESI-MS: 98%. Mp. 108-111 °C.

4.5.49 1-Azido-2-fluoroethane

2-Fluoroethyl-4-toluenesulfonate (0.05 ml, 0.18 mmol, 1.0 eq.) was dissolved in anhydrous

DMF (0.5 ml). Sodium azide (0.034 g, 0.53 mmol, 3.0 eq.) was added. The reaction was stirred

at rt for 24 h and monitored by TLC. Due to the instability and tendency to explode, the crude

mixture was added to the next reaction step without further workup.[141]

(2*R*,3*R*,4*S*,5*R*)-2-(2-Chloro-6-((4-(1-(2-fluoroethyl)-1*H*-1,2,3-triazol-4-

yl)benzyl)(propyl)amino)-9*H*-purin-9-yl)-5-(hydroxymethyl)tetrahydrofuran-3,4-diol
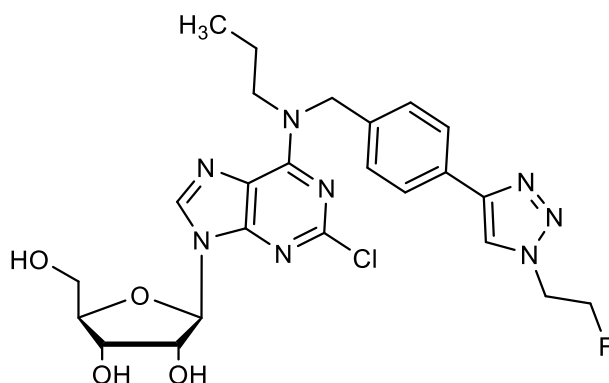
(2*R*,3*R*,4*S*,5*R*)-2-(2-Chloro-6-((4-ethynylbenzyl)(propyl)amino)-9*H*-purin-9-yl)-5-

(hydroxymethyl)tetrahydrofuran-3,4-diol (11, 0.080 g, 0.017 mmol, 1.0 eq.) was dissolved in a

solution of 1-azido-2-fluorethane in DMF (5 ml). TBTA (0.028 g, 0.052 mmol, 0.3 eq.) was

added the reaction mixture. Copper sulfate (0.008 g, 0.052 mmol, 0.3 eq.) and sodium ascorbate

(0.041 g, 0.21 mmol, 1.2 eq.) were premixed in 2 ml of water and then added to the reaction

mixture, which was then stirred overnight. After TLC indicated completion of the reaction, the

reaction mixture was diluted with water and extracted with ethyl acetate followed by washing with an aqueous lithium chloride solution (10%). The organic phase was dried over sodium sulfate, evaporated and then purified by normal phase column chromatography (silical gel, DCM/methanol 95/5). Appropriate fractions were pooled and the eluents were evaporated to give the desired compound as colorless solid (yield: 76%, 0.073 g).[169] ^{1}H NMR (600 MHz, DMSO-d_6) δ 8.55 (s, 1H, triazolyl), 8.49 – 8.36 (m, 1H, C8-H), 7.80 (d, J = 7.0 Hz, 2H, aryl), 7.42 – 7.31 (m, 2H, aryl), 5.86 (d, J = 5.8 Hz, 1H, C1′-H), 5.57 (d, J = 20.9 Hz, 1H, 1 x N-CH$_2$), 5.49 (s, 1H, OH), 5.20 (s, 1H, OH), 5.03 (s, 1H, OH), 4.95 (d, J = 21.2 Hz, 1H, 1 x N-CH$_2$), 4.89 (t, J = 4.7 Hz, 1H, F-CH$_2$-C$\underline{H}_2$), 4.81 (t, J = 4.7 Hz, 1H, F-CH$_2$-C$\underline{H}_2$), 4.76 (t, J = 4.7 Hz, 1H, F-C$\underline{H}_2$), 4.72 (t, J = 4.7 Hz, 1H, F-C$\underline{H}_2$), 4.52 (t, J = 5.3 Hz, 1H, C2′-H), 4.15 – 4.11 (m, 1H, C3′-H), 3.94 (q, J = 3.8 Hz, 1H, C4′-H), 3.65 (d, J = 11.9 Hz, 1H, C5′-H), 3.55 (d, J = 12.2 Hz, 1H, C5′-H), 1.71 – 1.57 (m, 2H, C$\underline{H}_2$CH$_3$), 0.90 – 0.82 (m, 3H, CH$_3$). ^{13}C NMR (151 MHz, DMSO-d_6) δ 154.43 (1C, C6), 152.76 (1C, C2), 151.73 (1C, C4), 146.43 (1C, C1-triazol), 137.88 (1C, C8), 137.41 (1C, C1-aryl), 129.83 (1C, C4-aryl), 128.14 (d, J = 35.1 Hz, 1C, C5-triazol), 125.54 (2C, aryl), 121.88 (2C, aryl), 118.42 (1C, C5), 87.46 (1C, C1′), 85.85 (1C, C4′), 82.01 (d, J = 168.3 Hz, F-CH$_2$), 73.84 (1C, C2′), 70.48 (1C, C3′), 61.44 (1C, C5′), 55.05 (1C, N-CH$_2$-aryl), 50.34 (d, J = 19.7 Hz, F-CH$_2$-C$\underline{H}_2$), 35.92, 30.92, 20.61 (d, J = 227.1 Hz, CH$_3$-C$\underline{H}_2$), 11.12 (d, J = 70.2 Hz, 1C, C$\underline{H}_3$). ^{19}F NMR (565 MHz, DMSO-d_6) δ -74.22. LC/ESI-MS (m/z): positive mode 547.40 [M+H]$^+$ Purity determined by HPLC-UV (254 nm)-ESI-MS: 98%. Mp. 180 – 183 °C.

4.5.50 (2*R*,3*S*,4*R*,5*R*)-2-(Hydroxymethyl)-5-(6-(prop-2-yn-1-ylamino)-9*H*-purin-9-yl)tetrahydrofuran-3,4-diol
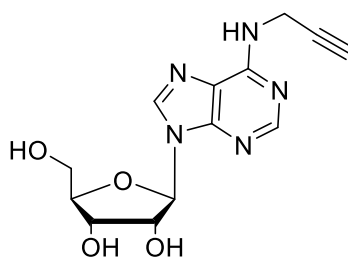
(2*R*,3*S*,4*R*,5*R*)-2-(Hydroxymethyl)-5-(6-(prop-2-yn-1-ylamino)-9*H*-purin-9-yl)tetrahydrofuran-3,4-diol was dissolved according to general procedure F (0.2 g, yield 75%). ^{1}H NMR (600 MHz, DMSO-*d*6) δ 8.40 (s, 1H, C8-H), 8.27 (s, 1H, C2-H), 5.89 (d, *J* = 6.0 Hz, 1H, C1′-H), 5.51 – 5.42 (m, 1H, OH), 5.25 – 5.12 (m, 1H, OH), 4.59 (t, *J* = 5.6 Hz, 1H, C2′-H), 4.24 (s br, 2H, N-CH2), 4.16 – 4.13 (m, 1H, C3′-H), 3.97 – 3.94 (m, 1H, C4′-H), 3.69 – 3.64 (m, 1H, C5′-H), 3.57 – 3.52 (m, 1H, C5′-H), 3.03 (s, 1H, CH). ^{13}C NMR (151 MHz, DMSO-*d*6) δ 154.01 (1C, C6), 152.36 (1C, C2), 148.81 (1C, C4), 140.34 (1C, C8), 120.02 (1C, C5), 88.02 (1C, C1′), 85.99 (1C, C4′), 81.97 (1C, C-CH), 73.69 (1C, C2′), 72.48 (1C, C3′), 70.74 (1C, C4′), 61.74 (1C, C5′), 45.63 (1C, N-CH2). LC-MS (m/z): positive mode 306.2 [M + H]$^+$. Purity determined by HPLC-UV (254 nm)-ESI-MS: 98%. 170 °C – 175 °C.
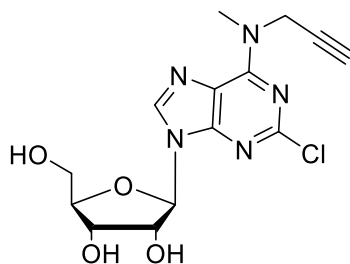
4.5.51 (2*R*,3*R*,4*S*,5*R*)-2-(2-Chloro-6-(prop-2-yn-1-ylamino)-9*H*-purin-9-yl)-5-(hydroxymethyl)tetrahydrofuran-3,4-diol
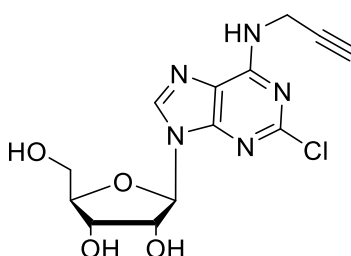
(2*R*,3*R*,4*S*,5*R*)-2-(2-Chloro-6-(prop-2-yn-1-ylamino)-9*H*-purin-9-yl)-5-(hydroxymethyl)tetrahydrofuran-3,4-diol was synthesized according to general procedure F. (0.25, yield: 96%). ^{1}H NMR (500 MHz, DMSO-*d₆*) δ 8.70 (s, 1H, NH), 8.43 (s, 1H, C8-H), 5.83 (d, *J* = 5.8 Hz, 1H, C1′-H), 5.46 (d, *J* = 6.0 Hz, 1H, OH), 5.17 (d, *J* = 5.0 Hz, 1H, OH), 5.02 (t, *J* = 5.6 Hz, 1H, OH), 4.51 (q, *J* = 5.4 Hz, 1H, C2′-H), 4.31 (s, 1H), 4.20 (s, 1H), 4.15 – 4.10 (m, 1H, C3′-H), 3.94 (q, *J* = 3.9 Hz, 1H, C4′-H), 3.68 – 3.62 (m, 1H, C5′-H), 3.59 – 3.52 (m, 1H, C5′-H), 3.47 – 3.40 (m, 2H, CH₂), 2.98 – 2.89 (m, 1H, CH), 1.13 (t, *J* = 7.2 Hz, 1H).^{13}C NMR (126 MHz, DMSO-*d₆*) δ 154.59 (1C, C6), 153.12 (1C, C2), 150.02 (1C, C4), 140.48 (1C, C8), 118.92 (1C, C5), 87.61 (C1′), 85.87 (C4′), 81.17 (1C, <u>C</u>-CH), 73.90 (1C, C2′), 72.99 (1C, CH), 70.49 (1C, C3′), 61.47 (1C, C5′), 29.51 (1C, N-CH₂) LC-MS (m/z): positive mode 340.1 [M + H]$^+$. Purity determined by HPLC-UV (254 nm)-ESI-MS: 95%. Mp. 83 - 85 °C.

4.5.52 (2*R*,3*R*,4*S*,5*R*)-2-(2-Chloro-6-(methyl(prop-2-yn-1-yl)amino)-9*H*-purin-9-yl)-5-(hydroxymethyl)tetrahydrofuran-3,4-diol
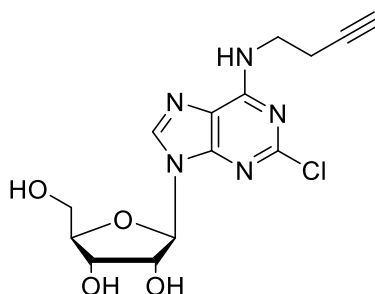

(2*R*,3*R*,4*S*,5*R*)-2-(2-Chloro-6-(methyl(prop-2-yn-1-yl)amino)-9*H*-purin-9-yl)-5-(hydroxymethyl)tetrahydrofuran-3,4-diol was synthesized according to general procedure F (0.04 g, yield: 36%). ^{1}H NMR (500 MHz, DMSO-*d₆*) δ 8.47 (s, 1H, C8-H), 5.86 (d, *J* = 5.6 Hz, 1H, C1′-H), 5.46 (d, *J* = 5.9 Hz, 1H, OH), 5.16 (d, *J* = 4.9 Hz, 1H, OH), 5.01 (t, *J* = 5.4 Hz, 1H, OH), 4.52 – 4.47 (m, 1H, C2′-H), 4.15 – 4.11 (m, 1H, C3′-H), 3.96 – 3.92 (m, 1H, C4′-H), 3.68 – 3.63 (m, 1H, C5′-H), 3.58 – 3.52 (m, 1H, C5′-H), 3.23 (s, 1H, CH). *N-CH₃ + N-CH₂ not visible* ^{13}C NMR (126 MHz, DMSO-*d₆*) δ 154.14 (1C, C6), 152.61 (1C, C2), 151.64 (1C, C4),

139.59 (1C, C8), 118.82 (1C, C5), 87.53 (1C, C1′), 85.81 (1C, C2′), 79.34 (1C, $\underline{C}$-CH), 75.20 (1C, CH), 73.90 (1C, C3′), 70.39 (1C, C4′), 61.36 (1C, C5′) 45.90 (1C, N-$\underline{C}H_2$) 34.58 (1C, CH_3).). LC-MS (m/z): positive mode 354.1 [M + H]+. Purity determined by HPLC-UV (254 nm)-ESI-MS: 92%. Mp. 74 °C.

4.5.53 (2R,3R,4S,5R)-2-(6-(But-3-yn-1-ylamino)-2-chloro-9H-purin-9-yl)-5-(hydroxymethyl)tetrahydrofuran-3,4-diol.

The compound was synthesized by Jianyu Hou under the supervision of Georg Rolshoven. (2R,3R,4S,5R)-2-(6-(But-3-yn-1-ylamino)-2-chloro-9H-purin-9-yl)-5-(hydroxymethyl)tetrahydrofuran-3,4-diol was synthesized according to general procedure F. (0.15 g, 64%). 1H NMR (500 MHz, DMSO-d_6) δ 8.39 (s, 1H, C8), 5.82 (d, J = 5.8 Hz, 1H, C1′), 5.46 (s, 1H, -OH), 5.18 (s, 1H, -OH), 5.02 (s, 1H, -OH), 4.54 – 4.47 (m, 1H, C2′), 4.18 – 4.08 (m, 1H, C3′), 3.96 – 3.89 (m, 1H, C4′), 3.70 – 3.62 (m, 1H, C5′), 3.63 – 3.48 (m, 3H, C5′+ NH-$C\underline{H}_2$), 2.81 (s, 1H, $\underline{H}C≡C$-), 2.53 – 2.44 (m, 1H, NH-CH_2-$C\underline{H}_2$, overlapped with $(CD_3)_2SO$ solvent peak). 13C NMR (126 MHz, DMSO-d_6) δ 155.05 (1C, C6), 153.26 (1C, C2), 149.75 (1C, C4), 140.18 (1C, C8), 118.72 (1C, C5), 87.59 (1C, C1′), 85.86 (1C, C4′), 82.10 (1C, HC≡$\underline{C}$-)), 73.85 (1C, C2′), 72.50 (1C, H$\underline{C}$≡C-), 70.49 (1C, C3′), 61.49 (1C, C5′), 56.16 (1C, NH-CH_2), 18.53 (1C, NHCH2-$C\underline{H}_2$). LC/ESI-MS (m/z): positive mode 354.2 [M+H]+.Purity determined by HPLC-DAD (200-600 nm)-ESI-MS: 97%. Mp. 70-73 ℃.

4.5.54 (((((2*R*,3*S*,4*R*,5*R*)-5-(6-(But-3-yn-1-ylamino)-2-chloro-9*H*-purin-9-yl)-3,4-dihydroxytetrahydrofuran-2-yl)methoxy)(hydroxy)phosphoryl)methyl)phosphonic acid.
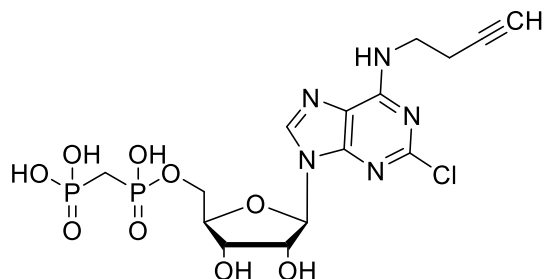
The compound was synthesized by Jianyu Hou under the supervision of Georg Rolshoven. (((((2*R*,3*S*,4*R*,5*R*)-5-(6-(But-3-yn-1-ylamino)-2-chloro-9*H*-purin-9-yl)-3,4-dihydroxytetrahydrofuran-2-yl)methoxy)(hydroxy)phosphoryl)methyl)phosphonic acid was synthesized according to general procedure G (0.011, 5%). ^{1}H NMR (600 MHz, D$_2$O+NaOD) δ 8.27 (s, 1H, C8-H), 5.71 (d, *J* = 5.4 Hz, 1H, C1′-H), 4.47 (t, *J* = 5.3 Hz, 1H, C2′-H), 4.17 – 4.12 (m, 1H, C3′-H), 4.11 – 4.08 (m, 1H, C4′-H), 4.02 – 3.96 (m, 1H, C5′-H), 3.95 – 3.86 (m, 1H, C5′-H), 3.63 – 3.51 (m, 2H, NH-C<u>H</u>$_2$), 2.48 (t, *J* = 6.7 Hz, 2H, NH-CH$_2$-C<u>H</u>$_2$), 1.89 (t, *J* = 19.3 Hz, 2H, PC<u>H</u>$_2$P). Alkyne proton has not been observed. ^{13}C NMR (151 MHz, D$_2$O) δ 157.94 (1C, C6), 156.90 (1C, C2), 151.26 (1C, C4), 118.14 (1C, C5), 90.97 (1C, C1′), 86.56 (1C, C4′), 85.08 (1C, HC≡<u>C</u>-), 77.20 (1C, C2′), 73.62 (1C, H<u>C</u>≡C-)72.55 (1C, C3′), 66.40 (1C, C5′), 54.91 (1C, NH-<u>C</u>H$_2$), 29.11 (1C, t, *J* = 127.9 Hz, P<u>C</u>H$_2$P), 21.13 (1C, NH-CH$_2$-<u>C</u>H$_2$).C8 has not been observed. ^{31}P NMR (243 MHz, D$_2$O+NaOD) δ 23.22 (d, *J* = 8.8 Hz), 12.67 (d, *J* = 8.8 Hz). LC/ESI-MS (m/z): positive mode 512.2 [M+H]$^{+}$ (calcd. mass for C$_{15}$H$_{21}$ClN$_5$O$_9$P$_2$ 512.1). Purity determined by HPLC-DAD (200-600 nm)-ESI-MS: 98%. Mp. 135 - 141 ℃

4.5.55 (((((2*R*,3*S*,4*R*,5*R*)-3,4-Dihydroxy-5-(6-(prop-2-yn-1-ylamino)-9*H*-purin-9-yl)tetrahydrofuran-2-yl)methoxy)(hydroxy)phosphoryl)methyl)phosphonic acid
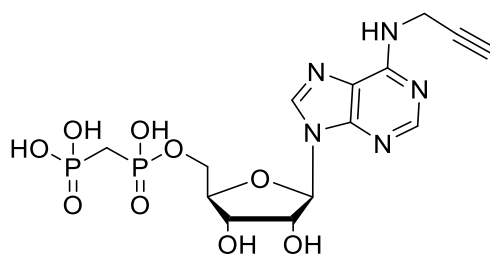
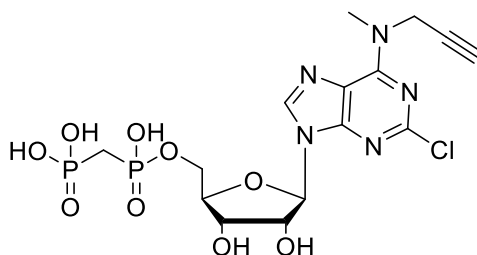(((((2*R*,3*S*,4*R*,5*R*)-3,4-Dihydroxy-5-(6-(prop-2-yn-1-ylamino)-9*H*-purin-9-yl)tetrahydrofuran-2-yl)methoxy)(hydroxy)phosphoryl)methyl)phosphonic acid was synthesized according to general procedure G (0.012 g, yield 8%).^{1}H NMR (600 MHz, D$_2$O) δ 8.66 (s, 1H, C2-H), 8.47 (s, 1H, C8-H), 6.17 (d, *J* = 5.0 Hz, 1H, C1′-H), 4.53 (t, *J* = 4.6 Hz, 1H, C2′-H), 4.44 (s br, 1H, C3′-H), 4.39 (q, *J* = 3.6 Hz, 1H, C4′-H), 4.27 – 4.16 (m, 2H, C5′-H), 2.77 (s, 1H, C-CH), 2.39 – 2.29 (m, 2H, P-CH$_2$-P). ^{13}C NMR (151 MHz, D$_2$O) δ 154.50 (1C, C6), 151.94 (1C, C2), 145.15 (1C, C4), 143.18 (1C, C8), 120.15 (1C, C5), 91.07 (1C, C1′), 87.01 (1C, C4′), 77.98 (1C, C-CH), 77.35 (1C, C2′), 73.30 (1C, C-CH), 72.97 (1C, C3′), 66.61 (1C, C5′), 34.26 (1C, N-CH$_2$), 29.19 (t, *J* = 127.6 Hz, PCP). ^{31}P NMR (243 MHz, D$_2$O) δ 19.74 (d, *J* = 10.5 Hz, P$_\alpha$), 16.73 (d, *J* = 10.7 Hz, P$_\beta$). LC-MS (*m/z*): positive mode 669.0 [M+H]$^+$. Purity determined by HPLC-UV (254 nm)-ESI-MS: 95%. Mp. 194 – 196 °C.

4.5.56 (((((2*R*,3*S*,4*R*,5*R*)-5-(2-Chloro-6-(prop-2-yn-1-ylamino)-9*H*-purin-9-yl)-3,4-dihydroxytetrahydrofuran-2-yl)methoxy)(hydroxy)phosphoryl)methyl)phosphonic acid
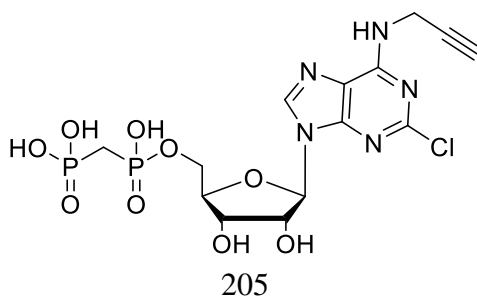
(((((2*R*,3*S*,4*R*,5*R*)-5-(2-Chloro-6-(prop-2-yn-1-ylamino)-9*H*-purin-9-yl)-3,4-dihydroxytetrahydrofuran-2-yl)methoxy)(hydroxy)phosphoryl)methyl)phosphonic acid was synthesized according to general procedure G (0.128 g, yield: 36%). ^{1}H NMR (600 MHz, D$_2$O) δ 8.65 (s, 1H, C8-H), 6.04 (d, J = 4.5 Hz, 1H, C1′-H), 4.70 (t, J = 4.8 Hz, 1H, C2′-H), 4.50 (t, J = 4.8 Hz, 1H, C3′-H), 4.38 (s br, 1H, C4′-H), 4.33 – 4.28 (m, 2H, N-C<u>H</u>$_2$), 4.27 – 4.24 (m, 1H, C5′-H), 4.22 – 4.17 (m, 1H, C5′-H), 2.65 (t, J = 2.4 Hz, 1H, C-CH), 2.39 (t, J = 19.8 Hz, 2H, P-C<u>H</u>$_2$-P). ^{13}C NMR (151 MHz, D$_2$O) δ 157.55 (1C, C6), 157.50 (1C, C4), 156.56 (1C, C2), 141.12 (1C, C8), 118.95 (1C, C5), 90.81 (1C, C1′), 86.57 (1C, C4′), 82.39 (1C, <u>C</u>-CH), 77.20 (1C, C2′), 75.28 (1C, N-<u>C</u>H$_2$) 72.59 (1C, C3′), 66.48 (1C, C5′), 57.84 (1C, C-<u>C</u>H), 29.11 (t, J = 127.7 Hz, PCP). ^{31}P NMR (243 MHz, D$_2$O) δ 19.86 (P$_\alpha$), 17.15 (P$_\beta$). LC-MS (*m/z*): positive mode 498.2 [M+H]$^+$. Purity determined by HPLC-UV (254 nm)-ESI-MS: 97%. Mp. 170 - 172 °C.

4.5.57 (((((2*R*,3*S*,4*R*,5*R*)-5-(2-Chloro-6-(methyl(prop-2-yn-1-yl)amino)-9*H*-purin-9-yl)-3,4-dihydroxytetrahydrofuran-2-yl)methoxy)(hydroxy)phosphoryl)methyl)phosphonic acid

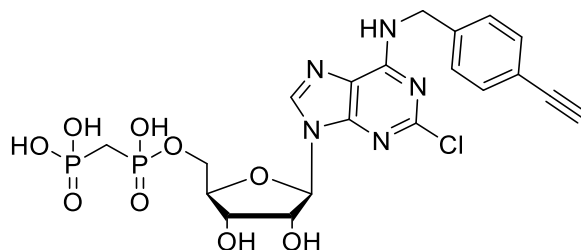(((((2*R*,3*S*,4*R*,5*R*)-5-(2-Chloro-6-(methyl(prop-2-yn-1-yl)amino)-9*H*-purin-9-yl)-3,4-dihydroxytetrahydrofuran-2-yl)methoxy)(hydroxy)phosphoryl)methyl)phosphonic acid was synthesized according to general procedure G (0.013 g, yield: 25%). ^{1}H NMR (600 MHz, D$_2$O) δ 8.32 (s, 1H, C8-H), 5.75 (d, J = 5.0 Hz, 1H, C1′-H), 4.64 (s br, 2H, N-CH$_2$), 4.48 (t, J = 5.1 Hz, 1H, C2′-H), 4.16 – 4.13 (m, 1H, C3′-H), 4.13 – 4.10 (m, 1H, C4′-H), 4.04 – 3.99 (m, 1H,

C5′-H), 3.97 – 3.93 (m, 1H, C5′-H), 3.35 (s, 3H, N-CH$_3$), 2.24 (d, J = 6.1 Hz, 1H, CH), 1.90 (t,

J = 19.3 Hz, 2H, P-CH$_2$-P). ^{13}C NMR (151 MHz, D$_2$O) δ 157.12 (1C, C6), 156.59 (1C, C2),

153.74 (1C, C4), 139.66 (1C, C8), 120.40 (1C, C8), 90.36 (1C, C1′), 86.48 (1C, C4′), 81.69

(1C, C-CH), 77.08 (1C, C2′), 72.82 (1C, C3), 66.59 (1C, C5′), 58.49 (1C, N-CH$_2$), 39.37 (1C,

N-CH$_3$), 28.96 (1C, PCP). ^{31}P NMR (243 MHz, D$_2$O) δ 23.19 (d, J = 8.2 Hz, P$_\alpha$), 12.62 (d, J =

8.5 Hz, P$_\beta$). LC-MS (*m/z*): positive mode 512.2 [M+H]$^+$. Neg: 510.10 [M-H]$^-$. Purity

determined by HPLC-UV (254 nm)-ESI-MS: 95%. Mp. 180 - 181 °C.

4.5.58 (((((2*R*,3*S*,4*R*,5*R*)-5-(2-Chloro-6-((4-ethynylbenzyl)amino)-9*H*-purin-9-yl)-3,4-dihydroxytetrahydrofuran-2-yl)methoxy)(hydroxy)phosphoryl)methyl)phosphonic acid

 (((((2*R*,3*S*,4*R*,5*R*)-5-(2,6-Dichloro-9*H*-purin-9-yl)-3,4-dihydroxytetrahydrofuran-2-

yl)methoxy)(hydroxy)phosphoryl)methyl)phos-phonic acid was dissolved in 5 ml of ethanol.

Triethylamin (2 eq.) and 4-ethinylphenylmethane amine (2 eq.) was added to the reaction

mixture, which was stirred for 3 h at 90 °C under reflux. After completion of the reaction, the

volatiles were evaporated and the obtained mixture of the desired nucleotide analog and side-

products was purified by RP-HPLC using a gradient of acetonitrile/water (containing 0.05%

TFA) from 20:80 to 80:20. Suitable fractions were pooled and lyophilized to obtain the desired

product. ^{1}H NMR (600 MHz, D$_2$O) δ 8.33 (s, 1H, C8-H), 7.31 (d, J = 8.4 Hz, 2H, aryl), 7.22

(d, J = 8.0 Hz, 2H, aryl), 5.80 – 5.72 (m, 1H, C1′-H), 4.67 – 4.56 (m, 2H, C2′-H, C3′-H), 4.51

(s br, 1H, C4′-H), 4.18 (s, 2H, N-CH2), 4.12 – 3.96 (m, 2H, C5′-H2), 3.55 – 3.49 (m, 1H, CH),

2.04 – 1.80 (m, 2H, P-CH$_2$-P). ^{13}C NMR (151 MHz, D$_2$O) δ 155.08 (1C, C6), 153.99 (1C, C2), 149.27 (1C, C4), 140.97 (1C, C2), 139.16 (1C, C1, aryl), 132.12 (2C, aryl), 127.29 (2C, aryl), 120.08 (1C, C4, aryl), 118.13 (1C, C5), 88.64 (1C, C1′), 84.49 (1C, C4′), 83.26 (1C, C-CH), 76.26 (1C, C2′), 71.58 (1C, C3′), 64.12 (1C, C5′), 52.82 (1C, CH), 45.29 (1C, N-CH2), 28.41 (dd, J = 126.4, 117.8 Hz, PCP). ^{31}P NMR (243 MHz, D$_2$O) δ 23.18 (d, J = 8.1 Hz, P$_\beta$), 12.56 (d, J = 8.2 Hz, P$_\alpha$). LC-MS (*m/z*): positive mode 574.10 [M+H]$^+$. Neg: 572.10 [M-H]$^-$. Purity determined by HPLC-UV (254 nm)-ESI-MS: 99%. Mp. >300 °C.

4.5.59 *tert*-Butyl (4-((propylamino)methyl)benzyl)carbamate
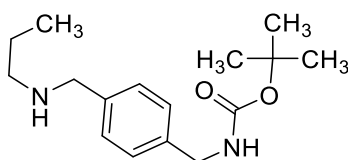
tert-Butyl (4-(aminomethyl)benzyl)carbamate (0.2 g, 0.847 mmol, 6 eq.) was dissolved in 5 ml DMF. 1-Brompropane (0.013 ml, 0.141 mmol, 1 eq.) was added to the reaction mixture which was then stirred overnight at room temperature. Then water was added to the reaction mixture and it was extracted three times with ethylacetate. The organic phase was dried over sodium sulfate and filtrated. The filtrate was evaporated to give the desired product. Without further purification it was used for the next reaction step. LC-MS (*m/z*): positive mode 279.0 [M+H]$^+$. Purity determined by HPLC-UV (254 nm)-ESI-MS: 84%.

4.5.60 *tert*-**Butyl-(4-(((2-chloro-9-((2*R*,3*R*,4*S*,5*R*)-3,4-dihydroxy-5-(hydroxymethyl) tetrahydrofuran-2-yl)-9*H*-purin-6-yl)(propyl)amino)methyl)benzyl)carbamate**
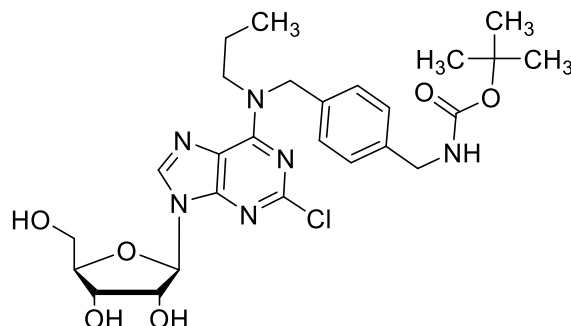
(2*R*,3*R*,4*R*,5*R*)-2-(Acetoxymethyl)-5-(2,6-dichloro-9*H*-purin-9-yl)tetrahydrofuran-3,4-diyl

diacetate (0.59 g, 0.933 mmol, 1 eq.) was dissolved in ethanol and triethylamine (0.12 ml, 0.86

mmol, 0.92 eq.). *tert*-Butyl (4-((propylamino)methyl)benzyl)carbamate (0.26 g, 0.94 mmol, 1

eq.) was added to the reaction mixture which was then refluxed at 90 °C for 3 h. After TLC

(DCM/methanol 9/1) indicated the end of the reaction, the volatiles were evaporated. The crude

mixture was then dissolved in 5 ml of methanol. After addition of 8 ml of 7N ammonia in

methanol to the reaction mixture it was stirred for 12 h at room temperature. Then, the volatiles

were evaporated and the crude mixture was purified by normal phase column chromatography

(DCM/methanol 40/1). Evaporation of the solvents yielded the desired product as a light brown

solid (0.25 g, yield: 38%).[102] ^{1}H NMR (600 MHz, DMSO-d_6) δ 8.44 – 8.34 (m, 1H, C8-H), 7.28

(t, *J* = 5.9 Hz, 1H, NH), 7.17 (s, 4H, aryl), 5.85 (d, *J* = 5.7 Hz, 1H, C1′-H), 5.56 – 5.42 (m, 2H,

NH-C<u>H</u>$_2$), 5.15 (s, 1H, OH), 5.02 (s, 1H, OH), 4.89 (q, *J* = 15.4 Hz, 1H, OH), 4.49 (t, *J* = 5.3

Hz, 1H, C4′-H), 4.15 – 4.11 (m, 1H, C2′-H), 4.08 (d, *J* = 5.9 Hz, 2H, C<u>H</u>$_2$-NH-CO), 3.94 (q, *J*

= 3.6 Hz, 1H, C3′-H), 3.65 (d, *J* = 10.4 Hz, 1H, C5′-H), 3.59 – 3.53 (m, 1H, C5′-H), 1.62 (s,

2H, C<u>H</u>$_2$-CH$_3$), 1.37 (s, 8H, (CH$_3$)$_3$), 0.85 (t, *J* = 7.4 Hz, 3H, CH$_2$-C<u>H</u>$_3$). ^{13}C NMR (151 MHz,

DMSO-d_6) δ 155.90 (1C, C=O), 154.40 (1C, C6), 152.74 (1C, C2), 151.62 (1C, C4), 139.27

(1C, C8), 136.38 (1C, C1, aryl), 135.92 (1C, C4, aryl), 127.57 (2C, aryl), 127.22 (2C, aryl),

118.34 (1C, C5), 87.50 (1C, C1′), 85.79 (1C, C4′), 77.85 (1C, $\underline{C}$(CH$_3$)$_3$), 73.89 (1C; C2′), 70.44 (1C, C3′), 61.41 (1C, C5′), 49.96 (1C, N-$\underline{C}$H$_2$), 49.81 (1C, N-$\underline{C}$H$_2$) 43.24 ($\underline{C}$H$_2$-NH-CO. 1C), 28.38 (($\underline{C}$H$_3$)$_3$, 3C), 21.28 ($\underline{C}$H$_2$-CH$_3$, 1C), 11.06 (CH$_3$, 1C). LC-MS (*m/z*): positive mode 563.1 [M+H]$^+$. Purity determined by HPLC-UV (254 nm)-ESI-MS: 94%.
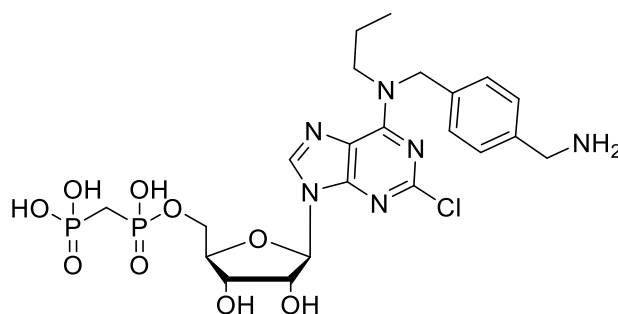
4.5.61 **(((((2R,3S,4R,5R)-5-(6-((4-(Aminomethyl)benzyl)(propyl)amino)-2-chloro-9H-purin-9-yl)-3,4-dihydroxytetrahydrofuran-2-yl)methoxy)-(hydroxy)phosphoryl)methyl)phosphonic acid**
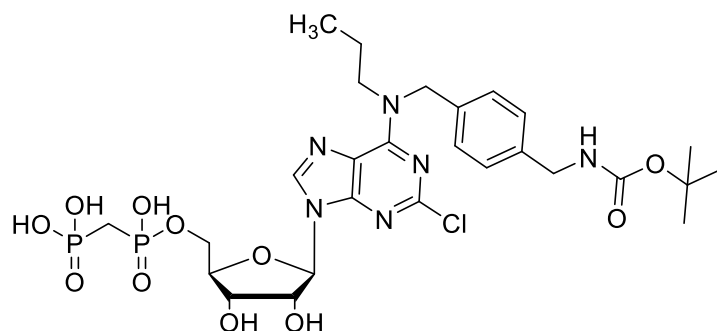
(((((2R,3S,4R,5R)-5-(6-((4-(Aminomethyl)benzyl)(propyl)amino)-2-chloro-9H-purin-9-yl)-3,4-dihydroxytetrahydrofuran-2-yl)methoxy)-(hydroxy)phosphoryl)methyl)phosphonic acid was synthesized according to general procedure G (0.0778 g, yield: 56%). ^{1}H NMR (600 MHz, D$_2$O) δ 8.36 (s, 1H, C8-H), 7.20 – 7.05 (m, 4H, aryl), 5.99 (d, *J* = 4.9 Hz, 1H, C1′-H), 4.70 – 4.65 (m, 1H, C2′-H), 4.52 – 4.47 (m, 1H, C3′-H), 4.37 – 4.31 (m, 1H, C4′-H), 4.21 – 4.06 (m, 4H, C5′-H$_2$ + CH$_2$-C$\underline{H}$$_2$), 3.21 – 3.10 (m, 2H, N-CH$_2$), 2.19 (t, *J* = 19.5 Hz, 2H, P-CH$_2$-P), 1.58 (s, 2H, C$\underline{H}$$_2$-CH$_3$), 1.37 – 1.20 (m, 9H, (C$\underline{H}$$_3$)$_3$), 0.80 (s, 3H, CH$_3$). ^{13}C NMR (151 MHz, D$_2$O) δ 160.74 (1C, C=O), 157.52 (1C, C6), 156.46 (1C, C2), 154.09 (1C, C4), 140.92 (1C, C8), 138.85 (2C, aryl), 130.53 (2C, aryl), 130.11 (2C, aryl), 120.69 (1C, C5), 89.68 (1C, C1′), 86.60 (1C, C4′), 83.62 (1C, CH$_2$-$\underline{C}$H$_2$), 77.13 (1C, C2′), 73.07 (1C, C4′), 66.47

(1C, C5′), 49.48 (2C, 2 x N-$\underline{C}$H$_2$), 46.28 (1C, aryl-$\underline{C}$H$_2$), 30.54 (3C, ($\underline{C}$H$_3$)$_3$), 31.18 – 29.26 (m, PCP), 20.01 (1C, $\underline{C}$H$_2$-CH$_3$), 11.08 (1C, CH$_3$). ^{31}P NMR (243 MHz, D$_2$O) δ 18.52 (P$_\alpha$), 15.34 (P$_\beta$). LC-MS (*m/z*): positive mode 720.13 [M+H]$^+$. Purity determined by HPLC-UV (254 nm)-ESI-MS: 100%. Mp. 234 - 236 °C.

4.5.62 (((((2*R*,3*S*,4*R*,5*R*)-5-(6-((4-(Aminomethyl)benzyl)(propyl)amino)-2-chloro-9*H*-purin-9-yl)-3,4-dihydroxytetrahydrofuran-2-yl)methoxy)(hydroxy)phosphoryl)methyl)phosphonic acid

((((((2*R*,3*S*,4*R*,5*R*)-5-(6-((4-(Aminomethyl)benzyl)(propyl)amino)-2-chloro-9*H*-purin-9-yl)-3,4-dihydroxytetrahydrofuran-2-yl)methoxy)-(hydroxy)phosphoryl)

methyl)phosphonic acid was suspended in DCM and a few drops of water while dtirring over an ice bath. TFA (0.5 ml) were carefully added to the reaction mixture, which was stirred over ice for 1-2 h, and subsequently at room temperature for 30 min. The volatiles were evaporated and the crude mixture was purified by RP-HPLC. Appropriate fractions were pooled, evaporated and lyophilised to give the desired compound (0.051 g, yield: 91%).[137] ^{1}H NMR (600 MHz, D$_2$O) δ 8.25 (s, 1H, C8-H), 7.15 (s, 4H, aryl), 5.77 (d, *J* = 5.1 Hz, 1H, C1′-H), 4.51 – 4.44 (m, 1H, C2′-H), 4.19 – 4.09 (m, 2H, C3′-H & C4′-H), 4.08 – 4.01 (m, 1H, C5′-H), 4.01 – 3.95 (m, 1H, C5′-H), 3.60 (s, 2H, N-C$\underline{H}_2$), 1.94 (t, J = 19.3 Hz, 2H, P-CH$_2$-P), 1.56 (s, 2H, C$\underline{H}_2$-CH$_3$), 0.82 – 0.67 (m, 3H, CH$_3$) *2 x CH$_2$ not visible*. ^{13}C NMR (151 MHz, D$_2$O) δ 157.82 (1C, C6), 156.47 (1C, C2), 154.41 (1C, C4), 144.57 (1C, C8), 138.74 (1C, Cq), 132.17 (1C,

Cq, aryl), 130.55 (2C, aryl), 130.42 (2C, aryl), 120.94 (1C, C5), 91.40 (1C,C1′), 87.38 (1C,

C2′), 79.04 (1C, C3′), 74.52 (1C, C4′), 67.17 (1C, C5′), 47.31 (2C, 2 x N-$\underline{C}H_2$), 31.34 (t, J =

122.1, 118.8 Hz, PCH$_2$P), 25.89 (1C, $\underline{C}H_2$-CH$_3$), 13.22 (1C, CH$_3$). ^{31}P NMR (243 MHz, D$_2$O)

δ 23.20 (P$_\alpha$, d, J = 8.1 Hz), 12.58 (P$_\beta$, d, J = 8.5 Hz). LC-MS (m/z): positive mode 621.4 [M+H]$^+$.

Purity determined by HPLC-UV (254 nm)-ESI-MS: 99%. Mp. <300 °C decomp.

4.5.63 General procedures H and I

General procedure H. The nucleoside was dissolved in DCM or DMF. The acid component

(2 eq.), DMAP (1 eq.) and DCC (4 eq.) were added to the reaction mixture which was then

stirred overnight at room temperature under argon atmosphere. After completion of the reaction,

dicyclohexylurea was filtered, the filtrate was evaporated to give the crude reaction mixture.[188]

General procedure I. The compound was dissolved in DCM and a few drops of water were

added. Then, while stirring over an ice bath, TFA (0.6 ml – 1 ml) was added to the reaction

mixture which was then allowed to reach room temperature. After stirring for 3 h, the volatiles

were evaporated to give the desired product in a crude reaction mixutre.

4.5.64 *N*-((((3a*R*,4*R*,6*R*,6a*R*)-6-(6-Amino-9*H*-purin-9-yl)-2,2-dimethyltetrahydrofuro[3,4-
d][1,3]dioxol-4-yl)methyl)-2-sulfamoyl acetamide
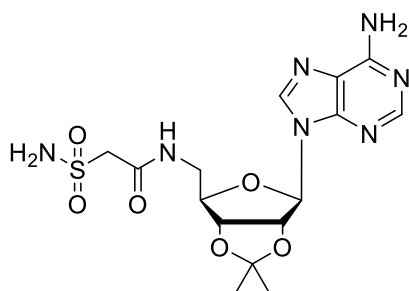
N-(((3a*R*,4*R*,6*R*,6a*R*)-6-(6-Amino-9*H*-purin-9-yl)-2,2-dimethyltetrahydrofuro[3,4-d][1,3]dioxol-4-yl)methyl)-2-sulfamoyl acetamide was synthesized according to general procedure H. ^{1}H NMR (600 MHz, DMSO-*d$_6$*) δ 8.49 (t, *J* = 5.8 Hz, 1H, NH), 8.32 (s, 1H, C8-H), 8.19 (s, 1H, C2-H), 7.34 (s, 2H, NH$_2$), 6.91 (s, 2H, NH$_2$), 6.11 (d, *J* = 3.2 Hz, 1H, C1′-H), 5.40 – 5.37 (m, 1H, C2′-H), 4.92 – 4.89 (m, 1H, C3′-H), 4.24 – 4.21 (m, 1H, C4′-H), 3.91 (d, *J* = 1.2 Hz, 2H, C5′-H), 3.47 – 3.37 (m, 2H, C<u>H</u>$_2$-CO$_2$NH$_2$). ^{13}C NMR (151 MHz, DMSO-*d$_6$*) δ 163.01 (1C, C=O), 156.37 (1C, C6), 152.91 (1C, C2), 148.88 (1C, C4), 140.23 (1C, C8), 119.45 (1C, C5), 113.71 (1C, C-(CH$_3$)$_2$), 89.28 (1C, C1′), 84.02 (1C, C4′), 82.94 (1C, C2′), 81.68 (1C, C3′), 60.10 (1C, C5′), 45.93 (1C, CH$_2$-SO$_2$NH$_2$), 27.22 (1C, CH$_3$), 25.39 (1C, CH$_3$). LC-MS (*m/z*): positive mode 428.1 [M+H]$^+$. Purity determined by HPLC-UV (254 nm)-ESI-MS: 95%.

4.5.65 *N*-(((2*R*,3*S*,4*R*,5*R*)-5-(6-Amino-9*H*-purin-9-yl)-3,4-dihydroxytetrahydrofuran-2-yl)methyl)-2-sulfamoyl acetamide
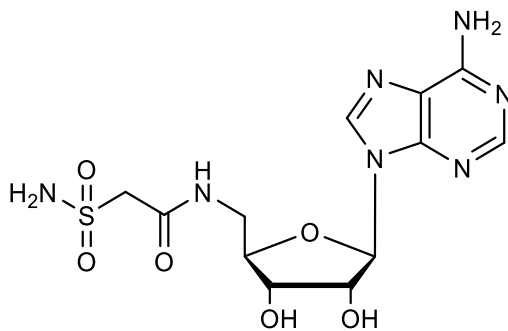
N-(((3a*R*,4*R*,6*R*,6a*R*)-6-(6-amino-9*H*-purin-9-yl)-2,2-dimethyltetrahydrofuro[3,4-d][1,3]dioxol-4-yl)methyl)-2-sulfamoyl acetamide (0.07 g, 0.16 mmol,) was deprotected following general procedure I. Upon addition of methanol, the desired product precipitated in the flask. It was filtrated and washed with methanol, and dried in the desiccator (0.042 g, yield: 67%). ^{1}H NMR (600 MHz, D$_2$O) δ 8.44 (s, 1H, C2-H), 8.41 (s, 1H, C8-H), 6.10 (d, *J* = 5.3 Hz, 1H, C1′-H), 4.84 – 4.82 (m, 1H, C2′-H), 4.36 (t, *J* = 4.9 Hz, 1H, C3′-H), 4.32 – 4.29 (m, 1H,

C4′-H), 4.18 (d, J = 3.5 Hz, 2H, <u>CH$_2$</u>-SO$_2$NH$_2$), 3.80 – 3.75 (m, 1H, C5′-H), 3.64 – 3.60 (m, 1H, C5′-H). ^{13}C NMR (151 MHz, D$_2$O) δ 167.58 (1C, C=O), 154.40 (1C, C6), 151.36 (1C, C4), 149.62 (1C, 1C), 122.00 (1C, C5), 91.20 (1C, C1′), 85.95 (1C, C4′), 76.34 (1C, C2′), 73.66 (1C, C4′), 62.84 (1C, C5′), 43.77 (1C, <u>C</u>H$_2$-SO$_2$NH$_2$). LC-MS (m/z): positive mode 388.1 [M+H]$^+$. Purity determined by HPLC-UV (254 nm)-ESI-MS: 96%.

4.5.66 (2-((((3aR,4R,6R,6aR)-6-(6-Amino-9H-purin-9-yl)-2,2-dimethyltetrahydrofuro[3,4-d][1,3]dioxol-4-yl)methyl)amino)-2-oxoethyl)phosphonic acid
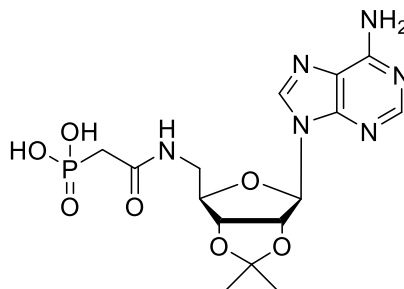
(2-(((((3aR,4R,6R,6aR)-6-(6-Amino-9H-purin-9-yl)-2,2-dimethyltetrahydrofuro[3,4-d][1,3]dioxol-4-yl)methyl)amino)-2-oxoethyl)phosphonic acid was synthesized according to general procedure H. (0.238, yield: 57%) ^{1}H NMR (600 MHz, DMSO-d_6) δ 8.92 (s, 1H, C8-H), 8.65 – 8.61 (m, 1H, NH), 8.16 (s, 1H, C2-H), 7.27 (s, 2H, NH$_2$), 5.99 (d, J = 4.6 Hz, 1H, C1′-H), 5.41 – 5.39 (m, 1H, C2′-H), 4.85 – 4.82 (m, 1H, C3′-H), 4.20 (q, J = 3.8 Hz, 1H, C4′-H), 1.51 (s, 3H, CH$_3$), 1.27 (s, 3H, CH$_3$). *CH$_2$ + C5′-H$_2$ signals overlayed by water peak.* ^{13}C NMR (151 MHz, DMSO-d_6) δ 170.07 (1C, C=O), 156.49 (1C, C6), 153.24 (1C, C2), 149.73 (1C, C4), 119.08 (1C, C5), 114.26 (C-(CH$_3$)$_2$), 87.86 (1C, C1′), 83.56 (1C, C4′), 83.24 (1C, C2′), 81.25 (1C, C3′), 27.59 (1C, CH$_3$), 25.71 (1C, CH$_3$). ^{31}P NMR (243 MHz, DMSO-d_6) δ 11.59 . LC-MS (m/z): positive mode 429.1 [M+H]$^+$. Purity determined by HPLC-UV (254 nm)-ESI-MS: 92%. Mp. 210 °C

4.5.67 (2-((((2R,3S,4R,5R)-5-(6-Amino-9H-purin-9-yl)-3,4-dihydroxytetrahydrofuran-2-yl)methyl)amino)-2-oxoethyl)phosphonic acid
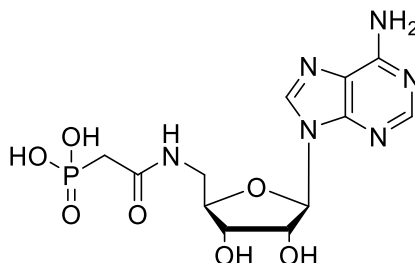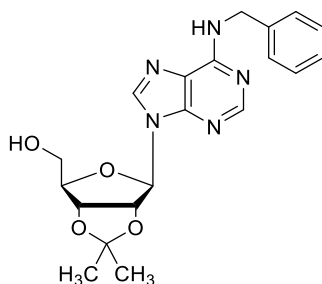

(2-(((((3aR,4R,6R,6aR)-6-(6-Amino-9H-purin-9-yl)-2,2-dimethyltetrahydrofuro[3,4-d][1,3]dioxol-4-yl)methyl)amino)-2-oxoethyl)phosphonic acid was deprotected following general procedure I. The crude mixture was purified employing RP-HPLC to give the desired product (0.058 g, yield: 64%). ^{1}H NMR (600 MHz, D$_2$O) δ 8.42 (s, 1H, C2-H), 8.39 (s, 1H, C8-H), 6.00 (d, J = 5.6 Hz, 1H, C1′-H), 4.75 (t, J = 5.5 Hz, 1H, C2′-H), 4.28 (q, J = 5.4, 4.2 Hz, 1H, C3′-H), 4.21 (q, J = 4.6 Hz, 1H, C4′-H), 3.64 – 3.60 (m, 1H, C5′-H), 3.50 – 3.46 (m, 1H, C5′-H), 2.64 (d, J = 20.5 Hz, 2H, C$\underline{H}_2$). ^{13}C NMR (151 MHz, D$_2$O) δ 173.47 (1C, C=O), 153.01 (1C, C6), 151.13 (1C, C2), 146.06 (1C, C4), 122.01 (1C, C5), 91.35 (1C, C1′), 86.51 (1C, C4′), 76.33 (1C, C2′), 73.66 (1C, C3′), 43.61 (1C, C5′), 40.66 (d, J = 120.8 Hz, $\underline{C}$H$_2$). ^{31}P NMR (243 MHz, D$_2$O) δ 14.56. LC-MS (*m/z*): positive mode 389.2 [M+H]$^+$. Purity determined by HPLC-UV (254 nm)-ESI-MS: 92%. Mp. 182-184 °C.

4.5.68 ((3a*R*,4*R*,6*R*,6a*R*)-6-(6-Chloro-9*H*-purin-9-yl)-2,2-dimethyltetrahydrofuro[3,4-d][1,3]dioxol-4-yl)methanol
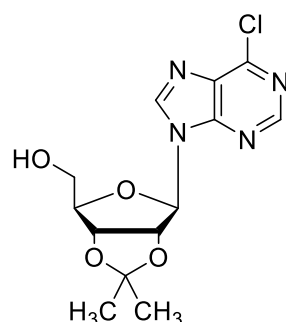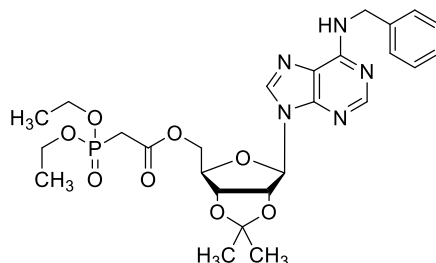

6-Chloro-9-(*β*-D-ribofuranosyl)purine (5.0 g, 0.027 mol, 1 eq.) was dissolved in 200 ml of acetone and 2,2-dimethoxypropane (25.0 ml, 0.20 mol, 12.1 eq.) was added. H_2SO_4 conc. (2.5 ml, 0.047 mol, 1.7 eq.) was then added to the reaction mixture, and the reaction mixture was stirred for 1 h at room temperature. The progress of the reaction was evaluated by normal phase TLC using DCM/methanol 9/1 as eluent. After TLC indicated completion of the reaction, triethylamine (15.0 ml, 0.11 mmol, 6.4 eq.) was added to the reaction mixture, which was subsequently stirred for another 30 minutes. The resulting crude mixture was evaporated and purified by column chromatography (silica gel, DCM/methanol 40:1). Precipitation during solvent evaporation led to the desired product (1.78 g, yield 31%).[102] ^{1}H NMR (500 MHz, DMSO-*d6*) *δ* 8.85 (s, 1H, C8-H), 8.81 (s, 1H, C2-H), 6.27 (d, *J* = 2.5 Hz, 1H, C1′-H), 5.40 (dd, *J* = 6.1, 2.5 Hz, 1H, C2′-H), 5.06 (t, *J* = 5.2 Hz, 1H, C3′-H), 4.97 (dd, *J* = 6.1, 2.4 Hz, 1H, C4′-H), 4.32 – 4.28 (m, 1H, OH), 3.58 – 3.50 (m, 2H, C5′-H), 1.54 (s, 3H, CH3), 1.33 (s, 3H, CH3). ^{13}C NMR (126 MHz, DMSO-*d6*) *δ* 151.71 (1C, C2), 151.25 (1C, C4), 149.22 (1C, C6), 145.75 (1C, C8), 131.35 (1C, C5), 112.93 (1C, (CH3)2-C), 90.50 (1C, C1′), 87.38 (1C, C4′), 83.75 (1C, C2′), 81.31 (1C, C3′), 61.34 (1C, C5′), 26.92 (1C, CH3), 25.10 (1C, CH3). LC-MS (m/z): positive mode 327.1 [M+H]+. Purity determined by HPLC-UV (254 nm)-ESI-MS: 98%.

4.5.69 ((3a*R*,4*R*,6*R*,6a*R*)-6-(6-(Benzylamino)-9*H*-purin-9-yl)-2,2-dimethyltetrahydrofuro[3,4-d][1,3]dioxol-4-yl)methanol


((3a*R*,4*R*,6*R*,6a*R*)-6-(6-Chloro-9*H*-purin-9-yl)-2,2-dimethyltetrahydrofuro[3,4-d][1,3]dioxol-4-yl)methanol (0.57 g, 1.74 mmol, 1 eq.) was dissolved in 10 ml ethanol. Benzylamine (0.19 ml, 1.76 mmol, 1 eq.) and triethylamine (0.22 ml, 1.60 mmol, 0.9 eq.) were added to the reaction mixture. The reaction was refluxed for 8 h at 90 °C. After TLC indicated completion of the reaction, the solvents were evaporated and the product was purified applying normal phase column chromatography (DCM/methanol 9:1). Precipitation during evaporation led to the desired product (0.67 g, yield: 91%).[102] ^{1}H NMR (500 MHz, DMSO-*d6*) δ 8.40 (s, 1H, NH), 8.35 (s, 1H, C8-H), 8.21 (s, 1H, C2-H), 7.36 – 7.16 (m, 5H, aryl), 6.13 (d, *J* = 3.0 Hz, 1H, C1′-H), 5.37 – 5.31 (m, 1H, C2′-H), 5.20 – 5.14 (m, 1H, C3′-H), 4.99 – 4.93 (m, 1H, C4′-H), 4.70 (s, 2H, NH-CH$_2$), 4.24 – 4.18 (m, 1H, OH), 3.60 – 3.47 (m, 2H, C5′-H$_2$), 1.54 (s, 3H, CH$_3$), 1.32 (s, 3H, CH$_3$). ^{13}C NMR (126 MHz, DMSO-*d6*) δ 154.44 (1C, C6), 152.53 (1C, C2), 148.34 (1C, C4), 141.26 (1C, C8), 139.94 (1C, C1, phe), 128.14 (2C, aryl), 127.10 (2C, aryl), 126.57 (1C, C4, aryl), 113.01 (1C, C5), 89.64 (1C, C1′), 86.43 (1C, C4′), 83.28 (1C, C2′), 81.33 (1C, C3′), 61.56 (1C, C5′), 42.88 (1C, C-(CH$_3$)), 27.05 (1C, CH$_3$), 25.17 (1C, CH$_3$). LC-MS (*m/z*): positive mode 398.0 [M+H]$^+$. Purity determined by HPLC-UV (254 nm)-ESI-MS: 96%.

4.5.70 ((3a*R*,4*R*,6*R*,6a*R*)-6-(6-(Benzylamino)-9*H*-purin-9-yl)-2,2-dimethyltetrahydro-furo[3,4-*d*][1,3]dioxol-4-yl)methyl 2-(diethoxyphosphoryl)acetate
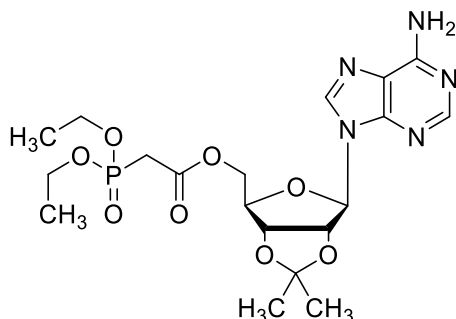

((3a*R*,4*R*,6*R*,6a*R*)-6-(6-(Benzylamino)-9*H*-purin-9-yl)-2,2-dimethyltetrahydrofuro[3,4-*d*][1,3]dioxol-4-yl)methyl 2-(diethoxyphosphoryl)acetate was synthesized following general procedure H. The crude mixture was purified by normal phase column chromatography (DCM/methanol 96/4). Appropriate fractions were pooled and evaporated to yield the desired product as colorless, viscous resin (0.052 g, yield: 56%). ^{1}H NMR (600 MHz, DMSO-*d6*) δ 8.44 (s, 1H, NH), 8.41 (s, 1H, C8-H), 8.21 (s, 1H, C2-H), 7.32 (d, *J* = 7.6 Hz, 2H, aryl), 7.30 – 7.26 (m, 2H, aryl), 7.21 – 7.18 (m, 1H, aryl), 5.92 (d, *J* = 5.4 Hz, 1H, C1′-H), 4.71 – 4.66 (m, 2H, N-CH$_2$), 4.34 (dd, *J* = 12.0, 3.5 Hz, 1H, C2′-H), 4.27 – 4.21 (m, 2H, C3′-H + C4′-H), 4.11 – 4.07 (m, 2H, C5′-H), 4.03 – 3.96 (m, 4H, 2 x C$\underline{H}_2$-CH$_3$), 3.14 (d, *J* = 21.3 Hz, 2H, C$\underline{H}_2$-C=O), 1.20 – 1.12 (m, 6H, 2 x CH$_3$). ^{13}C NMR (151 MHz, DMSO-*d6*) δ 165.58 (d, *J* = 5.9 Hz, 1C, C=O), 154.24 (1C, C6), 150.99 (1C, C2), 148.73 (1C, C4), 139.89 (1C, C8), 137.05 (1C, aryl), 128.16 (1C, aryl), 127.06 (1C, aryl), 126.58 (1C, aryl), 119.45 (1C, C5), 87.37 (1C, C1′), 81.56 (1C, C4′), 72.81 (1C, C2′), 70.23 (1C, C3′), 64.90 (1C, C5′), 61.97 (d, *J* = 5.8 Hz, 2C, 2 x C$\underline{H}_2$-CH$_3$), 54.87 (1C, N-CH$_2$), 33.31 (d, *J* = 130.8 Hz, C$\underline{H}_2$-C=O), 16.02 (d, *J* = 6.0 Hz, 2C, 2 x C$\underline{H}_3$). ^{31}P NMR (202 MHz, DMSO-*d6*) δ 20.95 (1P, P). LC-MS (*m/z*): positive mode 536.1 [M+H]$^{+}$. Purity determined by HPLC-UV (254 nm)-ESI-MS: 95%.

4.5.71 ((3a*R*,4*R*,6*R*,6a*R*)-6-(6-Amino-9*H*-purin-9-yl)-2,2-dimethyltetrahydrofuro[3,4-d][1,3]dioxol-4-yl)methanol
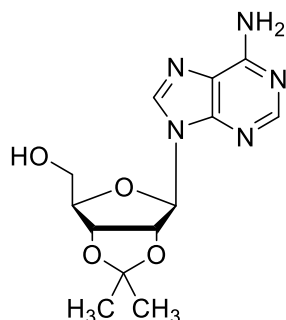

Adenosine (5 g, 0.019 mol, 1 eq.) was dissolved in 200 ml acetone. 2,2-Dimethoxypropane (25 ml, 0.21 mol, 12.1 eq.) was added. H_2SO_4 conc. (2.5 ml, 0.047 mol, 1.7 eq.) was then added to the reaction mixture, and the reaction mixture was stirred for 1 h at room temperature. The progress of the reaction was followed by TLC (DCM/methanol 12:1). After the reaction was finished, triethylamine (15.0 ml, 0.108 mmol, 6.4 eq.) was added to the reaction mixture, which was then stirred for another 30 minutes. The resulting solution was evaporated under high vacuum and purified by normal phase column chromatography (DCM/methanol 12:1). Precipitation during solvent evaporation led to the desired product (3.69 g, yield 64%).[102] ^{1}H NMR (600 MHz, DMSO-*d₆*) δ 8.33 (s, 1H, C2-H), 8.14 (s, 1H, C8-H), 7.31 (s, 2H, NH₂), 6.11 (d, *J* = 3.1 Hz, 1H, C1′-H), 5.35 – 5.31 (m, 1H, C2′-H), 5.21 (t, *J* = 5.5 Hz, 1H, C3′-H), 4.95 (dd, *J* = 6.1, 2.5 Hz, 1H, C4′-H), 4.22 – 4.19 (m, 1H, OH), 3.58 – 3.48 (m, 2H, C5-H₂), 1.53 (s, 3H, CH₃), 1.32 (s, 3H, CH₃). ^{13}C NMR (151 MHz, DMSO-*d₆*) δ 156.29 (1C, C6), 152.78 (1C, C2), 148.98 (1C, C4), 139.84 (1C, C8), 119.26 (1C, C5), 113.21 (1C, C-(CH₃)₂), 89.77 (1C, C1′), 86.52 (1C, C4′), 83.39 (1C, C2′), 81.52 (1C, C3′), 61.75 (1C, C5′), 52.95, 45.97, 27.24 (1C, CH₃), 25.36 (1C, CH₃). LC-MS (*m/z*): positive mode 308.1 [M+H]$^+$. Purity determined by HPLC-UV (254 nm)-ESI-MS: 96%.

4.5.72 ((3a*R*,4*R*,6*R*,6a*R*)-6-(6-Amino-9*H*-purin-9-yl)-2,2-dimethyltetrahydrofuro[3,4-*d*][1,3]dioxol-4-yl)methyl 2-(diethoxyphosphoryl)acetate

((3a*R*,4*R*,6*R*,6a*R*)-6-(6-Amino-9*H*-purin-9-yl)-2,2-dimethyltetrahydrofuro[3,4-*d*][1,3]dioxol-4-yl)methyl 2-(diethoxyphosphoryl)acetate was synthesized following general procedure H. The resulting crude mixture was purified by column chromatography (silica gel, DCM/methanol 94/6). Appropriate fractions were pooled and evaporated to give the product as colourless, viscous resin (0.053g, yield: 33%). ^{1}H NMR (600 MHz, DMSO-*d$_6$*) δ 8.39 (s, 1H, C8-H), 8.17 (s, 1H, C2-H), 7.28 (s, 2H, NH$_2$), 5.93 (d, *J* = 5.4 Hz, 1H, C1′-H), 5.55 (d, *J* = 6.0 Hz, 1H, OH), 5.38 (d, *J* = 5.3 Hz, 1H, OH), 4.70 (q, *J* = 5.5 Hz, 1H, C2′-H), 4.39 – 4.35 (m, 1H, C3′-H), 4.29 – 4.24 (m, 2H, C5′-H), 4.13 – 4.10 (m, 1H, C4′-H), 4.06 – 4.00 (m, 4H, 2 x CH$_2$-CH$_3$), 3.17 (d, *J* = 21.3 Hz, 2H, CH$_2$-C=O), 1.23 – 1.17 (m, 6H, 2 x CH$_3$). ^{13}C NMR (151 MHz, DMSO-*d$_6$*) δ 165.59 (d, *J* = 6.3 Hz, C=O), 156.22 (1C, C6), 152.79 (1C, C2), 149.61 (1C, C4), 139.89 (1C, C8), 119.25 (1C, C5), 87.48 (1C, C1′), 81.67 (1C, C4′), 72.93 (1C, C2′), 70.41 (1C, C3′), 65.08 (1C, C5′), 62.16 (d, *J* = 6.1 Hz, 2C, CH$_2$-CH$_3$), 33.49 (d, *J* = 130.8 Hz, CH$_2$-C=O), 16.20 (d, *J* = 6.1 Hz, 2 x CH$_3$). ^{31}P NMR (243 MHz, DMSO-*d$_6$*) δ 20.95 (1P, P). LC-MS (*m/z*): positive mode 446.1 [M+H]$^+$. Purity determined by HPLC-UV (254 nm)-ESI-MS: 97%.
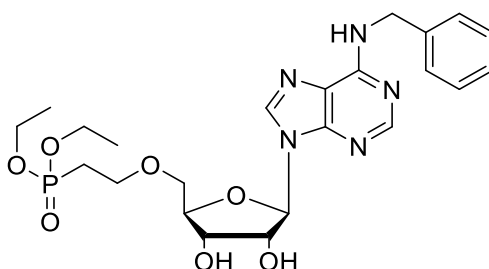
4.5.73 Diethyl (2-(((3a*R*,4*R*,6*R*,6a*R*)-6-(6-(Benzylamino)-9*H*-purin-9-yl)-2,2-dimethyltetrahydrofuro[3,4-d][1,3]dioxol-4-yl)methoxy)ethyl)phosphonate
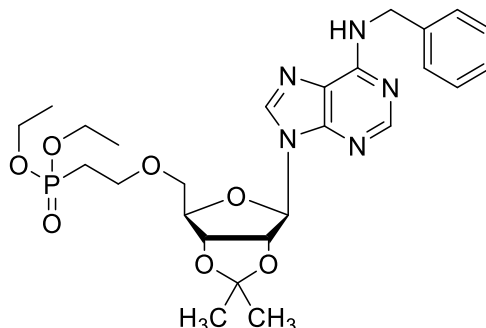
To a solution of ((3a*R*,4*R*,6*R*,6a*R*)-6-(6-(Benzylamino)-9*H*-purin-9-yl)-2,2-dimethyltetrahydrofuro[3,4-d][1,3]dioxol-4-yl)methanol (0.15 g, 0.38 mmol, 1 eq.) and diethyl-2-bromophosphonate (0.068 ml, 0.38 mmol, 1 eq.) in 3 ml toluene 2 ml of an aqueous sodium hydroxide solution (50.00%) were added. The reaction was stirred for 48 h. After completion of the reaction, the reaction mixture was diluted with water (5 ml) and diethylether (5 ml). The organic phase was separated and washed with 2 x 10 ml water and dried over sodium sulfate. The solution was filtrated and the filtrate evaporated and purified by normal phase column chromatography (DCM/methanol 98/2). Appropriate fractions were pooled and evaporated to give the desired compound as colorless, viscous oil. (0.065 g, yield 29%).[192] ^{1}H NMR (600 MHz, CDCl$_3$) δ 8.37 (s, 1H, C2-H), 7.76 (s, 1H, C8-H), 7.30 – 7.24 (m, 5H, aryl), 5.83 (d, *J* = 4.7 Hz, 1H, C1′-H), 5.59 (s, 1H, NH), 5.20 (t, *J* = 5.4 Hz, 1H, C2′-H), 5.12 (d, *J* = 5.6 Hz, 1H, C3′-H), 4.53 (s br, 1, C4′-H), 4.11 – 4.04 (m, 4H, 2 x C̲H̲$_2$-CH$_3$), 4.00 – 3.78 (m, 4H, C5′-H$_2$ + O-CH$_2$), 2.25 – 2.13 (m, 2H, P-CH$_2$), 1.62 (s, 3H, CH$_3$), 1.36 (s, 3H, CH$_3$), 1.30 (t, *J* = 7.1 Hz, 6H, 2 x CH$_3$). ^{13}C NMR (151 MHz, CDCl$_3$) δ 154.15 (1C, C6), 152.77 (1C, C2), 150.47 (1C, C4), 141.75 (1C, C8), 137.14 (1C, aryl), 128.73 (2C, aryl), 127,74 (2C, aryl), 127.66 (1C, aryl), 114.04 (1C, C5), 94.41 (1C, C1′), 85.94 (1C, C4′), 82.76 (1C, C2′), 81.73 (1C, C3′), 70.60 (1C, C5′), 63.36 (1C, C5′), 61.75 (d, *J* = 6.2 Hz, 2C, 2 x C̲H̲$_2$-CH$_3$), 29.68 , 27.65 (1C, CH$_3$), 25.24

(1C, CH₃), 16.39 (d, *J* = 6.2 Hz, 2 x CH₂-CH₃). ³¹P NMR (202 MHz, CDCl₃) *δ* 29.01. LC-MS (*m/z*): positive mode 562.2 [M+H]⁺. Purity determined by HPLC-UV (254 nm)-ESI-MS: 96%.

4.5.74 Diethyl   (2-(((2*R*,3*S*,4*R*,5*R*)-5-(6-(benzylamino)-9*H*-purin-9-yl)-3,4-dihydroxy-tetrahydrofuran-2-yl)methoxy)ethyl)phosphonate
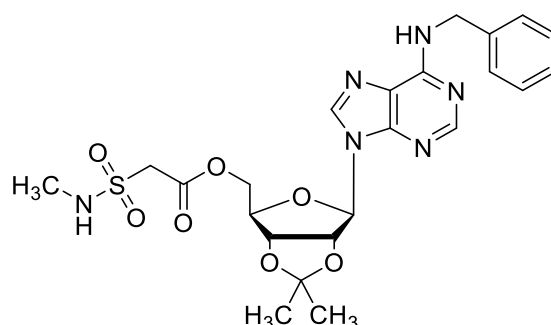

Diethyl(2-((((3a*R*,4*R*,6*R*,6a*R*)-6-(6-(benzylamino)-9*H*-purin-9-yl)-2,2-dimethyltetrahydrofuro[3,4-*d*][1,3]dioxol-4-yl)methoxy)ethyl)phosphonate (0.1 g, 0.17 mmol, 1 eq.) was deprotected following general procedure I. The crude mixture was purified by normal phase column chromatography (DCM/methanol 96/4). Appropriate fractions were pooled and evaporated to give the product as colorless, viscous resin. ¹H NMR (600 MHz, DMSO-*d₆*) *δ* 8.43 (s, 1H, C2-H), 8.30 (s, 1H, C8-H), 7.38 – 7.23 (m, 5H, aryl), 5.94 (d, *J* = 5.9 Hz, 1H, C1′-H), 5.44 (d, *J* = 6.1 Hz, 1H, OH), 5.29 – 5.24 (m, 1H, OH), 5.17 (d, *J* = 4.7 Hz, 1H, C2′-H), 4.60 (q, *J* = 5.8 Hz, 1H, C3′-H), 4.16 (q, *J* = 4.3 Hz, 1H, C4′-H), 4.04 – 4.00 (m, 1H, O-CH₂), 4.01 – 3.93 (m, 4H, 2 x CH₂-CH₃), 3.70 – 3.65 (m, 1H, C5′-H), 3.58 – 3.53 (m, 1H, C5′-H), 2.24 – 2.12 (m, 2H, P-CH₂), 1.22 (t, *J* = 7.0 Hz, 6H, 2 x CH₃). ¹³C NMR (151 MHz, DMSO-*d₆*) *δ* 154.07 (C6, 1C), 152.35 (C2, 1C), 150.83 (C4, 1C), 138.70 (1C, C8), 137.66 (1C, aryl), 129.07 (2C, aryl), 127.85 (2C, aryl), 127.68 (1C, aryl), 120.04 (1C, C5), 88.19 (1C, C1′), 86.24 (1C, C4′), 73.99 (1C, C2′), 70.97 (1C, C3′), 67.49 , 61.98 (1C, C5′), 61.58 (d, *J* = 6.0 Hz, 2C, 2 x CH₂CH₃), 55.37 (1C, P-CH₂-CH₂), 34.88 (1C, N-CH₂), 25.60 (1C, P-CH₂), 16.69 (d, *J* = 6.2

Hz, 2 x CH$_3$). ^{31}P NMR (243 MHz, DMSO-d_6) δ 29.64. LC-MS (*m/z*): positive mode 522.1 [M+H]$^+$. Purity determined by HPLC-UV (254 nm)-ESI-MS: 96%.

4.5.75 ((3a*R*,4*R*,6*R*,6a*R*)-6-(6-(Benzylamino)-9*H*-purin-9-yl)-2,2-dimethyltetrahydrofuro-[3,4-*d*][1,3]dioxol-4-yl)methyl 2-(*N*-methylsulfamoyl)acetate
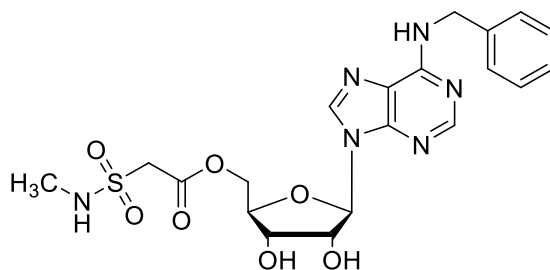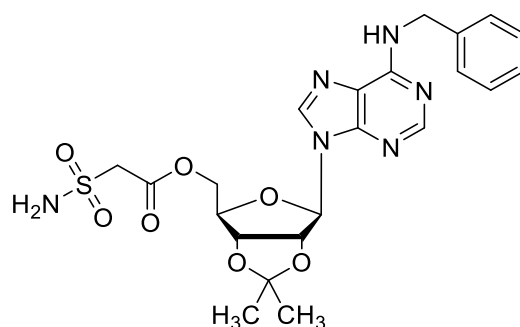

((3a*R*,4*R*,6*R*,6a*R*)-6-(6-(Benzylamino)-9*H*-purin-9-yl)-2,2-dimethyltetrahydrofuro-[3,4-*d*][1,3]dioxol-4-yl)methyl 2-(*N*-methylsulfamoyl)acetate was synthesized following general procedure H. The crude mixture was purified using normal phase column chromatography (DCM/methanol 9/1). Appropriate fractions were pooled and the eluents were evaporated to give the desired product (0.122 g, yield 61%). ^{1}H NMR (600 MHz, DMSO-d_6) δ 8.46 (s, 1H, NH), 8.36 (s, 1H, C2-H), 8.25 (s, 1H, C8-H), 7.35 (d, *J* = 7.6 Hz, 2H, aryl), 7.32 – 7.27 (m, 4H), 7.22 (t, *J* = 7.4 Hz, 1H), 6.22 (d, *J* = 2.7 Hz, 1H, C1′-H), 5.57 (d, *J* = 8.0 Hz, 1H, C2′-H), 5.48 – 5.45 (m, 1H, C3′-H), 5.10 – 5.07 (m, 1H, C4′-H), 4.72 (s, 2H, N-CH$_2$), 4.45 – 4.41 (m, 1H, NH), 4.39 – 4.35 (m, 1H, C5′-H), 4.31 – 4.27 (m, 1H, C5′-H), 4.19 (d, *J* = 1.7 Hz, 2H, CH$_2$-S), 2.59 (d, *J* = 4.9 Hz, 3H, NH-CH$_3$), 1.58 – 1.54 (m, 3H, CH$_3$), 1.37 – 1.33 (m, 3H, CH$_3$). ^{13}C NMR (151 MHz, DMSO-d_6) δ 163.44 (1C, C=O), 156.77 (1C, C6), 154.61 (1C, C4), 152.87 (1C, C2), 140.09 (1C, C8), 131.66 (1C, C1, aryl), 128.34 (2C, aryl), 127.29 (2C, aryl),

126.77 (1C, aryl), 119.67 (1C, C5), 113.68 (1C, $\underline{C}$-(CH$_3$)$_2$), 89.21 (1C, C1′), 83.34 (1C, C4′), 83.26 (1C, C2′), 81.11 (1C, C3′), 65.14 (1C, C5′), 54.65 (1C, $\underline{C}$H$_2$-NH) 33.50 (1C, $\underline{C}$H$_2$-C=O), 28.88 (1C, CH$_3$), 27.15 (1C, CH$_3$), 25.36 (1C, CH$_3$). LC-MS (*m/z*): positive mode 532.2 [M+H]$^+$. Purity determined by HPLC-UV (254 nm)-ESI-MS: 97%.

4.5.76 ((2*R*,3*S*,4*R*,5*R*)-5-(6-(Benzylamino)-9*H*-purin-9-yl)-3,4-dihydroxytetrahydrofuran-2-yl)methyl 2-(*N*-methylsulfamoyl)acetate

((3a*R*,4*R*,6*R*,6a*R*)-6-(6-(Benzylamino)-9*H*-purin-9-yl)-2,2-dimethyltetrahydrofuro-[3,4-*d*][1,3]dioxol-4-yl)methyl 2-(*N*-methylsulfamoyl)acetate (0.121 g, 0.227 mmol, 1 eq.) was deprotected according to general procedure I. The crude mixture was purified by normal phase column chromatography (DCM/methanol 94/6). Appropriate fractions were pooled and the eluents were evaporated to give the desired product. ^{1}H NMR (500 MHz, DMSO-*d$_6$*) δ 8.36 (s br, 2H, C8-H + SO$_2$N$\underline{H}$), 8.20 (s, 1H, C2-H), 7.33 (d, *J* = 7.2 Hz, 2H, aryl), 7.30 – 7.24 (m, 3H, aryl), 7.22 – 7.17 (m, 1H, NH), 5.92 (d, *J* = 5.4 Hz, 1H, C1′-H), 5.52 (d, *J* = 5.9 Hz, 1H, OH), 5.35 (d, *J* = 5.3 Hz, 1H, OH), 4.73 – 4.66 (m, 2H, C$\underline{H}$$_2$-C=O), 4.43 – 4.37 (m, 1H, C2′-H), 4.32 – 4.28 (m, 1H, C3′-H), 4.27 – 4.24 (m, 1H, C4′-H), 4.23 – 4.21 (m, 2H, C5′-H), 4.15 – 4.12 (m, 2H, NH-C$\underline{H}$$_2$), 2.59 (d, *J* = 4.7 Hz, 3H, CH$_3$). ^{13}C NMR (126 MHz, DMSO-*d$_6$*) δ 163.61 (1C, C=O), 156.15 (1C, C6), 154.59 (1C, C4), 152.73 (1C, C2), 140.16 (1C, C8), 128.32 (2C, aryl), 127.24 (2C, aryl), 126.72 (2C, aryl), 121.15 (1C, C5), 87.61, (1C, C1′), 81.60 (1C, C4′), 72.96

(1C, C2′), 70.41 (1C, C3′), 65.45 (1C, C5′), 61.79 (1C, NH-C$\underline{H}_2$), 54.81 (1C, $\underline{C}H_2$-C=O), 28.91 (1C, CH$_3$). LC-MS (*m/z*): positive mode 493.0 [M+H]$^+$. Purity determined by HPLC-UV (254 nm)-ESI-MS: 96%.

4.5.77 ((3a*R*,4*R*,6*R*,6a*R*)-6-(6-(Benzylamino)-9*H*-purin-9-yl)-2,2-dimethyltetrahydrofuro[3,4-*d*][1,3]dioxol-4-yl)methyl 2-sulfamoylacetate
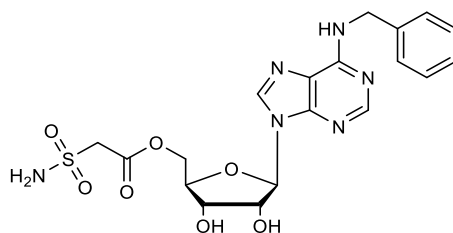

((3a*R*,4*R*,6*R*,6a*R*)-6-(6-(Benzylamino)-9*H*-purin-9-yl)-2,2-dimethyltetrahydrofuro[3,4-*d*][1,3]dioxol-4-yl)methyl 2-sulfamoylacetate was synthesized following general procedure H (0.131 g, yield 34%). ^{1}H NMR (500 MHz, DMSO-*d6*) δ 8.42 (s, 1H, NH), 8.33 (s, 1H, C8-H), 8.23 (s, 1H, C2-H), 7.33 (d, *J* = 7.3 Hz, 2H, NH$_2$), 7.28 (t, *J* = 7.6 Hz, 2H, aryl), 7.22 – 7.17 (m, 3H, aryl), 6.19 (d, *J* = 2.7 Hz, 1H, C1′-H), 5.45 – 5.41 (m, 1H, C2′-H), 5.09 – 5.04 (m, 1H, C3′-H), 4.70 (s br, 2H, C$\underline{H}_2$-C=O), 4.44 – 4.39 (m, 1H, C4′-H), 4.38 – 4.32 (m, 1H, C5′-H), 4.29 – 4.23 (m, 1H, C5′-H), 4.10 (s, 2H, NH-C$\underline{H}_2$), 1.54 (s, 3H, CH$_3$), 1.32 (s, 3H, CH$_3$). ^{13}C NMR (126 MHz, DMSO-*d6*) δ 163.31 (1C, C=O) , 158.96 (1C, C6), 153.77 (1C, C4), 152.69 (C2, 1C), 139.91 (1C, C8), 133.94 (1C, C1, aryl), 128.14 (2C, aryl), 127.11 (2C, aryl) 126.57 (aryl, 1C), 120.13 (1C, C5), 113.48 (1C, $\underline{C}$-(CH$_3$)$_2$), 88.99 (1C, C1′), 83.13 (1C, C4′), 83.09 (1C, C2′), 80.89 (1C, C3′), 64.94 (1C, C5′), 58.98 (1C, N-C$\underline{H}_2$), 26.96 (1C, CH$_3$), 25.17 (1C, CH$_3$). LC-MS (*m/z*): positive mode 493.0 [M+H]$^+$. Purity determined by HPLC-UV (254 nm)-ESI-MS: 82%.

4.5.78 ((2R,3S,4R,5R)-5-(6-(Benzylamino)-9H-purin-9-yl)-3,4-

       dihydroxytetrahydrofuran-2-yl)methyl 2-(diethoxyphosphoryl)acetate
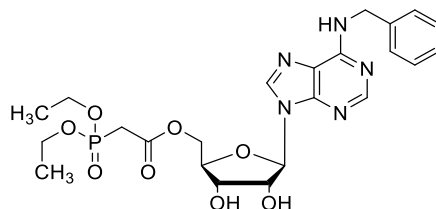
((2R,3S,4R,5R)-5-(6-(Benzylamino)-9H-purin-9-yl)-3,4-dihydroxytetrahydrofuran-2-yl)methyl 2-(diethoxyphosphoryl)acetate was synthesized according to general procedure I product as colourless, viscous resin (0.052 g, yield: 56%). ^{1}H NMR (600 MHz, DMSO-*d6*) δ 8.44 (s, 1H, NH), 8.41 (s, 1H, C8-H), 8.21 (s, 1H, C2-H), 7.32 (d, *J* = 7.6 Hz, 2H, aryl), 7.30 – 7.26 (m, 2H, aryl), 7.21 – 7.18 (m, 1H, aryl), 5.92 (d, *J* = 5.4 Hz, 1H, C1′-H), 4.71 – 4.66 (m, 2H, N-CH₂), 4.34 (dd, *J* = 12.0, 3.5 Hz, 1H, C2′-H), 4.27 – 4.21 (m, 2H, C3′-H + C4′-H), 4.11 – 4.07 (m, 2H, C5′-H), 4.03 – 3.96 (m, 4H, 2 x C̲H̲₂-CH₃), 3.14 (d, *J* = 21.3 Hz, 2H, C̲H̲₂-C=O), 1.20 – 1.12 (m, 6H, 2 x CH₃). ^{13}C NMR (151 MHz, DMSO-*d6*) δ 165.58 (d, *J* = 5.9 Hz, 1C, C=O), 154.24 (1C, C6), 150.99 (1C, C2), 148.73 (1C, C4), 139.89 (1C, C8), 137.05 (1C, aryl), 128.16 (1C, aryl), 127.06 (1C, aryl), 126.58 (1C, aryl), 119.45 (1C, C5), 87.37 (1C, C1′), 81.56 (1C, C4′), 72.81 (1C, C2′), 70.23 (1C, C3′), 64.90 (1C, C5′), 61.97 (d, *J* = 5.8 Hz, 2C, 2 x C̲H̲₂-CH₃), 54.87 (1C, N-CH₂), 33.31 (d, *J* = 130.8 Hz, C̲H̲₂-C=O), 16.02 (d, *J* = 6.0 Hz, 2C, 2 x C̲H̲₃). ^{31}P NMR (202 MHz, DMSO-*d6*) δ 20.95 (1P, P). LC-MS (*m/z*): positive mode 536.1 [M+H]$^+$. Purity determined by HPLC-UV (254 nm)-ESI-MS: 95%.

4.5.79 ((2R,3S,4R,5R)-5-(6-(Benzylamino)-9H-purin-9-yl)-3,4-

       dihydroxytetrahydrofuran-2-yl)methyl 2-sulfamoylacetate

((3a*R*,4*R*,6*R*,6a*R*)-6-(6-(Benzylamino)-9*H*-purin-9-yl)-2,2-dimethyltetrahydrofuro[3,4-d][1,3]dioxol-4-yl)methyl 2-sulfamoylacetate (0.131 g, 0.253 mmol, 1 eq.) was deprotected following general procedure I. The crude mixture was purified by normal phase column chromatography (DCM/methanol 8/2). Appropriate fractions were pooled and the eluents were evaporated to give the desired product (0.086 g, yield: 71%). ^{1}H NMR (500 MHz, DMSO-*d₆*) δ 8.35 (s, 1H, C2-H), 8.20 (s, 1H, C8-H), 7.33 (d, *J* = 7.3 Hz, 2H, NH₂), 7.28 (t, *J* = 7.6 Hz, 2H, aryl), 7.21 – 7.17 (m, 3H, aryl), 5.92 (d, *J* = 5.5 Hz, 1H, C1′-H), 5.50 (d, *J* = 5.9 Hz, 1H, OH), 5.34 (d, *J* = 5.3 Hz, 1H, OH), 4.71 (s, 1H, C2′-H), 4.70 – 4.64 (m, 2H, C$\underline{H}$₂-C=O), 4.43 – 4.38 (m, 1H, C3′-H), 4.30 (d, *J* = 5.9 Hz, 1H, C4′-H), 4.29 – 4.24 (m, 2H, C5′-H), 4.15 (d, *J* = 2.1 Hz, 2H, N-CH₂). ^{13}C NMR (126 MHz, DMSO-*d₆*) δ 163.49 (1C, C=O), 156.69 (1C, C6), 152.55 (1C, C2), 140.02 (1C, C8), 132.58 (1C, aryl), 128.13 (2C, aryl), 127.06 (2C, aryl), 126.54 (1C, aryl), 122.36 (1C, C5), 87.41 (1C, C1′), 81.44 (1C, C4′), 72.80 (1C, C2′), 70.22 (1C, C3′), 65.23 (1C, C5′), 59.06 (1C, N-$\underline{C}$H₂). LC-MS (*m/z*): positive mode 479.0 [M+H]⁺. Purity determined by HPLC-UV (254 nm)-ESI-MS: 95%.

4.5.80 General procedures J and K

General procedure J. General procedure J followed optimized previously published reaction conditions.[197] 7-(4-Bromobutyl)-8-bromo-theophylline (1.0 eq.) was dissolved in 10 ml of dry DMF. The aniline derivative (1.0 eq.) was added to the reaction mixture which was stirred for 10-12 h at 200 °C. After TLC indicated completion of the reaction, the solvents were evaporated

and the crude mixture was purified by column chromatography (DCM 100% - DCM/methanol 99/1). Appropriate fractions were pooled and the solvents were evaporated to give the desired compound.

**General procedure K.** 7-(4-Bromopropyl)-8-bromo-theophylline (1.0 eq.) was dissolved in 10 ml of dry DMF. The aniline derivative (1.0 eq.) was added to the reaction mixture which was stirred for 10-12 h at 150 - 160 °C. After TLC indicated completion of the reaction, the solvents were evaporated and the crude mixture was purified by column chromatography (DCM 100% - DCM/methanol 99/1). Appropriate fractions were pooled and the solvents were evaporated to give the desired compound.[197]

4.5.81 8-Bromotheophylline, (CAS-Nr. 10381-76-6)
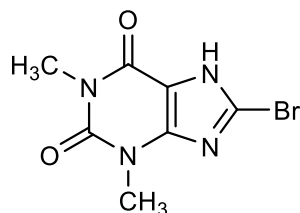
Theophylline (5 g, 0.029 mol, 1.0 eq.) were suspended in a mixture of 20 ml 1 M sodium acetate buffer and 15 ml of water in a 250 ml three-neck round bottomed flask, and was stirred over an ice bath. Via a dropping funnel ~ 2.5 ml of Bromine in 10 ml of water were added dropwise to the reaction mixture. After complete addition of the bromine solution, the ice bath was allowed to reach room temperature. The reaction was stirred overnight. After that, 20 ml of a 40% $NaHSO_3$ solution was added to the reaction mixture until the solution decolorized. The reaction stirred another 5 h. The resulting precipitate was filtered and washed subsequently with 40% $NaHSO_3$ and water and was dried overnight in a desiccator to give the a pale white/yellow solid (6.25 g, yield 87%).[102] ^{1}H NMR (500 MHz, DMSO-d_6) δ 3.36 (s, 3H, N1-CH$_3$), 3.19 (s, 3H, N3-CH$_3$). ^{13}C NMR (126 MHz, DMSO-d_6) δ 153.37 (1C, C2), 150.84 (1C, C6), 147.84 (1C,

C4), 124.23 (1C, C8), 109.15 (1C, C5), 29.81 (N1-C, 1C), 27.74 (N3-C, 1C). LC-MS (m/z): positive mode 259.1 [M+H]$^+$. Purity determined by HPLC-UV (254 nm)-ESI-MS: 99%. Mp. 295-297 °C.

**4.5.82 7-(4-Bromobutyl)-8-bromo-theophylline, CAS: 166274-43-7**
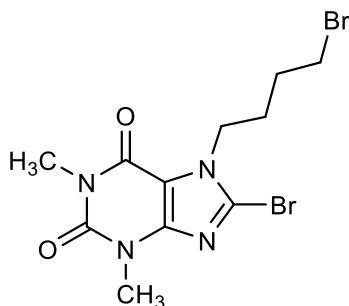
8-Bromotheophylline (2 g, 0.0077 mol, 1 eq.) was dissolved in 15 ml of DMF. The reaction mixture was raised to 85 °C. Triethylamine (3.2 ml, 0.023 mol, 3 eq.) and 1,4-dibromobutane (2.7 ml, 0.023 mol, 3 eq.) were added and the reaction mixture was stirred for 2 h ad 85 °C. When TLC (DCM/methanol 94/6) indicated the end of the reaction the volatiles were evaporated, and the crude mixture was purified by normal phase column chromatography (silica gel, DCM/methanol 98/2). The appropriate fractions were united and the solvents were evaporated to yield the desired product as light brown solid (2.5 g, yield: 82%).[203] ^{1}H NMR (600 MHz, DMSO-d_6) δ 4.29 (t, J = 6.9 Hz, 2H, N-CH$_2$), 3.53 (t, J = 6.4 Hz, 2H, Br-CH$_2$), 3.38 (s, 3H, N1-CH$_3$), 3.22 (s, 3H, N3-CH$_3$), 1.90 – 1.83 (m, 2H, CH$_2$), 1.82 – 1.77 (m, 2H, CH$_2$). ^{13}C NMR (151 MHz, DMSO-d_6) δ 153.67 (1C, C6), 150.83 (1C, C2), 147.98 (1C, C4), 127.81 (1C, C8), 108.37 (1C, C5), 46.17 (1C, N-$\underline{C}$H$_2$), 34.37 (1C, $\underline{C}$H$_2$-Br), 29.65 (N1-$\underline{C}$H$_3$, 1C), 29.15 ($\underline{C}$H$_2$, 1C), 28.44 ($\underline{C}$H$_2$, 1C), 27.82 (N3-$\underline{C}$H$_3$, 1C). LC-MS (m/z): positive mode 391.95 [M+H]$^+$. Purity determined by HPLC-UV (254 nm)-ESI-MS: 97%.

4.5.83 8-Bromo-7-(3-bromopropyl)-theophylline, CAS: 93883-68-2
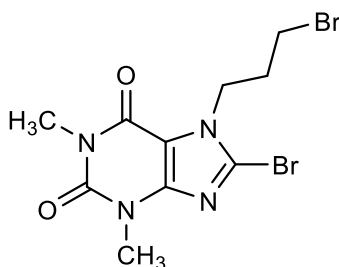
8-Bromotheophylline (2.0 g, 0.0077 mol, 1 eq.) was dissolved in 15 ml of DMF. The reaction mixture was raised to 85 °C. Triethylamine (3.2 ml, 0.023 mol, 3 eq.) and 1,4-dibromopropane (2.7 ml, 2.32 mmol, 3 eq.) were added to the reaction mixture which was then stirred for 2 h at 85 °C. When TLC (DCM/methanol 94/6) indicated the end of the reaction, the volatiles were evaporated, and the crude mixture was purified by normal column chromatography (silica gel, DCM/methanol 98/2). Appropriate fractions were united, the solvents were evaporated to give the desired product as light brown solid (2.5 g, yield: 83%).[197] ^{1}H NMR (600 MHz, DMSO-d_6) δ 4.35 (t, J = 7.1 Hz, 2H, N7-CH$_2$), 3.53 (t, J = 6.5 Hz, 2H, Br-CH$_2$), 3.37 (s, 3H, N1-CH$_3$), 3.20 (s, 3H, N-CH$_3$), 2.29 (t, J = 6.9 Hz, 2H, CH$_2$). ^{13}C NMR (151 MHz, DMSO-d_6) δ 153.49 (1C, C6), 150.65 (1C, C2), 147.87 (1C, C4), 127.89 (1C, C8), 108.26 (1C, C5), 45.78 (1C, N7-CH$_2$), 32.65 (CH$_2$-CH$_2$-CH$_2$, 1C), 30.57 (CH$_2$-Br, 1C), 29.50 (1C, N3-CH$_3$), 27.67 (1C, N1-CH$_3$). LC-MS (m/z): positive mode 380.6 [M+H]$^+$. Purity determined by HPLC-UV (254 nm)-ESI-MS: 95%.
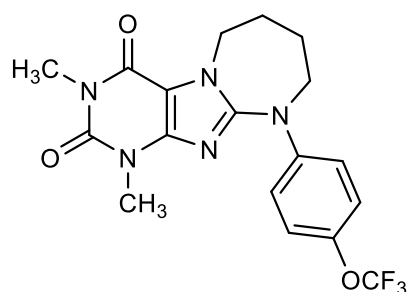
4.5.84 10-(4-Fluorophenyl)-1,3-dimethyl-7,8,9,10-tetrahydro-1*H*-[1,3]diazepino[2,1-*f*]purine-2,4(3*H*,6*H*)-dione
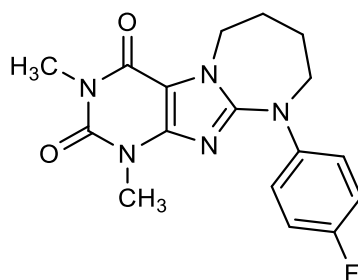
10-(4-Fluorophenyl)-1,3-dimethyl-7,8,9,10-tetrahydro-1*H*-[1,3]diazepino[2,1-*f*]purine-2,4(3*H*,6*H*)-dione was synthesized according to general procedure J (0.031 g, yield 24%). ^{1}H NMR (600 MHz, DMSO-*d6*) δ 7.26 – 7.22 (m, 2H, C3 + C5, phe), 7.14 (t, *J* = 8.8 Hz, 2H, C2 + C6, phe), 4.43 – 4.37 (m, 2H, C6-H$_2$), 3.78 – 3.73 (m, 2H, C8-H$_2$), 3.25 (s, 3H, N1-CH$_3$), 3.20 (s, 3H, N3-CH$_3$), 1.88 (s, 2H, C7-H$_2$), 1.84 (s, 2H, C8-H$_2$). ^{13}C NMR (151 MHz, DMSO-*d6*) δ 158.38 (d, *J* = 239.9 Hz, C4, phe), 154.76 (1C, C10a), 153.96 (1C, C4), 151.07 (1C, C2), 146.90 (1C, C11a), 141.98 (1C, C1, phe), 123.22 (d, *J* = 8.2 Hz, 2C, C3 + C5, phe), 115.73 (d, *J* = 22.5 Hz, 2C, C2 + C6, phe), 103.77 (1C, C4a), 51.09 (1C, C9), 45.30 (1C, C6), 29.55 (1C, N1-CH$_3$), 27.55 (1C, N3-CH$_3$), 27.44 (1C, C7), 25.28 (1C, C8). LC-MS (*m/z*): positive mode 344.1 [M+H]$^+$. HRMS (ESI): *m/z* [M + H]$^+$ calcd for C$_{17}$H$_{19}$FN$_5$O$_2$: 343.1523, found 344.1517. Purity determined by HPLC-UV (254 nm)-ESI-MS: 96%. Mp. 205 – 207 °C.

4.5.85 10-(4-Chlorophenyl)-1,3-dimethyl-7,8,9,10-tetrahydro-1*H*-[1,3]diazepino[2,1-*f*]purine-2,4(3*H*,6*H*)-dione
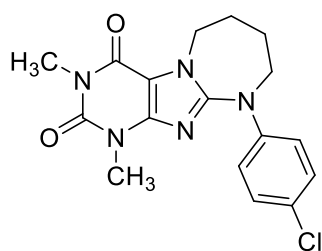
10-(4-Chlorophenyl)-1,3-dimethyl-7,8,9,10-tetrahydro-1*H*-[1,3]diazepino[2,1-*f*]purine-2,4(3*H*,6*H*)-dione was synthesized according to general procedure J (0.048 g, yield 35%).

^{1}H NMR (600 MHz, DMSO-*d6*) δ 7.34 – 7.30 (m, 2H, phe, C3-H + C5-H), 7.21 – 7.17 (m, 2H, phe, C2-H, C6-H), 4.42 – 4.37 (m, 2H, C4-H$_2$), 3.79 – 3.73 (m, 2H, C9-H$_2$), 3.29 (s, 3H, N1-CH$_3$), 3.21 (s, 3H, N3-CH$_3$), 1.89 – 1.80 (m, 4H, C7-H$_2$ + C8-H$_2$). ^{13}C NMR (151 MHz, DMSO-*d6*) δ 154.10 (1C, C10a), 153.27 (1C, C4), 151.06 (1C, C2), 146.66 (1C, C11a), 144.06 (1C, C1, phe), 128.99 (2C, C3 + C5, phe), 126.09 (1C, C4, phe), 121.13 (2C, C2 + C6, phe), 104.00 (C4a, 1C), 49.77 (1C, C9), 45.22 (1C, C6), 29.60 (1C, N1-CH$_3$), 27.60 (1C, N3-CH$_3$), 27.02 (1C, C7), 25.15 (1C, C8). LC-MS (m/z): positive mode 360.0. HRMS (ESI): *m/z* [M + H]$^+$ calcd. for C$_{17}$H$_{19}$ClN$_5$O$_2$: 360.1227; found: 360.1222. Purity determined by HPLC-UV (254 nm)-ESI-MS: 97%. Mp. 188-190 °C.

4.5.86 10-(4-Bromophenyl)-1,3-dimethyl-7,8,9,10-tetrahydro-1*H*-[1,3]diazepino[2,1-*f*]purine-2,4(3*H*,6*H*)-dione
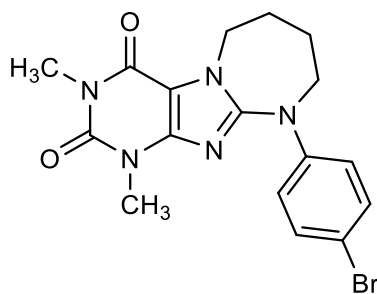
10-(4-Bromophenyl)-1,3-dimethyl-7,8,9,10-tetrahydro-1H-[1,3]diazepino[2,1-f]purine-2,4(3H,6H)-dione was synthesized according to general procedure J (2 mg, yield: 1%). ^{1}H NMR (500 MHz, DMSO-*d6*) δ 7.47 – 7.41 (m, 2H, C3-H + C5-H, phe), 7.15 – 7.09 (m, 2H, C2-H + C6-H, phe), 4.41 – 4.36 (m, 2H, C4-H$_2$), 3.78 – 3.73 (m, 2H, C9-H$_2$), 3.30 (s, 3H, *overlapping with solvent peak,* N1-CH$_3$), 3.21 (s, 3H, N3-CH$_3$), 1.88 – 1.80 (m, 4H, C7-H$_2$ + C8-H$_2$). ^{13}C NMR (126 MHz, DMSO-*d6*) δ 154.17 (1C, C10a), 153.12 (1C, C4), 151.12 (1C,

C2), 146.69 (1C, C11a), 144.48 (1C, C1, phe), 131.92 (2C, C3 + C5, phe), 121.40 (2C, C2 +

C6, phe), 113.92 (C4a, 1C), 49.65 (1C, C9), 45.22 (1C, C6), 29.64 (1C, N1-CH$_3$), 27.64 (1C,

N3-CH$_3$), 26.96 (1C, C7), 25.16 (1C, C8). LC-MS (m/z): positive mode 403.0 [M+H]+. Purity
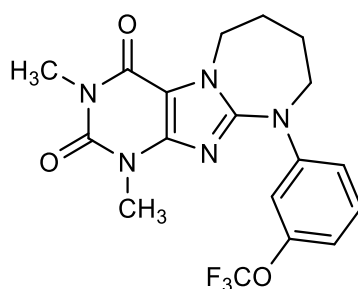
determined by HPLC-UV (254 nm)-ESI-MS: 95%.

4.5.87 1,3-Dimethyl-10-(4-(trifluoromethoxy)phenyl)-7,8,9,10-tetrahydro-1*H*-
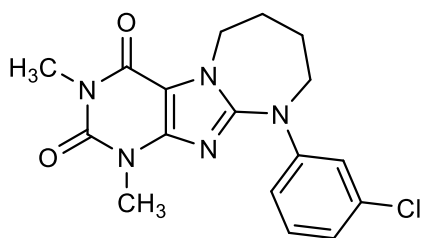[1,3]diazepino[2,1-*f*]purine-2,4(3*H*,6*H*)-dione

1,3-Dimethyl-10-(4-(trifluoromethoxy)phenyl)-7,8,9,10-tetrahydro-1*H*-[1,3]diazepino[2,1-

f]purine-2,4(3*H*,6*H*)-dione was synthesized according to general procedure J (0.057 g, yield

36%). ^{1}H NMR (600 MHz, DMSO-*d$_6$*) δ 7.27 (s, 4H, phe, C2-H + C3-H + C5-H + C6-H), 4.42

– 4.39 (m, 2H, C4-H$_2$), 3.81 – 3.76 (m, 2H, C9-H$_2$), 3.30 (s, 3H, N1-CH$_3$), 3.21 (s, 3H, N3-

CH$_3$), 1.88 – 1.82 (m, 4H, C7-H$_2$ + C8-H$_2$). ^{13}C NMR (151 MHz, DMSO-*d$_6$*) δ 153.94 (1C,

C10a), 152.89 (1C, C4), 150.88 (1C, C2), 146.45 (1C, C11a), 144.01 (1C, phe, C1), 142.80

(1C, phe, C4), 129.50 (1C, OCF$_3$), 121.85 (2C, C3/C5, phe), 120.27 (C2/C6, phe), 103.85 (1C,

C4a), 49.55 (1C, C9), 44.99 (1C, C6), 29.43 (1C, N1-CH$_3$), 27.42 (1C, N3-CH$_3$), 26.77 (1C,

C7), 24.93 (1C, C8). LC-MS (m/z): positive mode 409.9 [M+H]$^+$. HRMS (ESI): *m/z* [M + H]$^+$

calcd. for C$_{18}$H$_{19}$F$_3$N$_5$O$_3$: 410.1435; found: 410.1440. Purity determined by HPLC-UV (254

nm)-ESI-MS: 91%. Mp. 174 – 176 °C.

4.5.88 1,3-Dimethyl-10-(3-(trifluoromethyl)phenyl)-7,8,9,10-tetrahydro-1*H*-[1,3]diazepino[2,1-*f*]purine-2,4(3*H*,6*H*)-dione
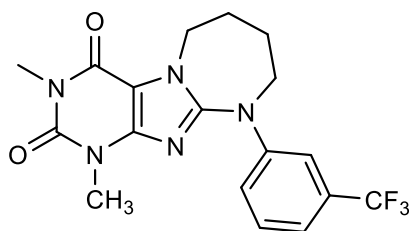
1,3-Dimethyl-10-(3-(trifluoromethyl)phenyl)-7,8,9,10-tetrahydro-1*H*-[1,3]diazepino[2,1-*f*]purine-2,4(3*H*,6*H*)-dione was synthesized according to general procedure J (0.052g, yield: 35%). ^{1}H NMR (500 MHz, DMSO-d_6) δ 7.54 (d, J = 2.1 Hz, 1H, C2, phe), 7.51 (t, J = 8.0 Hz, 1H, C6, phe), 7.46 – 7.43 (m, 1H, C4, phe), 7.32 – 7.29 (m, 1H, C5, phe), 4.43 (t, J = 4.5 Hz, 2H, C6-H$_2$), 3.84 (t, J = 4.8 Hz, 2H, C9-H$_2$), 3.31 (s, 3H, N1-CH$_3$), 3.22 (s, 3H, N3-CH$_3$), 1.90 – 1.82 (m, 4H, C7-H$_2$ + C8-H$_2$). ^{13}C NMR (126 MHz, DMSO-d_6) δ 154.13 (1C, C10a), 152.52 (1C, C4), 151.00 (1C, C2), 146.46 (1C, C11a), 145.58 (1C, C1, phe), 130.26 (1C, C5), 129.95 (d, J = 31.5 Hz, 1C, C3, phe), 124.23 (d, J = 272.6 Hz, 1C, CF$_3$), 122.48 (1C, C6, phe), 118.18 (d, J = 3.7 Hz, C4, phe), 114.96 (d, J = 3.8 Hz, C2, phe), 104.12 (1C, C4a), 49.37 (1C, C6), 45.11 (1C, C9), 29.50 (1C, N1-CH$_3$), 27.57 (1C, N3-CH$_3$), 26.82 (1C, C7), 25.01 (1C, C8). LC-MS (*m/z*): positive mode 393.9 [M + H]$^+$. HRMS (ESI): m/z [M + H]$^+$ calcd. for C$_{18}$H$_{19}$F$_3$N$_5$O$_2$: 394.1491; found: 394.1505. Purity determined by HPLC-UV (254 nm)-ESI-MS: 97%.

4.5.89 1,3-Dimethyl-10-(3-(trifluoromethoxy)phenyl)-7,8,9,10-tetrahydro-1*H*-[1,3]diazepino[2,1-*f*]purine-2,4(3*H*,6*H*)-dione

1,3-Dimethyl-10-(3-(trifluoromethoxy)phenyl)-7,8,9,10-tetrahydro-1*H*-[1,3]diazepino[2,1-*f*]purine-2,4(3*H*,6*H*)-dione was synthesized according to general procedure J. The product was obtained as a light brown oily substance (0.05 g, yield: 94%).[38] ^{1}H NMR (600 MHz, DMSO-*d6*) δ 7.38 (t, *J* = 8.3 Hz, 1H, C3-H, phe), 7.23 – 7.19 (m, 1H, C2-H, phe), 7.17 – 7.13 (m, 1H, C6-H, phe), 6.94 – 6.90 (m, 1H, C4-H, phe), 4.43 – 4.37 (m, 2H, C4-H$_2$), 3.83 – 3.78 (m, 2H, C9-H$_2$), 3.22 (s, 3H, N3-CH$_3$), 1.89 - 1.81 (m, 4H, C7-H$_2$ + C8-H$_2$). N1-CH$_3$ *signal overlaid with solvent peak* ^{13}C NMR (151 MHz, DMSO-*d6*) δ 154.22 (1C, C10a), 152.20 (1C, C5, phe), 151.07 (1C, C4), 149.20 (1C, C2), 146.51 (1C, C11a) , 146.48 (C1, phe), 130.75 (1C, C3, phe), 116.89 (1C, C2, phe), 113.50 (1C, C4, phe), 110.93 (1C, C6), 104.18 (1C, C4a), 49.20 (1C, C9), 45.14 (1C, C6), 29.53 (1C, N1-CH$_3$), 27.63 (1C, N3-CH$_3$), 26.71 (1C, C7), 25.03 (1C, C8). HRMS: calc 410.1435, det: 410.1432. LC-MS (m/z): positive mode 410.0 [M + H]$^+$. HRMS (ESI): *m/z* [M + H]$^+$ calcd. for C$_{18}$H$_{19}$F$_3$N$_5$O$_3$: 410.1440; found: 410.1440. Purity determined by HPLC-UV (254 nm)-ESI-MS: 95%. Mp. 75-77 °C.

4.5.90 10-(3-Chlorophenyl)-1,3-dimethyl-7,8,9,10-tetrahydro-1*H*-[1,3]diazepino[2,1-*f*]purine-2,4(3*H*,6*H*)-dione

10-(3-Chlorophenyl)-1,3-dimethyl-7,8,9,10-tetrahydro-1*H*-[1,3]diazepino[2,1-*f*]purine-2,4(3*H*,6*H*)-dione was synthesized according to general procedure J (0.039 g, yield: 43%). ^{1}H NMR (600 MHz, DMSO-*d6*) δ 7.29 (t, *J* = 8.1 Hz, 1H, C2-H, phe), 7.24 – 7.22 (m, 1H, C6-H, phe), 7.12 – 7.08 (m, 1H, C5-H, phe), 7.03 – 6.98 (m, 1H, C4-H, phe), 4.43 – 4.37 (m, 2H, C6-H$_2$), 3.80 – 3.76 (m, 2H, C7-H$_2$), 3.32 (s, 6H, N1-CH$_3$ *overlayed with sovlent peak*), 3.22 (s, 3H, N3-CH$_3$), 1.89 – 1.79 (m, 4H, C7-H$_2$ + C8-H$_2$). ^{13}C NMR (151 MHz, DMSO-*d6*) δ 154.20 (1C, C10a), 152.48 (1C, C6), 151.07 (1C, C1, phe), 146.55 (1C, C2), 146.40 (1C, C11a), 133.74 (1C, C3, phe), 130.76 (1C, C5), 121.55 (1C, C4) 118.22 (1C, C2) 117.12 (1C, C6), 104.18 (1C, C4a), 49.31 (1C, C6), 45.16 (1C, C9), 29.63 (1C, N1-CH$_3$), 27.62 (1C, N3-CH$_3$), 26.85 (1C, C7), 25.10 (1C, C8). LC-MS (m/z): positive mode 359.8 [M + H][+], HRMS (ESI): *m/z* [M + H][+] calcd. for C$_{17}$H$_{19}$ClN$_5$O$_2$: 360.1227; found: 360.1219. Purity determined by HPLC-UV (254 nm)-ESI-MS: 98%.

4.5.91 1,3-Dimethyl-9-(3-(trifluoromethoxy)phenyl)-6,7,8,9-tetrahydropyrimido[2,1-*f*]purine-2,4(1*H*,3*H*)-dione
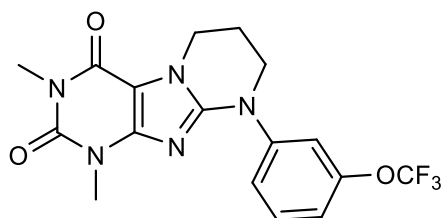
1,3-Dimethyl-9-(3-(trifluoromethoxy)phenyl)-6,7,8,9-tetrahydropyrimido[2,1-*f*]purine-2,4(1*H*,3*H*)-dione was synthesized according to general procedure K (0.080 g, yield 72%). [1]H

NMR (600 MHz, DMSO-d_6) δ 7.77 (s, 1H, C5-H, phe), 7.56 – 7.46 (m, 2H, C2-H + C6-H, phe), 7.11 (d, J = 7.8 Hz, 1H, C4-H, phe), 4.24 – 4.18 (m, 2H, C6-H$_2$), 3.87 (s, 2H, C8-H$_2$), 3.19 (s, 3H, N3-CH$_3$), 2.23 (s, 2H, C7-H$_2$). *N1-CH$_3$ overlayed with solvent peak.* ^{13}C NMR (151 MHz, DMSO-d_6) δ 153.24 (1C, C9a), 151.16 (1C, C4, phe), 148.37 (1C, C4) 147.20 (1C, C2), 144.41 (1C, C10a), 130.30 (1C, C5, phe), 121.51 (1C, C6, phe), 120.34 (1C, C5, phe), 120.30 (d, J = 256.3 Hz, CF$_3$), 116.11 (1C, C4, phe), 115.16 (1C, C2, phe) 102.52 (1C, C4a), 46.45 (1C, C6), 42.01 (1C, C9), 29.37 (1C, N1-CH$_3$), 27.46 (1C, N3-CH$_3$), 21.12 (1C, C7). LC-MS (m/z): positive mode 396.0 [M + H]$^+$. HRMS (ESI): m/z [M + H]$^+$ calcd. for C$_{17}$H$_{17}$F$_3$N$_5$O$_3$: 396.1283; found: 396.1294. Purity determined by HPLC-UV (254 nm)-ESI-MS: 97%. Mp. 203 °C.

4.5.92 10-(3-Chlorophenyl)-1,3-dimethyl-1*H*-[1,3]diazepino[2,1-*f*]purine-2,4(3*H*,10*H*)-dione
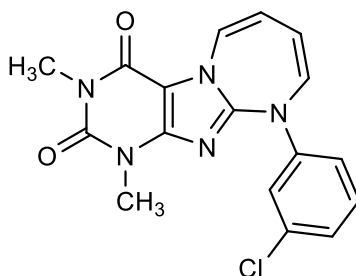
7-(4-Bromobutyl)-8-bromo-theophylline (0.15 g, 0.38 mmol, 1 eq.) was dissolved in 5 ml of Dowtherm^{TM}. 3-Chloroaniline (0.040 ml, 1 eq. 0.38 mmol) was added to the reaction mixture which was stirred for 3 h at 250 °C under argon with a reflux condenser installed. After 3 h, the reaction mixture was allowed to cool down to room temperature. Then, petrol ether was added and the mixture was filtered through a pore 4 filter and washed continuously with petrol ether. The precipitate was then dissolved in DCM. The filtrate was collected, and purified by normal phase column chromatography (DCM 100% to DCM/methanol 99.5/0.5). Appropriate fractions

were pooled and the solvents were evaporated. The resulting precipitate was was dried in the desiccator (0.024 g, yield: 26%).[208] ^{1}H NMR (600 MHz, DMSO-d_6) δ 8.66 (s, 1H, C6, phe), 8.58 – 8.55 (m, 1H, C7), 7.38 – 7.36 (m, 1H, C3-H, phe), 7.35 (t, J = 2.1 Hz, 1H, C4, phe), 7.33 – 7.30 (m, 1H, C2, phe), 7.30 – 7.27 (m, 1H, C6), 7.17 – 7.13 (m, 1H, C8), 7.01 – 6.98 (m, 1H, C9), 3.58 (s, 3H, N1-CH$_3$), 3.31 (s, 3H, N3-CH$_3$). ^{13}C NMR (151 MHz, DMSO-d_6) δ 154.43 (1C, C10a), 151.36 (1C, C4), 149.30 (1C, C2), 143.36 (1C, C11a), 141.02 (1C, C1, phe), 133.56, 131.24 (1C, C5, phe), 130.68 (1C, C9), 121.04 (1C, C3, phe), 118.67 (1C, C6, phe), 118.39 (1C, C2, phe), 117.11 (1C, C6), 115.17 (1C, C7), 110.81 (1C, C8), 102.04 (1C, C4a), 29.83 (N1-CH$_3$), 27.46 (1C, N3-CH$_3$). LC-MS (m/z): positive mode 356.0 [M + H]$^+$. HRMS (ESI): m/z [M + H]$^+$ calcd. for C$_{17}$H$_{14}$ClN$_5$O$_2$: 356.0914; found: 356.0897. Purity determined by HPLC-UV (254 nm)-ESI-MS: 92%.

4.5.93 9-(4-Fluorophenyl)-1,3-dimethyl-6,7,8,9-tetrahydropyrimido[2,1-*f*]purine-2,4(1*H*,3*H*)-dione
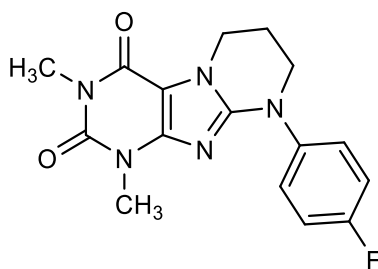
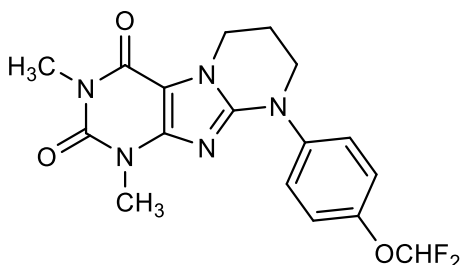9-(4-Fluorophenyl)-1,3-dimethyl-6,7,8,9-tetrahydropyrimido[2,1-*f*]purine-2,4(1*H*,3*H*)-dione was synthesized according to general procedure K (0.028 g, yield 90%). ^{1}H NMR (600 MHz, DMSO-d_6) δ 7.56 – 7.52 (m, 2H, C2 + C6-H, phe), 7.22 (t, *J* = 8.7 Hz, 2H, C3 + C5-H, phe), 4.20 (t, *J* = 6.0 Hz, 2H, C6-H), 3.79 (t, *J* = 5.5 Hz, 2H, C8-H), 3.27 (s, 3H, N1-CH$_3$), 3.18 (s, 3H, N3-CH$_3$), 2.24 – 2.19 (m, 2H, C7-H). ^{13}C NMR (151 MHz, DMSO-d_6) δ 159.47 (1C, d, *J* = 241.8 Hz, C4, phe), 153.40 (1C, C9a), 151.49 (1C, C4), 149.81 (C2, 1C), 147.93 (C10a, 1C), 139.93 (d, *J* = 2.7 Hz, C1, phe, 1C), 125.85 (d, *J* = 8.3 Hz, C2 + C6, phe, 2C), 115.81 (d, *J* =

22.5 Hz, C3 + C5, phe, 2C), 102.66 (C4a, 1C), 47.62 (C6, 1C), 42.29 (C8, 1C), 29.85 (N1-CH$_3$, 1C), 27.73 (N3-CH$_3$, 1C), 21.50 (C7, 1C). LC-MS (m/z): positive mode 330.1 [M + H]$^+$. HRMS (ESI): m/z [M + H]$^+$ calcd. for C$_{16}$H$_{17}$FN$_5$O$_2$: 330.1366; found: 330.1383. Purity determined by HPLC-UV (254 nm)-ESI-MS: 99%. Mp. 296 - 298 °C.

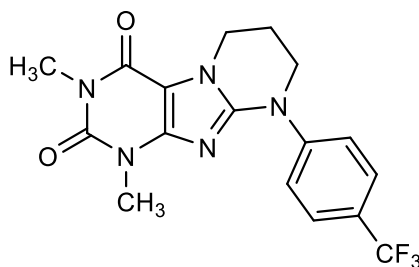### 4.5.94 9-(4-Chlorophenyl)-1,3-dimethyl-6,7,8,9-tetrahydropyrimido[2,1-*f*]purine-2,4(1*H*,3*H*)-dione
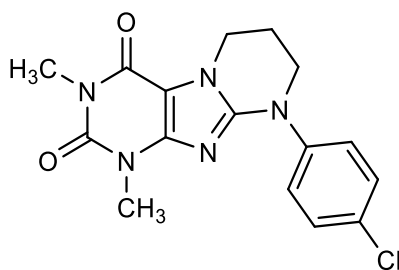
9-(4-Chlorophenyl)-1,3-dimethyl-6,7,8,9-tetrahydropyrimido[2,1-*f*]purine-2,4(1*H*,3*H*)-dione was synthesized according to general procedure K (0.050 g, yield 53%). ^{1}H NMR (600 MHz, DMSO-*d$_6$*) δ 7.67 – 7.64 (m, 1H, C6-H, phe), 7.45 – 7.41 (m, 1H, C3-H, phe), 7.21 (t, *J* = 8.9 Hz, 1H, C2-H, phe), 4.23 (t, *J* = 6.0 Hz, 2H, C6-H$_2$), 3.82 – 3.78 (m, 2H, C9-H$_2$), 3.32 (s, 3H, N1-CH$_3$), 3.20 (s, 3H, N3-CH$_3$), 2.27 – 2.22 (m, 2H, C7-H$_2$). ^{13}C NMR (151 MHz, DMSO-*d$_6$*) δ 154.16 (d, *J* = 245.5 Hz, C4, phe), 153.16 (1C, C9a), 151.05 (1C, C6), 148.51 (1C, C2), 147.25 (1C, C10a), 139.62 (d, *J* = 3.2 Hz, 1C, C1, phe), 124.76 (1C, C2, phe), 122.80 (d, *J* = 7.1 Hz, 1C, C6, phe), 119.59 (d, *J* = 18.6 Hz, 1C, C5, phe) 116.20 (d, *J* = 22.0 Hz, 1C, C3, phe), 102.49 (1C, C4a), 46.86 (C6, 1C), 41.73 (1C, C8), 29.25 (1C, N1-CH$_3$), 27.14 (1C, N3-CH$_3$), 21.10 (1C, C7). LC-MS (*m/z*): positive mode 364.0 [M + H]$^+$. HRMS (ESI): m/z [M + H]$^+$ calcd. for C$_{16}$H$_{16}$ClFN$_5$O$_2$: 364.0977; found: 364.0971. Purity determined by HPLC-UV (254 nm)-ESI-MS: 99%. Mp. >300 °C decomp.

4.5.95 1,3-Dimethyl-9-(4-(trifluoromethoxy)phenyl)-6,7,8,9-tetrahydropyrimido[2,1-*f*]purine-2,4(1*H*,3*H*)-dione
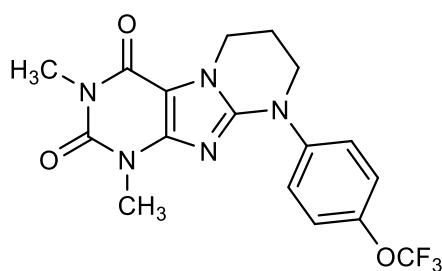
1,3-Dimethyl-9-(4-(trifluoromethoxy)phenyl)-6,7,8,9-tetrahydropyrimido[2,1-*f*]purine-2,4(1*H*,3*H*)-dione was synthesized according to general procedure K. The reaction mixture was cooled down to room temperature and the stirring was stopped. A precipitate occurred in the reaction mixture, which was then filtrated over a pore 5 filter and washed several times with acetone and H_2O. The precipitate was dried in the desiccator (0.017 g, yield: 16%). ^1H NMR (600 MHz, DMSO-d_6) δ 7.66 (d, J = 9.1 Hz, 2H, C3-H + C5-H, phe), 7.38 (d, J = 8.7 Hz, 2H, C2-H + C6-H, phe), 4.21 (t, J = 6.0 Hz, 2H, C6-H_2), 3.87 – 3.81 (m, 2H, C8-H_2), 3.29 (s, 3H, N1-CH_3), 3.19 (s, 3H, N3-CH_3), 2.25 – 2.19 (m, 2H, C7-H_2). ^{13}C NMR (151 MHz, DMSO-d_6) δ 153.00 (1C, C9a), 151.01 (1C, C4), 148.68 (1C, C2), 147.24 (1C, C10a), 144.31 (1C, C1, phe), 142.07 (1C, C4, phe), 124.17 (2C, C3 + C5, phe), 121.34 (2C, C2 + C6, phe), 120.13 (d, J = 255.7 Hz, 1C, CF_3), 102.30 (1C, C4a), 46.70 (1C, C6), 41.86 (1C, C8), 29.41 (1C, N1-CH_3), 27.27 (1C, N3-CH_3), 20.98 (1C, C7). LC-MS (*m/z*): positive mode 396.0 [M + H]$^+$. HRMS (ESI): m/z [M + H]$^+$ calcd. for $C_{17}H_{17}F_3N_5O_3$: 396.1283; found: 396.1278. Purity determined by HPLC-UV (254 nm)-ESI-MS: 99%. Mp. 202 - 204 °C.

4.5.96 4-(1,3-Dimethyl-2,4-dioxo-1,2,3,4,7,8-hexahydropyrimido[2,1-*f*]purin-9(6*H*)-yl)benzenesulfonamide
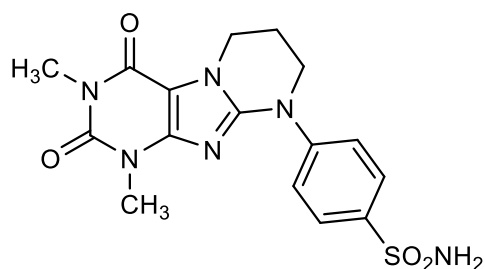
4-(1,3-Dimethyl-2,4-dioxo-1,2,3,4,7,8-hexahydropyrimido[2,1-*f*]purin-9(6*H*)-yl)benzenesulfonamide was synthesized according to general procedure K (0.044 g, yield 42%).

^{1}H NMR (600 MHz, DMSO-*d6*) δ 7.83 – 7.78 (m, 2H, C3-H + C5-H, phe), 7.68 – 7.62 (m, 2H, C2-H + C6-H, phe), 7.12 (s, 2H, SO$_2$NH$_2$), 4.32 – 4.22 (m, 2H, C6-H$_2$), 3.94 – 3.84 (m, 2H, C8-H$_2$), 2.32 – 2.25 (m, 2H, C7-H$_2$). ^{13}C NMR (151 MHz, DMSO-*d6*) δ 153.07 (C9a, 1C), 150.90 (C4, 1C), 147.77 (C1, phe, 1C), 146.95 (C2, 1C), 145.19 (C10a, 1C), 138.64 (C4, phe, 1C), 126.13 (C3 + C5, phe, 2C), 121.17 (C2 + C6, phe, 2C), 102.43 (C5, 1C), 46.16 (1C, C6), 41.65 (1C, C8), 29.12 (N1-CH$_3$, 1C), 27.00 (N3-CH$_3$, 1C), 20.97 (1C, C7). LC-MS (*m/z*): positive mode 391.1 [M + H]$^{+}$. HRMS (ESI): m/z [M + H]$^{+}$ calcd. for C$_{16}$H$_{19}$N$_6$O$_4$S: 391.1188; found: 391.1183. Purity determined by HPLC-UV (254 nm)-ESI-MS: 99%. Mp. > 300 °C.

4.5.97 9-(4-(Difluoromethoxy)phenyl)-1,3-dimethyl-6,7,8,9-tetrahydropyrimido[2,1-*f*]purine-2,4(1*H*,3*H*)-dione

9-(4-(Difluoromethoxy)phenyl)-1,3-dimethyl-6,7,8,9-tetrahydropyrimido[2,1-*f*]purine-2,4(1*H*,3*H*)-dione was synthesized according to general procedure K (0.062 g, yield: 64%). ^{1}H

NMR (600 MHz, DMSO-d_6) δ 7.81 – 7.78 (m, 1H, CHF$_2$), 7.75 – 7.72 (m, 2H, C3 + C5-H, phe), 7.28 (s, 2H, C2 + C6-H, phe), 4.22 (t, J = 6.0 Hz, 2H, C6-H$_2$), 3.90 – 3.87 (m, 2H, C8-H$_2$), 3.19 (s, 3H, N3-CH$_3$), 2.27 – 2.21 (m, 2H, C7-H$_2$). ^{13}C NMR (151 MHz, DMSO-d_6) δ 162.47 (1C, CHF$_2$), 153.23 (1C, C9a), 151.16 (1C, C4), 148.28 (1C, C2), 147.22 (1C, C10a), 145.70 (1C, C4, phe), 138.95 (1C, C1, phe), 126.43 (2C, C3 + C5, phe), 121.94 (2C, C2 + C6, phe), 102.59 (1C, C4a), 46.50 (1C, C6), 42.09 (1C, C8), 29.58 (1C, N1-CH$_3$), 27.48 (1C, N3-CH$_3$), 21.18 (1C, C7). LC-MS (*m/z*): positive mode 378.2 [M + H]$^+$.HRMS (ESI): m/z [M + H]$^+$ calcd. for C$_{17}$H$_{18}$F$_2$N$_5$O$_3$: 378.1378; found: 378.1379. Purity determined by HPLC-UV (254 nm)-ESI-MS: 99%. Mp. 279 – 281 °C.

4.5.98 1,3-Dimethyl-9-(4-(trifluoromethyl)phenyl)-6,7,8,9-tetrahydropyrimido[2,1-*f*]purine-2,4(1*H*,3*H*)-dione

1,3-Dimethyl-9-(4-(trifluoromethyl)phenyl)-6,7,8,9-tetrahydropyrimido[2,1-*f*]purine-2,4(1*H*,3*H*)-dione was synthesized according to general procedure K (0.032 g, yield: 32%). ^{1}H NMR (600 MHz, DMSO-d_6) δ 7.80 (d, J = 8.5 Hz, 2H, C3-H + C5-H, phe), 7.73 (d, J = 8.5 Hz, 2H, C2-H + C6-H, phe), 4.23 (t, J = 6.0 Hz, 2H, C6-H$_2$), 3.92 – 3.89 (m, 2H, C8-H$_2$), 3.20 (s, 3H, N3-CH$_3$), 2.28 – 2.22 (m, 3H, C7-H$_2$). *N1-CH$_3$ overlayed with solvent peak.* ^{13}C NMR (151 MHz, DMSO-d_6) δ 153.30 (1C, C9a), 151.20 (1C, C4), 148.20 (1C, C1, phe), 147.20 (1C, C2), 146.38 (1C, C10a), 125.86 (d, J = 3.9 Hz, 2C, C3 + C5, phe), 124.51 (d, J = 271.4 Hz, 1C, CF$_3$), 123.79 (d, J = 32.2 Hz, 1C, C4), 122.14 (2C, C2 + C6, phe), 102.64 (1C, C4a), 46.41 (1C, C6), 42.10 (1C, C8), 29.60 (1C, N1-CH$_3$), 27.49 (1C, N3-CH$_3$), 21.18 (1C, C8). LC-MS (*m/z*):

positive mode 380.1 [M + H]⁺. HRMS (ESI): m/z [M + H]⁺ calcd. for $C_{17}H_{16}F_3N_5O_2$: 380.1350; found: 380.1348. Purity determined by HPLC-UV (254 nm)-ESI-MS: 93%. Mp. 202 - 204 °C.

4.5.99 9-(3-Chloro-4-fluorophenyl)-1,3-dimethyl-6,7,8,9-tetrahydropyrimido[2,1-*f*]purine-2,4(1*H*,3*H*)-dione
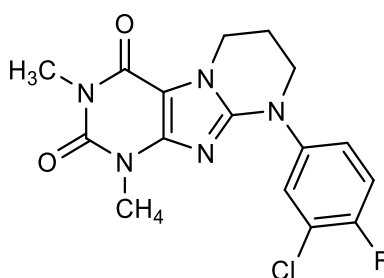

9-(3-Chloro-4-fluorophenyl)-1,3-dimethyl-6,7,8,9-tetrahydropyrimido[2,1-*f*]purine-2,4(1*H*,3*H*)-dione was synthesized according to general procedure K. After cooling down to room temperature and stopping the stirring, a white precipitate occurred in the reaction mixture, which was then filtrated and washed with 2 x 20 ml acetone and 2 x 20 ml H_2O. The precipitate was dried in the desiccator (0.050 g, yield: 53%). ¹H NMR (600 MHz, DMSO-*d₆*) δ 7.67 – 7.64 (m, 1H, C6-H, phe), 7.45 – 7.41 (m, 1H, C3-H, phe), 7.21 (t, *J* = 8.9 Hz, 1H, C2-H, phe), 4.23 (t, *J* = 6.0 Hz, 2H, C6-H₂), 3.82 – 3.78 (m, 2H, C9-H₂), 3.32 (s, 3H, N1-CH₃), 3.20 (s, 3H, N3-CH₃), 2.27 – 2.22 (m, 2H, C7-H₂). ¹³C NMR (151 MHz, DMSO-*d₆*) δ 154.16 (d, *J* = 245.5 Hz, C4, phe), 153.16 (1C, C9a), 151.05 (1C, C6), 148.51 (1C, C2), 147.25 (1C, C10a), 139.62 (d, *J* = 3.2 Hz, 1C, C1, phe), 124.76 (1C, C2, phe), 122.80 (d, *J* = 7.1 Hz, 1C, C6, phe), 119.59 (d, *J* = 18.6 Hz, 1C, C5, phe) 116.20 (d, *J* = 22.0 Hz, 1C, C3, phe), 102.49 (1C, C4a), 46.86 (C6, 1C), 41.73 (1C, C8), 29.25 (1C, N1-CH₃), 27.14 (1C, N3-CH₃), 21.10 (1C, C7). LC-MS (*m/z*): positive mode 364.0 [M + H]⁺. HRMS (ESI): m/z [M + H]⁺ calcd. for $C_{16}H_{16}ClFN_5O_2$:

364.0977; found: 364.0971. Purity determined by HPLC-UV (254 nm)-ESI-MS: 99%. Mp. >300 °C decomp.

4.5.100 4-(1,3-Dimethyl-2,4-dioxo-1,2,3,4,7,8-hexahydropyrimido[2,1-*f*]purin-9(6*H*)-yl)benzoic acid
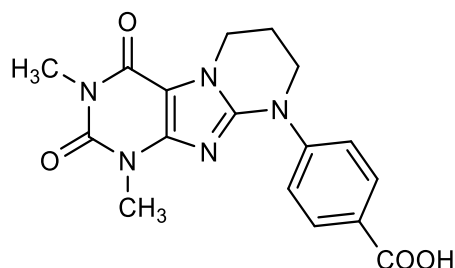
4-(1,3-Dimethyl-2,4-dioxo-1,2,3,4,7,8-hexahydropyrimido[2,1-*f*]purin-9(6*H*)-yl)benzoic acid was synthesized according to general procedure K (0.008 g, yield: 9%). ^{1}H NMR (500 MHz, DMSO-*d6*) δ 7.91 (d, *J* = 8.3 Hz, 2H, C3-H + C5-H, phe), 7.62 (d, *J* = 8.5 Hz, 2H, C2-H + C6-H, phe), 4.22 (t, *J* = 6.0 Hz, 2H, C6-H$_2$), 3.88 (t, *J* = 5.4 Hz, 2H, C8-H$_2$), 3.19 (s, 3H, N3-CH$_3$ *overlaid with solvent signal*), 2.26 – 2.19 (m, 2H, C7-H$_2$). ^{13}C NMR (126 MHz, DMSO-*d6*) δ 167.40 (1C, COOH), 156.11 (1C, C9a), 153.21 (1C, C4), 151.18 (1C, C2), 148.49 (1C, C10a), 147.35 (1C, C1, phe), 129.90 (2C, C3 + C5), 121.39 (1C, C2 + C6, phe) 102.49 (1C, C4a), 46.53 (1C, C6), 42.05 (1C, C8C), 29.55 (1C, N1-CH$_3$), 27.43 (1C, N3-CH$_3$), 21.19 (C7, 1C). LC-MS (*m/z*): positive mode 356.1 [M+H][+]. Purity determined by HPLC-UV (254 nm)-ESI-MS: 92%.

4.5.101 9-(3-Fluoropyridin-2-yl)-1,3-dimethyl-6,7,8,9-tetrahydropyrimido[2,1-*f*]purine-2,4(1*H*,3*H*)-dione
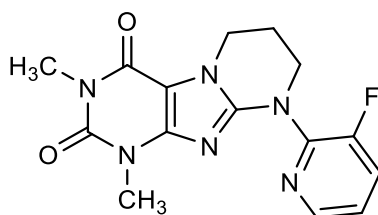
9-(3-Fluoropyridin-2-yl)-1,3-dimethyl-6,7,8,9-tetrahydropyrimido[2,1-*f*]purine-2,4(1*H*,3*H*)-dione was synthesized according to general procedure K. The reaction mixture was diluted with 3 ml of ethyl acetate and then extracted in total 35 ml of H_2O. The organic phase was dried over sodium sulfate, evaporated and purified by normal phase column chromatography (DCM/methanol 96/4). Since the obtained purity was not sufficient, it was subsequently purified by RP-HPLC to give an orange powder (0.004 g, yield: 5%). ^{1}H NMR (600 MHz, DMSO-*d6*) δ 7.47 (d, *J* = 6.9 Hz, 1H C5-H, phe), 7.43 – 7.39 (m, 1H, C3-H, phe), 6.47 – 6.42 (m, 1H, C4-H, phe), 4.71 (dd, *J* = 14.7, 5.6 Hz, 1H, C8-H), 3.98 (dd, *J* = 14.9, 5.0 Hz, 1H, C8-H), 3.57 – 3.50 (m, 2H, C6-H_2), 3.38 (s, 3H, N1-CH_3 *overlaid with solvent signal*), 3.20 (s, 3H, N3-CH_3), 1.84 – 1.78 (m, 1H, C7-H), 1.72 – 1.64 (m, 1H, C7-H). ^{13}C NMR (151 MHz, DMSO-*d6*) δ 153.74 (1C, C10a), 153.42 (1C, C4), 152.21 (d, *J* = 247.3 Hz, 1C, C2, phe), 151.27 (1C, C2, phe), 148.76 (1C, C11a), 144.06 (d, *J* = 16.5 Hz, C1, phe), 135.24 (d, *J* = 5.3 Hz, C5, phe), 119.54 (d, *J* = 19.1 Hz, 1C, C3, phe), 107.40 (d, *J* = 6.9 Hz, 1C, C4, phe), 101.36 (1C, C4a), 48.74 (1C, C6), 38.39 (1C, C8), 29.41 (1C, N1-CH_3), 27.40 (1C, N3-CH_3), 22.54 (1C, C7). HRMS (ESI): m/z [M + H]$^+$ calcd. for $C_{15}H_{16}FN_6O_2$: 331.1313; found: 331.1315. Purity determined by HPLC-UV (254 nm)-ESI-MS: 99%.

4.5.102 1,3-Dimethyl-9-(pyridin-2-yl)-6,7,8,9-tetrahydropyrimido[2,1-*f*]purine-2,4(1*H*,3*H*)-dione
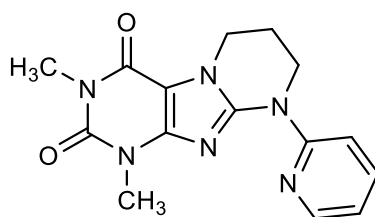
1,3-Dimethyl-9-(pyridin-2-yl)-6,7,8,9-tetrahydropyrimido[2,1-*f*]purine-2,4(1*H*,3*H*)-dione was synthesized according to general procedure K (0.006 g, yield: 7%). The reaction mixture was diluted with 3 ml of ethyl acetate and then extracted in total 35 ml of H_2O. The organic phase was dried over Na_2SO_3, evaporated and purified by normal phase column chromatography (DCM/methanol 96/4). The purified product was subsequently purified by RP-HPLC to give an orange powder. ^{1}H NMR (600 MHz, DMSO-*d6*) δ 7.60 – 7.57 (m, 1H, C5-H, phe), 7.45 – 7.41 (m, 1H, C3-H, phe), 6.75 (d, *J* = 9.0 Hz, 1H, C4-H, phe), 6.51 – 6.47 (m, 1H, C2-H, phe), 4.73 – 4.68 (m, 1H, C8-H), 3.93 – 3.88 (m, 1H, C8-H), 3.51 – 3.44 (m, 2H, C6-H_2) 3.36 (s, 3H, N1-CH_3, overlayed with solvent peak), 3.19 (s, 3H, N3-CH_3, overlayed with solvent peak), 1.82 – 1.75 (m, 1H, C7-H), 1.71 – 1.63 (m, 1H, C7-H). ^{13}C NMR (151 MHz, DMSO-*d6*) δ 154.69 (1C, C9a), 153.52 (1C, C1, phe), 151.70 (1C, C4), 151.60 (1C, C2), 149.24 (1C, C10a), 139.69 (1C, C5, phe), 138.42 (1C, C3, phe), 124.02 (1C, C4, phe), 110.14 (1C, C2, phe), 101.21 (1C, C4a), 48.79 (1C, C6), 38.64 (1C, C8), 29.68 (1C, N1-CH_3), 27.67 (1C, N3-CH_3), 23.04 (1C, C7). HRMS (ESI): m/z [M + H]$^+$ calcd. for $C_{15}H_{17}N_6O_2$: 313.1413; found: 313.1409. Purity determined by HPLC-UV (254 nm)-ESI-MS: 96%.

4.5.103 8-Bromo-1,3-dimethyl-7-(4-((4-(trifluoromethoxy)phenyl)amino)butyl)-3,7-

dihydro-1*H*-purine-2,6-dione
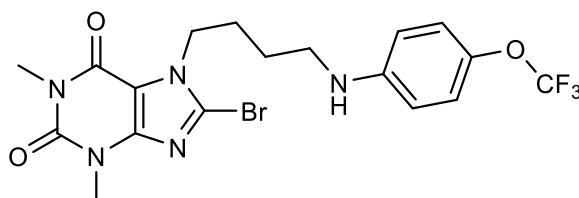
8-Bromo-1,3-dimethyl-7-(4-((4-(trifluoromethoxy)phenyl)amino)butyl)-3,7-dihydro-1*H*-purine-2,6-dione was synthesized according to general procedure J. The compounds was obtained as a side-product and was then isolated (no yield). ^{1}H NMR (500 MHz, DMSO-*d6*) δ 7.00 (d, *J* = 8.8 Hz, 2H, 2 x CH, phe), 6.54 (d, *J* = 9.0 Hz, 2H, 2 x CH, phe), 5.79 (t, *J* = 5.4 Hz, 1H, NH), 4.28 (t, *J* = 7.0 Hz, 2H, N-CH2), 3.38 (s, 3H, N1-CH3), 3.21 (s, 3H, N3-CH3) 2.99 (q, *J* = 6.5 Hz, 2H, NH-CH2), 1.83 (p, *J* = 7.2 Hz, 2H, CH2), 1.52 (p, *J* = 7.1 Hz, 2H, CH2). ^{13}C NMR (126 MHz, DMSO-*d6*) δ 153.60 (1C, C6), 150.78 (1C, C2), 148.22 (1C, C4), 147.94 (1 C, Cq, phe), 138.31 (1 C, Cq, phe), 127.81, 122.06 (2C, 2 x CH, phe), 120.50 (d, *J* = 253.8 Hz, CF3), 112.27 (2C, 2x CH, phe), 108.32 (1C, C5), 46.80 (1C, N-CH2), 42.55 (NH-CH2), 29.60 (1C, N1-CH3), 27.79 (1C, N3-CH3), 27.49 (1C, CH2), 25.36 (1C, CH2). LC-MS (*m/z*): positive mode 489.9 [M+H]$^{+}$. HRMS (ESI): m/z [M + H]$^{+}$ calcd. for $C_{18}H_{21}BrF_3N_5O_3$: 490.0702; found: 490.0705. Purity determined by HPLC-UV (254 nm)-ESI-MS: 95%.

5   References

(1) Drury, A. N.; Szent-Györgyi, A. The physiological activity of adenine compounds with especial reference to their action upon the mammalian heart. *J. Physiol.* **1929**, *68*, 213–237.

(2) Holton, P. The liberation of adenosine triphosphate on antidromic stimulation of sensory nerves. *J. Physiol.* **1959**, *145*, 494–504.

(3) Abbracchio, M. P.; Jacobson, K. A.; Müller, C. E.; Zimmermann, H. Professor Dr. Geoffrey Burnstock (1929–2020). *Purinergic Signal.* **2020**, *16*, 137–149.

(4) Burnstock, G. Physiology and pathophysiology of purinergic neurotransmission. *Physiol. Rev.* **2007**, *87*, 659–797.

(5) Burnstock, G. Purinergic nerves. *Pharmacol. Rev.* **1972**, *24*, 509–581.

(6) Allard, B.; Turcotte, M.; Stagg, J. Targeting CD73 and downstream adenosine receptor signaling in triple-negative breast cancer. *Expert Opin. Ther. Targets* **2014**, *18*, 863–881.

(7) Allard, B.; Longhi, M. S.; Robson, S. C.; Stagg, J. The ectonucleotidases CD39 and CD73: Novel checkpoint inhibitor targets. *Immunol. Rev.* **2017**, *276*, 121–144.

(8) Trautmann, A. Extracellular ATP in the immune system: more than just a "danger signal". *Sci. Signal.* **2009**, *2*, pe6.

(9) Zimmermann, H. Extracellular ATP and other nucleotides-ubiquitous triggers of intercellular messenger release. *Purinergic Signal.* **2016**, *12*, 25–57.

(10) Yegutkin, G. G. Enzymes involved in metabolism of extracellular nucleotides and nucleosides: functional implications and measurement of activities. *Crit. Rev. Biochem. Mol. Biol.* **2014**, *49*, 473–497.

(11) Harvey, J. B.; Phan, L. H.; Villarreal, O. E.; Bowser, J. L. CD73's Potential as an immunotherapy target in gastrointestinal cancers. *Front. Immunol.* **2020**, *11*, 508.

(12) Vijayan, D.; Young, A.; Teng, M. W. L.; Smyth, M. J. Targeting immunosuppressive adenosine in cancer. *Nat. Rev. Cancer* **2017**, *17*, 709–724.

(13) Cekic, C.; Linden, J. Purinergic regulation of the immune system. *Nat. Rev. Immunol.* **2016**, *16*, 177–192.

(14) Di Virgilio, F.; Sarti, A. C.; Falzoni, S.; Marchi, E. de; Adinolfi, E. Extracellular ATP and P2 purinergic signalling in the tumour microenvironment. *Nat. Rev. Cancer* **2018**, *18*, 601–618.

(15) Antonioli, L.; Pacher, P.; Vizi, E. S.; Haskó, G. CD39 and CD73 in immunity and inflammation. *Trends Mol. Med.* **2013**, *19*, 355–367.

(16) Antonioli, L.; Yegutkin, G. G.; Pacher, P.; Blandizzi, C.; Haskó, G. Anti-CD73 in cancer immunotherapy: awakening new opportunities. *Trends Cancer* **2016**, *2*, 95–109.

(17) Zimmermann, H.; Zebisch, M.; Sträter, N. Cellular function and molecular structure of ecto-nucleotidases. *Purinergic Signal.* **2012**, *8*, 437–502.

(18) Longhi, M. S.; Robson, S. C.; Bernstein, S. H.; Serra, S.; Deaglio, S. Biological functions of ecto-enzymes in regulating extracellular adenosine levels in neoplastic and inflammatory disease states. *J. Mol. Med.* **2013**, *91*, 165–172.

(19) Robson, S. C.; Sévigny, J.; Zimmermann, H. The E-NTPDase family of ectonucleotidases: Structure function relationships and pathophysiological significance. *Purinergic Signal.* **2006**, *2*, 409–430.

(20) Wang, T. F.; Guidotti, G. CD39 is an ecto-(Ca^{2+},Mg^{2+})-apyrase. *J. Biol. Chem.* **1996**, *271*, 9898–9901.

(21) Paavilainen, S.; Guidotti, G. Interactions between the transmembrane domains of CD39: identification of interacting residues by yeast selection. *ScienceOpen Research* **2014**, *2014*.

(22) Grinthal, A.; Guidotti, G. CD39, NTPDase 1, is attached to the plasma membrane by two transmembrane domains. Why? *Purinergic Signal.* **2006**, *2*, 391–398.

(23) Zhong, X.; Malhotra, R.; Woodruff, R.; Guidotti, G. Mammalian plasma membrane ecto-nucleoside triphosphate diphosphohydrolase 1, CD39, is not active intracellularly. The N-glycosylation state of CD39 correlates with surface activity and localization. *J. Biol. Chem.* **2001**, *276*, 41518–41525.

(24) Lecka, J.; Gillerman, I.; Fausther, M.; Salem, M.; Munkonda, M. N.; Brosseau, J.-P.; Cadot, C.; Martín-Satué, M.; d'Orléans-Juste, P.; Rousseau, E.; Poirier, D.; Künzli, B.; Fischer, B.; Sévigny, J. 8-BuS-ATP derivatives as specific NTPDase1 inhibitors. *Br. J. Pharmacol.* **2013**, *169*, 179–196.

(25) Schäkel, L.; Schmies, C. C.; Idris, R. M.; Luo, X.; Lee, S.-Y.; Lopez, V.; Mirza, S.; Vu, T. H.; Pelletier, J.; Sévigny, J.; Namasivayam, V.; Müller, C. E. Nucleotide analog ARL67156 as a lead structure for the development of CD39 and dual CD39/CD73 ectonucleotidase inhibitors. *Front. Pharmacol.* **2020**, *11*, 1294.

(26) Lecka, J.; Fausther, M.; Künzli, B.; Sévigny, J. Ticlopidine in its prodrug form is a selective inhibitor of human NTPDase1. *Mediators Inflamm.* **2014**, *2014*, 547480.

(27) Lee, S.-Y.; Fiene, A.; Li, W.; Hanck, T.; Brylev, K. A.; Fedorov, V. E.; Lecka, J.; Haider, A.; Pietzsch, H.-J.; Zimmermann, H.; Sévigny, J.; Kortz, U.; Stephan, H.; Müller, C. E. Polyoxometalates--potent and selective ecto-nucleotidase inhibitors. *Biochem. pharmacol.* **2015**, *93*, 171–181.

(28) Baqi, Y.; Weyler, S.; Iqbal, J.; Zimmermann, H.; Müller, C. E. Structure-activity relationships of anthraquinone derivatives derived from bromaminic acid as inhibitors of ectonucleoside triphosphate diphosphohydrolases (E-NTPDases). *Purinergic Signal.* **2009**, *5*, 91–106.

(29) Baqi, Y.; Rashed, M.; Schäkel, L.; Malik, E. M.; Pelletier, J.; Sévigny, J.; Fiene, A.; Müller, C. E. Development of anthraquinone derivatives as ectonucleoside triphosphate diphosphohydrolase (NTPDase) inhibitors with selectivity for NTPDase2 and NTPDase3. *Front. Pharmacol.* **2020**, *11*, 1282.

(30) Rücker, B.; Almeida, M. E.; Libermann, T. A.; Zerbini, L. F.; Wink, M. R.; Sarkis, J. J. F. Biochemical characterization of ecto-nucleotide pyrophosphatase/phosphodiesterase (E-NPP, E.C. 3.1.4.1) from rat heart left ventricle. *Mol. Cell. Biochem.* **2007**, *306*, 247–254.

(31) Massé, K.; Bhamra, S.; Allsop, G.; Dale, N.; Jones, E. A. Ectophosphodiesterase/nucleotide phosphohydrolase (Enpp) nucleotidases: cloning, conservation and developmental restriction. *Int. J. Dev. Biol.* **2010**, *54*, 181–193.

(32) Stefan, C.; Jansen, S.; Bollen, M. Modulation of purinergic signaling by NPP-type ectophosphodiesterases. *Purinergic Signal.* **2006**, *2*, 361–370.

(33) Sakagami, H.; Aoki, J.; Natori, Y.; Nishikawa, K.; Kakehi, Y.; Natori, Y.; Arai, H. Biochemical and molecular characterization of a novel choline-specific glycerophosphodiester phosphodiesterase belonging to the nucleotide pyrophosphatase/phosphodiesterase family. *J. Biol. Chem.* **2005**, *280*, 23084–23093.

(34) Nilsson, Å.; Duan, R.-D. Pancreatic and mucosal enzymes in choline phospholipid digestion. *Am. J. Physiol. Gastrointest. Liver Physiol.* **2019**, *316*, G425-G445.

(35) Sharma, U.; Pal, D.; Prasad, R. Alkaline phosphatase: an overview. *Indian J. Clin. Biochem.* **2014**, *29*, 269–278.

(36) Millán, J. L. Alkaline Phosphatases : Structure, substrate specificity and functional relatedness to other members of a large superfamily of enzymes. *Purinergic Signal.* **2006**, *2*, 335–341.

(37) Bogan, K. L.; Brenner, C. 5′-Nucleotidases and their new roles in NAD+ and phosphate metabolism. *New J. Chem.* **2010**, *34*, 845.

(38) Zhang, B. CD73: A novel target for cancer immunotherapy. *Cancer Res.* **2010**, *70*, 6407–6411.

(39) Knapp, K.; Zebisch, M.; Pippel, J.; El-Tayeb, A.; Müller, C. E.; Sträter, N. Crystal structure of the human ecto-5'-nucleotidase (CD73): insights into the regulation of purinergic signaling. *Structure* **2012**, *20*, 2161–2173.

(40) Heuts, D. P. H. M.; Weissenborn, M. J.; Olkhov, R. V.; Shaw, A. M.; Gummadova, J.; Levy, C.; Scrutton, N. S. Crystal structure of a soluble form of human CD73 with ecto-5'-nucleotidase activity. *Chembiochem.* **2012**, *13*, 2384–2391.

(41) Adzic, M.; Nedeljkovic, N. Unveiling the Role of Ecto-5'-Nucleotidase/CD73 in Astrocyte Migration by Using Pharmacological Tools. *Front. Pharmacol.* **2018**, *9*, 153.

(42) Airas, L.; Niemelä, J.; Salmi, M.; Puurunen, T.; Smith, D. J.; Jalkanen, S. Differential regulation and function of CD73, a glycosyl-phosphatidylinositol-linked 70-kD adhesion molecule, on lymphocytes and endothelial cells. *J. Cell Biol.* **1997**, *136*, 421–431.

(43) Schneider, E.; Rissiek, A.; Winzer, R.; Puig, B.; Rissiek, B.; Haag, F.; Mittrücker, H.-W.; Magnus, T.; Tolosa, E. Generation and Function of Non-cell-bound CD73 in Inflammation. *Front. Immunol.* **2019**, *10*, 1729.

(44) Martínez-Martínez, A.; Muñoz-Delgado, E.; Campoy, F.; Flores-Flores, C.; Rodríguez-López, J.; Fini, C.; Vidal, C. The ecto-5′-nucleotidase subunits in dimers are not linked by disulfide bridges but by non-covalent bonds. *Biochim. Biophys. Acta, Protein Struct. Mol. Enzymol.* **2000**, *1478*, 300–308.

(45) Klemens, M. R.; Sherman, W. R.; Holmberg, N. J.; Ruedi, J. M.; Low, M. G.; Thompson, L. F. Characterization of soluble vs membrane-bound human placental 5′-nucleotidase. *Biochem. Biophys. Res. Commun.* **1990**, *172*, 1371–1377.

(46) Grozio, A.; Sociali, G.; Sturla, L.; Caffa, I.; Soncini, D.; Salis, A.; Raffaelli, N.; Flora, A. de; Nencioni, A.; Bruzzone, S. CD73 protein as a source of extracellular precursors for sustained NAD+ biosynthesis in FK866-treated tumor cells. *J. Biol. Chem.* **2013**, *288*, 25938–25949.

(47) Xu, W.; Le Li; Zhang, L. NAD+ Metabolism as an emerging therapeutic target for cardiovascular diseases associated with sudden cardiac death. *Front. Physiol.* **2020**, *11*, 901.

(48) Koszałka, P.; Gołuńska, M.; Urban, A.; Stasiłojć, G.; Stanisławowski, M.; Majewski, M.; Składanowski, A. C.; Bigda, J. Specific activation of A3, A2A and A1 adenosine receptors in CD73-knockout mice affects B16F10 melanoma growth, neovascularization, angiogenesis and macrophage infiltration. *PLOS ONE* **2016**, *11*, e0151420.

(49) Neo, S. Y.; Yang, Y.; Record, J.; Ma, R.; Chen, X.; Chen, Z.; Tobin, N. P.; Blake, E.; Seitz, C.; Thomas, R.; Wagner, A. K.; Andersson, J.; Boniface, J. de; Bergh, J.; Murray, S.; Alici, E.; Childs, R.; Johansson, M.; Westerberg, L. S.; Haglund, F.; Hartman, J.; Lundqvist, A. CD73 immune checkpoint defines regulatory NK cells within the tumor microenvironment. *J. Clin. Investig.* **2020**, *130*, 1185–1198.

(50) Monteiro, I.; Vigano, S.; Faouzi, M.; Treilleux, I.; Michielin, O.; Ménétrier-Caux, C.; Caux, C.; Romero, P.; Leval, L. de. CD73 expression and clinical significance in human metastatic melanoma. *Oncotarget* **2018**, *9*, 26659–26669.

(51) Shevchenko, I.; Mathes, A.; Groth, C.; Karakhanova, S.; Müller, V.; Utikal, J.; Werner, J.; Bazhin, A. V.; Umansky, V. Enhanced expression of CD39 and CD73 on T cells in the regulation of anti-tumor immune responses. *Oncoimmunology* **2020**, *9*, 1744946.

(52) Gao, Z.; Dong, K.; Zhang, H. The roles of CD73 in cancer. *Biomed Res. Int.* **2014**, *2014*, 460654.

(53) Buisseret, L.; Pommey, S.; Allard, B.; Garaud, S.; Bergeron, M.; Cousineau, I.; Ameye, L.; Bareche, Y.; Paesmans, M.; Crown, J. P. A.; Di Leo, A.; Loi, S.; Piccart-Gebhart, M.; Willard-Gallo, K.; Sotiriou, C.; Stagg, J. Clinical significance of CD73 in triple-negative breast cancer: multiplex analysis of a phase III clinical trial. *Ann. Oncol.* **2018**, *29*, 1056–1062.

(54) Stagg, J.; Divisekera, U.; McLaughlin, N.; Sharkey, J.; Pommey, S.; Denoyer, D.; Dwyer, K. M.; Smyth, M. J. Anti-CD73 antibody therapy inhibits breast tumor growth and metastasis. *PNAS* **2010**, *107*, 1547–1552.

(55) Yegutkin, G. G.; Marttila-Ichihara, F.; Karikoski, M.; Niemelä, J.; Laurila, J. P.; Elima, K.; Jalkanen, S.; Salmi, M. Altered purinergic signaling in CD73-deficient mice inhibits tumor progression. *Eur. J. Immunol.* **2011**, *41*, 1231–1241.

(56) https://www.ema.europa.eu/en/documents/assessment-report/yervoy-epar-public-assessment-report_en.pdf. Available at https://www.ema.europa.eu/en/documents/assessment-report/yervoy-epar-public-assessment-report_en.pdf (accessed November 10, 2021).

(57) Robert, C. A decade of immune-checkpoint inhibitors in cancer therapy. *Nat. Commun.* **2020**, *11*, 3801.

(58) Yu, M.; Guo, G.; Huang, L.; Deng, L.; Chang, C.-S.; Achyut, B. R.; Canning, M.; Xu, N.; Arbab, A. S.; Bollag, R. J.; Rodriguez, P. C.; Mellor, A. L.; Shi, H.; Munn, D. H.; Cui, Y. CD73 on cancer-associated fibroblasts enhanced by the A2B-mediated feedforward circuit enforces an immune checkpoint. *Nat. Commun.* **2020**, *11*, 515.

(59) Allard, D.; Allard, B.; Gaudreau, P.-O.; Chrobak, P.; Stagg, J. CD73-adenosine: a next-generation target in immuno-oncology. *Immunother.* **2016**, *8*, 145–163.

(60) Hay, C. M.; Sult, E.; Huang, Q.; Mulgrew, K.; Fuhrmann, S. R.; McGlinchey, K. A.; Hammond, S. A.; Rothstein, R.; Rios-Doria, J.; Poon, E.; Holoweckyj, N.; Durham, N. M.; Leow, C. C.; Diedrich, G.; Damschroder, M.; Herbst, R.; Hollingsworth, R. E.; Sachsenmeier, K. F. Targeting CD73 in the tumor microenvironment with MEDI9447. *Oncoimmunology* **2016**, *5*, e1208875.

(61) Search of: MEDI9447 - List Results - ClinicalTrials.gov. Available at https://clinicaltrials.gov/ct2/results?cond=&term=MEDI9447+&cntry=&state=&city=&dist=, Published Online: August 16, 2021, last accessed November 10, 2021.

(62) MedImmune LLC. A Phase 1b/2 Study to Evaluate the Safety, Pharmacokinetics, and Clinical Activity of Oleclumab (MEDI9447) With or Without Durvalumab in Combination With Chemotherapy in Subjects With Metastatic Pancreatic Ductal Adenocarcinoma. Available at https://clinicaltrials.gov/ct2/show/NCT03611556, Published Online: July 13, 2021, last accessed August 05, 2021.

(63) ELI LILLY AND COMPANY; Merck Sharp & Dohme Corp. A Phase 1 Multicenter Global First in Human Study of the CD73 Inhibitor LY3475070 as Monotherapy or in Combination With Pembrolizumab in Patients With Advanced Solid Malignancies. Available at https://clinicaltrials.gov/ct2/show/NCT04148937, Published Online: May 21, 2021, last accessed August 09, 2021.

(64) Arcus Biosciences, Inc. A Phase 1 Study to Evaluate the Safety and Tolerability of AB680 Combination Therapy in Participants With Gastrointestinal Malignancies. Available at https://clinicaltrials.gov/ct2/show/NCT04104672, Published Online: July 19, 2021, last accessed September 10, 2021.

(65) Jeffrey, J. L.; Lawson, K. V.; Powers, J. P. Targeting metabolism of extracellular nucleotides via inhibition of ectonucleotidases CD73 and CD39. *J. Med. Chem.* **2020**, *63*, 13444–13465.

(66) Cogan, E. B.; Birrell, G. B.; Griffith, O. H. A robotics-based automated assay for inorganic and organic phosphates. *Anal. biochem.* **1999**, *271*, 29–35.

(67) Allard, B.; Cousineau, I.; Spring, K.; Stagg, J. Measurement of CD73 enzymatic activity using luminescence-based and colorimetric assays. *Meth. enzymol.* **2019**, *629*, 269–289.

(68) Baykov, A. A.; Evtushenko, O. A.; Avaeva, S. M. A malachite green procedure for orthophosphate determination and its use in alkaline phosphatase-based enzyme immunoassay. *Anal. biochem.* **1988**, *171*, 266–270.

(69) Christian Renn. *Assay development, identification, optimization and pharmacological characterization of inhibitors for ecto-5'-nucleotidase (CD73):* Bonn, 2019.

(70) Freundlieb, M.; Zimmermann, H.; Müller, C. E. A new, sensitive ecto-5'-nucleotidase assay for compound screening. *Anal. biochem.* **2014**, *446*, 53–58.

(71) Freundlieb, M. *Entwicklung und Charakterisierung von neuen und selektiven Inhibitoren für die Ecto-5'-Nucleotidase:* Bonn, 2016.

(72) Brunschweiger, A.; Müller, C. E. P2 receptors activated by uracil nucleotides--an update. *CMC* **2006**, *13*, 289–312.

(73) Burnstock, G. Purine and purinergic receptors. *Brain Neurosci. Adv.* **2018**, *2*, 2398212818817494.

(74) Thimm, D.; Knospe, M.; Abdelrahman, A.; Moutinho, M.; Alsdorf, B. B. A.; Kügelgen, I. von; Schiedel, A. C.; Müller, C. E. Characterization of new G protein-coupled adenine receptors in mouse and hamster. *Purinergic Signal.* **2013**, *9*, 415–426.

(75) Bender, E.; Buist, A.; Jurzak, M.; Langlois, X.; Baggerman, G.; Verhasselt, P.; Ercken, M.; Guo, H.-Q.; Wintmolders, C.; van den Wyngaert, I.; van Oers, I.; Schoofs, L.; Luyten, W.

Characterization of an orphan G protein-coupled receptor localized in the dorsal root ganglia reveals adenine as a signaling molecule. *PNAS* **2002**, *99*, 8573–8578.

(76) Knospe, M.; Müller, C. E.; Rosa, P.; Abdelrahman, A.; Kügelgen, I. von; Thimm, D.; Schiedel, A. C. The rat adenine receptor: pharmacological characterization and mutagenesis studies to investigate its putative ligand binding site. *Purinergic Signal.* **2013**, *9*, 367–381.

(77) Jacobson, K. A.; Gao, Z.-G. Adenosine receptors as therapeutic targets. *Nat. Rev. Drug Discov.* **2006**, *5*, 247–264.

(78) Abbracchio, M. P.; Burnstock, G.; Verkhratsky, A.; Zimmermann, H. Purinergic signalling in the nervous system: an overview. *Trends in Neurosci.* **2009**, *32*, 19–29.

(79) Müller, C. E.; Jacobson, K. A. Recent developments in adenosine receptor ligands and their potential as novel drugs. *Biochim. Biophys. Acta* **2011**, *1808*, 1290–1308.

(80) Beavis, P. A.; Divisekera, U.; Paget, C.; Chow, M. T.; John, L. B.; Devaud, C.; Dwyer, K.; Stagg, J.; Smyth, M. J.; Darcy, P. K. Blockade of A2A receptors potently suppresses the metastasis of CD73+ tumors. *PNAS* **2013**, *110*, 14711–14716.

(81) Boison, D.; Yegutkin, G. G. Adenosine metabolism: emerging concepts for cancer therapy. *Cancer Cell* **2019**, *36*, 582–596.

(82) Jacobson, K. A. Introduction to adenosine receptors as therapeutic targets. *Handb. Exp. Pharmacol* **2009**, 1–24.

(83) Rivera-Oliver, M.; Díaz-Ríos, M. Using caffeine and other adenosine receptor antagonists and agonists as therapeutic tools against neurodegenerative diseases: a review. *Life Sci.* **2014**, *101*, 1–9.

(84) Dungo, R.; Deeks, E. D. Istradefylline: first global approval. *Drugs* **2013**, *73*, 875–882.

(85) FDA approves new add-on drug to treat off episodes in adults with Parkinson's disease. *FDA, available at:* https://www.fda.gov/news-events/press-announcements/fda-approves-new-add-drug-treat-episodes-adults-parkinsons-disea*se,* last accesed on August 27, 2021.

(86) Ikeda, K.; Kurokawa, M.; Aoyama, S.; Kuwana, Y. Neuroprotection by adenosine A2A receptor blockade in experimental models of Parkinson's disease. *Journal of neurochemistry* **2002**, *80*, 262–270.

(87) Cunha, G. M. A.; Canas, P. M.; Melo, C. S.; Hockemeyer, J.; Müller, C. E.; Oliveira, C. R.; Cunha, R. A. Adenosine A2A receptor blockade prevents memory dysfunction caused by beta-amyloid peptides but not by scopolamine or MK-801. *Exp. neurol.* **2008**, *210*, 776–781.

(88) Paton, D. M. Istradefylline: adenosine A2A receptor antagonist to reduce "OFF" time in Parkinson's disease. *Drugs Today* **2020**, *56*, 125–134.

(89) Gendaszewska-Darmach, E.; Kucharska, M. Nucleotide receptors as targets in the pharmacological enhancement of dermal wound healing. *Purinergic Signal.* **2011**, *7*, 193–206.

(90) Oliveira, Á.; Illes, P.; Ulrich, H. Purinergic receptors in embryonic and adult neurogenesis. *Neuropharmacology* **2016**, *104*, 272–281.

(91) North, R. A. P2X receptors. *Philos. Trans. R. Soc. Lond., B, Biol. Sci.* **2016**, *371*.

(92) Hattori, M.; Gouaux, E. Molecular mechanism of ATP binding and ion channel activation in P2X receptors. *Nature* **2012**, *485*, 207–212.

(93) Kügelgen, I. von; Hoffmann, K. Pharmacology and structure of P2Y receptors. *Neuropharmacology* **2016**, *104*, 50–61.

(94) Kügelgen, I. von. Pharmacological profiles of cloned mammalian P2Y-receptor subtypes. *Pharmacol. Ther.* **2006**, *110*, 415–432.

(95) Guzman, S. J.; Gerevich, Z. P2Y Receptors in synaptic transmission and plasticity: therapeutic potential in cognitive dysfunction. *Neural Plast.* **2016**, *2016*, 1207393.

(96) Zhang, L.; Lu, J.; Dong, W.; Tian, H.; Feng, W.; You, H.; He, H.; Ma, J.; Dong, Y. Meta-analysis of comparison of the newer P2Y12 inhibitors (oral preparation or intravenous) to clopidogrel in patients with acute coronary syndrome. *J. Cardiovasc. Pharmacol.* **2017**, *69*, 147–155.

(97) Briasoulis, A.; Telila, T.; Palla, M.; Siasos, G.; Tousoulis, D. P2Y12 receptor antagonists: which one to choose? A systematic review and meta-analysis. *Curr. Pharm. Des.* **2016**, *22*, 4568–4576.

(98) Shah, R.; Rashid, A.; Hwang, I.; Fan, T.-H. M.; Khouzam, R. N.; Reed, G. L. Meta-analysis of the relative efficacy and safety of oral P2Y12 inhibitors in patients with acute coronary syndrome. *Am. J. Cardiol.* **2017**, *119*, 1723–1728.

(99) Keating, G. M. Diquafosol ophthalmic solution 3 %: a review of its use in dry eye. *Drugs* **2015**, *75*, 911–922.

(100) Lau, O. C. F.; Samarawickrama, C.; Skalicky, S. E. P2Y2 receptor agonists for the treatment of dry eye disease: a review. *Clin. Ophthalmol.* **2014**, *8*, 327–334.

(101) Jumblatt, J. E.; Jumblatt, M. M. Regulation of ocular mucin secretion by P2Y2 nucleotide receptors in rabbit and human conjunctiva. *Exp. Eye Res.* **1998**, *67*, 341–346.

(102) Bhattarai, S.; Freundlieb, M.; Pippel, J.; Meyer, A.; Abdelrahman, A.; Fiene, A.; Lee, S.-Y.; Zimmermann, H.; Yegutkin, G. G.; Sträter, N.; El-Tayeb, A.; Müller, C. E. α,β-Methylene-ADP (AOPCP) derivatives and analogues: development of potent and selective ecto-5'-Nucleotidase (CD73) inhibitors. *J. Med. Chem.* **2015**, *58*, 6248–6263.

(103) Bhattarai, S.; Pippel, J.; Meyer, A.; Freundlieb, M.; Schmies, C.; Abdelrahman, A.; Fiene, A.; Lee, S.-Y.; Zimmermann, H.; El-Tayeb, A.; Yegutkin, G. G.; Sträter, N.; Müller, C. E. X-Ray co-crystal structure guides the way to subnanomolar competitive ecto-5′-nucleotidase (CD73) inhibitors for cancer immunotherapy. *Adv. Therap.* **2019**, *2*, 1900075.

(104) Bhattarai, S.; Pippel, J.; Scaletti, E.; Idris, R.; Freundlieb, M.; Rolshoven, G.; Renn, C.; Lee, S.-Y.; Abdelrahman, A.; Zimmermann, H.; El-Tayeb, A.; Müller, C. E.; Sträter, N. 2-Substituted α,β-methylene-ADP derivatives: potent competitive ecto-5'-nucleotidase (CD73) inhibitors with variable binding modes. *J. Med. Chem.* **2020**, *63*, 2941–2957.

(105) Naito, Y.; Lowenstein, J. M. 5'-Nucleotidase from rat heart membranes. Inhibition by adenine nucleotides and related compounds. *Biochem J.* **1985**, *226*, 645–651.

(106) Grondal, E. J.; Zimmermann, H. Purification, characterization and cellular localization of 5'-nucleotidase from Torpedo electric organ. *Biochem. J.* **1987**, *245*, 805–810.

(107) Iqbal, J.; Jirovsky, D.; Lee, S.-Y.; Zimmermann, H.; Müller, C. E. Capillary electrophoresis-based nanoscale assays for monitoring ecto-5'-nucleotidase activity and inhibition in preparations of recombinant enzyme and melanoma cell membranes. *Anal. biochem.* **2008**, *373*, 129–140.

(108) Zimmermann, H. 5'-Nucleotidase: molecular structure and functional aspects. *Biochem. J.* **1992**, *285 (Pt 2)*, 345–365.

(109) Bhattarai, S.; Rolshoven, G. *unpublished work*, 2021.

(110) Bowman, C. E.; Da Silva, R. G.; Pham, A.; Young, S. W. An exceptionally potent inhibitor of human CD73. *Biochemistry* **2019**, *58*, 3331–3334.

(111) Bhattarai, S. *Synthesis and structure-activity relationships of α,β-methylene-ADP derivatives: potent and selective ecto-5'-nucleotidase inhibitors:* Bonn, 2015.

(112) Fredholm, B. B.; IJzerman, A. P.; Jacobson, K. A.; Linden, J.; Müller, C. E. International union of basic and clinical pharmacology. LXXXI. Nomenclature and classification of adenosine receptors--an update. *Pharmacol. rev.* **2011**, *63*, 1–34.

(113) Lawson, K. V.; Kalisiak, J.; Lindsey, E. A.; Newcomb, E. T.; Leleti, M. R.; Debien, L.; Rosen, B. R.; Miles, D. H.; Sharif, E. U.; Jeffrey, J. L.; Tan, J. B. L.; Chen, A.; Zhao, S.; Xu, G.; Fu, L.; Jin, L.; Park, T. W.; Berry, W.; Moschütz, S.; Scaletti, E.; Sträter, N.; Walker, N. P.; Young, S. W.; Walters, M. J.; Schindler, U.; Powers, J. P. Discovery of AB680: A potent and selective inhibitor of CD73. *J. Med. Chem.* **2020**, *63*, 11448–11468.

(114) USPTO.report. Inhibitors Of Cd73-mediated Immunosuppression Patent Application. Available at https://uspto.report/patent/app/20200062797, Published Online: August 05, 2021, last accessed August 05, 2021.

(115) Debien, L. P. P.; Jaen, J.C.; Kalisiak, J.; Modulators of ecto-5'-nucleotidase and the use thereof. 2017, WO 2017/120508.

(116) Du, X.; Moore, J.; Blank, B. R.; Eksterowicz, J.; Sutimantanapi, D.; Yuen, N.; Metzger, T.; Chan, B.; Huang, T.; Chen, X.; Chen, Y.; Duong, F.; Kong, W.; Chang, J. H.; Sun, J.; Zavorotinskaya, T.; Ye, Q.; Junttila, M. R.; Ndubaku, C.; Friedman, L. S.; Fantin, V. R.; Sun, D. Orally bioavailable small-molecule CD73 inhibitor (OP-5244) reverses immunosuppression through blockade of adenosine production. *J. Med. Chem.* **2020**, *63*, 10433–10459.

(117) Xiaohui Du. Orally bioavailable small molecule CD73 inhibitor reverses immunosuppression by reduction of adenosine receptors. Available at https://oricpharma.com/wp-content/uploads/2020/06/5244_oral_AACR_V12.pdf, last accessed November 15, 2021.

(118) Sharif, E. U.; Kalisiak, J.; Lawson, K. V.; Miles, D. H.; Newcomb, E.; Lindsey, E. A.; Rosen, B. R.; Debien, L. P. P.; Chen, A.; Zhao, X.; Young, S. W.; Walker, N. P.; Sträter, N.; Scaletti, E. R.; Jin, L.; Xu, G.; Leleti, M. R.; Powers, J. P. Discovery of potent and selective methylenephosphonic acid CD73 inhibitors. *J. Med. Chem.* **2021**, *64*, 845–860.

(119) Dumontet, C.; Peyrottes, S.; Rabeson, C.; Cros-Perrial, E.; Géant, P. Y.; Chaloin, L.; Jordheim, L. P. CD73 inhibition by purine cytotoxic nucleoside analogue-based diphosphonates. *Eur. J. Med. Chem.* **2018**, *157*, 1051–1055.

(120) Ghoteimi, R.; Braka, A.; Rodriguez, C.; Cros-Perrial, E.; van Tai Nguyen; Uttaro, J.-P.; Mathé, C.; Chaloin, L.; Ménétrier-Caux, C.; Jordheim, L. P.; Peyrottes, S. 4-Substituted-1,2,3-triazolo nucleotide analogues as CD73 inhibitors, their synthesis, in vitro screening, kinetic and in silico studies. *Bioorg. Chem.* **2021**, *107*, 104577.

(121) Junker, A.; Renn, C.; Dobelmann, C.; Namasivayam, V.; Jain, S.; Losenkova, K.; Irjala, H.; Duca, S.; Balasubramanian, R.; Chakraborty, S.; Börgel, F.; Zimmermann, H.; Yegutkin, G. G.; Müller, C. E.; Jacobson, K. A. Structure-activity relationship of purine and pyrimidine nucleotides as ecto-5'-nucleotidase (CD73) inhibitors. *J. Med. Chem.* **2019**, *62*, 3677–3695.

(122) Cacatian, S.; Claremon, D. A.; Jia, L.; Morales-Ramos, A.; Singh, S. B.; Venkatraman, S.; Xu, Z.; Zheng, Y. Purine dervatives as CD73 inhibitors for the treatment of cancer. 2015, WO 2015/164573.

(123) Billedeau, R.; Li, J.; Chen, L. Ectonucleotidase inhibitors and methods of use thereof. 2018, WO 2018/119284 A1.

(124) Wang, B.; Yang H., B. K.; Wehn P.; Rizzi J.P. CD73 inhibitors and uses thereof, 2018, WO 2018/183635A1

(125) Baqi, Y.; Lee, S.-Y.; Iqbal, J.; Ripphausen, P.; Lehr, A.; Scheiff, A. B.; Zimmermann, H.; Bajorath, J.; Müller, C. E. Development of potent and selective inhibitors of ecto-5'-nucleotidase based on an anthraquinone scaffold. *J. Med. Chem.* **2010**, *53*, 2076–2086.

(126) Carvalho, D.; Paulino, M.; Polticelli, F.; Arredondo, F.; Williams, R. J.; Abin-Carriquiry, J. A. Structural evidence of quercetin multi-target bioactivity: A reverse virtual screening strategy. *Eur. J. Pharm. Sci.* **2017**, *106*, 393–403.

(127) Braganhol, E.; Tamajusuku, A. S. K.; Bernardi, A.; Wink, M. R.; Battastini, A. M. O. Ecto-5'-nucleotidase/CD73 inhibition by quercetin in the human U138MG glioma cell line. *Biochim. Biophys. Acta* **2007**, *1770*, 1352–1359.

(128) Iqbal, J.; Saeed, A.; Raza, R.; Matin, A.; Hameed, A.; Furtmann, N.; Lecka, J.; Sévigny, J.; Bajorath, J. Identification of sulfonic acids as efficient ecto-5'-nucleotidase inhibitors. *Eur. J. Med. Chem.* **2013**, *70*, 685–691.

(129) Ripphausen, P.; Freundlieb, M.; Brunschweiger, A.; Zimmermann, H.; Müller, C. E.; Bajorath, J. Virtual screening identifies novel sulfonamide inhibitors of ecto-5'-nucleotidase. *J. Med. Chem.* **2012**, *55*, 6576–6581.

(130) Lyu, S.; Zhao, Y.; Zeng, X.; Chen, X.; Meng, Q.; Ding, Z.; Zhao, W.; Qi, Y.; Gao, Y.; Du, J. Identification of phelligridin-based compounds as novel human CD73 inhibitors. *J. Chem. Inf. Model.* **2021**, *61*, 1275–1286.

(131) Baell, J.; Walters, M. A. Chemistry: Chemical con artists foil drug discovery. *Nature* **2014**, *513*, 481–483.

(132) Jasial, S.; Hu, Y.; Bajorath, J. How frequently are pan-assay interference compounds active? Large-scale analysis of screening data reveals diverse activity profiles, low global hit frequency, and many consistently inactive compounds. *J. Med. Chem.* **2017**, *60*, 3879–3886.

(133) Rahimova, R.; Fontanel, S.; Lionne, C.; Jordheim, L. P.; Peyrottes, S.; Chaloin, L. Identification of allosteric inhibitors of the ecto-5'-nucleotidase (CD73) targeting the dimer interface. *PLoS Comput. Biol.* **2018**, *14*, e1005943.

(134) Beatty, J. W.; Lindsey, E. A.; Thomas-Tran, R.; Debien, L.; Mandal, D.; Jeffrey, J. L.; Tran, A. T.; Fournier, J.; Jacob, S. D.; Yan, X.; Drew, S. L.; Ginn, E.; Chen, A.; Pham, A. T.; Zhao, S.; Jin, L.; Young, S. W.; Walker, N. P.; Leleti, M. R.; Moschütz, S.; Sträter, N.; Powers, J. P.; Lawson, K. V. Discovery of potent and selective non-nucleotide small molecule inhibitors of CD73. *J. Med. Chem.* **2020**, *63*, 3935–3955.

(135) Adams J.L.; Ator L. E.; Duffy, K. J.; Graybill T. L.; Kiesow T. J.; Lian Y.; Moore, M. L.; Ralph, J. M.; Ridgers, L. H. Benzothiadiazine compounds, 2017, WO 2017/098421.

(136) Dally, R. D.; Garcia Paredes, M. C.; Heinz, L. J., II; Howell, J. M.; Njoroge, F. G.; Wang, Y.; Zhao, G. CD73 Inhibitors, 2019 Int. Appl. PCT/US2019/019074, WO Patent WO2019168744.

(137) Schmies, C. C.; Rolshoven, G.; Idris, R. M.; Losenkova, K.; Renn, C.; Schäkel, L.; Al-Hroub, H.; Wang, Y.; Garofano, F.; Schmidt-Wolf, I. G. H.; Zimmermann, H.; Yegutkin, G. G.; Müller, C. E. Fluorescent probes for ecto-5'-nucleotidase (CD73). *ACS Med. Chem. Lett.* **2020**, *11*, 2253–2260.

(138) Witkowski, J. T.; Robins, R. K.; Sidwell, R. W.; Simon, L. N. Design, synthesis, and broad spectrum antiviral activity of 1- -D-ribofuranosyl-1,2,4-triazole-3-carboxamide and related nucleosides. *J. Med. Chem.* **1972**, *15*, 1150–1154.

(139) Niedballa, U.; Vorbrüggen, H. A general synthesis of pyrimidine nucleosides. *Angew. Chem. Int. Ed. Engl.* **1970**, *9*, 461–462.

(140) Sekiya, M.; Yoshino, T.; Tanaka, H.; Ishido, Y. On the mechanism of the acid catalysis and new activating agents in the fusion reaction of an acylated sugar with a purine derivative. *BCSJ* **1973**, *46*, 556–561.

(141) Constanze Schmies. *Design, synthesis and optimization of nucleotide-derived inhibitors and probes for the ecto-nucleotidases CD39 and CD73:* Bonn, 2019.

(142) Francom, P.; Janeba, Z.; Shibuya, S.; Robins, M. J. Nucleic acid related compounds. 116. Nonaqueous diazotization of aminopurine nucleosides. Mechanistic considerations and efficient procedures with tert-butyl nitrite or sodium nitrite. *J. Org. Chem.* **2002**, *67*, 6788–6796.

(143) Francom, P.; Robins, M. J. Nucleic acid related compounds. 118. Nonaqueous diazotization of aminopurine derivatives. Convenient access to 6-halo- and 2,6-dihalopurine nucleosides and 2'-deoxynucleosides with acyl or silyl halides. *J. Org. Chem.* **2003**, *68*, 666–669.

(144) Lebleu, T.; Ma, X.; Maddaluno, J.; Legros, J. Selective monomethylation of primary amines with simple electrophiles. *Chem. Commun.* **2014**, *50*, 1836–1838.

(145) Salvatore, R. N.; Yoon, C. H.; Jung, K. W. Synthesis of secondary amines. *Tetrahedron* **2001**, *57*, 7785–7811.

(146) Ramos-Villaseñor, J. M.; Rodríguez-Cárdenas, E.; Barrera Díaz, C. E.; Frontana-Uribe, B. A. Review—Use of 1,1,1,3,3,3–hexafluoro–2–propanol (HFIP) Co-Solvent Mixtures in Organic Electrosynthesis. *J. Electrochem. Soc.* **2020**, *167*, 155509.

(147) PubChem. Methyl trifluoromethanesulfonate. Available at https://pubchem.ncbi.nlm.nih.gov/compound/Methyl-trifluoromethanesulfonate, Published Online: July 12, 2021, last accessed July 12, 2021.

(148) Yin, J.; Zhang, J.; Cai, C.; Deng, G.-J.; Gong, H. Catalyst-free transamidation of aromatic amines with formamide derivatives and tertiary amides with aliphatic amines. *Org. Let.* **2019**, *21*, 387–392.

(149) Jianyu Hou. *Design, synthesis and pharmacological evaluation of nucleotide-derived inhibitors and fluorescent tools for ecto-5'-nucleotidase (CD73):* Bonn, 2021.

(150) Yung-Chi, C.; Prusoff, W. H. Relationship between the inhibition constant (KI) and the concentration of inhibitor which causes 50 per cent inhibition (I50) of an enzymatic reaction. *Biochem. pharmacol.* **1973**, *22*, 3099–3108.

(151) Riham Idris. *unpublished work*, 2021.

(152) Steinebach, C.; Kehm, H.; Lindner, S.; Vu, L. P.; Köpff, S.; López Mármol, Á.; Weiler, C.; Wagner, K. G.; Reichenzeller, M.; Krönke, J.; Gütschow, M. PROTAC-mediated crosstalk between E3 ligases. *Chem. Commun.* **2019**, *55*, 1821–1824.

(153) Brown, J. M.; Dahlman, J. E.; Neuman, K. K.; Prata, C. A. H.; Krampert, M. C.; Hadwiger, P. M.; Vornlocher, H.-P. Ligand conjugated multimeric siRNAs enable enhanced uptake and multiplexed gene silencing. *Nucleic Acid Ther.* **2019**, *29*, 231–244.

(154) Lee, S.-Y.; Luo, X.; Namasivayam, V.; Geiss, J.; Mirza, S.; Pelletier, J.; Stephan, H.; Sévigny, J.; Müller, C. E. Development of a selective and highly sensitive fluorescence assay for nucleoside triphosphate diphosphohydrolase1 (NTPDase1, CD39). *Analyst* **2018**, *143*, 5417–5430.

(155) Zhang, X.-F.; Zhang, J.; Liu, L. Fluorescence properties of twenty fluorescein derivatives: lifetime, quantum yield, absorption and emission spectra. *J. Fluoresc.* **2014**, *24*, 819–826.

(156) El-Tayeb, A.; Gollos, S. Synthesis and structure-activity relationships of 2-hydrazinyladenosine derivatives as A(2A) adenosine receptor ligands. *Bioorg. Med. Chem.* **2013**, *21*, 436–447.

(157) Shendage, D. M.; Fröhlich, R.; Haufe, G. Highly efficient stereoconservative amidation and deamidation of alpha-amino acids. *Org. Let.* **2004**, *6*, 3675–3678.

(158) Vrettos, E. I.; Sayyad, N.; Mavrogiannaki, E. M.; Stylos, E.; Kostagianni, A. D.; Papas, S.; Mavromoustakos, T.; Theodorou, V.; Tzakos, A. G. Unveiling and tackling guanidinium peptide coupling reagent side reactions towards the development of peptide-drug conjugates. *RSC Adv.* **2017**, *7*, 50519–50526.

(159) Rafehi, M.; Burbiel, J. C.; Attah, I. Y.; Abdelrahman, A.; Müller, C. E. Synthesis, characterization, and in vitro evaluation of the selective P2Y2 receptor antagonist AR-C118925. *Purinergic Signal.* **2017**, *13*, 89–103.

(160) Rafehi, M.; Malik, E. M.; Neumann, A.; Abdelrahman, A.; Hanck, T.; Namasivayam, V.; Müller, C. E.; Baqi, Y. Development of potent and selective antagonists for the UTP-activated P2Y4 receptor. *J. Med. Chem.* **2017**, *60*, 3020–3038.

(161) Attah, I. Y.; Neumann, A.; Al-Hroub, H.; Rafehi, M.; Baqi, Y.; Namasivayam, V.; Müller, C. E. Ligand binding and activation of UTP-activated G protein-coupled P2Y2 and P2Y4 receptors elucidated by mutagenesis, pharmacological and computational studies. *Biochim. Biophys. Acta Gen. Subj.* **2020**, *1864*, 129501.

(162) Loudet, A.; Burgess, K. BODIPY dyes and their derivatives: syntheses and spectroscopic properties. *Chem. Rev.* **2007**, *107*, 4891–4932.

(163) Martin, M. M.; Lindqvist, L. The pH dependence of fluorescein fluorescence. *J. Lumin.* **1975**, *10*, 381–390.

(164) Sun, W.-C.; Gee, K. R.; Klaubert, D. H.; Haugland, R. P. Synthesis of Fluorinated Fluoresceins. *J. Org. Chem.* **1997**, *62*, 6469–6475.

(165) Díaz-García, M. E.; Badía-Laíño, R. Fluorescence | Fluorescence Labeling. In *Reference Module in Chemistry, Molecular Sciences and Chemical Engineering;* Elsevier.

(166) Zlatić, K.; Antol, I.; Uzelac, L.; Mikecin Dražić, A.-M.; Kralj, M.; Bohne, C.; Basarić, N. Labeling of proteins by BODIPY-quinone methodes utilizing anti-kasha photochemistry. *ACS Appl. Mater. Interfaces* **2020**, *12*, 347–351.

(167) Kim, D.; Ma, D.; Kim, M.; Jung, Y.; Kim, N. H.; Lee, C.; Cho, S. W.; Park, S.; Huh, Y.; Jung, J.; Ahn, K. H. Fluorescent labeling of protein using blue-emitting 8-amino-BODIPY derivatives. *J. Fluoresc.* **2017**, *27*, 2231–2238.

(168) Ulrich, G.; Ziessel, R.; Harriman, A. The chemistry of fluorescent bodipy dyes: versatility unsurpassed. *Angew. Chem. Int. Ed. Engl.* **2008**, *47*, 1184–1201.

(169) Rostovtsev, V. V.; Green, L. G.; Fokin, V. V.; Sharpless, K. B. A stepwise Huisgen Cycloaddition process: Copper(I)-catalyzed regioselective "Ligation" of azides and terminal alkynes. *Angew. Chem. Int. Ed.* **2002**, *41*, 2596–2599.

(170) Himo, F.; Lovell, T.; Hilgraf, R.; Rostovtsev, V. V.; Noodleman, L.; Sharpless, K. B.; Fokin, V. V. Copper(I)-catalyzed synthesis of azoles. DFT study predicts unprecedented reactivity and intermediates. *Chem. Eur. J.* **2005**, *127*, 210–216.

(171) Sun, C.; Du, W.; Wang, B.; Dong, B.; Wang, B. Research progress of near-infrared fluorescence probes based on indole heptamethine cyanine dyes in vivo and in vitro. *BMC Chem.* **2020**, *14*, 21.

(172) Li, Y.; Zhou, Y.; Yue, X.; Dai, Z. Cyanine conjugates in cancer theranostics. *Bioact. mater.* **2021**, *6*, 794–809.

(173) Grimm, J. B.; Heckman, L. M.; Lavis, L. D. The chemistry of small-molecule fluorogenic probes. *Prog. Mol. Biol. Transl. Sci.* **2013**, *113*, 1–34.

(174) Ilina, K.; Henary, M. Cyanine dyes containing quinoline moieties: history, synthesis, optical properties, and applications. *Chem. Eur. J.* **2021**, *27*, 4230–4248.

(175) Tim Harms. *unpublished work:* Bonn, 2021.

(176) Clemens Dobelmann. *unpublished work:* Münster, 2021.

(177) Meinecke, J.; Koert, U. Copper-free click reaction sequence: A chemoselective layer-by-layer approach. *Org. Let.* **2019**, *21*, 7609–7612.

(178) Jewett, J. C.; Bertozzi, C. R. Cu-free click cycloaddition reactions in chemical biology. *Chem. Soc. Rev.* **2010**, *39*, 1272–1279.

(179) Baskin, J. M.; Prescher, J. A.; Laughlin, S. T.; Agard, N. J.; Chang, P. V.; Miller, I. A.; Lo, A.; Codelli, J. A.; Bertozzi, C. R. Copper-free click chemistry for dynamic in vivo imaging. *PNAS* **2007**, *104*, 16793–16797.

(180) Feng, L.; Dong, Z.; Tao, D.; Zhang, Y.; Liu, Z. The acidic tumor microenvironment: a target for smart cancer nano-theranostics. *Natl. Sci. Rev.* **2018**, *5*, 269–286.

(181) Nuhn, L.; Hartmann, S.; Palitzsch, B.; Gerlitzki, B.; Schmitt, E.; Zentel, R.; Kunz, H. Water-soluble polymers coupled with glycopeptide antigens and T-cell epitopes as potential antitumor vaccines. *Angew. Chem. Int. Ed.* **2013**, *52*, 10652–10656.

(182) Nuhn, L.; Vanparijs, N.; Beuckelaer, A. de; Lybaert, L.; Verstraete, G.; Deswarte, K.; Lienenklaus, S.; Shukla, N. M.; Salyer, A. C. D.; Lambrecht, B. N.; Grooten, J.; David, S. A.; Koker, S. de; Geest, B. G. de. pH-degradable imidazoquinoline-ligated nanogels for lymph node-focused immune activation. *PNAS* **2016**, *113*, 8098–8103.

(183) Nuhn, L.; Koker, S. de; van Lint, S.; Zhong, Z.; Catani, J. P.; Combes, F.; Deswarte, K.; Li, Y.; Lambrecht, B. N.; Lienenklaus, S.; Sanders, N. N.; David, S. A.; Tavernier, J.; Geest, B. G. de. Nanoparticle-conjugate TLR7/8 agonist localized immunotherapy provokes safe antitumoral responses. *Adv. Mater.* **2018**, *30*, e1803397.

(184) Talelli, M.; Barz, M.; Rijcken, C. J.; Kiessling, F.; Hennink, W. E.; Lammers, T. Core-crosslinked polymeric micelles: Principles, preparation, biomedical applications and clinical translation. *Nano Today* **2015**, *10*, 93–117.

(185) Nuhn, L.; van Hoecke, L.; Deswarte, K.; Schepens, B.; Li, Y.; Lambrecht, B. N.; Koker, S. de; David, S. A.; Saelens, X.; Geest, B. G. de. Potent anti-viral vaccine adjuvant based on pH-degradable nanogels with covalently linked small molecule imidazoquinoline TLR7/8 agonist. *Biomaterials* **2018**, *178*, 643–651.

(186) Henderson, W. A.; Schultz, C. J. The Nucleophilicity of Amines. *J. Org. Chem.* **1962**, *27*, 4643–4646.

(187) Castillo, J.-C.; Orrego-Hernández, J.; Portilla, J. Cs 2 CO 3 -Promoted direct N-alkylation: Highly chemoselective synthesis of N-alkylated benzylamines and anilines. *Eur. J. Org. Chem.* **2016**, *2016*, 3824–3835.

(188) Vertuani, S.; Baldisserotto, A.; Varani, K.; Borea, P. A.; Marcos Maria Cruz, B. de; Ferraro, L.; Manfredini, S.; Dalpiaz, A. Synthesis and in vitro stability of nucleoside 5'-phosphonate derivatives. *Eur. J. Med. Chem.* **2012**, *54*, 202–209.

(189) Brunschweiger, A. *Darstellung und Charakterisierung von Uracil- und Adeninnucleotid-Mimetika als selektive Ectonucleotidase-Inhibitoren*: Bonn, 2007.

(190) Carpino, L. A. 1-Hydroxy-7-azabenzotriazole. An efficient peptide coupling additive. *J. Am. Chem. Soc.* **1993**, *115*, 4397–4398.

(191) Ghoteimi, R.; van Nguyen, T.; Rahimova, R.; Grosjean, F.; Cros-Perrial, E.; Uttaro, J.-P.; Mathé, C.; Chaloin, L.; Jordheim, L. P.; Peyrottes, S. Synthesis of substituted 5′-aminoadenosine derivatives and evaluation of their inhibitory potential towards CD73. *ChemMedChem* **2019**, *14*, 1431–1443.

(192) Lai, A. C.; Toure, M.; Hellerschmied, D.; Salami, J.; Jaime-Figueroa, S.; Ko, E.; Hines, J.; Crews, C. M. Modulares PROTAC-Design zum Abbau von onkogenem BCR-ABL. *Angew. Chem.* **2016**, *128*, 818–821.

(193) Neises, B.; Steglich, W. Simple method for the esterification of carboxylic acids. *Angew. Chem. Int. Ed. Engl.* **1978**, *17*, 522–524.

(194) Wiemer, A. J.; Wiemer, D. F. Prodrugs of phosphonates and phosphates: crossing the membrane barrier. *Top. Curr. Chem.* **2015**, *360*, 115–160.

(195) Marianne Freundlieb. *Entwicklung und Charakterisierung von neuen und selektiven Inhibitoren für die Ecto-5'-Nucleotidase:* Bonn, 2016.

(196) Compound library, AK Müller. Available at https://www.pharmchem1.uni-bonn.de/www-en/pharmchem1-en/mueller-laboratory/compound-library, last accessed July 13, 2021.

(197) Drabczyńska, A.; Karcz, T.; Szymańska, E.; Köse, M.; Müller, C. E.; Paskaleva, M.; Karolak-Wojciechowska, J.; Handzlik, J.; Yuzlenko, O.; Kieć-Kononowicz, K. Synthesis,

biological activity and molecular modelling studies of tricyclic alkylimidazo-, pyrimido- and diazepinopurinediones. *Purinergic Signal.* **2013**, *9*, 395–414.

(198) Drabczyńska, A.; Müller, C. E.; Karolak-Wojciechowska, J.; Schumacher, B.; Schiedel, A.; Yuzlenko, O.; Kieć-Kononowicz, K. N9-benzyl-substituted 1,3-dimethyl- and 1,3-dipropyl-pyrimido2,1-fpurinediones: synthesis and structure-activity relationships at adenosine A1 and A2A receptors. *Bioorg. Med. Chem.* **2007**, *15*, 5003–5017.

(199) Koch, P.; Akkari, R.; Brunschweiger, A.; Borrmann, T.; Schlenk, M.; Küppers, P.; Köse, M.; Radjainia, H.; Hockemeyer, J.; Drabczyńska, A.; Kieć-Kononowicz, K.; Müller, C. E. 1,3-Dialkyl-substituted tetrahydropyrimido1,2-fpurine-2,4-diones as multiple target drugs for the potential treatment of neurodegenerative diseases. *Bioorg. Med. Chem.* **2013**, *21*, 7435–7452.

(200) Schoeder, C. T.; Mahardhika, A. B.; Drabczyńska, A.; Kieć-Kononowicz, K.; Müller, C. E. Discovery of tricyclic xanthines as agonists of the cannabinoid-activated orphan G-Protein-coupled receptor GPR18. *ACS Med. Chem. Lett.* **2020**, *11*, 2024–2031.

(201) Załuski, M.; Stanuch, K.; Karcz, T.; Hinz, S.; Latacz, G.; Szymańska, E.; Schabikowski, J.; Doroż-Płonka, A.; Handzlik, J.; Drabczyńska, A.; Müller, C. E.; Kieć-Kononowicz, K. Tricyclic xanthine derivatives containing a basic substituent: adenosine receptor affinity and drug-related properties. *Medchemcomm* **2018**, *9*, 951–962.

(202) Müller, C. E.; Jacobson, K. A. Xanthines as adenosine receptor antagonists. *Handb. Exp. Pharmacol.* **2011**, 151–199.

(203) Brunschweiger, A.; Koch, P.; Schlenk, M.; Rafehi, M.; Radjainia, H.; Küppers, P.; Hinz, S.; Pineda, F.; Wiese, M.; Hockemeyer, J.; Heer, J.; Denonne, F.; Müller, C. E. 8-Substituted 1,3-dimethyltetrahydropyrazino2,1-fpurinediones: Water-soluble adenosine receptor antagonists and monoamine oxidase B inhibitors. *Bioorg. Med. Chem.* **2016**, *24*, 5462–5480.

(204) Romio, M.; Reinbeck, B.; Bongardt, S.; Hüls, S.; Burghoff, S.; Schrader, J. Extracellular purine metabolism and signaling of CD73-derived adenosine in murine Treg and Teff cells. *Am. J. Physiol. Cell Physiol.* **2011**, *301*, C530-9.

(205) Sträter, N. Ecto-5'-nucleotidase: Structure function relationships. *Purinergic Signal.* **2006**, *2*, 343–350.

(206) Young, A.; Ngiow, S. F.; Barkauskas, D. S.; Sult, E.; Hay, C.; Blake, S. J.; Huang, Q.; Liu, J.; Takeda, K.; Teng, M. W.; Sachsenmeier, K.; Smyth, M. J. Co-inhibition of CD73 and A2AR adenosine signaling improves anti-tumor immune responses. *Cancer Cell* **2016**, *30*, 391–403.

(207) Geoghegan, J. C.; Diedrich, G.; Lu, X.; Rosenthal, K.; Sachsenmeier, K. F.; Wu, H.; Dall'Acqua, W. F.; Damschroder, M. M. Inhibition of CD73 AMP hydrolysis by a therapeutic antibody with a dual, non-competitive mechanism of action. *mAbs* **2016**, *8*, 454–467.

(208) Brouet, J.-C.; Gu, S.; Peet, N. P.; Williams, J. D. Survey of solvents for the Conrad–Limpach synthesis of 4-hydroxyquinolones. *Synth. Commun.* **2009**, *39*, 1563–1569.

(209) Scaletti, E.; Huschmann, F. U.; Mueller, U.; Weiss, M. S.; Sträter, N. Substrate binding modes of purine and pyrimidine nucleotides to human ecto-5'-nucleotidase (CD73) and inhibition by their bisphosphonic acid derivatives. *Purinergic Signal.* **2021**, 1–12.

(210) Servos, J.; Reilnder, H.; Zimmermann, H. Catalytically active soluble ecto-5?-nucleotidase purified after heterologous expression as a tool for drug screening. *Drug Dev. Res.* **1998**, *45*, 269–276.

(211) Sévigny, J.; Levesque, F. P.; Grondin, G.; Beaudoin, A. R. Purification of the blood vessel ATP diphosphohydrolase, identification and localisation by immunological techniques. *Biochim. Biophys. Acta Gen. Subj.* **1997**, *1334*, 73–88.

(212) Kukulski, F.; Levesque, S. A.; Lavoie, E. G.; Lecka, J.; Bigonnesse, F.; Knowles, A. F.; Robson, S. C.; Kirley, T. L.; Sevigny, J. Erratum to: Comparative hydrolysis of P2 receptor agonists by NTPDases 1, 2, 3 and 8. *Purinergic Signal.* **2005**, *1*, 293.

6   Abbreviations

Ado	Adenosine
ACN	Acetonitrile
ADP	Adenosine diphosphate
AdeR	Adenine receptor
AMP	Adenosine monophosphate
AMPCP	*α,β*-methylene-ADP, adenosine-5′-*O*-[(phosphonomethyl)phosphonic acid]
AP	Alkaline phosphatase
AR	Adenosine receptor
ASAP-MS	Atmospheric solid analysis probe mass spectrometry
ATP	Adenosine triphosphate
BAIB	(Diacetoxyiodo)benzene

Balb/c	Bagg albino
Boc	*tert*-butyloxycarbonyl
Br	Broad
BSA	*N*-Trimethylsilyl-1-trimethylsilyloxyethanimine
CD39	Cluster of differentiation 39
CD73	Cluster of differentiation 73
CE	Capillary electrophoresis
CE-UV	Capillary electrophoresis coupled with UV detector
CHES	*N*-Cyclohexyl-2-aminoethanesulfonic acid
CTLA4	Cytotoxic T-lymphocyte-associated protein 4
CD26	Colon Tumor #26
d	Doublet
DAD	Diode array detector
DIPEA	*N*,*N*-Diisopropylethylamine
DCC	*N, N′*-Dicyclohexylcarbodiimide
DCM	Dichloromethane
DMAP	4-Dimethylaminopyridine
DMF	*N*,*N*-Dimethylformamide
DMSO	Dimethyl sulfoxide
*e*N	*ecto*-5′-Nucleotidase
*e*NPP	*ecto*-Nucleotide pyrophosphatases/ phosphodiesterase
*e*NTPDase	*ecto*-Nucleoside triphosphate diphosphohydrolases
EDTA	Ethylenediaminetetraacetic acid
GCAP	Gem cell alkaline phosphatase
GMP	Guanosine monophosphate
GPCR	G protein-coupled receptor
GPI	Glycosylphosphatidylinositol
HATU	1-[Bis(dimethylamino)methylene]-1*H*-1,2,3-triazolo[4,5-b]pyridinium 3-oxide hexafluorophosphate
HFIP	1,1,1,3,3,3-Hexafluoro-2-propanole

266

HEPES	4-(2-Hydroxyethyl)-1-piperazineethanesulfonic acid
HObt	1-Hydroxybenzotriazole
HPLC	High performance liquid chromatography
IAP	Intestinal alklaine phosphatase
IFN	Interferon
IMP	Inosine monophosphate
IMDQ	Imidazoquinoline
LC-MS	Liquid chromatography-mass spectrometry
LOD	Limit of detection
m	Multiplet
mAb	monoclonal antibody
mTEGMA	methoxy triethylene glycol methacrylate
N	Normal
NMR	Nuclear magnetic resonance
PD1	Programmed cell death protein 1
PD-L1	Programmed cell death protein 1
PEG	Polyethyleneglycol
PFP	Pentafluorophenyl
PFPMA	Pentafluorophenyl methacrylate
PLAP	Placental alkaline phosphatase
PROTAC	Proteolysis targeting chimera
q	Quartet
RP	Reversed-phase
RP-HPLC	Reversed-phase high performance liquid chromatography
r.t.	Room temperature
s	Singlet
SAR	Structure-activity relationship
TBAHS	Tetrabutyl ammoniumhydrogensulfate
TBME	*tert*-butylmethyl ether
TBN	*tert*-Butyl nitrite

TEAC	Triethyl ammoniumhydrogencarbonate buffer
TEMPO	2,2,6,6-Tetramethylpiperidinyloxyl
TFA	Trifluoroacetic acid
THF	Tetrahydrofuran
TLC	Thin-layer chromatography
TLC-MS	Thin-layer chromatography-coupled mass spectrometry
TLR	Toll-like receptor
TMSBr	Bromotrimethylsilane
TNAP	Tisse non-specific alkaline phosphatase
t	Triplet
UDP	Uridine diphosphate
UMP	Uridine monophosphate
UTP	Uridine triphosphate

7 List of tables

9   List of figures

272

10   Publications

Schmies, C. C.;* Rolshoven, G.;* Idris, R. M.; Losenkova, K.; Renn, C.; Schäkel, L.; Al-Hroub, H.; Wang, Y.; Garofano, F.; Schmidt-Wolf, I. G. H.; Zimmermann, H.; Yegutkin, G. G.; Müller, C. E. Fluorescent probes for *ecto*-5'-nucleotidase (CD73). *ACS Med. Chem. Lett.* **2020**, *11*, 2253–2260. *shared first-authorship. https://doi.org/10.1021/acsmedchemlett.0c00391

Bhattarai, S.; Pippel, J.; Scaletti, E.; Idris, R.; Freundlieb, M.; Rolshoven, G.; Renn, C.; Lee, S.-Y.; Abdelrahman, A.; Zimmermann, H.; El-Tayeb, A.; Müller, C. E.; Sträter, N. 2-Substituted α,β- methylene-ADP derivatives: potent competitive *ecto*-5'-nucleotidase (CD73) inhibitors with variable binding modes. *J. Med. Chem.* **2020**, *63*, 2941–2957. https://doi.org/10.1021/acs.jmedchem.9b01611

Losenkova, K.; Takeda, A.; Ragauskas, S.; Kaja, S.; Paul, M.L.; Schmies, C.C.; Rolshoven, G.; Müller, C.E.; Sandholm, J.; Jalkanen, S.; Kalesnykas, G.; Yegutkin, G.G. CD73 Controls Ocular Adenosine Levels and Protects Retina from Light-Induced Phototoxicity, August 06, 2021, PREPRINT (Version 1) available at Research Square [https://doi.org/10.21203/rs.3.rs-743701/v1]. This preprint is under consideration at Cellular and Molecular Life Sciences. Current Status: *Under Revision.*

11 Danksagung

Ich danke weiterhin Tobias Claff, Jonathan Schlegel, Viktoria Vaaßen, Dr. Lukas L. Wendt, Dr. Anton Ivanov und Dr. Yvonne Riedel für die zahlreichen gemeinsamen Besuche in der Mensa. Hier konntem wir gemeinsam für einen kurzen Moment von der Uni Abstand nehmen und wunderbar über Probleme, Offenbarungen, Sorgen und ganz generell die verschiedensten Themen des Lebens philosophieren. Weniger das Essen an sich als das tägliche Ritual des gemeinsamen Ausfluges war für uns alle Bedeutsam und belebte neben der wissenschaftlichen auch die transzendentale Seite einer Doktorandenseele. Die ca. anderthalbjährige kulinarische Zwangspause, die wir aufgrund der Corona-Schutzmaßnahmen einlegen mussten, lehrte uns einmal mehr auch die Speisen der Mensa Poppelsdorf zu schätzen. Ein herzhaftes Dankeschön!

Ich danke außerdem Dr. Constanze Schmies, mit der ich nicht nur eine Erstautorenschaft, sondern auch die Karnevalsregentschaft des AK Müllers im Jahre 2019 teilte. Unsere wissenschaftlichen Projekte waren eng miteinander verbunden und deshalb danke ich dir sehr für den regen fachlichen Austausch, für die Unterweisung an der HPLC und insbesondere die Initiierung der Feierabendbiergruppe, welche im Arbeitskreis regen Anklang fand.

Ich danke darüberhinaus allen Kolleginnen und Kollegen, mit denen ich das Praktikum im 4. Semester betreut habe. Namentlich zu nennen sind Jan Voss, Dr. Lukas L. Wendt, Lukas Gockel, Katrin Nekipelov, Dr. Markus Kuschak, Dr Ali El-Tayeb und insbesondere PD. Dr. Martin Schlesinger, der das Praktikum über Jahre hinweg perfekt organisiert hat. Einen besseren Semesterleiter hätte man sich als Doktorand nicht wünschen können. Außerdem möchte ich meinem ehemaligen Masteranden Jianyu Hou für die konstruktive Zusammenarbeit danken. Meinem Projektnachfolger Eugen Potaptschuk danke ich ebenfalls für neue, frische Ideen und wünsche viel Erfolg mit diesem tollen Projekt!

Allen namentlich nicht genannten Mitgliederinnen und Mitgliedern des Arbeitskreises Müller möchte ich ebenfalls ausdrücklich danken. Ihr alle habt zum erfolgreichen Abschluss meiner

Dissertation beigetragen. Aus einigen Kollegen sind während der Zeit der Promotion Freunde geworden und auch dafür möchte ich natürlich danken.

Mein größter Dank gilt meiner Freundin Pia, die mich immer unterstützt hat und mir in allen Phasen der doktoralen Stimmungsmplitude zur Seite stand. Ich danke außerdem meiner Familie für die immer fortwährende Unterstüzung, sowie meinen Freunden, die mich auf diesem Weg begleitet haben.